Blind Channel Estimation Using Redundant Precoding: New Algorithms, Analysis, and Theory

Thesis by

Borching Su

In Partial Fulfillment of the Requirements

for the Degree of

Doctor of Philosophy

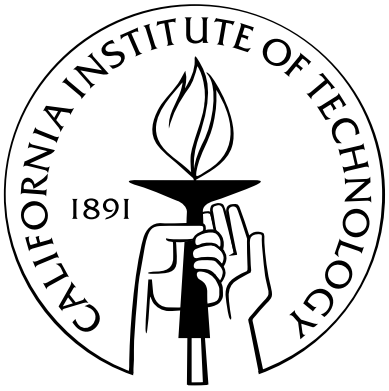

California Institute of Technology

Pasadena, California

2008

(Defended January 9th, 2008)

© 2008

Borching Su

All Rights Reserved

Acknowledgments

I would like to first express my sincerest gratitude to my thesis advisor, Professor P. P. Vaidyanathan, for his excellent guidance, encouragement, and patience during the years of my Ph.D. study at Caltech. P. P. not only has taught me valuable skills for doing research, but has also influenced me with invaluable attitudes required for a real scholar. His advices have been inspiring and motivating, and his words of encouragement have always been a strong support especially when I faced difficulties. He made me understand the importance of being confident yet polite, assertive yet consistent, and disciplined yet humorous. And the fact that he lives with these values himself uncompromisingly is a stronger source, than words, of stimulation and reinforcement for my research endeavors. He is in every aspect a great teacher and advisor, and I feel really grateful and fortunate to be one of his students.

I would also like to thank the members of my defense and candidacy examining committees for their interest: Professor Robert McEliece, Professor Babak Hassibi, Professor Yaser Abu-Mostafa, Professor Tracey Ho, and Dr. Andre Tkacenko. Generous support from Moore Fellowship, National Science Foundation, and the Office of Naval Research is gratefully acknowledged. I would also like to thank DSP lab alumni and frequent visitors Professor See-May Phoong and Professor Yuan-Pei Lin, whose comments have in my early years helped me find my initial research direction.

I would like to thank my labmates, Andre Tkacenko, Michael Larsen, Sriram Murali, Byung-Jun Yoon, Chun-Yang Chen, and Ching-Chih Weng, for their friendship and sharing experience in learning and research during my stay in the DSP lab. I would especially like to thank Byung-Jun, with whom I shared the longest time in the lab, for his constant thoughtful support since my first day in the lab. I would also like to Chun-Yang and Ching-Chih for all the stimulating discussions and memorable joyful moments we have shared in the lab.

Finally, I would like to thank my parents for their unconditional love and their endless support for my pursue of studying in the United States. Without their sacrifices and endeavors to provide

me with the best education in every step in my life, I could not have had any of the opportunities I currently enjoy. I would like to take this remarkable moment to say to parents: “I love you, Dad and Mom. Thank you for everything you have done for me!”

Abstract

Digital signal processing (DSP) techniques have played an important role in channel equalization and estimation in communication systems. While channel equalization and estimation are usually done by pilot-assisted methods in most systems, algorithms for blind channel estimation have also been largely studied due to high bandwidth efficiency. However, up to date, most blind methods possess disadvantages such as slow convergence speed, high complexity, poor performance, etc., compared to pilot-assisted methods. These drawbacks have made many consider blind methods as inapplicable in modern communication systems which feature fast-varying channels.

In this thesis, we consider the blind channel estimation problem in block transmission systems with linear redundant precoding (LRP) which have been widely adopted in modern communication systems in recent years. The main contribution of this thesis is to considerably reduce the amount of received data required for blind estimation and suggest blind methods which are applicable even in fast-varying environments (e.g., in wireless channels). New algorithms are proposed, performance analysis derived, and theoretical issues studied.

The first part of the thesis focuses on new algorithms for blind channel estimation and blind block synchronization in LRP systems. Two major types of linear redundant precoding, namely zero-padding (ZP) and cyclic prefixing (CP), are considered in this thesis. We first propose a generalized, subspace-based algorithm for blind channel estimation in ZP systems of which two previously reported algorithms are special cases. The generalization uses an integer parameter called *repetition index* which represents the number of repeated uses of each received block. The number of received blocks required for subspace-based blind estimation is roughly inversely proportional to the repetition index. By choosing a larger repetition index, the amount of received data can be significantly reduced.

The concept of repetition index is also applied in blind channel estimation in CP systems, which are more widely used than ZP systems in many current communication standards such as orthog-

onal frequency division multiplexing (OFDM) systems. The use of repetition index in CP systems is much less obvious and conceptually more complicated than in ZP systems. By choosing a repetition index larger than unity, the number of received blocks needed for blind estimation is significantly reduced compared to all previously reported methods. Theoretically, the proposed method can perform blind estimation using only three received blocks in absence of noise. In practice, the number of received blocks needed to yield a satisfactory bit error rate performance is usually on the order of half the block size. The proposed algorithm can be directly applied in OFDM systems without any modification of transmitter structure. A semiblind algorithm for channel estimation in OFDM systems is also proposed based on the extension of the blind algorithm.

Another important problem, namely the blind block synchronization, is also studied. Most existing blind estimation methods in LRP systems assume the block boundaries of the received streams are perfectly known to the receiver, but this assumption is usually not true in practice since no extra known samples are transmitted. Two algorithms for blind block synchronization are proposed for ZP and CP systems, respectively. In particular, the block synchronization problem in CP systems is a broader version of the timing synchronization problem in the OFDM systems. The proposed algorithms exploit the concept of repetition index and both theoretical and simulation results suggest their advantages over all previously reported algorithms, especially when the amount of received data is limited.

The second part of the thesis deals with theoretical issues related to blind channel estimation. Performance analysis of the generalized blind channel estimation algorithm in ZP systems is first given and shows that the system performance in terms of channel estimation mean square error (MSE) is very close to the Cramer-Rao bound (CRB), even when only two received blocks are available. Another important theoretical problem, namely the signal richness preservation problem, is also studied. Signal richness is an essential property for input signals in subspace-based blind channel estimation algorithms studied in this thesis. This property, however, may be altered by a linear precoder. Necessary and sufficient conditions for a linear precoder to preserve signal richness are explored. Several relevant interesting mathematical problems are also studied.

Contents

Acknowledgments **iii**

Abstract **v**

1 Introduction **1**

1.1 Brief History of Blind Channel Estimation 2

1.1.1 Early Developments of Blind Estimation in SISO Systems 3

1.1.2 Using Second Order Statistics in SIMO Systems 4

1.2 Blind Channel Estimation Using Redundant Precoding 6

1.2.1 Block Transmission Systems With Linear Redundant Precoders 7

1.2.2 Blind Channel Estimation in LRP Systems: Subspace v.s. Finite Alphabet Algorithms 9

1.3 Outline of the thesis 10

1.3.1 Scope of the thesis 10

1.3.2 Generalized Algorithms for Blind Channel Estimation in ZP Systems (Chapter 2) 10

1.3.3 Blind and Semi-Blind Channel Estimation in Cyclic Prefix Systems (Chapter 3) 11

1.3.4 New Algorithms for Blind Block Synchronization In LRP Systems (Chapter 4) 12

1.3.5 Performance Analysis of Blind Estimation Algorithms in ZP Systems (Chapter 5) 12

1.3.6 Theoretical Issues on Signal Richness Preservation for Blind Estimation (Chapters 6 and 7) 13

1.4 Notations 14

2 Generalized Algorithms for Blind Channel Estimation in Zero-Padding Systems **16**

2.1 Outline . . . 17
2.2 Problem Formulation and Literature Review . . . 18
2.2.1 Redundant Filter Bank Precoders . . . 18
2.2.2 Trailing Zeros as Transmitter Guard Interval and the SGB method . . . 19
2.2.3 The MNP Method: Finding the Greatest Common Divisor . . . 20
2.2.4 Connection to the Earlier Literature . . . 21
2.3 A Generalized Algorithm . . . 22
2.3.1 Algorithm Description . . . 22
2.3.2 Q-Repetition and Shifting Operation . . . 24
2.3.3 Special Cases of the Algorithm . . . 24
2.4 Frequency Domain Approach . . . 25
2.5 Generalized Signal Richness . . . 28
2.5.1 Measure of Generalized Signal Richness . . . 29
2.5.2 Connection to Earlier Literature . . . 31
2.5.3 Remarks on Generalized Signal Richness . . . 32
2.6 Simulations and Discussions . . . 32
2.6.1 Simulations of time domain Approaches . . . 33
2.6.2 Simulations of frequency domain Approaches . . . 34
2.6.3 Complexity Analysis . . . 35
2.6.4 Simulations for Time-varying Channels . . . 35
2.6.5 Remarks on Choosing the Optimal Parameters . . . 38
2.6.6 Noise Handling for large J . . . 38
2.7 Concluding Remarks . . . 39
2.8 Appendix: Proof of Lemmas . . . 39

3 Blind and Semi-Blind Channel Estimation in Cyclic-Prefix Systems 42

3.1 Outline . . . 44
3.2 Problem Formulation . . . 44
3.2.1 Cyclic Prefix System Overview . . . 44
3.2.2 Subspace-based Blind Channel Estimation in CP Systems . . . 46
3.2.3 Limitations . . . 49
3.3 Proposed Method . . . 50

3.3.1 The Repetition Index . . . 51
3.3.2 Necessary Condition for Persistency of Excitation . . . 58
3.3.3 Repetition Index for the Forgetting Factor . . . 59
3.3.4 Summary of the Proposed Algorithm . . . 60
3.3.5 System Complexity . . . 60
3.3.6 Equalization and Resolving the Scalar Ambiguity . . . 61
3.4 Semi-Blind Channel Estimation in OFDM Systems . . . 62
3.4.1 Problem Formulation . . . 62
3.4.2 Pure pilot-Assisted Channel Estimation . . . 64
3.4.3 Proposed Algorithm . . . 65
3.5 On The Probability That $\mathbf{U}_Q^{(J)}$ Has Full Rank . . . 66
3.6 Simulation Results and Discussions . . . 69
3.6.1 Static Channels . . . 69
3.6.2 Simulations with smaller J . . . 70
3.6.3 Time-Varying Channels . . . 74
3.6.4 Simulation Results for Semi-Blind . . . 76
3.7 Conclusions . . . 78
3.8 Appendix . . . 79
3.8.1 Proofs of Theorems . . . 79
3.8.2 Probability of $\mathbf{U}_Q^{(J)}$ having full rank for different precoders . . . 81

4 Blind Block Synchronization for Transceivers Using Redundant Precoders 83
4.1 Outline . . . 84
4.2 Problem Formulation . . . 85
4.2.1 Redundant Block Transmission Systems . . . 85
4.2.2 Blind Block Synchronization for LRP Systems . . . 87
4.3 Proposed Algorithm for ZP Systems . . . 88
4.3.1 Derivation of the Proposed Algorithm . . . 89
4.3.2 Comparison with An Earlier Algorithm . . . 92
4.4 Proposed Algorithm for CP Systems . . . 93
4.4.1 Derivation of the Proposed Algorithm . . . 93
4.4.2 Comparisons with a Previously Reported Algorithm . . . 97

4.5 Simulation Results and Discussions . . . 98
4.5.1 Simulation Results for Zero Padding Systems . . . 99
4.5.2 Simulation Results for Cyclic Prefix Systems . . . 104
4.6 Conclusions . . . 108
4.7 Appendix . . . 108

5 Performance Analysis of Blind Estimation Algorithms in ZP Systems 115
5.1 Outline . . . 116
5.2 Review of the Generalized Algorithm . . . 116
5.2.1 Problem Formulation . . . 116
5.2.2 Generalized Algorithm . . . 117
5.3 Performance Analysis in Additive Noise . . . 119
5.3.1 Cramer-Rao Bound . . . 121
5.4 Simulations . . . 122
5.5 Conclusions . . . 123
5.6 Appendix . . . 123

6 Theoretical Issues on Linear Precoders that Preserve Signal Richness 128
6.1 Outline . . . 129
6.2 Formulation and Examples . . . 130
6.2.1 Examples that Do not Preserve Richness . . . 131
6.2.2 Examples that Preserve Richness . . . 133
6.3 Main Theorem . . . 134
6.3.1 Proof of a Special Case . . . 135
6.4 Properties of Richness-Preserving Systems . . . 137
6.4.1 Cascaded Systems . . . 137
6.4.2 Enriching Systems . . . 139
6.4.3 Restriction on Output Range . . . 140
6.4.4 Proof of Theorems 3 and 4 . . . 141
6.4.5 Paraunitary and Unimodular matrices . . . 141
6.5 Strict Definition of Richness . . . 142
6.6 Proof of the Main Theorems . . . 143

6.6.1 Sketch of the Proof . . . 143
6.6.2 Proof of Sufficiency . . . 144
6.6.3 Relationship between RP and SRP Systems . . . 144
6.6.4 Lemmas for Proof of Necessity . . . 145
6.6.5 Coefficient Rank of an RP System . . . 147
6.6.6 Completion of Proof of Necessity for RP Systems . . . 149
6.6.7 Necessary Conditions for Preserving Strict Richness . . . 150
6.7 Relationship with Persistent Excitation . . . 151
6.8 Concluding Remarks and Open Issues . . . 152

7 Generalized Signal Richness Preservation Problem and Vandermonde-Form Preserving Matrices 154

7.1 Outline . . . 155
7.1.1 Notations . . . 155
7.2 Generalized Signal Richness . . . 156
7.2.1 Definition of Generalized Signal Richness . . . 156
7.2.2 Properties of $(1/Q)$-richness . . . 158
7.2.3 Vandermonde Form Vectors and Generalized Zero Location . . . 160
7.3 Preserving Generalized Signal Richness . . . 163
7.3.1 Problem Statement . . . 163
7.3.2 The Special Case When $Q = M - 1$ . . . 164
7.4 Vandermonde-form preserving Matrices . . . 165
7.4.1 Representation of Vandermonde-form preserving Matrices . . . 165
7.4.2 Zero-Location Transformation . . . 168
7.4.3 Other Properties of VFP matrices . . . 171
7.4.4 VFP matrices as a Linear Precoder . . . 173
7.5 Main Theorem . . . 173
7.5.1 Necessary Conditions . . . 173
7.5.2 Hankel-form Preservation . . . 174
7.5.3 Main Theorem . . . 175
7.6 Other Relevant Issues on $(1/Q)$-richness . . . 176
7.6.1 Relationship between degree of richness and rank of a signal . . . 176

7.6.2 Distribution of Degree of Non-richness 179
7.7 Concluding Remarks 180
7.8 Appendix: Proof of Theorems 180

8 Conclusions **187**

Bibliography **190**

List of Figures

1.1 Baseband representation of a digital communication channel. (a) Analog model with a bandlimited channel impulse response $h_c(t)$; (b) Equivalent digital model with channel transfer function $H(z)$. 3

1.2 Single-input-multiple-output channel model. (a) Oversampling of a SISO channel; (b) A SIMO channel; (c) Equivalent system with an upsampled source signal. 5

1.3 Schematic of subspace based system identification. 6

1.4 Illustration of a zero-padding precoder and a cyclic-prefixing precoder. 7

1.5 A block transmission system with a linear redundant precoder $\mathbf{R}(z)$. 8

2.1 Communication System with Redundant Filter Bank Precoders. 17

2.2 The zero-padding system with precoder $\mathbf{R}_1$. 18

2.3 Q-repetition and shifting operation. 24

2.4 Receiver structure for frequency domain approach. 26

2.5 Normalized least squared channel error estimation. 32

2.6 Bit error rate performance of the blind algorithm. 33

2.7 Normalized least squared channel error estimation. 34

2.8 Normalized Channel MSE performance for a time-varying channel. 37

2.9 Bit error rate performance for a time-varying channel. 37

3.1 A typical cyclic prefix system. 44

3.2 The transceiver system equipped with a method to resolve scale-factor ambiguity. . . 61

3.3 A CP-based orthogonal frequency division multiplexing (OFDM) system. 63

3.4 Illustration of the approach of the proposed semi-blind estimation algorithm. 64

3.5 The probability of $\mathbf{U}_Q^{(J)}$ having full rank in SC-CP systems. 67

3.6 The probability of $\mathbf{U}_Q^{(J)}$ having full rank in OFDM systems. 68

3.7 Normalized mean squared error of channel estimation for static channels with the QPSK constellation in SC-CP systems. 71
3.8 Bit error rate performance for static channels with the QPSK constellation in SC-CP systems. 71
3.9 Bit error rate performance for static channels with the 16-QAM constellation in SC-CP systems. 71
3.10 Bit error rate performance for static channels with the QPSK constellation in OFDM systems. 72
3.11 Bit error rate performance for static channels with the QPSK constellation in SC-CP systems when J is small. 73
3.12 Bit error rate performance for blind estimation systems when the Doppler frequency is 5 Hz (5.4 km/hr). 73
3.13 Bit error rate performance for blind estimation systems when the Doppler frequency is 50 Hz (54 km/hr). 73
3.14 Pilot positions for $K = 20$ (left) and $K = 15$ (right). 76
3.15 Comparison of pilot-based and semi-blind methods in channel estimation mean square error performance. 77
3.16 Comparison of pilot-based and semi-blind methods in bit error rate performance. . . 78

4.1 Block transmission systems using linear redundant precoders. 85
4.2 Illustration of blind block synchronization problem in ZP and CP systems. 85
4.3 Function $\lambda(d)$ v.s. time mismatch d for a channel with zeros at $(0.8, -0.8, 0.5j, -0.5j)$ in absence of noise. 100
4.4 Blind block synchronization error rate performance for a channel with zeros at $(0.8, -0.8, 0.5j, -0.5j)$ when $J = 20$ in ZP systems. 100
4.5 Function $\lambda(d)$ v.s. time mismatch d for a channel with zeros at $(1.2, -0.9, 0.7j, -0.7j)$ in absence of noise when $J = 20$. 101
4.6 Blind block synchronization error rate performance for a channel with zeros at $(1.2, -0.9, 0.7j, -0.7j)$ when $J = 20$ in ZP systems. 101
4.7 Blind block synchronization error rate performance for a Rayleigh random channel with $J = 20$ in ZP systems. 102

4.8 Blind block synchronization error rate performance for a Rayleigh random channel with small J in ZP systems. 102
4.9 Blind block synchronization error rate performance for a channel with zeros at $(0.8, -0.8, 0.5j)$ when $J = 40$ in CP systems. 104
4.10 Blind block synchronization error rate performance for a channel with zeros at $(1.2, -0.9, 0.7j)$ when $J = 40$ in CP systems. 105
4.11 Blind block synchronization error rate performance for a third-order Rayleigh random channel with $J = 40$ in CP systems. 105
4.12 Blind block synchronization error rate performance for a fourth-order Rayleigh random channel with $J = 40$ in CP systems. 106
4.13 Blind block synchronization error rate performance for a third-order Rayleigh random channel in CP systems when J is small. 106

5.1 Channel estimation MSE versus SNR obtained by simulations, theoretical values in (5.7), and CRB in (5.11) with 16 blocks. 123
5.2 Channel estimation MSE versus SNR obtained by simulations, theoretical values in (5.7), and CRB in (5.11) with 5 blocks. 124

7.1 A multi-input multi-output LTI system. 163
7.2 Distribution of degree of non-richness of signals whose entries are from BPSK constellation. 180
7.3 Distribution of degree of non-richness of signals whose entries are from QPSK constellation. 181
7.4 Distribution of degree of non-richness of signals whose entries are from 16-QAM constellation. 182

List of Tables

2.1 Coefficients for the Time-Varying Channel. 36

3.1 Power delay profile of the channel model used in Section 3.6 69

5.1 Comparison of Eq. (33) in [2] and Eq. (5.11); the data length per block is $M = 12$ . . . 125

7.1 Relationship between degree of non-richness and rank of $\mathbf{s}(n)$. Notice ambiguity of finite values for $M \geq 5$. See text. 178

Chapter 1

Introduction

In digital communication systems, channel equalization and channel estimation are essential to successful data transmission. While channel equalization and estimation are usually done by pilot-assisted-based methods (i.e., inserting pilot samples that are known to the receiver into the transmitted data sequence), *blind* methods have also been developed (see [8] and references therein) which do not require use of pilot samples and possess desirable advantages such as a better bandwidth efficiency. Although many blind methods in various types of communication systems have been developed since the early 80s, they generally suffer from several drawbacks which prevent them from widespread use.

As block transmission systems using redundant precoding, such as orthogonal frequency division multiplexing (OFDM) systems, become increasingly popular, research on blind channel estimation has also been shifted to these types of systems. Recent work on block transmission systems with redundant precoding [45] has shown that the redundancy, originally introduced for the purpose of eliminating interblock interference (IBI), is also beneficial to blind channel estimation. Many blind methods have been developed for block transmission with different types of redundant precoding and prove to be free from several problems present in conventional blind channel estimation [30]. These new algorithms, however, still have several problems such as slow convergence speed (i.e., requirement of a large amount of received data), which makes them less applicable in an environment where the channel status is fast-varying (e.g., in a wireless link). Other problems include computational complexity, constraints on data constellations, etc.

This thesis presents a contribution to further reduction of convergence time for blind channel estimation using redundant precoding. Some other important problems that arise from blind channel estimation problem, such as the blind block synchronization problem, the semi-blind channel

estimation, and the signal richness preservation problem, will also be considered in this thesis. In this introductory chapter, we give an overview of the basic concepts and a brief history of blind channel estimation. Every attempt is made to make the present text as self-contained as possible, and the introduction is meant to primarily serve this purpose. Due to the large volume of the blind channel estimation literature, the summary here is only directly related to the thesis topics and is by no means a complete treatment of all past work. The readers interested in more comprehensive treatments are referred to [8, 11].

1.1 Brief History of Blind Channel Estimation

Figure 1.1 depicts the baseband representation of a digital communication system. The communication channel is characterized as a linear time invariant (LTI) system which has a finite impulse response (FIR) due to finite delay spread of the channel. The impulse response $h_c(t)$ is a cascade of the pulse shaping filter in the transmitter, the physical multipath fading channel, and the receive filter. Assume the symbol interval of the input signal is T. The output signal can be written as

$$x(t) = \sum_n s(n)h_c(t - nT) + w(t).$$

When the output signal is sampled at the baud rate (i.e., at the rate $1/T$), the system can be simplified as in Figure 1.1-(b), where the equivalent channel, $H(z)$, is a discrete LTI system. The received signal $x(n)$ is a noise corrupted version of the convolution of the input signal $s(n)$ and the channel impulse response $h_c(t)$. A successful communication aims at recovering the transmitted symbols $s(n)$ at the receiver. A large number of methods have been developed to equalize, or deconvolve, the effect of $H(z)$ assuming the channel transfer function $H(z)$ is known. Therefore, channel estimation, i.e., obtaining an estimate of $H(z)$, is a critical problem. A straightforward way of channel estimation is to insert in the transmitted signal pilot samples that are known to the receiver, and to compare the pilot samples with corresponding received samples. Blind channel estimation, however, seeks to estimate the channel $H(z)$ without explicit knowledge of $s(n)$. Mathematically, it is similar to blind deconvolution problem in control or image processing literature.

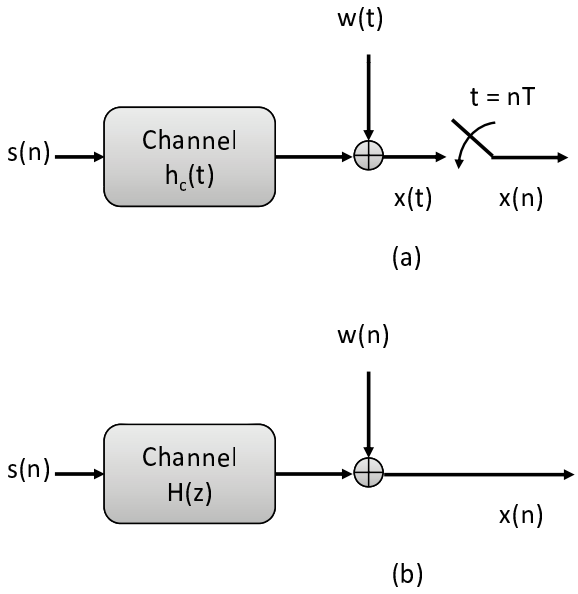

Figure 1.1: Baseband representation of a digital communication channel. (a) Analog model with a bandlimited channel impulse response $h_c(t)$; (b) Equivalent digital model with channel transfer function $H(z)$.

1.1.1 Early Developments of Blind Estimation in SISO Systems

Since the late 70s, many blind equalization algorithms have been proposed [40, 12, 3, 47]. Most of these early developments of blind methods are based on adaptive algorithms. They generally share the following features. First of all, although the explicit knowledge of $s(n)$ is unknown, the constellation used by $s(n)$ must be known and is usually quadrature amplitude modulation (QAM), pulse amplitude modulation (PAM), or phase shift keying (PSK). A special class of these algorithms is the constant modulus algorithm (CMA) [12], which works by setting constant modulus constraints on samples equalized by adaptive filters. Also, higher-than-second-order-statistics (HOS) of the received stream is required in these algorithms. The requirement for HOS may be explained as follows. Evaluating the spectral density function of the output signal, we have

$$S_{xx}(z) = |H(z)|^2 S_{ss}(z) + S_{ww}(z),$$

where $S_{xx}(z) \triangleq \sum_m E\left[x(n)x^*(n-m)\right] z^{-m}$, $S_{ss}(z) \triangleq \sum_m E\left[s(n)s^*(n-m)\right] z^{-m}$, and $S_{ww}(z) \triangleq \sum_m E\left[x(n)x^*(n-m)\right] z^{-m}$. Assume the input spectral density function $S_{ss}(z)$ is known (usually assumed white). Then the amplitude of the channel can be identified but the phase information of

$H(z)$ is missing. In order to obtain the full information of the channel, higher-than-second-order statistics (HOS) of $x(n)$ is employed in many blind algorithms (e.g., 4th order) [47].

These early algorithms in general share the following common drawbacks. First of all, the convergence of the adaptive algorithms depends on the initial values of the equalizer parameters, and the solution is subject to local convergence. Secondly, due to the use of HOS, the required amount of received data is usually very large, and this makes the algorithms have slow convergence time and inapplicable in time-varying environments. Finally, the computational complexity is high for HOS of received data. These drawbacks limit their applicability in practical situations.

1.1.2 Using Second Order Statistics in SIMO Systems

It is shown above that second order statistics (SOS) of received samples alone cannot give the full information of a frequency selective channel. However, since algorithms based on second order statistics converge much faster than those using higher-order statistics, researchers have searched for newer methods. The work proposed by Tong *et al.* in 1991 which first used only SOS of the received samples for blind channel estimation in the context of single-input-multiple-output (SIMO) systems is widely considered as a major breakthrough. As shown in Figure 1.2, a set of virtual multiple channels can be achieved by oversampling at the receiver in a physically SISO system. The work in [64] suggests SOS alone is sufficient to estimate channel coefficients blindly as long as the oversampled channel satisfies a channel diversity condition. Following this, considerable research has been done to study blind channel estimation in SIMO systems using SOS [26, 27, 30, 46, 74]. Among these, a representative is a subspace based algorithm proposed by Moulines *et al.* in [30], which explicitly exploits the signal and noise subspace separation and also the special structure of the channel matrix. First used in the famous multiple signal classification (MUSIC) algorithm [42], the basic idea of subspace-based methods are illustrated in Figure 1.3 and are elaborated below.

The first principle of subspace-based algorithms is that the dimension of the observation space, q, must be strictly larger than that of the signal space, p. The matrix $\mathbf{H}_{\boldsymbol{\theta}}$ has a known structure in terms of an unknown parameter vector $\boldsymbol{\theta}$. By evaluating the autocorrelation matrix of $\mathbf{y}(n)$ and an eigen-decomposition of $\mathbf{R}_{\mathbf{yy}}$, the basis vectors of signal space and noise space can be found. Finally, using the fact that the noise space is orthogonal to the space spanned by all columns of the matrix $\mathbf{H}_{\boldsymbol{\theta}}$, the parameter vector $\boldsymbol{\theta}$ can be found. In the case of blind estimation in SIMO channels, the parameter vector $\boldsymbol{\theta}$ contains coefficients of the impulse response of all virtual channels, and

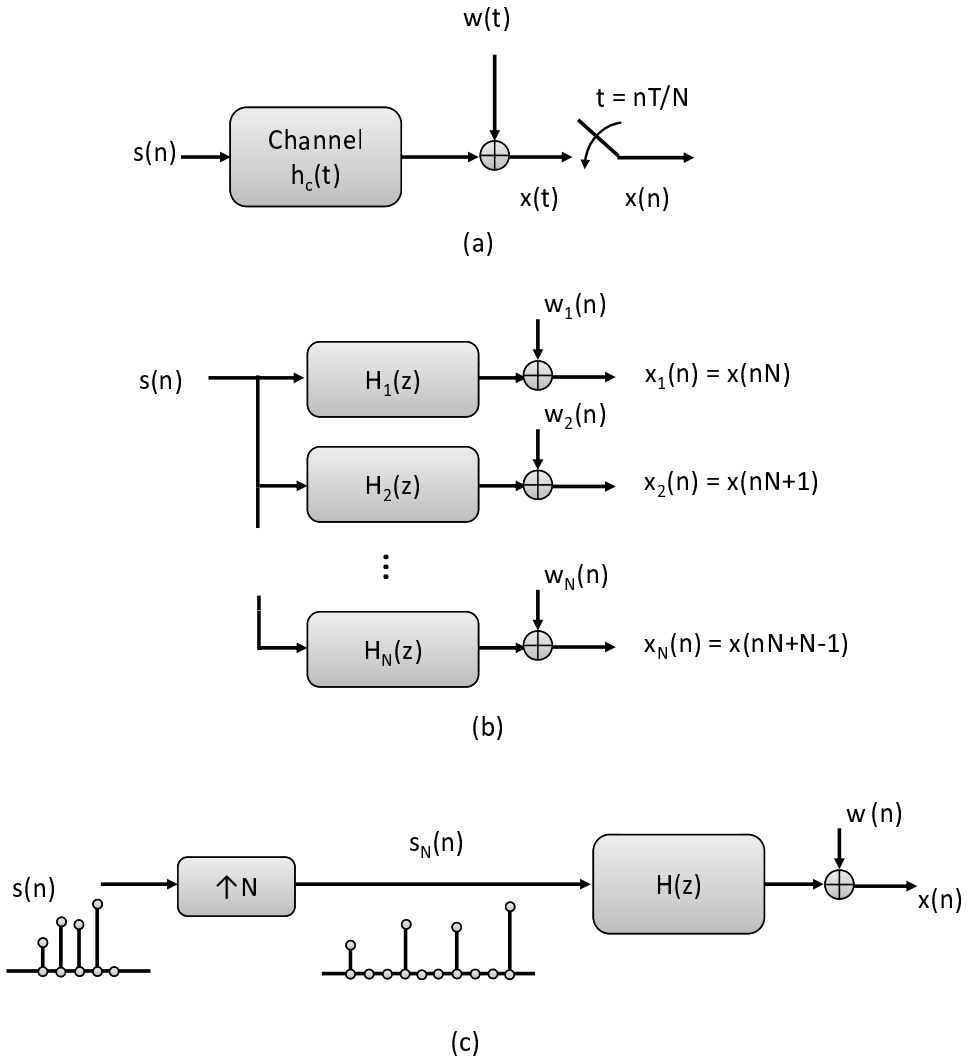

Figure 1.2: Single-input-multiple-output channel model. (a) Oversampling of a SISO channel; (b) A SIMO channel; (c) Equivalent system with an upsampled source signal.

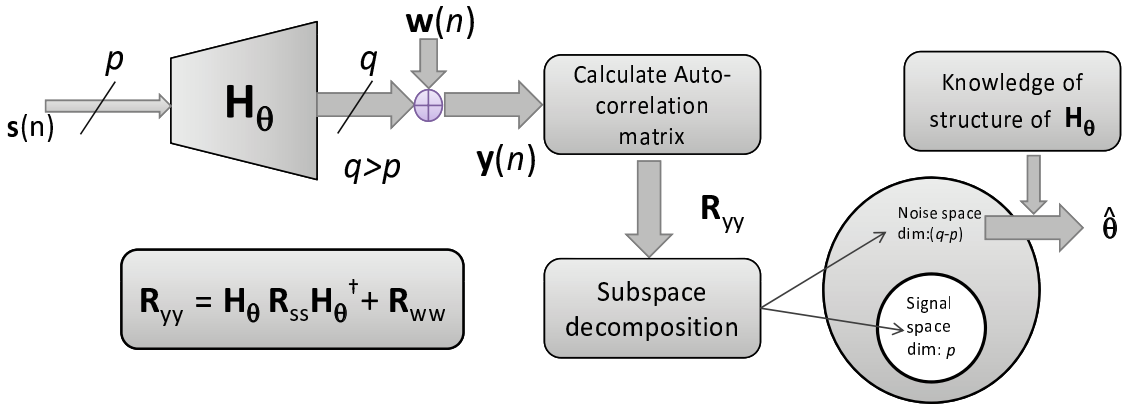

Figure 1.3: Schematic of subspace based system identification.

the matrix $\mathbf{H}_{\boldsymbol{\theta}}$ has a special block Toeplitz structure [30]. Subspace-based algorithms have since played an important role and are still widely used in the development of blind channel estimation algorithms nowadays.

There are two problems with blind methods in SIMO systems which prevent them from practical applications. First of all, most of these methods are very sensitive to channel order overestimation: they require the maximum channel order among the multiple channels to be exactly known. This information, however, is usually unavailable in most situations. The second problem is the bandwidth expansion caused by oversampling at the receiver. As illustrated in Figure 1.2-(c), the SIMO channel is equivalent to a SISO channel where the source signal is upsampled by a factor of N [9].

1.2 Blind Channel Estimation Using Redundant Precoding

In the previous section we learned that blind channel estimation using SOS alone is possible only when some redundancy is introduced in the transmitter. The virtual SIMO systems implemented by oversampling the received signal are one way to introduce redundancy. There are, however, different ways to introduce redundancy. In recent years, block transmission systems using linear redundant precoders (LRP) have become popular due to their capability to facilitate block channel equalization of frequency-selective channels. The redundant structure is also found to be beneficial to blind channel estimation [10]. Blind estimation with LRP has a small bandwidth expansion factor

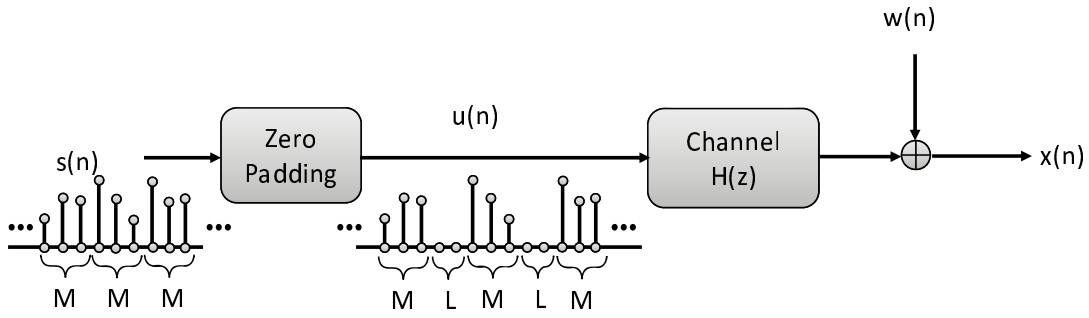

Figure 1.4: Illustration of a zero-padding precoder and a cyclic-prefixing precoder.

(asymptotically unity) and is robust to channel order overestimation. So blind methods developed in LRP systems are in general superior to those in SIMO systems. In this section, we will first review block transmission systems with linear redundant precoders and then review blind channel estimation algorithms with redundant precoding.

1.2.1 Block Transmission Systems With Linear Redundant Precoders

To illustrate the idea of linear redundant precoding, we first explain a special case called "zero-padding." As shown in Figure 1.4, the source sequence $s(n)$ is divided into blocks of size M. A zero block of length L is inserted after each block. Suppose $P = M + L$. Then mathematically,

$$u(nP+k) = \begin{cases} s(nM+k) & \text{if } 0 \le k \le M-1 \\ 0 & \text{if } M \le k \le P-1 \end{cases}.$$

The zero-padding precoder introduces bandwidth expansion by a factor $(M+L)/M$. While the redundancy length L is usually chosen as an integer comparable to the channel order, the block size M can be chosen as any positive integer. When M is chosen as a large integer, the bandwidth expansion factor is asymptotically unity. The general form of a block transmission system with linear redundant precoder is shown in Figure 1.5. The source sequence $s(n)$ is blocked into vectors $\mathbf{s}(n)$ of size M:

$$\mathbf{s}(n) = \begin{bmatrix} s(nM) & s(nM+1) & \cdots & s(nM+M-1) \end{bmatrix}^T.$$

The vectors $\mathbf{s}(n)$ go through a linear precoder characterized as a $P \times M$ polynomial matrix in z^{-1}, $\mathbf{R}(z) = \sum_{k=0}^{K} \mathbf{R}_k z^{-k}$, resulting in a P-vector $\mathbf{u}(n) = \sum_{k=0}^{K} \mathbf{R}_k \mathbf{s}(n-k)$. The vectors $\mathbf{u}(n)$ are

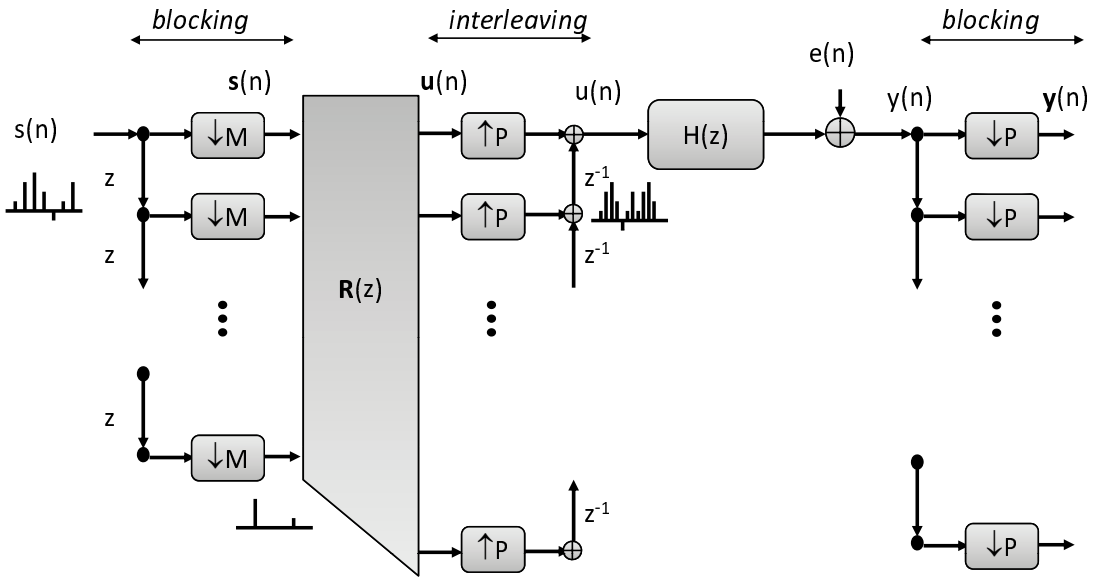

Figure 1.5: A block transmission system with a linear redundant precoder $\mathbf{R}(z)$.

interleaved into the precoded sequence $u(n)$ which is sent over the channel $H(z)$.

The zero-padding precoder illustrated in Figure 1.4 is a special case where $\mathbf{R}(z)$ is chosen as

$$\mathbf{R}(z) = \begin{bmatrix} \mathbf{I}_M \\ \mathbf{0} \end{bmatrix},$$

where $\mathbf{I}_M$ is the $M \times M$ identity matrix. A more general zero-padding precoder has transfer function of the form

$$\mathbf{R}(z) = \begin{bmatrix} \mathbf{R}_1(z) \\ \mathbf{0} \end{bmatrix},$$

where $\mathbf{R}_1(z)$ is an $M \times M$ polynomial matrix in z^{-1}.

Another important class of linear redundant precoders is cyclic prefix (CP) precoders. A CP precoder has a transfer function

$$\mathbf{R}(z) = \begin{bmatrix} \mathbf{R}_{cp}(z) \\ \mathbf{R}_2(z) \end{bmatrix},$$

where $\mathbf{R}_2(z)$ is an $M \times M$ polynomial matrix in z^{-1} and $\mathbf{R}_{cp}(z)$ is an $L \times M$ matrix whose elements are copied from the last L rows of $\mathbf{R}_2(z)$. This arrangement inserts a cyclic prefix of length L in front of a data block of size M. The popular orthogonal frequency division multiplexing (OFDM) systems are a special case of CP systems where $\mathbf{R}_2(z)$ is chosen as the inverse DFT matrix.

The linear redundant precoders were proposed in an attempt to eliminate interblock interference (IBI) of the received blocks caused by the frequency selective channel $H(z)$ [73]. If the channel order of $H(z)$ is upper-bounded by L, the received blocks will be free of interblock interference and channel equalization can be performed block-by-block without worries of interblock error propagation. Noise amplification can be avoided in the channel equalization phase even if the channel has zeros outside the unit circle. It turns out the redundancy introduced by LRPs are also helpful in blind channel estimation, as discussed below.

1.2.2 Blind Channel Estimation in LRP Systems: Subspace v.s. Finite Alphabet Algorithms

The blind channel estimation algorithms in LRP systems can be roughly divided into two categories: finite-alphabet-based algorithms and non-finite-alphabet algorithms. Algorithms that exploit knowledge of the finite-alphabet of the source data generally have a shorter converge time but may be computationally exhausting when the constellation size is large [76, 6]. Most non-finite-alphabet-based algorithms exploit (second order) statistics of the received data [15, 35]. These methods naturally require a longer convergence time than finite alphabet counterparts before an accurate channel estimate can be obtained due to use of statistics. Another important category of non-finite-alphabet-based algorithms uses subspace decomposition [5, 21, 45], and they can even be implemented deterministically [45, 36, 5, 21, 32].

Subspace-based algorithms can be used in any kind of constellation, but require a longer convergence time. We will discuss subspace based channel estimation algorithms for ZP systems and CP systems here. In ZP systems, the first subspace-based blind channel estimation algorithm was proposed by Scaglione *et al.* [45]. Subspace algorithms in CP systems require more sophisticated designs [5, 21, 32]. These methods all need the persistency of excitation property of the input signal (i.e., signal richness) to render the data covariance matrix to have full rank. This requirement demands the receiver to collect at least a number of blocks equal to the block size for one channel estimate and thus makes the approach less applicable when the channel is fast-varying.

In summary, the basic trade-off between finite-alphabet methods and subspace-based methods is that finite-alphabet methods have a faster convergence speed, while subspace-based methods can be operated in any constellations without any increase of computational complexity. It seemed difficult to have both desirable properties at the same time. However, it was more recently pointed

out by Manton *et al.* [28] that a blind estimation without knowledge of finite alphabet in ZP systems is possible with only *two* received blocks. An algorithm based on viewing the channel estimation problem as finding the greatest common divisors (GCD) of polynomials representing received blocks was proposed in [36].

Although many blind algorithms in LRP systems have been developed, they mostly tend to suffer from several common drawbacks such as slow convergence speed, high complexity, poorer performance, etc., as opposed to pilot-assisted methods. In this thesis, we propose new algorithms and theories that suggest blind algorithms can in general be developed with small amount of received data, satisfactory system performance, and reasonable complexity.

1.3 Outline of the thesis

1.3.1 Scope of the thesis

There are two major parts in this thesis. In the first part (Chapters 2, 3, and 4), new algorithms for blind channel estimation using redundant precoding as well as other related problems, including blind block synchronization and semi-blind channel estimation, are proposed. The second part of the thesis (Chapters 5, 6, and 7) deals with theoretical aspects of the blind channel estimation problems, including performance analysis of the blind algorithms, and the signal richness preservation problem. In this section we will briefly introduce the scope of each chapter.

1.3.2 Generalized Algorithms for Blind Channel Estimation in ZP Systems (Chapter 2)

The material in Chapters 2 and 3 presents new algorithms for blind channel estimation in LRP systems. Chapter 2 studies the blind channel estimation algorithm in ZP systems, i.e., the precoder $\mathbf{R}(z)$ has a form of $\mathbf{R}(z) = \left[\begin{array}{cc} \mathbf{R}_1(z)^T & \mathbf{0}^T \end{array} \right]^T$. The proposed algorithm is a generalization of two algorithms previously reported in [45, 36]. In [45], the first deterministic blind method in ZP systems was proposed by Scaglione *et al.* which we will call the SGB method. The SGB method assumes the input sequence is *rich*. That is, the matrix composed of finite source blocks achieves full rank. This implies the requirement that the receiver has to accumulate at least M blocks before channel coefficients can be identified. The method reported in [36] by Manton *et al.*, which we will call the MNP method, is based on viewing the channel identification problem as finding the greatest

common divisor (GCD) of polynomials representing received blocks. The MNP algorithm requires only two blocks to work but has much more computational complexity.

Although the MNP method is based on the idea of the greatest common divisor of polynomials, the mathematical formulation of its implementation still involves subspace decomposition (in a space of a larger dimension). This fact puts the MNP method and the SGB method into the same category, and we can generalize them using a concept called *repetition index*. In Chapter 2, we will propose a generalized algorithm of which the SGB algorithm proposed in [45] and the MNP algorithm in [36] are both special cases. The idea of repetition index is to repeatedly use each received block. In the conventional subspace method, the receiver needs to accumulate M blocks in order to achieve sufficient rank. By repeated use of each received block by a factor of Q, the number of blocks needed to achieve the required rank can be significantly reduced and is roughly inversely proportional to the repetition index Q. The MNP method essentially uses a large repetition index ($Q = P$) and requires only two received blocks. The use of a large Q also increases the receiver side computational complexity. By carefully choosing parameters, the system performance and computational complexity can be jointly optimized.

1.3.3 Blind and Semi-Blind Channel Estimation in Cyclic Prefix Systems (Chapter 3)

In Chapter 3 we study the blind channel estimation problem in cyclic prefix systems. As more and more new communication standards adopt cyclic-prefix based systems such as orthogonal frequency division multiplexing (OFDM) and signal carrier cyclic prefix (SC-CP) systems, the importance of studying CP systems is increasing. Unlike in ZP systems, some parts of a received block in a CP system contain interblock interference (IBI). This fact makes the formulation of a blind algorithm more difficult than in ZP systems. In [5], [31], and [32], Muquet *et al.* and Cai *et al.* independently developed a subspace-based algorithm which requires at least $2M + 1$ received blocks. This requirement of minimum number of received blocks again limits the application of these algorithms in a fast-varying channel environment. The idea of repetition index which first arises in ZP systems can also be applied in CP systems. In Chapter 3, a generalization to algorithms reported in [31, 5, 32] is proposed using the idea of repetition index, whose value is unity for these previously reported methods. When the repetition index is chosen to be greater than unity, the number of received blocks needed will be significantly reduced. Theoretical limit allows

the proposed method to perform blind identification using only three received blocks in absence of noise. We also study a semi-blind channel estimation algorithm in OFDM systems which is a special case of CP systems. The proposed semi-blind estimation algorithm is a combination of the blind channel estimation method and a pure pilot-assisted method. Simulation results show that, under the same number of pilot samples, the semi-blind algorithm has a clear improvement over the pure pilot-assisted method.

1.3.4 New Algorithms for Blind Block Synchronization In LRP Systems (Chapter 4)

Many algorithms for blind channel estimation in LRP systems, including those proposed in Chapters 2 and 3, are based on the assumption that block synchronization is perfect, i.e., block boundaries of the received streams are perfectly known to the receiver. In practical applications, however, this assumption is usually not true since no extra known samples are transmitted. The problem of blind block synchronization is therefore important. However, up to date, this problem has not yet been given as much attention as blind channel estimation has. Chapter 4 studies the blind block synchronization problem in both ZP and CP systems. These algorithms exploit the presence of rank deficiency in the matrix composed of received blocks when the block synchronization is perfect. The formulated matrices, when block synchronization is not correct, have a higher rank instead. In order to make the matrices have sufficiently large rank, a large amount of received data is required for both algorithms. The algorithms proposed in Chapter 4 use the concept of repetition index and guarantee correct block synchronization in absence of noise using only two and three received blocks in ZP and CP systems, respectively, when the repetition index is chosen appropriately.

1.3.5 Performance Analysis of Blind Estimation Algorithms in ZP Systems (Chapter 5)

The second part of the thesis will deal with theoretical issues. The material addressed in Chapters 5, 6, and 7 will be related to blind channel estimation in ZP systems. In Chapter 5 we analyze the performance of the blind channel estimation algorithm proposed in Chapter 2. As we have seen in the simulation results reported in Chapter 2, with repetition index and the number of received blocks adjusted appropriately, the performance of the generalized algorithm is superior to those of the SGB and MNP algorithms. The goal here is to quantify this performance improvement the-

oretically. We study the channel estimation error (MSE) in the algorithm of [49] and compare it with the corresponding Cramer-Rao bound. We will derive in this chapter performance analysis of the generalized algorithm proposed in Chapter 2. When the number of received blocks is small, however, there is an obvious gap between the performance of the SGB algorithm and the corrected CRB given in [58] when a small number of received blocks are available. Both theory and simulation results suggest that the performance of the generalized algorithm is usually closer to the CRB when the repetition index is larger but the performance does not achieve the CRB for any repetition index.

1.3.6 Theoretical Issues on Signal Richness Preservation for Blind Estimation (Chapters 6 and 7)

In Chapters 6 and 7, we study in detail theoretical issues on signal richness in ZP systems, specifically the richness preservation problem. The richness property of input signals is essential to blind channel estimation algorithms we discussed in Chapter 2. Since the property of signal richness may be altered by a linear precoder, we are interested in finding the conditions on which a this linear precoder will "preserve" the property of signal richness. For different blind channel estimation algorithms, the definition of signal richness may be different. Conventionally, signal richness can be defined as follows. A signal of M-vectors $\mathbf{x}(n), n \geq 0$, is said to be *rich* or *rank rich* if the matrix

$$\left[\begin{array}{cccc} \mathbf{x}(0) & \mathbf{x}(1) & \cdots & \mathbf{x}(K_x) \end{array} \right]$$

has rank M for sufficiently large K_x. This definition of signal richness is required for input signals used in the SGB method [45] (see Sec. 1.3.2). We say a ZP precoder $\mathbf{R}(z)$ is richness-preserving if for any rich input signal $\mathbf{x}(n)$, the output of $\mathbf{R}(z)$ is also rich. The mathematical problem on richness-preserving precoders, rather than the application itself, is the focus of Chapter 6. It turns out that there exist only two major types of systems which preserve richness.

In Chapter 7, we extend the signal richness preservation problem to different definitions of signal richness. In the generalized blind algorithm for ZP systems proposed in Chapter 2, the requirement of signal richness is relaxed, and the concept of "generalized signal richness" is established. The conditions on the precoders which preserve the generalized signal richness are different from those which preserve conventional signal richness. The necessary and sufficient conditions on memoryless precoders which preserve generalized signal richness are studied in Chapter 7. In

finding the solution of the problem, a new class of invertible matrices, namely the *Vandermonde-form preserving (VFP) matrices*, is introduced. Several interesting properties of the VFP matrices are also studied.

1.4 Notations

The notations used throughout this thesis are defined as follows. Boldfaced lower case letters represent column vectors. Boldfaced upper case letters and calligraphic upper case letters are reserved for matrices. Superscripts *, ^{T}, and † as in a^*, $\mathbf{A}^T$, and $\mathbf{A}^\dagger$ denote the conjugate, transpose, and transpose-conjugate operations, respectively. $\mathbf{A}^\#$ represents the pseudo-inverse of $\mathbf{A}$. $\widetilde{\mathbf{H}}(z)$ represents $\mathbf{H}^\dagger(1/z^*)$. $[\mathbf{v}]_i$ denotes the ith element of vector $\mathbf{v}$, $[\mathbf{A}]_i$ denotes the ith row of matrix $\mathbf{A}$, and $[\mathbf{A}]_{ij}$ denotes the entry at the ith row and the jth column of matrix $\mathbf{A}$. Column and row indices of all vectors and matrices begin at one. $\mathbf{e}_{i,M}$ denotes the ith column of the identity matrix $\mathbf{I}_M$ and is often abbreviated as $\mathbf{e}_i$ when there is no ambiguity about the value of M. All the vectors and matrices in this paper are complex-valued. The notation W_M denotes $e^{-j2\pi/M}$, and $\mathbf{W}_M$ is the $M \times M$ normalized DFT matrix whose kl-th entry is $W_M^{(k-1)(l-1)}/\sqrt{M}$. Column and row indices of all matrices and vectors begin at one. $\mathbf{A}_{k,l}$ is the entry at the kth row and the lth column of $\mathbf{A}$. $\mathbf{I}_n$ is the $n \times n$ identity matrix, and $\mathbf{0}_{m\times n}$ is the $m \times n$ zero matrix. In figures, "$\uparrow N$" and "$\downarrow N$" denote the signal downsampler and upsampler, respectively [67]. The notation vec$(\mathbf{A})$ represents the column vector constructed by concatenating columns of $\mathbf{A}$. $\mathbf{A} \otimes \mathbf{B}$ denotes the Kronecker product[17] of the matrices $\mathbf{A}$ and $\mathbf{B}$.

A matrix $\mathbf{T}$ is said to be a *Toeplitz matrix* if $\mathbf{T}$ has constant values along diagonals, i.e., $[\mathbf{T}]_{ij} = [\mathbf{T}]_{i+k,j+k}$ for all i, j, k such that the indices of $\mathbf{T}$ in the above equation are within the size of $\mathbf{T}$. A matrix $\mathbf{H}$ is said to be a *Hankel matrix* if $\mathbf{H}$ has constant values along all skew diagonals, i.e., $[\mathbf{H}]_{ij} = [\mathbf{H}]_{i+k,j-k}$ for all i, j, k such that the indices of $\mathbf{H}$ in the above equation are within the size of $\mathbf{H}$. Notations for commonly used matrix structures in this paper are presented below. If $\mathbf{v} = \begin{bmatrix} v_1 & v_2 & \cdots & v_m \end{bmatrix}^T$ is an $m \times 1$ vector, we use $\mathcal{T}_n(\mathbf{v})$ to denote the $(m + n - 1) \times n$ full-

banded Toeplitz matrix

$$\mathcal{T}_n(\mathbf{v}) = \begin{bmatrix} v_1 & 0 & \cdots & 0 \\ v_2 & v_1 & \ddots & \vdots \\ \vdots & v_2 & \ddots & 0 \\ v_m & \vdots & \ddots & v_1 \\ 0 & v_m & & v_2 \\ \vdots & \ddots & \ddots & \vdots \\ 0 & \cdots & 0 & v_m \end{bmatrix} \tag{1.1}$$

and $\mathcal{K}_l(\mathbf{v})$ to denote the $l \times (m-l+1)$ Hankel matrix

$$\mathcal{K}_l(\mathbf{v}) = \begin{bmatrix} v_1 & v_2 & v_3 & \cdots & v_{m-l+1} \\ v_2 & v_3 & \iddots & \iddots & \vdots \\ \vdots & \iddots & \iddots & \iddots & v_{m-1} \\ v_l & \cdots & \cdots & v_{m-1} & v_m \end{bmatrix}. \tag{1.2}$$

Due to the special property of cyclic prefixes, we will use the following notation extensively in this paper. Suppose $\mathbf{y}$ is an $m \times 1$ column vector $\mathbf{y} = \begin{bmatrix} y_1 & y_2 \cdots & y_m \end{bmatrix}^T$. Then, the notation $[\mathbf{y}]_{a:b}$ denotes the $(b-a+1) \times 1$ vector

$$[\mathbf{y}]_{a:b} = \begin{bmatrix} y_a & y_{a+1} & \cdots & y_b \end{bmatrix}^T$$

if $1 \leq a \leq b \leq m$. An extension of this definition to any arbitrary pair of integers a and b satisfying $a \leq b$ is made by defining y_k as $y_{(k-1 \bmod m)+1}$ for any $k > m$ or $k < 1$. For example, if $\mathbf{y} = \begin{bmatrix} y_1 & y_2 & y_3 \end{bmatrix}^T$, then $[\mathbf{y}]_{-1:7}$ denotes the vector $\begin{bmatrix} y_2 & y_3 & y_1 & y_2 & y_3 & y_1 & y_2 & y_3 & y_1 \end{bmatrix}^T$. If $a > b$, then $[\mathbf{y}]_{a:b}$ denotes an empty vector.

Chapter 2

Generalized Algorithms for Blind Channel Estimation in Zero-Padding Systems

In this chapter, we study the problem of blind channel estimation in zero-padding (ZP) systems. As shown in Chapter 1, redundancy introduced at the transmitter facilitates blind identifiability of channel coefficients using only second order statistics (SOS) of received samples. The problem of blind channel estimation in ZP systems was first studied in [45]. By exploiting the padded zeros between data blocks, Scaglione *et al.* proposed a subspace based method, which we will call the SGB method. The SGB method not only works with SOS of received samples, but can also be implemented using deterministic received data, as long as the source signal is *rich* or *rank rich*. That is, the matrix composed of finite source blocks achieves full rank. The SGB method is robust to channel order overestimation. Furthermore, the bandwidth expansion factor is asymptotically unity when the block size goes to infinity. These two advantages make the SGB method superior to other blind channel estimation algorithms in virtual SIMO systems.

However, the signal richness assumption implies the number of received blocks should be at least the size of a data block. This prevents the algorithm from identifying channel coefficients accurately when the channel is fast-varying, especially when the block size is large. More recently, Manton *et al.* pointed out that the channel could be identifiable with only two received blocks [28]. An algorithm based on viewing the channel identification problem as finding the greatest common divisor (GCD) of polynomials was proposed in [36], which we will call the MNP method. This greatly reduces the number of received blocks needed for channel estimation. Although the MNP method takes a completely different approach from the SGB method, the implementation of

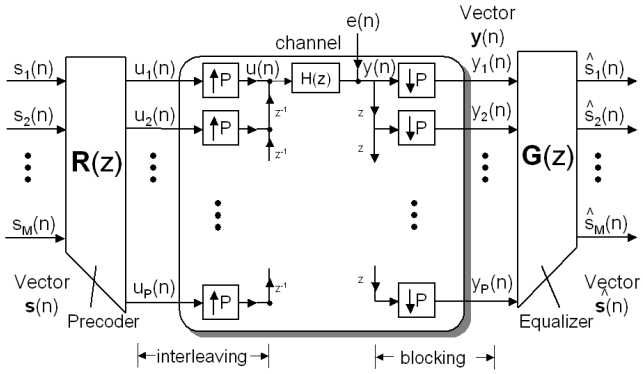

Figure 2.1: Communication System with Redundant Filter Bank Precoders.

the GCD idea is also based on subspace decomposition [39]. This similarity of the two algorithms suggests a possibility of generalization.

In this chapter, we propose such a generalized, subspace-based algorithm of which both the SGB method [45] and the MNP method [36] are special cases. The generalization uses an integer parameter called *repetition index* which represents the number of repeated uses of each received block. The choice of the repetition index is roughly inversely proportional to the number of required received blocks. When the repetition index is chosen as unity, the algorithm reduces to the SGB method; when it is equal to the size of a received block, it becomes the MNP algorithm. The large repetition index of the MNP method explains its speedy convergence and suitability in fast-varying environments but also imposes a high computational complexity. The introduction of repetition index provides a way to achieve a system performance similar to or better than that of the MNP method with a much less computational load.

The content of this chapter is mainly drawn from [49], and portions of it have been presented in [51]. Other relevant results will be presented in later chapters. The performance analysis of the generalized algorithm will be presented in Chapter 5. Some theoretical issues on signal richness will be studied in Chapters 6 and 7.

2.1 Outline

The organization of this chapter is as follows. Section 2.2 describes the system structure with ZP precoders and reviews two existing blind algorithms: the SGB method[45] and the MNP method [36]. In Section 2.3 we present the generalized algorithm and derive the conditions on the input

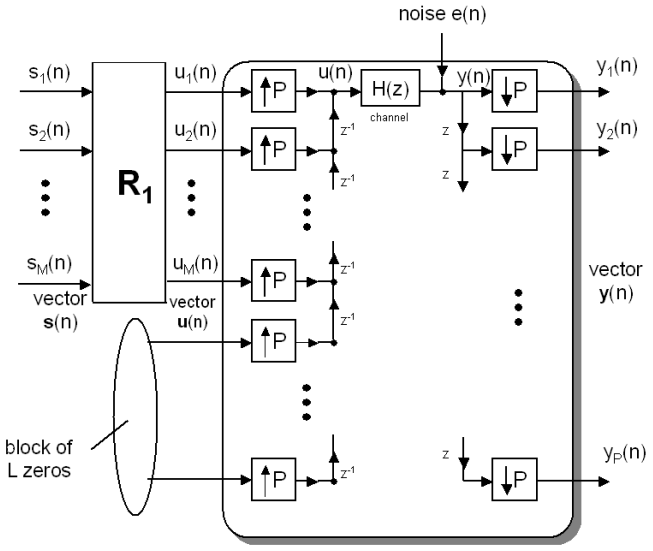

Figure 2.2: The zero-padding system with precoder $\mathbf{R}_1$.

sequence under which the algorithm operates properly. In Section 2.4 a variation of the generalized algorithm, namely the frequency domain version of the generalized algorithm, is proposed.

The conditions on the input signal under which the proposed algorithms work properly result in the concept of *generalized signal richness*. In Section 2.5, a mathematical treatment of generalized signal richness is presented, and some basic properties thereof are studied in detail. More advanced materials on generalized signal richness will be studied later in Chapters 6 and 7.

Simulation results and complexity analysis of both time and frequency domain approaches are presented in Section 2.6. In particular, simulations under time-varying channel environments are presented to demonstrate the strength of the proposed algorithm against channel variation. Finally, conclusions are made in Section 2.7.

2.2 Problem Formulation and Literature Review

2.2.1 Redundant Filter Bank Precoders

Consider the multirate communication system [25] depicted in Figure 2.1. The source symbols $s_1(n), s_2(n), ..., s_M(n)$ may come from M different users or from a serial-to-parallel operation on data of a single user. For convenience we consider the blocked version $\mathbf{s}(n)$ as indicated. The vector $\mathbf{s}(n)$ is precoded by a $P \times M$ matrix $\mathbf{R}(z)$ where $P > M$. The information with redundancy is then sent over the channel $H(z)$. We assume $H(z)$ is an FIR channel with a maximum order L,

i.e.,

$$H(z) = \sum_{k=0}^{L} h_k z^{-k}.$$

The signal is corrupted by channel noise $e(n)$. The received symbols $y(n)$ are divided into $P \times 1$ block vectors $\mathbf{y}(n)$. The $M \times P$ matrix $\mathbf{G}(z)$ is the channel equalizer, and $\hat{s}_1(n), \hat{s}_2(n), ..., \hat{s}_M(n)$ are the recovered symbol streams. Also, for simplicity we define $\mathbf{h}$ as the column vector $\begin{bmatrix} h_0 & h_1 & \cdots & h_L \end{bmatrix}^T$. We set

$$P = M + L,$$

that is, the redundancy introduced in a block is equal to the maximum channel order.

2.2.2 Trailing Zeros as Transmitter Guard Interval and the SGB method

Suppose we choose the precoder $\mathbf{R}(z) = \begin{bmatrix} \mathbf{R}_1 \\ \mathbf{0} \end{bmatrix}$, where $\mathbf{R}_1$ is an $M \times M$ constant invertible matrix and the $L \times M$ zero matrix $\mathbf{0}$ represents zero-padding with length L in each transmitted block, as indicated in Fig. 2.2. For simplicity of describing the algorithms, in this section we assume the noise is absent. Now, the received blocks can be written as

$$\begin{aligned} & \underbrace{\begin{bmatrix} \mathbf{y}(1) & \mathbf{y}(2) & \cdots & \mathbf{y}(J) \end{bmatrix}}_{\mathbf{Y} \text{ matrix; size } P \times J} \\ = \; & \mathcal{H}_M \mathbf{R}_1 \underbrace{\begin{bmatrix} \mathbf{s}(1) & \mathbf{s}(2) & \cdots & \mathbf{s}(J) \end{bmatrix}}_{\mathbf{S} \text{ matrix; size } M \times J}, \end{aligned}$$

where $\mathcal{H}_M = \mathcal{T}_M(\mathbf{h})$ is the full-banded Toeplitz channel matrix. As long as vector $\mathbf{h}$ is nonzero, the matrix $\mathcal{H}_M$ has full column rank M. Now we assume the signal $\mathbf{s}(n)$ is *rich*, that is, there exists an integer J such that the matrix $\mathbf{S}$ has full row rank M. Since $\mathbf{R}_1$ is an $M \times M$ invertible matrix, we conclude that the $P \times J$ matrix $\mathbf{Y}$ has rank M. So there exist L linearly independent vectors that are left annihilators of $\mathbf{Y}$. In other words, there exists a $P \times L$ matrix $\mathbf{U}_0$ such that $\mathbf{U}_0^\dagger \mathbf{Y} = \mathbf{U}\mathcal{H}_M \mathbf{R}_1 \mathbf{S} = \mathbf{0}$. Now that $\mathbf{R}_1\mathbf{S}$ has rank M, this implies

$$\mathbf{U}_0^\dagger \mathcal{H}_M = \mathbf{0}. \tag{2.1}$$

The channel coefficients $\mathbf{h}$ can then be determined by solving Eq. (2.1). In practice, where *channel*

noise is present, the computation of the annihilators is replaced with the computation of the eigenvectors corresponding to the smallest L singular values of $\mathbf{Y}$. In this and the following sections, the channel noise term is not shown explicitly.

Note that this algorithm [45] works under the assumption that $\mathbf{S}$ has full row rank M. Obviously $J \geq M$ is a necessary condition for this assumption. This means the receiver must accumulate at least M blocks (i.e., a duration of $M(M+L)$ symbols) before channel identification can be performed. This could be a disadvantage when the system is working over a fast-varying channel.

2.2.3 The MNP Method: Finding the Greatest Common Divisor

Another approach proposed in [36] requires only two received blocks for blind channel identification. Recall that the channel is described by $\mathbf{y} = \mathcal{H}_M \mathbf{u} = \mathcal{T}_M(\mathbf{h})\,\mathbf{u}$, or

$$\begin{bmatrix} y_1 \\ y_2 \\ \vdots \\ y_P \end{bmatrix} = \begin{bmatrix} h_0 & & \mathbf{0} \\ h_1 & \ddots & \\ \vdots & & h_0 \\ h_L & & h_1 \\ & \ddots & \vdots \\ \mathbf{0} & & h_L \end{bmatrix} \begin{bmatrix} u_1 \\ u_2 \\ \vdots \\ u_M \end{bmatrix}. \tag{2.2}$$

By multiplying $\begin{bmatrix} 1 & x & x^2 & \cdots & x^{P-1} \end{bmatrix}$ to both sides of Eq. (2.2), we obtain

$$y(x) = h(x)u(x),$$

where

$$y(x) \triangleq \sum_{k=0}^{P-1} y_{k+1}x^k, h(x) \triangleq \sum_{k=0}^{L} h_k x^k,$$

and

$$u(x) \triangleq \sum_{k=0}^{M-1} u_{k+1}x^k$$

are polynomial representations of the output vector, channel vector, and input vector, respectively. This means Eq. (2.2) is nothing but a polynomial multiplication. Now, suppose we have two received blocks $\mathbf{y}(1)$ and $\mathbf{y}(2)$, and let $y_1(x) = h(x)u_1(x)$ and $y_2(x) = h(x)u_2(x)$ represent the polynomial forms of these. Then, the channel polynomial $h(x)$ can be found as the GCD of $y_1(x)$ and $y_2(x)$, given that the input polynomials $u_1(x)$ and $u_2(x)$ are co-prime to each other.

To compute the GCD of $y_1(x)$ and $y_2(x)$, we first construct a $(2P-1)\times 2P$ matrix [39]

$$\mathbf{Y}_P \triangleq \begin{bmatrix} y_{11} & 0 & \cdots & 0 & y_{21} & 0 & \cdots & 0 \\ y_{12} & y_{11} & \ddots & \vdots & y_{22} & y_{21} & \ddots & \vdots \\ \vdots & y_{12} & \ddots & 0 & \vdots & y_{22} & \ddots & 0 \\ y_{1P} & \vdots & & y_{11} & y_{2P} & \vdots & & y_{21} \\ 0 & y_{1P} & & y_{12} & 0 & y_{2P} & & y_{22} \\ \vdots & \ddots & \ddots & \vdots & \vdots & \ddots & \ddots & \vdots \\ 0 & \cdots & 0 & y_{1P} & 0 & \cdots & 0 & y_{2P} \end{bmatrix}.$$

One can verify that

$$\mathbf{Y}_P = \underbrace{\begin{bmatrix} h_0 & & \mathbf{0} \\ h_1 & \ddots & \\ \vdots & & h_0 \\ h_L & & h_1 \\ & \ddots & \vdots \\ \mathbf{0} & & h_L \end{bmatrix}}_{\text{matrix } \mathcal{H}_{M+P-1}} \underbrace{\begin{bmatrix} u_{11} & & \mathbf{0} & u_{21} & & \mathbf{0} \\ u_{12} & \ddots & & u_{22} & \ddots & \\ \vdots & & u_{11} & \vdots & & u_{21} \\ u_{1M} & & u_{12} & u_{2M} & & u_{22} \\ & \ddots & \vdots & & \ddots & \vdots \\ \mathbf{0} & & u_{1M} & \mathbf{0} & & u_{2M} \end{bmatrix}}_{\text{matrix } \mathcal{U}}.$$

size $(2P-1)\times(M+P-1)$; size $(M+P-1)\times 2P$

When $u_1(x)$ and $u_2(x)$ are co-prime to each other, it can be shown that the matrix $\mathcal{U}$ has full rank $M+P-1$ (see section 2.5). Since $\mathcal{H}_{M+P-1}$ also has rank $M+P-1$, rank($\mathbf{Y}_P$) $= M+P-1$ and hence $\mathbf{Y}_P$ has L left annihilators (i.e., there exists a $(2P-1)\times L$ full rank matrix $\mathbf{U}_0$ such that $\mathbf{U}_0^\dagger \mathbf{Y} = \mathbf{0}$). These annihilators are also annihilators of each column of matrix $\mathcal{H}_{M+P-1}$, and we can therefore, in absence of noise, identify channel coefficients $h_0, h_1, ..., h_L$ up to a scalar ambiguity. In presence of noise, the columns of $\mathbf{U}_0$ would be selected as the eigenvectors associated with the smallest singular values of $\mathbf{Y}_P$.

2.2.4 Connection to the Earlier Literature

The MNP method described above can be viewed as a dual version of the subspace methods proposed in the earlier literature in multi-channel blind identification [30][65]. In the subspace method in [30], the single source can be estimated as the GCD of the received data from two (more gener-

ally N) different antennas. The MNP method [36] swaps the roles of data blocks and multi-channel coefficients.

2.3 A Generalized Algorithm

In this section we propose a generalized algorithm of which each of the two algorithms described in the previous section is a special case. Comparing the two algorithms described above, we find that the MNP approach needs much fewer received blocks for blind identifiability. However, it has more computational complexity. Each received block is repeated P times to build a big matrix. Using the generalized algorithm, we can choose the number of repetitions and the number of received blocks freely as long as they satisfy a certain constraint.

2.3.1 Algorithm Description

Observe Eq. (2.2) again and note that it can be rewritten as

$$\mathcal{T}_Q(\mathbf{y}) = \mathcal{T}_{M+Q-1}(\mathbf{h})\,\mathcal{T}_Q(\mathbf{u}), \tag{2.3}$$

where the notation $\mathcal{T}.(\cdot)$ is defined as in Section 1.4. Here Q can be any positive integer. Note that in the MNP method, Q is chosen as P, as described in the previous section. Suppose the receiver gathers J blocks with $J \geq 2$. Then we have $\mathbf{Y}_Q^{(J)} = \mathcal{H}_{M+Q-1}\mathbf{U}_Q^{(J)}$, where

$$\mathbf{Y}_Q^{(J)} = \left[\begin{array}{cccc} \mathcal{T}_Q(\mathbf{y}(1)) & \mathcal{T}_Q(\mathbf{y}(2)) & \cdots & \mathcal{T}_Q(\mathbf{y}(J)) \end{array}\right], \tag{2.4}$$

$$\mathcal{H}_{M+Q-1} = \mathcal{T}_{M+Q-1}(\mathbf{h}),$$

and

$$\mathbf{U}_Q^{(J)} = \left[\begin{array}{ccc} \mathcal{T}_P(\mathbf{u}(1)) & \cdots & \mathcal{T}_P(\mathbf{u}(J)) \end{array}\right]. \tag{2.5}$$

Note that $\mathbf{U}_Q^{(J)}$ has size $(M+Q-1)\times QJ$, and $\mathbf{Y}_Q^{(J)}$ has size $(P+Q-1)\times QJ$. For notational simplicity, from now on we will use subscript Q as in N_Q to denote $N_Q = N+Q-1$ where N denotes a positive integer. In particular,

$$M_Q = M+Q-1$$

and

$$P_Q = P + Q - 1.$$

Notice that they still have the relationship $P_Q = M_Q + L$.

Assume now the matrix $\mathbf{U}_Q^{(J)}$ has full row rank M_Q. Taking singular-value decomposition (SVD) of $\mathbf{Y}_Q^{(J)}$ we have

$$\mathbf{Y}_Q^{(J)} = \begin{bmatrix} \mathbf{U}_r & \mathbf{U}_0 \end{bmatrix} \begin{bmatrix} \mathbf{\Sigma} & \\ & \mathbf{0} \end{bmatrix} \begin{bmatrix} \mathbf{V}_r & \mathbf{V}_0 \end{bmatrix}^\dagger. \tag{2.6}$$

The size of $\mathbf{\Sigma}$ is $M_Q \times M_Q$ since both $\mathcal{H}_{M_Q}$ and $\mathbf{U}_Q^{(J)}$ have full rank M_Q. The columns of the $M_Q \times L$ matrix $\mathbf{U}_0$ are left annihilators of matrix $\mathbf{Y}^{(J)}$ and also of $\mathbf{H}$ since $\mathbf{U}^{(J)}$ has full row rank. Suppose

$$\mathbf{U}_0^\dagger = \begin{bmatrix} u_{11} & u_{12} & \cdots u_{1,P+Q-1} \\ u_{21} & u_{22} & \cdots u_{2,P+Q-1} \\ \vdots & & \vdots \\ u_{L1} & u_{L2} & \cdots u_{L,P+Q-1} \end{bmatrix}.$$

Form the Hankel matrices

$$\mathcal{U}_k \triangleq \begin{bmatrix} u_{k1} & u_{k2} & \cdots & u_{k,L+1} \\ u_{k2} & u_{k3} & \cdots & u_{k,L+2} \\ \vdots & & \vdots & \\ u_{k,M_Q} & u_{k,M_Q+1} & \cdots & u_{k,P_Q} \end{bmatrix}$$

for $k, 1 \le k \le L$. Then we have

$$\underbrace{\begin{bmatrix} \mathcal{U}_1 \\ \mathcal{U}_2 \\ \vdots \\ \mathcal{U}_L \end{bmatrix}}_{\mathcal{U} \text{ matrix; size } LM_Q \times (L+1)} \mathbf{h} = \mathbf{0}. \tag{2.7}$$

Vector $\mathbf{h}$ can thus be identified up to a scalar ambiguity.

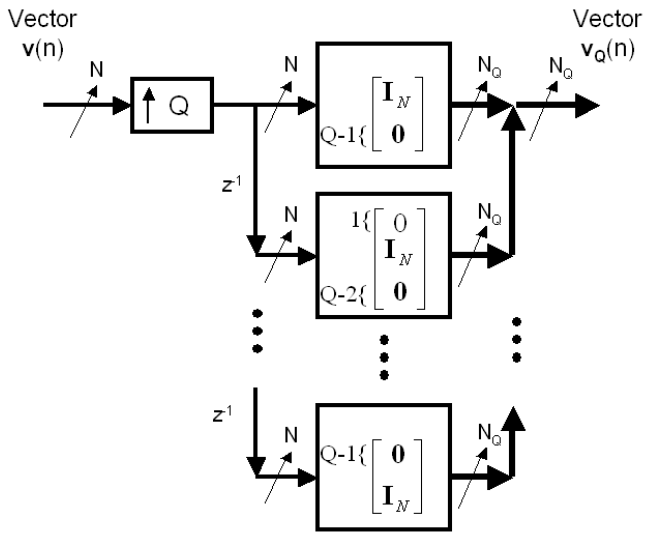

Figure 2.3: Q-repetition and shifting operation.

2.3.2 Q-Repetition and Shifting Operation

As we can see in the previous subsection, the repetition and shifting operation on a vector signal is crucial in the generalized algorithm. Figure 2.3 gives a block diagram of this operation. For future notational convenience, the subscript Q as in $\mathbf{v}_Q(n)$ denotes the result of this operation on a vector signal. By viewing Eq. (2.3) and applying this operation on $\mathbf{y}(n)$ and $\mathbf{u}(n)$, we obtain the relationship

$$\mathbf{y}_Q(n) = \mathcal{H}_{M+Q-1}\mathbf{u}_Q(n)$$

for any positive integer Q. We call the integer Q the *repetition index* since it represents the number of repeated uses of each received block.

2.3.3 Special Cases of the Algorithm

The blind channel identification algorithm described above uses two parameters: (a) the number of received blocks J, and (b) the repetition index Q. A number of points should be noted here:

1. The algorithm works for any J and Q as long as $\mathbf{U}_Q^{(J)}$ has full row rank M_Q. *This is the only constraint for choosing parameters J and Q.*

2. Note that if we choose $Q = 1$ and $J \geq M$, then the algorithm reduces to the *SGB algorithm* [45].

3. If we choose $Q = P$ and $J = 2$, it becomes the *MNP algorithm* [36].

So both the SGB method and the MNP method are a special case of the proposed algorithm. Since $\mathbf{U}_Q^{(J)}$ has size $M_Q \times QJ$, $\mathbf{U}_Q^{(J)}$, having full row rank, implies $QJ \geq M_Q = M + Q - 1$, or

$$Q \geq \frac{M-1}{J-1}. \tag{2.8}$$

Also note that we cannot choose $J = 1$ since $\mathbf{U}_Q^{(J)}$ can never have full rank unless the block size $M = 1$. This is consistent with the theory that two blocks are required for blind channel identification [28]. While the inequality (2.8) is a necessary condition for $\mathbf{U}_Q^{(J)}$ to have full rank, it is not sufficient because it also depends on the values of entries of $\mathbf{u}(n)$. Nevertheless, when inequality (2.8) is satisfied, the probability of $\mathbf{U}_Q^{(J)}$ having full rank is usually close to unity in practice, especially when a large symbol constellation is used. Thus,

$$Q = \left\lceil \frac{M-1}{J-1} \right\rceil$$

appears to be a selection that minimizes the computational cost given the number of received blocks J. A detailed study on the conditions for $\mathbf{U}_Q^{(J)}$ to have full rank is presented in Section 2.5.

When $J = 2$, Q can be chosen as small as $M-1$ rather than P. If we take $J = 3$, $Q = \lceil (M-1/2) \rceil$ makes the matrix $\mathbf{Y}$ twice smaller. We can choose $Q = 1$ only when $J \geq M$. This coincides with the SGB algorithm which uses a richness assumption [45].

2.4 Frequency Domain Approach

In this section we slightly modify the blind identification algorithm and directly estimate the frequency responses of the channel at different frequency bins and equalize the channel in the frequency domain. We call the modified algorithm *frequency domain approach*. Some of the ideas come from [70]. The receiver structure for the frequency domain approach is shown in Fig. 2.4. To demonstrate how this system works, observe the $P_Q \times M_Q$ *full-banded Toeplitz* channel matrix

$$\mathcal{H}_{M_Q} = \mathcal{T}_{M_Q}(\mathbf{h}).$$

Define a row vector $\mathbf{v}_\rho^T = \begin{bmatrix} 1 & \rho^{-1} & \cdots & \rho^{-(P_Q-1)} \end{bmatrix}$ with ρ a nonzero complex number. Due to

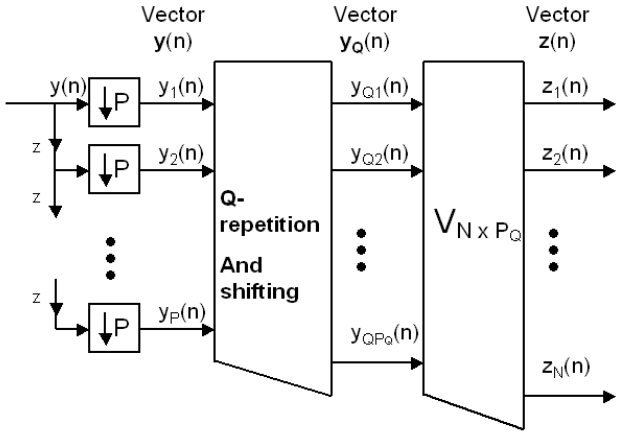

Figure 2.4: Receiver structure for frequency domain approach.

full-banded Toeplitz structure of $\mathcal{H}_{M_Q}$, we have

$$\mathbf{v}_\rho^T \mathcal{H}_{M_Q} = \left[\begin{array}{cccc} H(\rho) & \rho^{-1}H(\rho) & \cdots & \rho^{-(M_Q-1)}H(\rho) \end{array} \right],$$

where $H(\rho) = \sum_{k=0}^{L} h_k \rho^{-k}$ is the channel z-transform evaluated at $z = \rho$.

Let N be chosen as an integer greater than or equal to P_Q, and ρ_1, ρ_2, ..., ρ_N be distinct nonzero complex numbers. Consider an $N \times P_Q$ matrix $\mathbf{V}_{N\times P_Q}$ whose ith row is $\mathbf{v}_{\rho_i}^T$:

$$\mathbf{V}_{N\times P_Q} = \left[\begin{array}{cccc} 1 & \rho_1^{-1} & \rho_1^{-2} & \cdots & \rho_1^{-(P_Q-1)} \\ 1 & \rho_2^{-1} & \rho_2^{-2} & \cdots & \rho_2^{-(P_Q-1)} \\ & & \vdots & & \\ 1 & \rho_N^{-1} & \rho_N^{-2} & \cdots & \rho_N^{-(P_Q-1)} \end{array} \right].$$

It is easy to verify that

$$\mathbf{V}_{N\times P_Q}\mathcal{H}_{M_Q} = \mathbf{\Lambda}_N \underbrace{\left[\begin{array}{cccc} 1 & \rho_1^{-1} & \cdots & \rho_1^{-(M_Q-1)} \\ 1 & \rho_2^{-1} & \cdots & \rho_2^{-(M_Q-1)} \\ & & \vdots & \\ 1 & \rho_N^{-1} & \cdots & \rho_N^{-(M_Q-1)} \end{array} \right]}_{\mathbf{V}_{N\times M_Q} \text{ matrix}},$$

where

$$\mathbf{\Lambda}_N = \text{diag}(\begin{bmatrix} H(\rho_1) & H(\rho_2) & \cdots & H(\rho_N) \end{bmatrix}) \triangleq \text{diag}(\tilde{\mathbf{h}}_N)$$

is a diagonal matrix with frequency domain channel coefficients as the diagonal entries. Now, when we gather receiving blocks and repeat them as in Eq. (2.4), we get the following matrix.

$$\mathbf{Y}_Q^{(J)} = \begin{bmatrix} \mathcal{T}_Q(\mathbf{y}(1)) & \mathcal{T}_Q(\mathbf{y}(2)) & \cdots & \mathcal{T}_Q(\mathbf{y}(J)) \end{bmatrix}.$$

Since we have $\mathbf{Y}_Q^{(J)} = \mathcal{H}_{M_Q}\mathbf{U}_Q^{(J)}$ in absence of noise, by multiplying $\mathbf{V}_{N\times P_Q}$ and $\mathbf{Y}_Q^{(J)}$, we have

$$\begin{aligned} \mathbf{Z} = \mathbf{V}_{N\times P_Q}\mathbf{Y}_Q^{(J)} &= \mathbf{V}_{N\times P_Q}\mathcal{H}_{M_Q}\mathbf{U}_Q^{(J)} \\ &= \mathbf{\Lambda}_N\mathbf{V}_{N\times M_Q}\mathbf{U}_Q^{(J)}. \end{aligned}$$

Recall that $\text{rank}(\mathbf{Y}_Q^{(J)}) = \text{rank}(\mathbf{U}_Q^{(J)}) = M_Q$. Since $\rho_1, \rho_2, ..., \rho_N$ are all distinct, the matrix $\mathbf{Z}$ has the same rank as $\mathbf{Y}_Q^{(J)}$. The dimension of the null space of matrix $\mathbf{Z}$ is hence $N - M_Q$. By performing SVD on $\mathbf{Z}$, we can find these $N - M_Q$ left annihilators of $\mathbf{Z}$, which are also annihilators of $\mathbf{\Lambda}_N\mathbf{V}_{N\times M_Q}$. There exists an $(N - M_Q)\times N$ matrix $\mathbf{U}_0^\dagger$ such that $\mathbf{U}_0^T\mathbf{Z} = \mathbf{0}$. Since $\mathbf{U}_Q^{(J)}$ has full rank, this implies

$$\mathbf{U}_0^\dagger\mathbf{\Lambda}_N\mathbf{V}_{N\times M_Q} = \mathbf{0}. \tag{2.9}$$

Suppose

$$\mathbf{U}_0^\dagger = \begin{bmatrix} u_{11} & u_{12} & \cdots & u_{1N} \\ u_{21} & u_{22} & \cdots & u_{2N} \\ \vdots & \vdots & & \vdots \\ u_{N-M_Q,1} & u_{N-M_Q,2} & \cdots & u_{N-M_Q,N} \end{bmatrix}.$$

Then by observing the ijth entry of Eq.(2.9), we have

$$\mathbf{u}_{ij}^\dagger\tilde{\mathbf{h}}_N = 0 \tag{2.10}$$

for all i, j , $1 \le i \le N - M_Q$, and $1 \le j \le M_Q$, where $\mathbf{u}_{ij} = \begin{bmatrix} u_{i1}\rho_1^{-(j-1)} & u_{i2}\rho_2^{-(j-1)} & \cdots & u_{iN}\rho_N^{-(j-1)} \end{bmatrix}^\dagger$.

Form the $M_Q \times N$ matrices

$$\mathcal{U}_i = \begin{bmatrix} u_{i1} & u_{i2} & \cdots & u_{iN} \\ u_{i1}\rho_1^{-1} & u_{i2}\rho_2^{-1} & \cdots & u_{iN}\rho_N^{-1} \\ u_{i1}\rho_1^{-2} & u_{i2}\rho_2^{-2} & \cdots & u_{iN}\rho_N^{-2} \\ & & \vdots & \\ u_{i1}\rho_1^{-(M_Q-1)} & u_{i2}\rho_2^{-(M_Q-1)} & \cdots & u_{iN}\rho_N^{-(M_Q-1)} \end{bmatrix},$$

and let $\mathcal{U} = \begin{bmatrix} \mathcal{U}_1^T & \mathcal{U}_2^T & \cdots & \mathcal{U}_{N-M_Q}^T \end{bmatrix}^T$. Then, from Eq. (2.10) we have $\mathcal{U}\tilde{\mathbf{h}}_N = \mathbf{0}$. Then the *frequency domain channel coefficients* $\tilde{\mathbf{h}}_N$ can be estimated by solving this equation. After the frequency domain channel coefficients are estimated, the received symbols can be equalized directly in the frequency domain, as in DMT systems.

Recall that we have the freedom to choose N as any integer greater than or equal to P_Q and the values of $\rho_i, 1 \leq i \leq N$ as any nonzero complex number in the z-domain. In this paper, we use $N = P_Q$ and

$$\rho_k = \exp\left(\frac{j2k\pi}{N}\right), k = 0, 1, ..., N-1.$$

Note that since $H(z)$ is an Lth order system, there are at most L values among $H(\rho_i)$ which can be zero (channel nulls). By choosing $N \geq P_Q$, there are at least M_Q nonzero values among $H(\rho_i), i = 1, 2, ..., P_Q$. In practice we can choose to equalize the received symbols in frequency bins associated with the largest M_Q frequency responses $H(\rho_i)$ to enhance the system performance. This provides resistance to channel nulls.

2.5 Generalized Signal Richness

For the generalized blind channel identification method proposed in this paper to work properly, the matrix $\mathbf{U}_Q^{(J)}$ defined in Eq. (2.5) must have full row rank for given parameters J and Q. An obvious necessary condition has been presented as inequality (2.8) in Section 2.3. The sufficiency, however, depends on the content of signal $\mathbf{u}(n)$. When $Q = 1$ and $\mathbf{u}(n)$ is *rich*, then there exists J such that $\mathbf{U}_Q^{(J)} = \begin{bmatrix} \mathbf{u}(0) & \mathbf{u}(1) & \cdots & \mathbf{u}(J-1) \end{bmatrix}$ has full rank. When $Q > 1$, $\mathbf{u}(n)$ requires another kind of richness property so that $\mathbf{U}_Q^{(J)}$ has full rank for a finite integer J. We call this property the *generalized signal richness* and define it as follows:

Definition 2.1: An $M \times 1$ sequence $\mathbf{u}(n), n \geq 0$, is said to be $(1/Q)$-*rich* if there exists a finite integer J such that the $(M+Q-1) \times JQ$ matrix

$$\mathbf{U}_Q^{(J)} = \left[\begin{array}{cccc} \mathcal{T}_Q\left(\mathbf{s}(0)\right) & \mathcal{T}_Q\left(\mathbf{s}(1)\right) & \cdots & \mathcal{T}_Q\left(\mathbf{s}(J-1)\right) \end{array} \right]$$

has full row rank $M+Q-1$. □

Several interesting properties of generalized signal richness will be presented in this section. The reason why we use the notation of $(1/Q)$ will soon be clear when these properties are presented.

2.5.1 Measure of Generalized Signal Richness

Lemma 2.1: If an $M \times 1$ sequence $\mathbf{s}(n)$ is $(1/Q)$-rich, then $\mathbf{s}(n)$ is $(1/(Q+1))$-rich.

Proof: See Appendix. □ □

Lemma 2.1 states a basic property of generalized signal richness: the smaller the value of Q is, the "stronger" the condition of $(1/Q)$-richness is. For example, if an $M \times 1$ sequence $\mathbf{s}(n)$ is 1-rich, or simply *rich*, then it is $(1/Q)$-rich for any positive integer Q. On the contrary, a $(1/2)$-rich signal $\mathbf{s}(n)$ is not necessarily 1-rich. We can thus define a measure of generalized signal richness for a given $M \times 1$ sequence $\mathbf{s}(n)$ as follows:

Definition 2.2: Given an $M \times 1$ sequence $\mathbf{s}(n), n \geq 0$, the *degree of non-richness* of $\mathbf{s}(n)$ is defined as:

$$Q_{min} \triangleq \min_{Q} \left(\mathbf{s}(n) \text{ is } \frac{1}{Q}\text{-rich} \right). \tag{2.11}$$

□

Recall that the larger the degree of non-richness Q_{min} is, the weaker the richness of the signal $\mathbf{s}(n)$ is. If $\mathbf{s}(n)$ is not $(1/Q)$-rich for any Q, then $Q_{min} = \infty$. The property of an infinite degree of non-richness can be described in the following lemma. We use the notation $\mathbf{p}_M(x)$ to denote the column vector:

$$\mathbf{p}_M(x) = \left[\begin{array}{ccccc} 1 & x & x^2 & \cdots & x^{M-1} \end{array} \right]^T.$$

Lemma 2.2: Consider an $M \times 1$ sequence $\mathbf{s}(n)$. The following statements are equivalent:

(1) $\mathbf{s}(n)$ is not $(1/Q)$-rich for any Q.

(2) The degree of non-richness of $\mathbf{s}(n)$ is infinity.

(3) Either there exists a complex number α such that $\begin{bmatrix} 1 & \alpha & \cdots & \alpha^{M-1} \end{bmatrix}$ is an annihilator of $\mathbf{s}(n)$ or $\begin{bmatrix} 0 & \cdots & 0 & 1 \end{bmatrix}$ is an annihilator of $\mathbf{s}(n)$.

(4) Either polynomials $p_n(x) = \mathbf{p}_M^T(x)\mathbf{s}(n), n \geq 0$ share a common zero (at α), or their orders are all less than $M-1$. □

Proof: See Appendix. □

Note that the statement $\begin{bmatrix} 0 & \cdots & 0 & 1 \end{bmatrix}$ is an annihilator of $\mathbf{s}(n)$ in condition (3), and the statement that polynomials $p_n(x)$ have orders less than $M-1$ in condition (4) can be interpreted as the special situation when the common zero α is at infinity.

If an $M \times 1$ sequence $\mathbf{s}(n)$ has a finite degree of non-richness, or $\mathbf{s}(n)$ is $(1/Q)$-rich for some integer Q, then it can be shown that the maximum possible value of Q_{min} is $M-1$, as described in the following lemma.

Lemma 2.3: If $M > 1$ and an $M \times 1$ sequence $\mathbf{s}(n)$ is not $(1/(M-1))$-rich, then it is not $(1/Q)$-rich for any Q. □

Proof: See Appendix. □

With Lemma 2.3, we can see that for an $M \times 1$ sequence $\mathbf{s}(n)$, the possible values of the degree of non-richness Q_{min} are $1, 2, ..., M-1$, and ∞. $(1/(M-1))$-richness is thus the weakest form of generalized richness. When using the MNP method [39], this weakest form of generalized richness is very crucial. If this weakest form of richness of $\mathbf{s}(n)$ is not achieved, then by Lemma 2.2, $\mathbf{s}(n)$ has an infinite degree of non-richness and polynomials $\mathbf{p}_M^T(x)\mathbf{s}(n)$ have a common factor $(x-\alpha)$. Then, as in Section 2.2.3, when we take GCD of the polynomials representing the received blocks, the receiver would be unable to determine whether the factor $(x-\alpha)$ belongs to the channel polynomial or is a common factor of the symbol polynomials. *Therefore, if the input signal $\mathbf{s}(n)$ has infinite degree of non-richness, all methods proposed in this paper will fail for all repetition index Q.*

Furthermore, the MNP method proposed in [36] and [39] uses $Q = P$. Using Lemma 2.3, we see that using $Q = M-1$ is sufficient if we are computing the GCD of polynomials representing received blocks, and the following two conditions are true: (1) the GCD is known to have a degree less than or equal to L, (2) the degree of each symbol polynomial is less than or equal to $M-1$.

Using $Q = P$ not only is computationally unnecessary, but also, as we will see in simulation results in Section 2.6, has sometimes a worse performance than using $Q = M - 1$ in presence of noise.

The sufficiency of $Q = M - 1$ can also be understood from the point of view of polynomial theory. Suppose polynomials $a(x)$ and $b(x)$ have degrees less than or equal to $P - 1$ and have a greatest common denominator $d(x)$ whose degree is less than or equal to L. Suppose $a(x) = d(x)a_1(x)$ and $b(x) = d(x)b_1(x)$ and both $a_1(x)$ and $b_1(x)$ have degrees less than or equal to $M - 1$ and they are co-prime to each other. Then there exists polynomials $p(x)$ and $q(x)$ whose degrees are less than or equal to $M-2$ such that $1 = p(x)a_1(x)+q(x)b_1(x)$ and thus $d(x) = p(x)a(x)+q(x)b(x)$.

2.5.2 Connection to Earlier Literature

An earlier proposition mathematically equivalent to Lemma 2.3 has been presented in the single-input-multiple-output (SIMO) blind equalization literature [65],[23]. We review it here briefly:

Proposition: Let $\mathbf{h}[n]$ be $J \times 1$ vectors. Suppose a $QJ \times (Q+M-1)$ block Toeplitz matrix $\mathcal{T}_Q(\mathbf{h}) =$

$$\begin{bmatrix} \mathbf{h}[0] & \mathbf{h}[1] & \cdots & \mathbf{h}[M-1] & \mathbf{0} & \cdots & \mathbf{0} \\ \mathbf{0} & \mathbf{h}[0] & \mathbf{h}[1] & \cdots & \mathbf{h}[M-1] & \ddots & \vdots \\ \vdots & \ddots & \ddots & \ddots & \ddots & \ddots & \mathbf{0} \\ \mathbf{0} & \cdots & \mathbf{0} & \mathbf{h}[0] & \mathbf{h}[1] & \cdots & \mathbf{h}[M-1] \end{bmatrix}$$

satisfies the following conditions:

(1) $\mathbf{h}[0] \neq \mathbf{0}$ and $\mathbf{h}[M-1] \neq \mathbf{0}$;

(2) $\mathbf{h}[n] = \mathbf{0}$ for $n < 0$ and $n \geq M$;

(3) $Q \geq M - 1$.

Then, $\mathcal{T}_Q(\mathbf{h})$ has full column rank if and only if

$$\mathbf{h}(z) \triangleq \sum_{i=0}^{M} \mathbf{h}[i]z^{-i} \neq \mathbf{0}, \qquad \forall z.$$

□

Here, $\mathbf{h}[n]$ was used to refer to the impulse response of a $J \times 1$ channel. Q stands for the observation period in the multiple-channel receiver end. Conditions (1) and (2) imply that the channel has finite impulse response. Condition (3) can be met by increasing the observation period Q. While this old proposition focuses on the coefficients of multiple channels rather than values of transmitted symbols, it is mathematically equivalent to the statement that $\mathbf{s}(n)$ is $(1/(M-1))$-rich

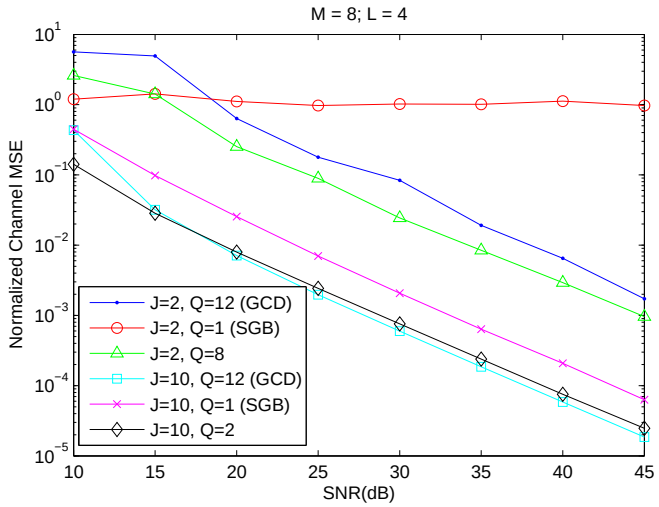

Figure 2.5: Normalized least squared channel error estimation.

if and only if polynomials $\mathbf{p}_M^T(x)\mathbf{s}(n)$ do not share common zeros. The case of $Q < M-1$, however, has not been considered earlier in the literature, to the best of our knowledge.

2.5.3 Remarks on Generalized Signal Richness

In this section we introduced the concept of generalized signal richness. Given an $M \times 1$ signal $\mathbf{s}(n), n \geq 0$, the *degree of non-richness* Q_{min} was defined. For an input signal with a degree of non-richness Q_{min}, we can choose any

$$Q \geq Q_{min}$$

and some finite J for the generalized algorithm proposed in Section 2.3 to work properly. The possible values of Q_{min} are $1, 2, ..., M-1$, and ∞. If $\mathbf{s}(n)$ has an infinite degree of non-richness, the algorithm proposed in this paper will fail for all Q. The degree of non-richness of a signal $\mathbf{s}(n)$ directly depends on its content. A deeper study of degree of non-richness will be presented in Chapter 7 [56].

2.6 Simulations and Discussions

In this section, several simulation results, comparisons, and discussions will be presented. We will first test our proposed method and compare it with the existing methods [45, 36] described in Sec. 2.2. Secondly, we will compare the performances of time domain versus frequency do-

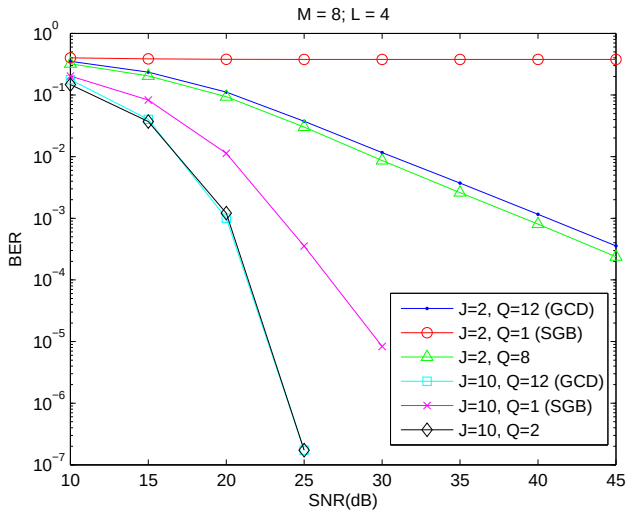

Figure 2.6: Bit error rate performance of the blind algorithm.

main approaches and show that under some channel conditions the frequency domain approach outperforms the time domain approach. Finally, we will analyze and compare the computational complexity of algorithms proposed in this chapter.

2.6.1 Simulations of time domain Approaches

A Rayleigh fading channel of order $L = 4$ is used. The size of transmitted blocks is $M = 8$ and received block size is $P = M + L = 12$. The normalized least squared channel estimation error, denoted as E_{ch}, is used as the figure of merit for channel identification and is defined as follows:

$$E_{ch} = \frac{||\hat{\mathbf{h}} - \mathbf{h}||^2}{||\mathbf{h}||^2},$$

where $\hat{\mathbf{h}}$ and $\mathbf{h}$ are the estimated and the true channel vectors, respectively. The simulated normalized channel estimation error is shown in Figure 2.5, and the corresponding BER is presented in Figure 2.6. When the number of blocks $J = 10$, the MNP method (with the number of block repetitions $Q = 12$) outperforms the SGB method ($Q = 1$) by a considerable range. Taking $Q = 2$ saves a lot of computation and yet yields a good performance as indicated. Furthermore, in the case of $J = 2$, the system with $Q = 8$ even outperforms the original MNP method with $Q = 12$. This also strengthens our argument in Section 2.5 that choosing Q as large as P is unnecessary.

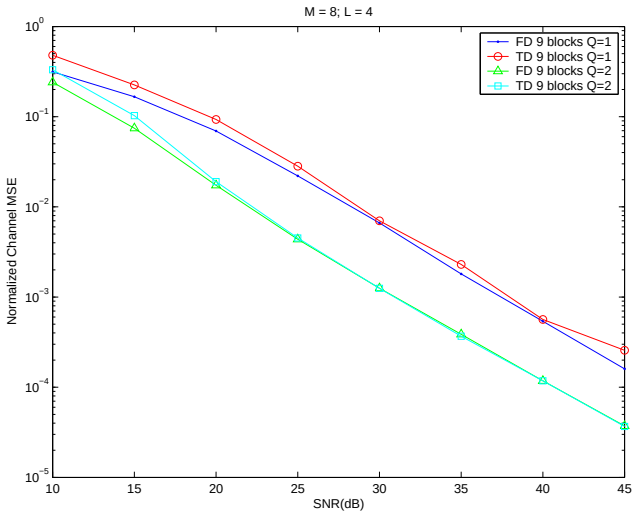

Figure 2.7: Normalized least squared channel error estimation.

2.6.2 Simulations of frequency domain Approaches

Fig. 2.7 shows the comparison of frequency domain approach and time domain approach under the channel coefficients $H(z) = 1 - jz^{-1} + (-1 + 0.01j)z^{-2} + (0.01 + j)z^{-3} - 0.01jz^{-4}$.

For frequency domain approach, the normalized least squared channel error is defined as

$$E_{ch} = \frac{||\hat{\tilde{\mathbf{h}}} - \tilde{\mathbf{h}}||^2}{||\tilde{\mathbf{h}}||^2},$$

where

$$\tilde{\mathbf{h}} = \left[\begin{array}{cccc} H(\rho_1) & H(\rho_2) & \cdots & H(\rho_N) \end{array} \right]$$

and $\hat{\tilde{\mathbf{h}}}$ is the estimation of $\tilde{\mathbf{h}}$. Simulation results show that frequency domain approach outperforms time domain approach especially when the noise level is high. While the frequency domain approach does not in general beat the time domain approach for a random channel, it has been consistently observed that frequency domain approach performs better than time domain approach when the last channel coefficient $h(L)$ has a small magnitude (i.e., at least one zero of $H(z)$ is close to the origin).

Since we have the freedom to choose values of coefficients ρ_i, the receiver can adjust ρ_i dynamically according to the *a priori* knowledge of the approximated channel zero locations. This is especially useful when the channel coefficients are changing slowly from block to block.

2.6.3 Complexity Analysis

For the algorithms presented in Section 2.3, the SVD computation dominates the computational complexity. The number of blocks J, the number of repetitions per block Q, and the received block size P decide the size of the matrix on which SVD is taken. The complexity of SVD operation on an $n \times m$ matrix [13] is on the order of $\mathcal{O}(mn^2)$ with $m \geq n$. Since $\mathbf{Y}_Q^{(J)}$ has size $(P+Q-1) \times QJ$, the complexity is $\mathcal{O}(QJ(P+Q-1)^2)$. We can see that the complexity can be greatly reduced by choosing a smaller Q. Recall that the SGB method [45] uses $Q = 1$ and the MNP method [36] uses $Q = P$. We thus have the following arguments:

1. the MNP method has a complexity around $4P$ times the complexity of the SGB method for any J. A choice of Q between 1 and P could be seen as a compromise between system performance and complexity.

2. When J is large, we have the freedom to choose a smaller Q, as explained in the previous subsection.

For the frequency domain approach presented in Section 2.4, an additional matrix multiplication is required. This demands extra computational complexity of the order of $\mathcal{O}(JP_Q^2)$. However, if the values ρ_i are chosen as equally spaced on the unit circle, an FFT algorithm can be exploited and the computational complexity will be reduced to $\mathcal{O}(JP_Q \log P_Q)$ and is negligible compared to the complexity of SVD operations.

2.6.4 Simulations for Time-varying Channels

In this subsection, we demonstrate the capability of the proposed generalized blind identification algorithm in time-varying channels environments. The received symbols can be expressed as

$$y(n) = \sum_{k=0}^{L} h(n,k)x(n-k),$$

where the $(L+1)$-tap channel coefficients $h(n,k)$ vary as the time index n changes. We generate the channel coefficients as follows. During a time interval T, the channel coefficients change from $h_1(k)$ to $h_2(k)$, where $h_1(k)$ and $h_2(k), 0 \leq k \leq L$ represent two sets of $(L+1)$-tap independent

coefficients. The variation of the coefficient is done by linear interpolation such that

$$h(n,k) = \begin{cases} h_1(k), & \text{if } n = 0 \\ h_2(k), & \text{if } n = T \\ \frac{T-n}{T}h_1(k) + \frac{n}{T}h_2(k) & \text{otherwise} \end{cases} .$$

In our simulation, we choose $T = 180$. Coefficients of $h_1(k)$ and $h_2(k)$ are given in Table I. The size of transmitted blocks is $M = 8$, and received block size is $P = M + L = 12$ (so the channel coefficients completely change after 15 blocks). Simulations are performed under different choices of J and Q, as indicated in Figures 2.8 and 2.9. The normalized least squared channel error is defined as

$$E_{ch} = \frac{||\hat{\mathbf{h}} - \overline{\mathbf{h}}||^2}{||\overline{\mathbf{h}}||^2},$$

where $\hat{\mathbf{h}}$ is the estimated channel and $\overline{\mathbf{h}}$ is the averaged coefficients during the time the channel is being estimated:

$$\overline{\mathbf{h}} = \frac{1}{JP} \sum_{n=n_0}^{n_0+JP-1} \begin{bmatrix} h(n,0) & h(n,1) & \cdots & h(n,L) \end{bmatrix}^T .$$

In Figure 2.8 we see that when $J = 10$ (SGB), the time range is too large for the algorithm to estimate the time-varying channel accurately. The performance for $J = 2$ (MNP) is much better in high SNR region because the channel does not vary too much during the time of two blocks. However, in low SNR region the performance for $J = 2$ becomes bad. The case for $J = 4$ has the best performance among all other choices because the channel does not vary too much during the duration of four receiving blocks, and more data are available for accurate estimation. This simulation result provides clues about how we can choose the optimal J: if the channel variation is fast (T is smaller) we need a smaller J while we can use a larger J when T is larger.

k	$h_1(k)$	$h_2(k)$
0	-0.6563 + 0.7059i	-1.2519 + 0.2295i
1	-0.6534 + 1.1774i	0.9347 + 0.1237i
2	-0.4229 - 0.2362i	0.0346 - 0.6180i
3	0.2145 - 0.2207i	0.7272 - 1.4084i
4	-0.1478 + 0.2802i	0.8612 + 0.3455i

Table 2.1: Coefficients for the Time-Varying Channel.

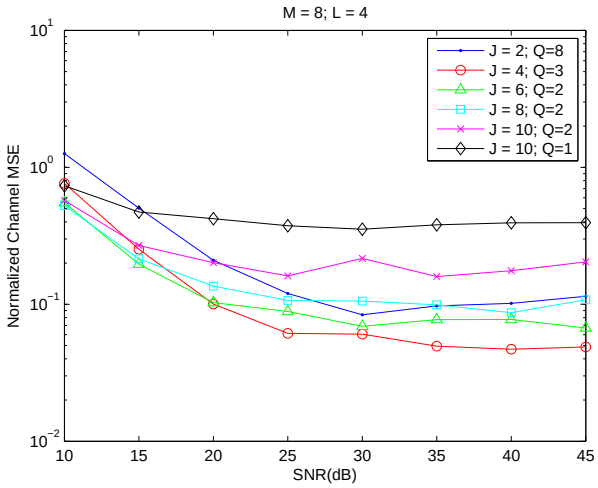

Figure 2.8: Normalized Channel MSE performance for a time-varying channel.

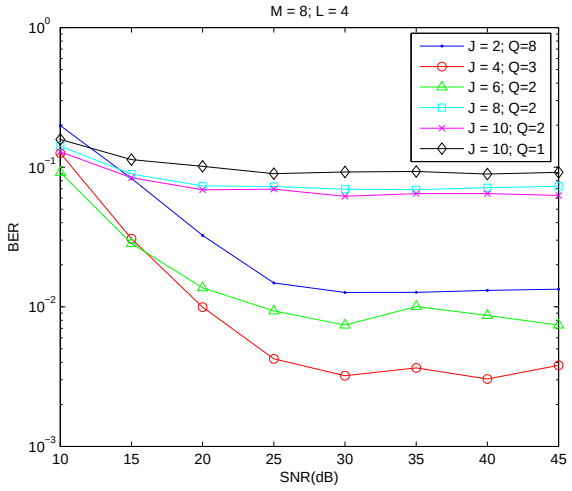

Figure 2.9: Bit error rate performance for a time-varying channel.

2.6.5 Remarks on Choosing the Optimal Parameters

According to the simulations results above, we summarize here a general guideline to choose a set of optimal parameters in practice.

1. When the channel is constant and for a fixed Q, a larger J appears to have a better performance (as shown in Fig. 2.5) since more data are available for accurate estimation.

2. When the channel is time-varying, the optimal choice of J depends on the speed of channel variation. Simulation results in Figures 2.8 and 2.9 suggest when the channel coefficients completely change in N blocks, a choice of $J \approx N/4$ could be appropriate.

3. Suppose J is given, a choice of Q as the smallest integer that satisfies inequality (2.8) often has a satisfactory performance. A slightly larger Q can sometimes be better (see Fig. 2.5 for $J = 10$) at the expense of a slightly increased complexity. However, if Q is too large, the performance could be even worse (see Fig. 2.5 for $J = 2, Q = 12$).

The guidelines above are given by observing the simulation results. An analytically optimal set of J and Q is still under investigation.

2.6.6 Noise Handling for large J

It should be noted that when J is very large (and $Q = 1$), the proposed method behaves like a traditional subspace method using second-order statistics. Suppose

$$\mathbf{Y}^{(J)} = \mathbf{H}\mathbf{U}^{(J)} + \mathbf{E}^{(J)},$$

where $\mathbf{E}^{(J)}$ is composed of J columns of noise vectors $\mathbf{e}(n)$. The autocorrelation matrix of received blocks can be estimated as

$$\mathbf{R}_{yy} = E[\mathbf{y}(n)\mathbf{y}^{\dagger}(n)] \approx \frac{1}{J}\mathbf{Y}^{(J)}\mathbf{Y}^{(J)\dagger}.$$

If the input signal and channel noise are uncorrelated, we can write $\mathbf{R}_{yy}$ as

$$\mathbf{R}_{yy} = \mathbf{H}\mathbf{R}_{uu}\mathbf{H}^{\dagger} + \mathbf{R}_{ee},$$

where $\mathbf{R}_{uu} = E[\mathbf{u}(n)\mathbf{u}^{\dagger}(n)]$ and $\mathbf{R}_{ee} = E[\mathbf{e}(n)\mathbf{e}^{\dagger}(n)]$ are autocorrelation matrices of input blocks and noise vectors, respectively. If $\mathbf{R}_{ee}$ is known (e.g., if the noise is white and noise variance is N_0,

then $\mathbf{R}_{ee} = N_0\mathbf{I}_P$), an improved estimation of annihilators of matrix $\mathbf{H}$ can be performed by taking eigen-decomposition of $\mathbf{R}_{yy} - \mathbf{R}_{ee}$, which results in better channel estimation [45]. This technique, however, does not apply when J is small.

2.7 Concluding Remarks

In this chapter we proposed a generalized algorithm for blind channel estimation in ZP systems. The number of received blocks $J \geq 2$ can be chosen freely depending on the speed of channel variation. An integer parameter called *repetition index* is introduced representing the number of repeated uses of each block. The minimum repetition index Q is derived to optimize the computational complexity while retaining good performance. Simulation shows that when the system parameter Q is properly chosen, the generalized algorithm outperforms previously reported special cases, especially in time-varying channel environments.

A *frequency domain* version of the generalized algorithm is also presented. Simulation result shows that it outperforms time domain approach at low SNR region for certain types of channels, e.g., channels with a zero close to the origin. Since we have the freedom to choose different frequency parameters in the frequency domain approach, certain choices other than equally spaced grids on the unit circle can be used to improve the system performance for different channel zero locations. An even more challenging problem might be to analytically derive the optimal frequency points for a specific type of channel.

The concept of *generalized signal richness* for a vector signal was introduced. With the *degree of non-richness* of the input signal decided, we can determine the minimum repetition index theoretically. A complete set of necessary and sufficient conditions for signals satisfying generalized signal richness is still under investigation. The study of effect of a linear precoder on the property of generalized signal richness will be presented in Chapter 7 [56].

2.8 Appendix: Proof of Lemmas

Proof of Lemma 2.1: Suppose $\mathbf{s}(n)$ is $(1/Q)$-rich but not $(1/(Q+1))$-rich, then there exists a $1\times(M+Q)$ nonzero vector $\mathbf{v}^T = \begin{bmatrix} v_1 & v_2 & \cdots & v_{M+Q} \end{bmatrix}$ such that

$$\mathbf{v}^T\mathcal{T}(\mathbf{s}(n), Q+1) = \mathbf{0}_{1\times(Q+1)}, \forall n. \tag{2.12}$$

Observing the first Q elements of the vector equation above, we obtain

$$\left[\begin{array}{cccc} v_1 & v_2 & \cdots & v_{M+Q-1} \end{array}\right] \mathcal{T}(\mathbf{s}(n), Q) = \mathbf{0}_{1\times Q}, \forall n.$$

Without loss of generality, we can assume $\left[\begin{array}{cccc} v_1 & v_2 & \cdots & v_{M+Q-1} \end{array}\right]$ to be nonzero and an annihilator of $\mathcal{T}(\mathbf{s}(n), Q)$. This violates the assumption that $\mathbf{s}(n)$ is $(1/Q)$-rich. □

Proof of Lemma 2.2: Conditions (1) and (2) are equivalent by definition. The equivalence of conditions (3) and (4) can also be easily examined. If condition (3) is true, then either $\mathbf{p}_{M+Q-1}^T(\alpha)$ or $\left[\begin{array}{cccc} 0 & \cdots & 0 & 1 \end{array}\right]$ is an annihilator of $\mathbf{s}_Q(n)$ (as defined in Sec. 2.3.2) for all Q and, hence, condition (1) is also true. In the case condition (1) is true, assume there exists $n \geq 0$ such that the degree of the polynomial $\mathbf{p}_M^T(x)\mathbf{s}(n)$ is $M-1$. Then for any Q, there exists a row vector $\mathbf{v}^T = \left[\begin{array}{cccc} v_1 & v_2 & \cdots & v_{M+Q-1} \end{array}\right]$ such that $\mathbf{v}^T\mathbf{s}_Q(n) = 0, \forall n$. This implies

$$\sum_{l=1}^{M} v_{k+l} \left[\mathbf{s}(n)\right]_l = 0, \forall n, k \geq 0, \tag{2.13}$$

where $[\cdot]_l$ represents the lth element of a column vector. So the series $\{v_k\}_{k=1}^{M+Q-1}$ must satisfy the recurrence equation (2.13) for any $n \geq 0$. This requires the characteristic polynomials $\mathbf{p}_M^T(x)\mathbf{s}(n), n \geq 0$ to share at least one zero. So condition (4) must be true. By the arguments above, these four conditions are equivalent. □

Proof of Lemma 2.3: If $\mathbf{s}(n)$ is proportional to a same nonzero vector $\mathbf{x}$ for all n, then it is obviously not $(1/Q)$-rich for any Q. We thus assume without loss of generality that $\mathbf{s}(0)$ and $\mathbf{s}(1)$ are linearly independent. Suppose polynomials $\mathbf{p}_M^T(x)\mathbf{s}(0)$ and $\mathbf{p}_M^T(x)\mathbf{s}(1)$ have two sets of *distinct* zeros $\{\alpha_{01}, \alpha_{02}, ..., \alpha_{0,M-1}\}$ and $\{\alpha_{11}, \alpha_{12}, ..., \alpha_{1,M-1}\}$, respectively. Since $\mathbf{s}(n)$ is not $(1/Q)$-rich, there exists a $(2M-2)$-row vector $\mathbf{v}^T = \left[\begin{array}{cccc} v_1 & v_2 & \cdots & v_{2M-2} \end{array}\right]$ such that $\mathbf{v}^T\mathcal{T}(\mathbf{s}(n), M-1) = \mathbf{0}_{1\times(M-1)}$. We have that the nonzero row vector $\mathbf{v}^T$ must have the form of

$$\begin{aligned} \mathbf{v}^T &= \sum_{k=1}^{M-1} c_k \left[\begin{array}{ccccc} 1 & \alpha_{0,k}^{-1} & \alpha_{0,k}^{-2} & \cdots & \alpha_{0,k}^{-(M-2)} \end{array}\right] \\ &= \sum_{k=1}^{M-1} d_k \left[\begin{array}{ccccc} 1 & \alpha_{1,k}^{-1} & \alpha_{1,k}^{-2} & \cdots & \alpha_{1,k}^{-(M-2)} \end{array}\right] \end{aligned}$$

for some coefficients $c_1, c_2, ..., c_{M-1}, d_1, d_2, ..., d_{M-1}$. This implies

$$\left[\begin{array}{cc} \mathbf{c}^T & -\mathbf{d}^T \end{array} \right] \mathbf{V} = \mathbf{0}^T, \tag{2.14}$$

where $\mathbf{c}^T = \left[\begin{array}{cccc} c_1 & c_2 & \cdots & c_{M-1} \end{array} \right]$, $\mathbf{d}^T = \left[\begin{array}{cccc} d_1 & d_2 & \cdots & d_{M-1} \end{array} \right]$, and

$$\mathbf{V} = \left[\begin{array}{c} \mathbf{p}_{2M-2}^T(\alpha_{01}) \\ \vdots \\ \mathbf{p}_{2M-2}^T(\alpha_{0,M-1}) \\ \mathbf{p}_{2M-2}^T(\alpha_{11}) \\ \vdots \\ \mathbf{p}_{2M-2}^T(\alpha_{1,M-1}) \end{array} \right]$$

is a Vandermonde matrix. If all zeros $\{\alpha_{ij}\}$ are distinct, $\mathbf{V}$ is a $(2M-2) \times (2M-2)$ invertible matrix and Eq. (2.14) implies $\mathbf{c}^T = \mathbf{d}^T = \mathbf{0}^T$ and hence $\mathbf{v}^T = \mathbf{0}^T$. This contradicts the assumption that $\mathbf{s}(n)$ is not $(1/(M-1))$-rich. Therefore, if $\mathbf{s}(n)$ is not $(1/(M-1))$-rich, there must be a common zero shared by $\mathbf{p}_{2M-2}^T(x)\mathbf{s}(0)$ and $\mathbf{p}_{2M-2}^T(x)\mathbf{s}(1)$. Similarly, we can obtain that there exists an α such that $\mathbf{p}_{2M-2}^T(\alpha)\mathbf{s}(n) = 0$ for all n. Using Lemma 2.2, this implies that $\mathbf{s}(n)$ is not $(1/Q)$-rich for all Q. In the case where the polynomial $\mathbf{p}_{2M-2}^T(x)\mathbf{s}(n)$ has multiple zeros for some n, the matrix $\mathbf{V}$ in Eq. (2.14) can be replaced with a *confluent Vandermonde matrix* [13] which is still invertible. □

Chapter 3

Blind and Semi-Blind Channel Estimation in Cyclic-Prefix Systems

In this chapter we study the blind channel estimation problem in cyclic prefix (CP) systems, which are more widely used than zero-padding (ZP) systems in many current standards such as orthogonal frequency division multiplexing (OFDM) and single carrier cyclic prefix (SC-CP) systems. Many blind estimation methods in CP systems (mostly OFDM systems) have been proposed in the literature [76, 35, 24, 15, 5, 21, 77, 31, 32, 6]. Depending on whether the knowledge of source constellations is used in the receiver, these methods can be roughly divided into two categories. Methods exploiting knowledge of source constellations usually discard the IBI-containing part of received blocks before channel estimation [76, 6] and can be computationally prohibitive unless a small constellation is used. Algorithms that do not use knowledge of source constellations generally exploit the statistical information of the source samples. Heath *et al.* proposed a statistical blind method [15] which exploits cyclostationarity induced by cyclic prefixes. Another statistics-based algorithm was proposed by Petropulu *et al.* [35, 24] using a special linear precoding. Zhuang *e*t al. proposed a statistical method that can estimate channels whose length is larger than the CP length. All these statistics-based algorithms require a larger amount of received data to obtain an accurate estimate.

Another class of blind algorithms that do not exploit knowledge of source constellations is the subspace-based algorithms. They not only work well with second order statistics, but can also be implemented deterministically as long as the persistency of excitation (p.o.e.) criterion of the input signal is satisfied. Unlike in ZP systems, where each received block is free from interblock interference (IBI), in CP systems, some parts of a received block contain IBI and present a difficulty for subspace-based blind channel estimation. Muquet *et al.* proposed a subspace-based algorithm for

OFDM systems by exploiting information obtained from concatenating two consecutive received blocks[31, 32]. Cai and Akansu proposed a similar deterministic algorithm of blind channel estimation for OFDM systems [5]. Li and Roy further exploited the presence of virtual carriers of OFDM systems[21]. All these previously reported methods require the number of received blocks to be at least as large as *two times the block size* to satisfy the p.o.e. criterion of the input, which limits the application in a fast-varying channel environment.

Inspired by the idea of repetition index proposed in Chapter 2, we propose in this chapter a generalization to some of previously reported subspace-based blind methods for CP systems [5, 32, 21]. The value of repetition index is unity for these previously reported methods. When the repetition index is chosen to be greater than unity, the number of received blocks needed will be significantly reduced. Note that OFDM systems and SC-CP systems are both special cases of CP systems, so the proposed method can be directly applicable in these systems without modifying transmitter structures.

The other part of this chapter deals with semiblind channel estimation in OFDM systems. In the context of channel estimation, one of the most important advantages of blind methods over pilot-assisted methods is better bandwidth efficiency. The bandwidth saving of blind methods, however, usually comes at the expense of computational complexity, a slower convergence speed, and worst of all, a poorer system performance than in pilot-assisted counterparts. A hybrid of these two types of channel estimation therefore has been studied in an attempt to combine advantages of both schemes [76, 16, 32, 16, 75, 7]. Several semi-blind algorithms have been proposed for OFDM systems [76, 16, 32, 16, 75, 7]. Similarly, these methods either rely on the knowledge of source statistics[7, 32], or require the knowledge of source constellation [76, 16, 75]. Methods relying on source statistics inevitably need to collect a sufficiently large amount of received data to obtain an accurate statistics. This fact makes these methods inapplicable to fast-varying channels since the channel status may have changed significantly by the time the data is collected. On the other hand, the methods using the knowledge of source constellations usually rely on using a small constellation. When the constellation size is large, these methods become either inapplicable or computationally prohibitive. We propose a semiblind algorithm based on a combination of a pure pilot-assisted algorithm and the subspace-based blind channel estimation algorithm proposed in this chapter. The new semiblind algorithm is applicable with any source constellation and any pilot sample configuration and is suitable for fast-varying channels.

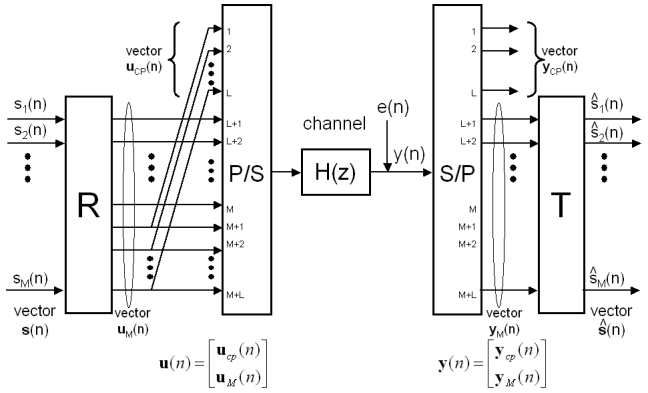

Figure 3.1: A typical cyclic prefix system.

The content of this chapter is mainly drawn from [60], and portions of it have been presented in [53, 52, 55].

3.1 Outline

The rest of the chapter is organized as follows. In Section 3.2 we review the basic ideas of subspace-based blind estimation methods in CP systems that have been reported so far in the literature [32, 21, 5]. In Section 3.3 we present the generalized blind algorithm.

In Section 3.4, we extend the idea to a semiblind algorithm by joint use of a purely pilot-assisted criterion and the blind criterion. In Section 3.5 we study in detail the conditions on input signal under which the proposed algorithm works properly.

In Section 3.6, simulations of the proposed blind algorithm are performed both in static and time-varying channel environments and the results are presented. We also conduct a performance comparison of the proposed blind algorithm, semiblind algorithm, and the purely pilot-assisted algorithm. Conclusions are made in Section 3.7.

3.2 Problem Formulation

3.2.1 Cyclic Prefix System Overview

Consider the communication system using cyclic prefixes (CP) depicted in Figure 3.1. The source symbols $s_1(n), s_2(n), ..., s_M(n)$ may come from M different users or from a serial-to-parallel operation on data of a single user. For convenience we consider the blocked version $\mathbf{s}(n)$ as indicated.

The vector $\mathbf{s}(n)$ is precoded by an $M \times M$ constant matrix $\mathbf{R}$ and results in precoded data $\mathbf{u}_M(n)$. In particular, for OFDM or multi-carrier (MC) systems, $\mathbf{R} = \mathbf{W}_M^{\dagger}$ is the normalized IDFT matrix; for single-carrier cyclic prefix (SC-CP) systems, $\mathbf{R}$ is chosen as $\mathbf{I}_M$. A cyclic prefix of length L, taking from the last L elements of $\mathbf{u}_M(n)$, is defined as $\mathbf{u}_{cp}(n) = \begin{bmatrix} \mathbf{0}_{L\times(M-L)} & \mathbf{I}_L \end{bmatrix} \mathbf{u}_M(n)$. We assume $L+1 < M$. The cyclic prefix is appended to $\mathbf{u}_M(n)$, forming a vector

$$\mathbf{u}(n) = \begin{bmatrix} \mathbf{u}_{cp}(n) \\ \mathbf{u}_M(n) \end{bmatrix} = [\mathbf{u}_M(n)]_{-L+1:M}$$

whose length is $P = M + L$. The vector $\mathbf{u}(n)$, after parallel-to-serial conversion, is sent over the channel $H(z)$. We assume $H(z)$ is an FIR channel with a maximum order L, i.e.,

$$H(z) = \sum_{k=0}^{L} h_k z^{-k}, \tag{3.1}$$

and define $\mathbf{h}$ as the $(L+1)$-column vector $\begin{bmatrix} h_0 & h_1 & \cdots & h_L \end{bmatrix}^T$. The signal is corrupted by channel noise $e(n)$. The received symbols $y(n)$ are blocked into $P \times 1$ vectors $\mathbf{y}(n)$. We assume perfect block synchronization between the transmitter and receiver. Also let $\mathbf{e}(n)$ denote the blocked version of the noise $e(n)$. Denote $\mathbf{y}_{cp}(n)$ as the first L entries and $\mathbf{y}_M(n)$ as the last M entries of $\mathbf{y}(n)$ so that $\mathbf{y}(n) = \begin{bmatrix} \mathbf{y}_{cp}(n)^T & \mathbf{y}_M(n)^T \end{bmatrix}^T$. It can be shown that

$$\mathbf{y}_M(n) = \mathbf{H}_{cir}\mathbf{u}_M(n) + \mathbf{e}_M(n), \tag{3.2}$$

where

$$\mathbf{H}_{cir} = \begin{bmatrix} h_0 & \mathbf{0} & h_L & \cdots & h_1 \\ \vdots & \ddots & \ddots & \ddots & \vdots \\ h_L & & \ddots & \ddots & h_L \\ & \ddots & & \ddots & \mathbf{0} \\ \mathbf{0} & & h_L & \cdots & h_0 \end{bmatrix}$$

is an $M \times M$ circulant matrix [67] and $\mathbf{e}_M(n) = [\mathbf{e}(n)]_{L+1:P}$ is the noise vector. The $L \times 1$ vector $\mathbf{y}_{cp}(n)$ contains inter-block interference (IBI) and can be expressed as

$$\mathbf{y}_{cp}(n) = \mathbf{H}_l\mathbf{u}_{cp}(n) + \mathbf{H}_u\mathbf{u}_{cp}(n-1) + \mathbf{e}_{cp}(n), \tag{3.3}$$

where

$$\mathbf{H}_l \triangleq \begin{bmatrix} h_0 & & \mathbf{0} \\ \vdots & \ddots & \\ h_{L-1} & \cdots & h_0 \end{bmatrix} \text{ and } \mathbf{H}_u \triangleq \begin{bmatrix} h_L & \cdots & h_1 \\ & \ddots & \vdots \\ \mathbf{0} & & h_L \end{bmatrix}$$

are $L \times L$ matrices and $\mathbf{e}_{cp}(n) = [\mathbf{e}(n)]_{1:L}$ is the noise component. For channel equalization, $\mathbf{y}_{cp}(n)$ is usually dropped and only $\mathbf{y}_M(n)$ passes the $M \times M$ equalizer $\mathbf{T}$ and results in recovered symbol $\hat{\mathbf{s}}(n)$. When the channel coefficients are known, the optimal equalizer $\mathbf{T}$ can be derived to minimize mean square error of equalized symbols.

3.2.2 Subspace-based Blind Channel Estimation in CP Systems

While $\mathbf{y}_{cp}(n)$ is often dropped before equalization, the information from $\mathbf{y}_{cp}(n)$ is useful to estimate the channel coefficients. In this section we review the essences of blind estimation algorithms which have been used in earlier methods reported in [5], [32], and [21]. For simplicity, we first ignore the noise term $\mathbf{e}(n)$. Define a *composite block* $\bar{\mathbf{y}}(n)$ which has a length $2M + L$ and contains information from two consecutive blocks as follows:

$$\bar{\mathbf{y}}(n) = \begin{bmatrix} \mathbf{y}_M(n-1)^T & \mathbf{y}_{cp}(n)^T & \mathbf{y}_M(n)^T \end{bmatrix}^T. \tag{3.4}$$

Then, from Eqs. (3.2) and (3.3) we have

$$\bar{\mathbf{y}}(n) = \begin{bmatrix} \mathbf{H}_{cir}\mathbf{u}_M(n-1) \\ \mathbf{H}_l\mathbf{u}_{cp}(n) + \mathbf{H}_u\mathbf{u}_{cp}(n-1) \\ \mathbf{H}_{cir}\mathbf{u}_M(n) \end{bmatrix} = \tilde{\mathbf{H}}\tilde{\mathbf{u}}(n), \tag{3.5}$$

where

$$\tilde{\mathbf{H}} = \left[\begin{array}{c|c} \mathbf{H}_{cir} & \mathbf{0}_{M\times M} \\ \hline \left[\begin{array}{c|c} \mathbf{0}_{L\times(M-L)} & \mathbf{H}_u \end{array}\right] & \left[\begin{array}{c|c} \mathbf{0}_{L\times(M-L)} & \mathbf{H}_l \end{array}\right] \\ \hline \mathbf{0}_{M\times M} & \mathbf{H}_{cir} \end{array}\right]$$

and $\tilde{\mathbf{u}}(n) = \left[\begin{array}{cc} \mathbf{u}_M(n-1)^T & \mathbf{u}_M(n)^T \end{array} \right]^T$. Note that $\tilde{\mathbf{H}}$ is a $(2M+L) \times 2M$ matrix. A special case of Eq. (3.5) when $M = 4$ and $L = 2$ is shown as

$$\left[\begin{array}{c} y_{01} \\ y_{02} \\ y_{03} \\ y_{04} \\ \hline y_{cp1} \\ y_{cp2} \\ \hline y_{11} \\ y_{12} \\ y_{13} \\ y_{14} \end{array}\right] = \left[\begin{array}{cccc|cccc} h_0 & 0 & h_2 & h_1 & 0 & 0 & 0 & 0 \\ h_1 & h_0 & 0 & h_2 & 0 & 0 & 0 & 0 \\ h_2 & h_1 & h_0 & 0 & 0 & 0 & 0 & 0 \\ 0 & h_2 & h_1 & h_0 & 0 & 0 & 0 & 0 \\ \hline 0 & 0 & h_2 & h_1 & 0 & 0 & h_0 & 0 \\ 0 & 0 & 0 & h_2 & 0 & 0 & h_1 & h_0 \\ \hline 0 & 0 & 0 & 0 & h_0 & 0 & h_2 & h_1 \\ 0 & 0 & 0 & 0 & h_1 & h_0 & 0 & h_2 \\ 0 & 0 & 0 & 0 & h_2 & h_1 & h_0 & 0 \\ 0 & 0 & 0 & 0 & 0 & h_2 & h_1 & h_0 \end{array}\right] \left[\begin{array}{c} u_{01} \\ u_{02} \\ u_{03} \\ u_{04} \\ \hline u_{11} \\ u_{12} \\ u_{13} \\ u_{14} \end{array}\right], \tag{3.6}$$

where we set $y_{0k} = [\mathbf{y}_M(n-1)]_k$, $y_{1k} = [\mathbf{y}_M(n)]_k$, and $y_{cpk} = [\mathbf{y}_{cp}(n)]_k$ for notational convenience.

Theorem 3.1: If $H(z) = \sum_{k=0}^{L} h_k z^{-k}$ does not have any zero on the unit circle grid $W_M^l, 0 \le l \le M-1$, then $\tilde{\mathbf{H}}$ has full column rank $2M$. □

Proof: See [32].

□

We now review some of the key ideas in [32]. Suppose we gather J consecutive received blocks $\mathbf{y}(0), \mathbf{y}(1), \cdots, \mathbf{y}(J-1)$ at the receiver. Then, we have $J-1$ composite blocks $\bar{\mathbf{y}}(n)$ defined in Eq.(3.4) for $n = 1, 2, ..., J-1$. We can construct the $(2M+L) \times (J-1)$ matrix by placing these composite blocks together as

$$\mathbf{Y}^{(J)} = \left[\begin{array}{cccc} \bar{\mathbf{y}}(1) & \bar{\mathbf{y}}(2) & \cdots & \bar{\mathbf{y}}(J-1) \end{array} \right].$$

Then, we have

$$\mathbf{Y}^{(J)} = \tilde{\mathbf{H}}\mathbf{U}^{(J)}, \tag{3.7}$$

where

$$\mathbf{U}^{(J)} = \left[\begin{array}{cccc} \tilde{\mathbf{u}}(1) & \tilde{\mathbf{u}}(2) & \cdots & \tilde{\mathbf{u}}(J-1) \end{array} \right]$$

is a $2M \times (J-1)$ matrix. Assume there exists an integer $J \geq 2M+1$ such that $\mathbf{U}^{(J)}$ has full row rank $2M$. Then, rank$(\mathbf{Y}^{(J)}) = 2M$ and, hence, $\mathbf{Y}^{(J)}$ has L linearly independent left annihilators. Let $\mathbf{g}_k^\dagger$ be the kth annihilator of $\mathbf{Y}^{(J)}, 1 \leq k \leq L$, i.e., $\mathbf{g}_k^\dagger \mathbf{Y}^{(J)} = \mathbf{0}$. Then, $\mathbf{g}_k^\dagger \tilde{\mathbf{H}} = \mathbf{0}$ since $\mathbf{U}^{(J)}$ has full rank. Write $\mathbf{g}_k^\dagger$ as

$$\mathbf{g}_k^\dagger = \left[\begin{array}{ccc|ccc|ccc} g_{01} & \cdots & g_{0M} & g_{c1} & \cdots & g_{cL} & g_{11} & \cdots & g_{1M} \end{array}\right].$$

For notational simplicity, we ignore the index k in the contents of $\mathbf{g}_k^\dagger$. By observing the columns of $\tilde{\mathbf{H}}$, we can construct a $2M \times (L+1)$ matrix $\mathcal{G}_k$ as follows such that $\mathcal{G}_k \mathbf{h} = \mathbf{0}$:

$$\mathcal{G}_k = \left[\begin{array}{cccc} g_{01} & g_{02} & \cdots & g_{0,1+L} \\ g_{02} & g_{03} & \cdots & g_{0,2+L} \\ \vdots & \vdots & & \vdots \\ g_{0,M-L} & g_{0,M-L+1} & \cdots & g_{0M} \\ \hline g_{0,M-L+1} & \cdots & g_{0M} & g_{01}+g_{c1} \\ \vdots & \iddots & \iddots & \vdots \\ g_{0M} & g_{01}+g_{c1} & \cdots & g_{0L}+g_{cL} \\ \hline g_{11} & g_{12} & \cdots & g_{1,1+L} \\ g_{12} & g_{13} & \cdots & g_{1,2+L} \\ \vdots & \vdots & & \vdots \\ g_{1,M-L} & g_{1,M-L+1} & \cdots & g_{1M} \\ \hline g_{1,M-L+1}+g_{c1} & \cdots & g_{1M}+g_{cL} & g_{11} \\ \vdots & \iddots & \iddots & \vdots \\ g_{1M}+g_{cL} & g_{11} & \cdots & g_{1L} \end{array}\right]. \tag{3.8}$$

Define $\mathcal{G} = \left[\begin{array}{cccc} \mathcal{G}_1^T & \mathcal{G}_2^T & \cdots & \mathcal{G}_L^T \end{array}\right]^T$. Then, the channel coefficients $\mathbf{h}$ can be recovered within a scalar ambiguity by finding the only right-annihilating vector of $\mathcal{G}$ [32].

Although the developments above are based on the assumption that $\tilde{\mathbf{H}}$ has full column rank (i.e., $H(z)$ has no zeros on DFT grid), a slight modification of the algorithm when this is not true can be found in [32]. Due to the length of the text, we do not elaborate this special case throughout this chapter.

In presence of noise, Eq. (3.7) becomes

$$\mathbf{Y}^{(J)} = \tilde{\mathbf{H}}\mathbf{U}^{(J)} + \mathbf{N}^{(J)},$$

where the noise component $\mathbf{N}^{(J)}$ comes accordingly from Eqs. (3.2) and (3.3). In this case, $\mathbf{Y}^{(J)}$ usually becomes full rank and no longer has L left annihilators. The left annihilators of $\tilde{\mathbf{H}}$, i.e., the noise space, can be estimated by taking singular value decomposition (SVD) of $\mathbf{Y}^{(J)}$. In the equation

$$\mathbf{Y}^{(J)} = \begin{bmatrix} \mathbf{U}_s & \mathbf{U}_n \end{bmatrix} \begin{bmatrix} \mathbf{\Sigma}_s & \mathbf{0} \\ \mathbf{0} & \mathbf{\Sigma}_n \end{bmatrix} \begin{bmatrix} \mathbf{V}_s & \mathbf{V}_n \end{bmatrix}^{\dagger}, \tag{3.9}$$

$\mathbf{U}_n$ contains the singular-vectors associated with the smallest L singular values of $\mathbf{Y}^{(J)}$ and $\mathbf{g}_k$ is chosen as the kth column of $\mathbf{U}_n$.

Note that in Eq. (3.9) if the matrix $\mathbf{Y}^{(J)}$ is replaced with the estimated autocorrelation matrix

$$\mathbf{R}_{\bar{\mathbf{y}}\bar{\mathbf{y}}} = \mathbf{Y}^{(J)}[\mathbf{Y}^{(J)}]^{\dagger}.$$

Then, the null space $\mathbf{U}_n$ obtained by singular value decomposition will remain unchanged. Since the size of $\mathbf{R}_{\bar{\mathbf{y}}\bar{\mathbf{y}}}$ is usually smaller than $\mathbf{Y}^{(J)}$, especially when J is large, taking SVD on $\mathbf{R}_{\bar{\mathbf{y}}\bar{\mathbf{y}}}$ rather than on $\mathbf{Y}^{(J)}$ actually saves computational complexity, although an additional computation will be needed for creating matrix $\mathbf{R}_{\bar{\mathbf{y}}\bar{\mathbf{y}}}$. However, the matrix $\mathbf{R}_{\bar{\mathbf{y}}\bar{\mathbf{y}}}$, once created, can be easily updated each time a new block is received (see Eq. (18) in [32]). The idea of maintaining an autocorrelation matrix further develops into a strategy where newer blocks can be put a greater weighting than older blocks. Specifically, after an initial estimate of $\mathbf{R}_{\bar{\mathbf{y}}\bar{\mathbf{y}}}$ is established, $\mathbf{R}_{\bar{\mathbf{y}}\bar{\mathbf{y}}}$ is updated each time a new composite block $\bar{\mathbf{y}}(n)$ is obtained using

$$\hat{\mathbf{R}}^{(N)}_{\bar{\mathbf{y}}\bar{\mathbf{y}}} = \alpha\hat{\mathbf{R}}^{(N-1)}_{\bar{\mathbf{y}}\bar{\mathbf{y}}} + (1-\alpha)\bar{\mathbf{y}}(N)\bar{\mathbf{y}}(N)^{\dagger}. \tag{3.10}$$

The parameter $\alpha \in [0, 1]$ is called the *forgetting factor*. The technique of using a forgetting factor has been applied especially in time-varying channel environments.

3.2.3 Limitations

In order for the above method to work, the $2M \times (J-1)$ matrix $\mathbf{U}^{(J)}$ must have full row rank $2M$. This is also known as the property of persistency of excitation[32]. Obviously, $\mathbf{U}^{(J)}$ has full row rank only when the number of columns is not smaller than the number of rows, i.e., $J - 1 \geq 2M$. This requires the receiver to wait for at least $(2M+1)P$ symbol durations before a channel esti-

mation can be performed. This limitation makes these previously reported algorithms unrealistic in environments with fast-fading channels since the channel coefficients may have changed significantly during accumulation of the data. Even though a forgetting factor can be used to give a larger weighting to newer blocks than to older blocks, the use of blocks as old as $2M + 1$ blocks earlier is still unavoidable. The method we propose in Sec. 3.3 will overcome this fundamental limit present in previously reported methods.

3.3 Proposed Method

For a subspace method, it is always necessary to write an equation

$$\mathbf{Y} = \mathbf{HU} + \mathbf{N} \tag{3.11}$$

or

$$\mathbf{R_y} = \mathbf{HR_u H}^\dagger + \mathbf{R_n}, \tag{3.12}$$

where $\mathbf{H}$ contains unknown information on the channel, $\mathbf{U}$ or $\mathbf{R_u}$ contain unknown information of transmitted symbols, and $\mathbf{Y}$ or $\mathbf{R_y}$ contain the noise-corrupted observation of received data. Note that Eq. (3.12) can always be obtained from Eq. (3.11) by setting $\mathbf{R_y} = \mathbf{YY}^\dagger$, $\mathbf{R_u} = \mathbf{UU}^\dagger$, and $\mathbf{R_n} = \mathbf{NN}^\dagger$, as long as the input symbols and the noise are uncorrelated. The following discussions will be focused on Eq. (3.11) only. In order to make the subspace method work, Eq. (3.11) must satisfy the following two conditions:

1. $\mathbf{H}$ must be a tall matrix. That is, if $\mathbf{H}$ has a size $p \times m$, then $p > m$.

2. $\mathbf{U}$ must have full row rank, i.e., rank$(\mathbf{U}) = m$.

The idea of accumulating two consecutive blocks and keeping the ISI-containing CP between the two blocks, as reviewed in the previous section, was actually intended to satisfy condition 1). To satisfy condition 2), the minimum number of blocks must be at least as large as the number of rows of $\mathbf{U}$, since each composite block $\bar{\mathbf{y}}(n)$ defined in Eq. (3.4) can at most increase the rank of $\mathbf{U}$ only by one (as can be seen in Eq. (3.7) and the equation after Eq. (3.7)).

In this section, we reformulate Eq. (3.11) in such a way that each new composite block $\bar{\mathbf{y}}(n)$ can increase the rank of $\mathbf{U}$ by more than one. By repeated use of the same blocks, the "speed" of rank growth of matrix $\mathbf{U}$ will be faster so that a smaller number of received blocks is needed to satisfy

condition 2). The idea of repeated use of the same blocks originated in the work of Pham and Manton [36] and was later generalized by Su and Vaidyanathan [49]. These developments were originally for ZP systems. We now show that for CP systems, similar extensions are possible. The generalized method works well in situations in which the previously reported methods [32, 5, 21] either fail or do not perform well, as we shall demonstrate next.

3.3.1 The Repetition Index

In this subsection, we will present the idea of repetition index. We will first present the development using an example with small values M and L.

We first rewrite Eq. (3.5) so that the channel matrix has a more symmetric and "tidy" form. The rearranged version of Eq. (3.5) is

$$\bar{\mathbf{y}}(n) = \bar{\mathbf{H}}\bar{\mathbf{u}}(n), \tag{3.13}$$

where

$$\bar{\mathbf{H}} = \left[\begin{array}{c|c} \mathbf{H}_{cir} & \mathbf{0}_{M\times M} \\ \hline \left[\begin{array}{c|c} \mathbf{0}_{L\times(M-L)} & \mathbf{H}_u \end{array}\right] & \left[\begin{array}{c|c} \mathbf{H}_l & \mathbf{0}_{L\times(M-L)} \end{array}\right] \\ \hline \mathbf{0}_{M\times M} & \mathbf{H}_{cir2} \end{array}\right],$$

$$\bar{\mathbf{u}}(n) = \begin{bmatrix} \mathbf{u}_M(n-1) \\ \mathbf{u}'_M(n) \end{bmatrix}, \text{ and } \mathbf{u}'_M(n) = [\mathbf{u}_M(n)]_{-L+1:M-L}\,.$$

$\mathbf{H}_{cir2}$ is obtained by permuting columns of $\mathbf{H}_{cir}$ and is still a circulant matrix. Note that this rewriting is simply to cut the last L columns of $\tilde{\mathbf{H}}$ and insert them into the middle. Accordingly, we permute elements of $\mathbf{u}_M(n)$ such that $\mathbf{u}'_M(n) = [\mathbf{u}_M(n)]_{-L+1:M-L}$. A special case of Eq. (3.13) when

$M = 4$ and $L = 2$ is shown as in

$$\left[\begin{array}{c} y_{01} \\ y_{02} \\ y_{03} \\ y_{04} \\ \hline y_{cp1} \\ y_{cp2} \\ \hline y_{11} \\ y_{12} \\ y_{13} \\ y_{14} \end{array}\right] = \left[\begin{array}{cccc|cccc} h_0 & 0 & h_2 & h_1 & 0 & 0 & 0 & 0 \\ h_1 & h_0 & 0 & h_2 & 0 & 0 & 0 & 0 \\ h_2 & h_1 & h_0 & 0 & 0 & 0 & 0 & 0 \\ 0 & h_2 & h_1 & h_0 & 0 & 0 & 0 & 0 \\ \hline 0 & 0 & h_2 & h_1 & h_0 & 0 & 0 & 0 \\ 0 & 0 & 0 & h_2 & h_1 & h_0 & 0 & 0 \\ \hline 0 & 0 & 0 & 0 & h_2 & h_1 & h_0 & 0 \\ 0 & 0 & 0 & 0 & 0 & h_2 & h_1 & h_0 \\ 0 & 0 & 0 & 0 & h_0 & 0 & h_2 & h_1 \\ 0 & 0 & 0 & 0 & h_1 & h_0 & 0 & h_2 \end{array}\right] \left[\begin{array}{c} u_{01} \\ u_{02} \\ u_{03} \\ u_{04} \\ \hline u_{13} \\ u_{14} \\ u_{11} \\ u_{12} \end{array}\right]. \tag{3.14}$$

This might give a clearer view of the structure of the channel matrix $\bar{\mathbf{H}}$. Observe that $\bar{\mathbf{H}}$ is nearly a Toeplitz matrix except for some sparse terms present in the top and bottom L rows. This Toeplitz-like structure of $\bar{\mathbf{H}}$ will become very useful in the following development. For the sake of clarity, the following developments will start from Eq. (3.14).

We take advantage of the property of circulant matrices. Notice that since

$$\left[\begin{array}{c} y_{01} \\ y_{02} \\ y_{03} \\ y_{04} \end{array}\right] = \left[\begin{array}{cccc} h_0 & 0 & h_2 & h_1 \\ h_1 & h_0 & 0 & h_2 \\ h_2 & h_1 & h_0 & 0 \\ 0 & h_2 & h_1 & h_0 \end{array}\right] \left[\begin{array}{c} u_{01} \\ u_{02} \\ u_{03} \\ u_{04} \end{array}\right],$$

we have

$$\begin{bmatrix} y_{03} \\ y_{04} \\ y_{01} \\ y_{02} \\ y_{03} \\ y_{04} \end{bmatrix} = \begin{bmatrix} h_2 & h_1 & h_0 & 0 \\ 0 & h_2 & h_1 & h_0 \\ h_0 & 0 & h_2 & h_1 \\ h_1 & h_0 & 0 & h_2 \\ h_2 & h_1 & h_0 & 0 \\ 0 & h_2 & h_1 & h_0 \end{bmatrix} \begin{bmatrix} u_{01} \\ u_{02} \\ u_{03} \\ u_{04} \end{bmatrix}$$

$$= \left[\begin{array}{cccc|cc} h_0 & 0 & h_2 & h_1 & 0 & 0 \\ h_1 & h_0 & 0 & h_2 & 0 & 0 \\ h_2 & h_1 & h_0 & 0 & 0 & 0 \\ 0 & h_2 & h_1 & h_0 & 0 & 0 \\ \hline 0 & 0 & h_2 & h_1 & h_0 & 0 \\ 0 & 0 & 0 & h_2 & h_1 & h_0 \end{array}\right] \begin{bmatrix} u_{03} \\ u_{04} \\ u_{01} \\ u_{02} \\ u_{03} \\ u_{04} \end{bmatrix}. \tag{3.15}$$

In general, we can show that if $\mathbf{y}_M(n-1) = \mathbf{H}_{cir}\mathbf{u}_M(n-1)$ is true, then we have

$$[\mathbf{y}_M(n-1)]_{1-k:M} = \begin{bmatrix} \mathbf{H}_{cir} & \mathbf{0}_{M\times k} \\ \mathbf{0}_{k\times(M-L)} & \mathcal{H}_k \end{bmatrix} [\mathbf{u}_M(n-1)]_{M:1-k} \tag{3.16}$$

for any $k \geq 0$. Here

$$\mathcal{H}_k = \begin{bmatrix} h_L & h_{L-1} & \cdots & h_0 & 0 & \cdots & 0 \\ 0 & h_L & h_{L-1} & \cdots & h_0 & \ddots & \vdots \\ \vdots & \ddots & \ddots & \ddots & & \ddots & 0 \\ 0 & \cdots & 0 & h_L & h_{L-1} & \cdots & h_0 \end{bmatrix} \tag{3.17}$$

is a $k \times (L+k)$ Toeplitz matrix. Eq. (3.15) was a special case when $k = 2$. Similarly if $\mathbf{y}_M(n) = \mathbf{H}_{cir2}\mathbf{u}'_M(n)$, then we have

$$[\mathbf{y}_M(n)]_{1:M+l} = \begin{bmatrix} \mathcal{H}_l & \mathbf{0}_{l\times(M-L)} \\ \mathbf{0}_{M\times l} & \mathbf{H}_{cir2} \end{bmatrix} [\mathbf{u}'_M(n)]_{1:M+l} \tag{3.18}$$

for any $l \geq 0$. Combining knowledge of Eqs. (3.16) and (3.18), we can "expand" the composite block $\bar{\mathbf{y}}(n)$ in Eq. (3.13) by k symbols upward and l symbols downward for any nonnegative integers k and l. If we choose k and l such that $k + l = Q - 1$ for some positive integer Q, we will be able to write a new channel equation as follows.

$$\bar{\mathbf{y}}_{kl}(n) = \bar{\mathbf{H}}_Q \bar{\mathbf{u}}_{kl}(n), \tag{3.19}$$

where

$$\bar{\mathbf{y}}_{kl}(n) = \begin{bmatrix} [\mathbf{y}_M(n-1)]_{-k+1:M} \\ \mathbf{y}_{cp}(n) \\ [\mathbf{y}_M(n)]_{1:M+l} \end{bmatrix},$$

$$\bar{\mathbf{H}}_Q = \begin{bmatrix} \mathbf{H}_{cir} & & \mathbf{0}_{M\times(M+Q-1)} \\ \mathbf{0}_{(L+Q-1)\times(M-L)} & \mathcal{H}_{L+Q-1} & \mathbf{0}_{(L+Q-1)\times(M-L)} \\ \mathbf{0}_{M\times(M+Q-1)} & & \mathbf{H}_{cir2} \end{bmatrix}, \tag{3.20}$$

and

$$\bar{\mathbf{u}}_{kl}(n) = \begin{bmatrix} [\mathbf{u}_M(n-1)]_{-k+1:M} \\ [\mathbf{u}'_M(n)]_{1:M+l} \end{bmatrix}.$$

Note that if we choose $Q = 1$, then $k = l = 0$ and Eq. (3.19) reduces to Eq. (3.13). Now, by combining cases when k is chosen from 0 to $Q-1$ (and so l from $Q-1$ to 0) in Eq. (3.19), we get

$$\mathbf{Y}_Q(n) = \bar{\mathbf{H}}_Q \mathbf{U}_Q(n), \tag{3.21}$$

where

$$\mathbf{Y}_Q(n) = \begin{bmatrix} \bar{\mathbf{y}}_{0,Q-1}(n) & \bar{\mathbf{y}}_{1,Q-2}(n) & \cdots & \bar{\mathbf{y}}_{Q-1,0}(n) \end{bmatrix}$$

is a $(2M+Q+L-1)\times Q$ matrix and

$$\mathbf{U}_Q(n) = \begin{bmatrix} \bar{\mathbf{u}}_{0,Q-1}(n) & \bar{\mathbf{u}}_{1,Q-2}(n) & \cdots & \bar{\mathbf{u}}_{Q-1,0}(n) \end{bmatrix} \tag{3.22}$$

is a $(2M+Q-1)\times Q$ matrix. A special case of Eq. (3.21) when $M = 4, L = 2$, and $Q = 3$ is shown as

$$\left[\begin{array}{ccc} y_{01} & y_{04} & y_{03} \\ y_{02} & y_{01} & y_{04} \\ y_{03} & y_{02} & y_{01} \\ y_{04} & y_{03} & y_{02} \\ \hline y_{cp1} & y_{04} & y_{03} \\ y_{cp2} & y_{cp1} & y_{04} \\ y_{11} & y_{cp2} & y_{cp1} \\ y_{12} & y_{11} & y_{cp2} \\ \hline y_{13} & y_{12} & y_{11} \\ y_{14} & y_{13} & y_{12} \\ y_{11} & y_{14} & y_{13} \\ y_{12} & y_{11} & y_{14} \end{array}\right] = \left[\begin{array}{cccc|cc|cccc} h_0 & 0 & h_2 & h_1 & 0 & 0 & 0 & 0 & 0 & 0 \\ h_1 & h_0 & 0 & h_2 & 0 & 0 & 0 & 0 & 0 & 0 \\ h_2 & h_1 & h_0 & 0 & 0 & 0 & 0 & 0 & 0 & 0 \\ 0 & h_2 & h_1 & h_0 & 0 & 0 & 0 & 0 & 0 & 0 \\ \hline 0 & 0 & h_2 & h_1 & h_0 & 0 & 0 & 0 & 0 & 0 \\ 0 & 0 & 0 & h_2 & h_1 & h_0 & 0 & 0 & 0 & 0 \\ 0 & 0 & 0 & 0 & h_2 & h_1 & h_0 & 0 & 0 & 0 \\ 0 & 0 & 0 & 0 & 0 & h_2 & h_1 & h_0 & 0 & 0 \\ \hline 0 & 0 & 0 & 0 & 0 & 0 & h_2 & h_1 & h_0 & 0 \\ 0 & 0 & 0 & 0 & 0 & 0 & 0 & h_2 & h_1 & h_0 \\ 0 & 0 & 0 & 0 & 0 & 0 & h_0 & 0 & h_2 & h_1 \\ 0 & 0 & 0 & 0 & 0 & 0 & h_1 & h_0 & 0 & h_2 \end{array}\right] \left[\begin{array}{ccc} u_{01} & u_{04} & u_{03} \\ u_{02} & u_{01} & u_{04} \\ u_{03} & u_{02} & u_{01} \\ u_{04} & u_{03} & u_{02} \\ \hline u_{13} & u_{04} & u_{03} \\ u_{14} & u_{13} & u_{04} \\ \hline u_{11} & u_{14} & u_{13} \\ u_{12} & u_{11} & u_{14} \\ u_{13} & u_{12} & u_{11} \\ u_{14} & u_{13} & u_{12} \end{array}\right]. \quad (3.23)$$

Note that Eq. (3.13) implies Eq. (3.21) without any additional assumptions. We can see this, for example, by verifying that Eq. (3.14) is equivalent to Eq. (3.23). This may provide more insight for Eq. (3.19). The new channel matrix $\bar{\mathbf{H}}_Q$ with a parameter Q maintains a Toeplitz-like structure plus some sparse components: two triangular-shaped "residues" in the top and bottom few rows. As Q increases, the Toeplitz component of $\bar{\mathbf{H}}_Q$ is elongated while the triangular-shaped components keep the same size. We call the parameter Q the *repetition index* since for each composite block $\bar{\mathbf{y}}(n)$ we can generate a matrix $\mathbf{Y}_Q(n)$ whose number of columns is Q.

Finally, if we accumulate J consecutive blocks ($J \geq 2$) $\mathbf{y}(n)$, $0 \leq n \leq J-1$, we have $J-1$ composite blocks $\bar{\mathbf{y}}(n)$, $1 \leq n \leq J-1$. Construct the $(2M+Q+L-1) \times Q(J-1)$ matrix

$$\mathbf{Y}_Q^{(J)} = \left[\begin{array}{cccc} \mathbf{Y}_Q(1) & \mathbf{Y}_Q(2) & \cdots & \mathbf{Y}_Q(J-1) \end{array}\right]. \quad (3.24)$$

Then, we have

$$\mathbf{Y}_Q^{(J)} = \bar{\mathbf{H}}_Q \mathbf{U}_Q^{(J)},$$

where

$$\mathbf{U}_Q^{(J)} = \left[\begin{array}{cccc} \mathbf{U}_Q(1) & \mathbf{U}_Q(2) & \cdots & \mathbf{U}_Q(J-1) \end{array}\right] \quad (3.25)$$

is a $(2M+Q-1) \times Q(J-1)$ matrix.

Theorem 3.2: $\bar{\mathbf{H}}_Q$ has full column rank $2M+Q-1$ if and only if $H(z)$ as defined in Eq. (3.1) does not have any zero at $z = W_M^l$, $0 \le l \le M-1$. □

Proof: If $H(W_M^l) = 0$ for some l, then

$$\begin{bmatrix} 1 & W_M^l & W_M^{2l} & \cdots & W_M^{l(2M+Q-2)} \end{bmatrix}^T$$

is a right annihilator of $\bar{\mathbf{H}}_Q$ and, hence, $\bar{\mathbf{H}}_Q$ does not have full rank. On the other hand, when $H(W_M^l) \neq 0$ for any l, suppose $\bar{\mathbf{H}}_Q$ does not have full rank. Then there exists a nonzero vector $\mathbf{v} = \begin{bmatrix} \mathbf{v}_{M1}^T & \mathbf{v}_{Q-1}^T & \mathbf{v}_{M2}^T \end{bmatrix}^T$ such that $\bar{\mathbf{H}}_Q\mathbf{v} = \mathbf{0}$. The lengths of $\mathbf{v}_{M1}$, $\mathbf{v}_{Q-1}$, and $\mathbf{v}_{M2}$ are M, $Q-1$, and M, respectively. Note that when $Q = 1$, the segment $\mathbf{v}_{Q-1}$ has a zero length (i.e., this segment simply does not exist). Observe that $\mathbf{H}_{cir}\mathbf{v}_{M1} = \mathbf{0}$. Since

$$\det(\mathbf{H}_{cir}) = \prod_{l=0}^{M-1} H(W_M^l) \neq 0,$$

we have $\mathbf{v}_{M1} = \mathbf{0}$. Similarly, $\mathbf{v}_{M2} = \mathbf{0}$ since $\det(\mathbf{H}_{cir2}) \neq 0$. If $Q = 1$, this already leads to a contradiction. In the case when $Q > 1$, $\bar{\mathbf{H}}_Q\mathbf{v} = \mathbf{0}$ implies $\mathcal{T}_{Q-1}(\mathbf{h})\mathbf{v}_{Q-1} = \mathbf{0}$ (see Eq. (1.1) for definition of notation $\mathcal{T}_{Q-1}(\mathbf{h})$). But $\mathcal{T}_{Q-1}(\mathbf{h})$ has full rank, so $\mathbf{v}_{Q-1}$ must also be zero. This contradicts the fact that $\mathbf{v}$ is nonzero, and so $\bar{\mathbf{H}}_Q$ must have full column rank.

□

Note that when $Q = 1$, Theorem 3.2 reduces to Theorem 1. Theorem 3.2 states that the necessary and sufficient conditions for $\bar{\mathbf{H}}_Q$ to have full column rank does not change whatever the repetition index Q we use. Assume the channel $H(z)$ does not have zeros at $z = W_M^l$ for any l. Then, $\bar{\mathbf{H}}_Q$ has full column rank $2M+Q-1$. This assumption is usually reasonable since the probability that a channel $H(z)$ has a zero exactly at $z = W_M^l$ is zero. We also assume that there exists J such that $\mathbf{U}_Q^{(J)}$ achieves full row rank $2M+Q-1$. Under these two assumptions, we obtain that the $(2M+L+Q-1)$-row matrix $\mathbf{Y}_Q^{(J)}$ has rank $2M+Q-1$. This means there exist L linearly independent vectors $\mathbf{g}_k, 1 \le k \le L$ such that

$$\mathbf{g}_k^\dagger \mathbf{Y}_Q^{(J)} = \mathbf{0}^T. \tag{3.26}$$

Since $\mathbf{U}_Q^{(J)}$ has full row rank, these vectors $\mathbf{g}_k^\dagger$ are also annihilators of $\bar{\mathbf{H}}_Q$.

For each annihilator $\mathbf{g}_k^\dagger$ of $\bar{\mathbf{H}}_Q$, we can construct a $(2M+Q-1) \times (L+1)$ matrix $\mathcal{G}_k$ in a way

similar to Eq. (3.8) in Section 3.2 such that

$$\mathcal{G}_k \mathbf{h} = \mathbf{0}. \tag{3.27}$$

The construction of $\mathcal{G}_k$ is conceptually easy. We simply inspect each column of $\bar{\mathbf{H}}_Q$ and find locations of each channel coefficient $h_i, 0 \leq i \leq L$. For example, in the special case where $M = 4, L = 2$, and $Q = 3$, the structure of $\mathcal{G}_k$ is given as

$$\mathcal{G}_k = \begin{bmatrix} g_{k1} & g_{k2} & g_{k3} \\ g_{k2} & g_{k3} & g_{k4} \\ g_{k3} & g_{k4} & g_{k5} + g_{k1} \\ g_{k4} & g_{k5} + g_{k1} & g_{k6} + g_{k2} \\ g_{k5} & g_{k6} & g_{k7} \\ g_{k6} & g_{k7} & g_{k8} \\ g_{k7} + g_{k,11} & g_{k8} + g_{k,12} & g_{k9} \\ g_{k8} + g_{k,12} & g_{k9} & g_{k,10} \\ g_{k9} & g_{k,10} & g_{k,11} \\ g_{k,10} & g_{k,11} & g_{k,12} \end{bmatrix},$$

where g_{kl} denotes the lth element of $\mathbf{g}_k^\dagger$. A systematic way of construction of $\mathcal{G}_k$ is given as follows.

First note that $\bar{\mathbf{H}}_Q = \mathcal{H}_{2M+Q+L-1}\mathbf{A}$, where the notation $\mathcal{H}_k$ was defined in Eq. (3.17) and $\mathbf{A}$ is a sparse matrix defined as follows.

$$\mathbf{A} = \begin{bmatrix} \mathbf{A}_1^T & \mathbf{I}_{2M+Q-1} & \mathbf{A}_2^T \end{bmatrix}^T,$$

where

$$\mathbf{A}_1 = \begin{bmatrix} \mathbf{0}_{L\times(M-L)} & \mathbf{I}_L & \mathbf{0}_{L\times(M+Q-1)} \end{bmatrix}$$

and

$$\mathbf{A}_2 = \begin{bmatrix} \mathbf{0}_{L\times(M+Q-1)} & \mathbf{I}_L & \mathbf{0}_{L\times(M-L)} \end{bmatrix}.$$

Now we have

$$\begin{aligned}\mathbf{0}^T = \mathbf{g}_k^\dagger \bar{\mathbf{H}}_Q &= \mathbf{g}_k^\dagger \mathcal{H}_{2M+Q+L-1}\mathbf{A} \\ &= \begin{bmatrix} h_L & \cdots & h_0 \end{bmatrix} \mathcal{T}_{L+1}^T(\mathbf{g}_k^\dagger)\mathbf{A} \\ &= \mathbf{h}^T \mathbf{G}_k \mathbf{A},\end{aligned}$$

where $\mathbf{G}_k = \mathcal{K}_{L+1}([\mathbf{0}_{1\times L}, (\mathbf{g}_k^\dagger)^T, \mathbf{0}_{1\times L}])$ is a Hankel matrix (see Eq. (1.2) for definition of the notation) composed of elements of $\mathbf{g}_k^\dagger$. Now, by simply choosing

$$\mathcal{G}_k = \mathbf{A}^T \mathbf{G}_k^T,$$

Eq. (3.27) is satisfied. By defining

$$\mathcal{G} = \begin{bmatrix} \mathcal{G}_1^T & \mathcal{G}_2^T & \cdots & \mathcal{G}_L^T \end{bmatrix}^T, \tag{3.28}$$

we now have $\mathcal{G}\mathbf{h} = \mathbf{0}$. The channel coefficients $\mathbf{h}$ can be identified within a scalar ambiguity.

In presence of noise, the estimated annihilators $\mathbf{g}_k^\dagger$ can be found by taking SVD on $\mathbf{Y}_Q^{(J)}$ and choosing the L singular vectors associated with the L smallest singular values (similar to the description after Eq. (3.9)). Also, after constructing the $\mathcal{G}$ matrix, we use the vector $\mathbf{h}$ which minimizes the norm of $\mathcal{G}\mathbf{h}$ as the estimated channel coefficients. This optimal estimation can be written as

$$\hat{\mathbf{h}} = \arg \min_{||\mathbf{h}||=1} ||\mathcal{G}\mathbf{h}||^2 = \arg \min_{||\mathbf{h}||=1} \mathbf{h}^\dagger (\mathcal{G}^\dagger \mathcal{G})\mathbf{h}. \tag{3.29}$$

3.3.2 Necessary Condition for Persistency of Excitation

Recall that the matrix $\mathbf{U}_Q^{(J)}$ defined in Eq. (3.25) must have full row rank. If $\mathbf{U}_Q^{(J)}$ does not have full rank, some annihilators of $\mathbf{Y}_Q^{(J)}$ as defined in Eq. (3.26) may not be annihilators of $\bar{\mathbf{H}}_Q$ and will result in failure of the proposed algorithm. Since $\mathbf{U}_Q^{(J)}$ has size $(2M+Q-1)\times(J-1)Q$, it has full row rank only when

$$(J-1)Q \geq 2M + Q - 1, \tag{3.30}$$

or

$$Q \geq \frac{2M-1}{J-2}. \tag{3.31}$$

This necessary condition for $\mathbf{U}_Q^{(J)}$ to have full row rank $(2M+Q-1)$ is not sufficient since it still depends on the values of transmitted symbols $\mathbf{u}_M(n)$. However, simulations in Section 3.5 show that (for most choices of M and input constellations) once inequality (3.31) is satisfied, the probability that $\mathbf{U}_Q^{(J)}$ has full rank is very close to unity. Thus,

$$Q = \left\lceil \frac{2M-1}{J-2} \right\rceil \tag{3.32}$$

is usually a valid choice in practice. A detailed study on the conditions of $\mathbf{U}_Q^{(J)}$ having full rank is presented in Section 3.5. Now, if we choose

$$J \geq 3,$$

then there exists Q such that $\mathbf{U}_Q^{(J)}$ can possibly have full rank. This suggests that the proposed algorithm is *potentially capable of identifying the channel from only three blocks*. In Section 3.6 we will demonstrate these with examples.

3.3.3 Repetition Index for the Forgetting Factor

The idea of using a repetition index Q can also be applied when a forgetting factor is used. The technique of using a forgetting factor has been reviewed in Section 3.2 right before Eq. (3.10). The "autocorrelation matrix" $\mathbf{R}_{\bar{\mathbf{y}}\bar{\mathbf{y}},Q}^{(0)}$ is initiated as $\mathbf{R}_{\bar{\mathbf{y}}\bar{\mathbf{y}},Q}^{(0)} = \mathbf{0}$ and updated each time when a new composite block $\bar{\mathbf{y}}(N-1)$ is received as

$$\mathbf{R}_{\bar{\mathbf{y}}\bar{\mathbf{y}},Q}^{(N)} = \alpha \mathbf{R}_{\bar{\mathbf{y}}\bar{\mathbf{y}},Q}^{(N-1)} + (1-\alpha)\mathbf{Y}_Q(N-1)[\mathbf{Y}_Q(N-1)]^\dagger, \tag{3.33}$$

where $\alpha \in [0,1]$ is the forgetting factor. The SVD of $\mathbf{R}_{\bar{\mathbf{y}}\bar{\mathbf{y}},Q}^{(N)}$ is then taken, and the estimated annihilators $\mathbf{g}_k^\dagger$ chosen as the singular vectors associated with the smallest L singular values of $\mathbf{R}_{\bar{\mathbf{y}}\bar{\mathbf{y}},Q}^{(N)}$. Note that N must satisfy $N \geq (2M+Q-1)/Q$ to render $\mathbf{R}_{\bar{\mathbf{y}}\bar{\mathbf{y}},Q}^{(N)}$ full rank. This means the first channel estimation after initialization can be requested only when $N \geq (2M+Q-1)/Q$. After this, an estimation can be requested at any time instant N.

3.3.4 Summary of the Proposed Algorithm

The proposed algorithm can be summarized as follows:

1. Given M and the CP length L, choose J and the repetition index Q such that

$$Q \geq \frac{2M-1}{J-2}.$$

   Some remarks on choosing a good pair of J and Q will be presented in Section 3.6.

2. Collect J blocks $\mathbf{y}(n)$ at the receiver and construct a $(2M+L+Q-1)\times(J-1)Q$ matrix $\mathbf{Y}_Q^{(J)}$ as defined in Eq. (3.24). Let $\mathbf{Z} = \mathbf{Y}_Q^{(J)}\mathbf{Y}_Q^{(J)\dagger}$.

3. Perform SVD on $\mathbf{Z}$ so that

$$\mathbf{Z} = \begin{bmatrix} \mathbf{U}_s & \mathbf{U}_n \end{bmatrix} \begin{bmatrix} \mathbf{\Sigma}_s & \mathbf{0} \\ \mathbf{0} & \mathbf{\Sigma}_n \end{bmatrix} \begin{bmatrix} \mathbf{U}_s^\dagger \\ \mathbf{U}_n^\dagger \end{bmatrix},$$

   where the diagonal entries of $\mathbf{\Sigma}_n$ are the L smallest singular values of $\mathbf{Z}$.

4. Let $\mathbf{g}_k$ be chosen as the kth column of $\mathbf{U}_n$. Construct the $(2M+Q-1)L\times(L+1)$ matrix $\mathcal{G}$ as in Eq. (3.28).

5. Let $\hat{\mathbf{h}}$ be the eigenvector of $\mathcal{G}^\dagger\mathcal{G}$ associated with the smallest eigenvalue. This is the estimated channel vector within a scalar ambiguity.

When a forgetting factor is used, steps 1 and 2 are modified as follows.

1. Choose $\alpha \in [0,1]$ and the repetition index Q. Some remarks of choosing a good α will be presented in Section 3.6.

2. Update the "autocorrelation matrix" $\mathbf{R}_{\bar{\mathbf{y}}\bar{\mathbf{y}},Q}^{(N)}$ as received blocks are accumulated. Choose $\mathbf{Z} = \mathbf{R}_{\bar{\mathbf{y}}\bar{\mathbf{y}},Q}^{(N)}$ as defined in Eq. (3.33), where N is the block index when a channel estimation is requested.

3.3.5 System Complexity

The computational complexity of the proposed algorithm is dominated by the SVD of the matrix $\mathbf{Z}$, whose size is $2M+Q+L-1$. The computational complexity is proportional to $\mathcal{O}((2M+Q+L-1)^3)$.

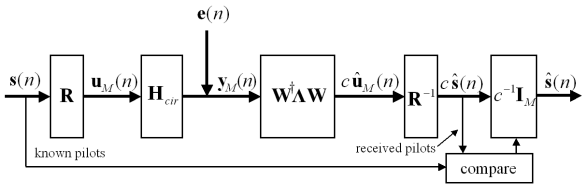

Figure 3.2: The transceiver system equipped with a method to resolve scale-factor ambiguity.

A larger repetition index Q leads to a greater complexity. However, when M and L are much larger than Q, this complexity increase due to increase of Q is not very serious. On the other hand, if Q is chosen as large as $2M-1$ (e.g., when $J=3$), the complexity increase can be significant.

3.3.6 Equalization and Resolving the Scalar Ambiguity

After estimating the channel coefficients, the receiver proceeds to equalize the effects of the frequency-selective channels. A standard linear minimum mean square error (L-MMSE) equalizer is used at the receiver. Figure 3.2 depicts the equalizer structure of the system. Here, $\mathbf{\Lambda}$ is a diagonal matrix whose kth diagonal entry is

$$\mathbf{\Lambda}_{k,k} = \frac{E_s \hat{H}^*(W_M^k)}{E_s|\hat{H}(W_M^k)|^2 + N_0}, \tag{3.34}$$

where E_s is the average energy of transmitted symbols, N_0 is the channel noise variance, and $\hat{H}(W_M^k) = \sum_{l=0}^{L}[\hat{\mathbf{h}}]_l {W_M}^{-kl}$ is the frequency response of the estimated channel. Since there is a scalar ambiguity in the estimated channel coefficients, all equalized symbols will be scaled by an unknown complex-valued scalar c. A usual way to resolve this scalar is to introduce *one* extra pilot symbol and compare it with the corresponding received symbol. If several blocks are using the same channel estimate $\hat{\mathbf{h}}$, the scalar ambiguity can be estimated as follows:

$$\hat{c} = \arg\min_{c\in\mathbb{C}} \sum_n ||s_{rec}(n) - c s_{pil}(n)||^2 \tag{3.35}$$

$$= \frac{\sum_n s_{pil}^*(n) s_{rec}(n)}{\sum_n |s_{pil}(n)|^2}, \tag{3.36}$$

where $s_{pil}(n)$ is the pilot symbol of the nth block and $s_{rec}(n)$ is the corresponding received pilot. We set the first symbol of each source block $\mathbf{s}(n)$ as the known symbol (i.e., $s_{pil}(n) = [\mathbf{s}(n)]_1$) defined as

$$s_{pil}(n) = \sqrt{E_s} p_{(n \bmod 4)},$$

where $\begin{bmatrix} p_0 & p_1 & p_2 & p_3 \end{bmatrix} = \begin{bmatrix} 1 & j & -j & -1 \end{bmatrix}$. There are definitely many other alternative designs of these pilot symbols. The choice here is just to make sure that $\mathbf{U}_Q^{(J)}$ defined in Eq. (3.25) would not become rank deficient due to the introduction of these pilot symbols.

3.4 Semi-Blind Channel Estimation in OFDM Systems

In this section, we extend the blind algorithm proposed above into a semiblind scenario. That is, we assume there are some pilot samples at the transmitter that are known to the receiver. Specifically, we study the special case when $\mathbf{R} = \mathbf{W}_M^{\dagger}$, where the CP system become an OFDM system. In traditional pilot-assisted transmission, channel estimation is done by comparing the pilot samples with the corresponding received pilots. In this section, we will develop a semiblind technique that involves the blind technique proposed above and see how this can help improve system performance.

3.4.1 Problem Formulation

Figure 3.3 shows a cyclic prefix (CP)-based OFDM system. It is a special case of Figure 3.1 where the precoder $\mathbf{R}$ is set as the normalized inverse Fourier transform (IDFT) matrix. From (3.2), it can be shown that

$$\mathbf{y}_M(n) = \mathbf{H}_{cir}\mathbf{u}_M(n) + \text{ noise.}$$

The vector $\mathbf{y}_M(n)$ goes through an FFT operation and $\mathbf{x}(n)$ is obtained. Using the property that the DFT matrix $\mathbf{W}_M$ diagonalizes circulant matrices, the relationship of vectors $\mathbf{x}(n)$ and $\mathbf{s}(n)$ can be written as

$$\mathbf{x}(n) = \text{diag}(\mathbf{s}(n)) \begin{bmatrix} H(e^{j0}) \\ H(e^{j2\pi/M}) \\ \vdots \\ H(e^{j2\pi(M-1)/M}) \end{bmatrix} + \text{ noise.} \tag{3.37}$$

Suppose some samples of $\mathbf{s}(n)$ are chosen as pilot samples known to the receiver and do not carry user information. Specifically, define the set of pilot indices

$$\mathcal{C}_{pil} = \{(m,n)\,|0 \le m \le M-1, n \ge 0, s_m(n) \text{ is known}\}.$$

Consider the case where each channel estimate is obtained by using J consecutive received blocks

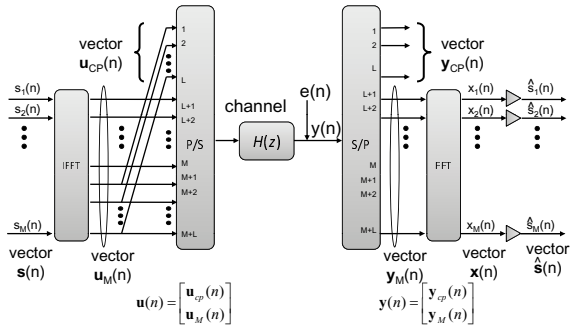

Figure 3.3: A CP-based orthogonal frequency division multiplexing (OFDM) system.

$\mathbf{y}(n)$, $n = t, t+1, ..., t+J-1$. Let

$$\mathcal{C}^{(t,J)} = \{(n,m) | t \le n \le t+J-1, 0 \le m \le M-1\}$$

and let $\mathcal{C}_{pil}^{(t,J)} = \mathcal{C}_{pil} \bigcap \mathcal{C}^{(t,J)}$ be the pilot indices in the J blocks. Suppose $\mathcal{C}_{pil}^{(t,J)}$ has a size K, and denote the kth element of $\mathcal{C}_{pil}^{(t,J)}$ as (n_k, m_k). Let

$$\mathbf{s}_{pil} = \begin{bmatrix} s_{m_1}(n_1) & s_{m_2}(n_2) & \cdots & s_{m_K}(n_K) \end{bmatrix}^T \tag{3.38}$$

be the vector containing all pilot samples in these J blocks. The problem can be formulated as follows. Given J received blocks $\mathbf{y}(n), n = t, t+1, ..., t+J-1$, $\mathbf{s}_{pil}$, and $\mathcal{C}_{pil}^{(t,J)}$, how do we estimate the channel coefficients $\mathbf{h}$?

The proposed semi-blind algorithm presented in this section is a combination of a pure pilot-assisted algorithm and the blind channel estimation algorithm proposed previously in this chapter. We will first review the pure pilot-assisted algorithm and then present the proposed algorithm. As shown in Figure 3.4, all received samples, including the CP parts, will be used for a blind estimation procedure. After FFT operation, received samples at the pilot positions will be used for pilot-assisted estimation. These results will be combined to obtain an even more accurate estimate than both the blind and the pure pilot-assisted algorithms.

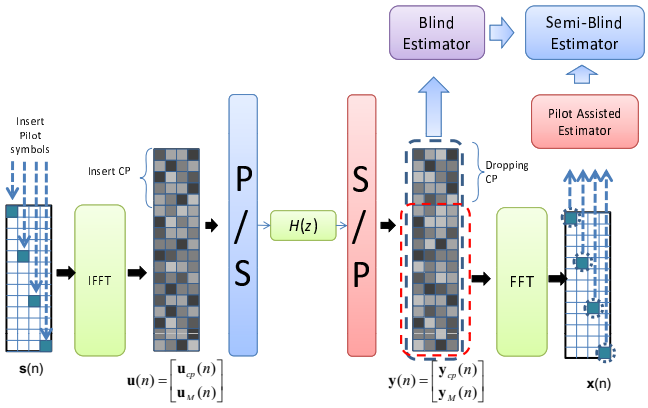

Figure 3.4: Illustration of the approach of the proposed semi-blind estimation algorithm.

3.4.2 Pure pilot-Assisted Channel Estimation

A pure pilot-assisted channel estimation method can be deployed (see [63] and the references therein). From (3.37), it is readily verified that

$$\mathbf{x}(n) \quad = \quad \sqrt{M}\text{diag}(\mathbf{s}(n))\mathbf{W}_{M,L+1}\mathbf{h} + \text{ noise}, \tag{3.39}$$

where $\mathbf{W}_{M,L+1}$ is an $M \times (L+1)$ matrix composed of the first $(L+1)$ columns of $\mathbf{W}_M$. Let $\mathbf{s}_{pil}$ be the pilot sample vector defined as in (3.38) and

$$\mathbf{x}_{pil} = \left[\begin{array}{cccc} x_{m_1}(n_1) & x_{m_2}(n_2) & \cdots & x_{m_K}(n_K) \end{array} \right] \tag{3.40}$$

be the corresponding received pilot samples. Then from (3.39), we have

$$\mathbf{x}_{pil} = \text{diag}(\mathbf{s}_{pil})\mathbf{F}_{pil}\mathbf{h} + \text{ noise},$$

where $\mathbf{F}_{pil}$ is a $K \times (L+1)$ matrix whose kth row is the m_kth row of $\mathbf{W}_{M,L+1}$ and can be expressed as

$$\left[\begin{array}{cccc} 1 & e^{-j2\pi m_k/M} & \cdots & e^{-j2\pi m_k L/M} \end{array} \right]. \tag{3.41}$$

A least-square estimate of $\mathbf{h}$ is given by

$$\hat{\mathbf{h}} = \arg\min_{\mathbf{h}} ||\mathbf{x}_{pil} - \text{diag}(\mathbf{s}_{pil})\mathbf{F}_{pil}\mathbf{h}||^2.$$

3.4.3 Proposed Algorithm

Note that the blind channel estimation algorithm proposed in Section 3.3 does not impose any constraints on the input samples $\mathbf{s}(n)$ except for the requirement that $\mathbf{U}_Q^{(J)}$ as defined in (3.25) must have full rank. This property is an advantage in adaption in semi-blind schemes: the positions of pilot samples can be freely chosen, and their values do not have to be selected from a given constellation. A semi-blind estimation technique can be devised by using both the information obtained from the blind method and the pilot-assisted method described above. Specifically, we can use the following expression as the objective function for channel estimation:

$$||\mathbf{x}_{pil} - \text{diag}(\mathbf{s}_{pil})\mathbf{F}_{pil}\mathbf{h}||^2 + \beta||\mathcal{G}\mathbf{h}||^2, \tag{3.42}$$

where $\beta \geq 0$ is a constant which can be adjusted according to how much we are relying on the information obtained from blind method and from pilot-assisted method, respectively. The proposed semi-blind algorithm is summarized as follows.

1. Collect J consecutive blocks $\mathbf{y}(n), n = t, t+1, ..., t+J-1$ at the receiver, and construct a $(2M+L+Q-1) \times (J-1)Q$ matrix $\mathbf{Y}_Q^{(J)}$ as defined in (3.24).

2. Perform SVD on $\mathbf{Y}_Q^{(J)}$ so that

$$\mathbf{Y}_Q^{(J)} = \begin{bmatrix} \mathbf{U}_s & \mathbf{U}_n \end{bmatrix} \begin{bmatrix} \mathbf{\Sigma}_s & \mathbf{0} \\ \mathbf{0} & \mathbf{\Sigma}_n \end{bmatrix} \begin{bmatrix} \mathbf{V}_s^\dagger \\ \mathbf{V}_n^\dagger \end{bmatrix},$$

   where the diagonal entries of $\mathbf{\Sigma}_n$ are the L smallest singular values of $\mathbf{Y}_Q^{(J)}$.

3. Let $\mathbf{g}_k$ be chosen as the kth column of $\mathbf{U}_n$. Construct the $(2M+Q-1)L \times (L+1)$ matrix $\mathcal{G}$ as in (3.28).

4. Collect the received pilot samples and form the vector $\mathbf{x}_{pil}$ as defined in (3.40). Also construct vector $\mathbf{s}_{pil}$ and matrix $\mathbf{F}_{pil}$ as defined in (3.38) and (3.41), respectively.

5. Take the estimate $\hat{\mathbf{h}}$ to be the value of $\mathbf{h}$ which minimizes the objective function defined in (3.42), that is,

$$\hat{\mathbf{h}} = \arg\min_{\mathbf{h}} \left(||\mathbf{x}_{pil} - \text{diag}(\mathbf{s}_{pil})\mathbf{F}_{pil}\mathbf{h}||^2 + \beta||\mathcal{G}\mathbf{h}||^2 \right). \tag{3.43}$$

3.5 On The Probability That $\mathbf{U}_Q^{(J)}$ Has Full Rank

Before presenting simulation results which demonstrate the performance of the above algorithms, we discuss the technical issue of rank requirement of the matrix $\mathbf{U}_Q^{(J)}$ defined in Eq. (3.25) in greater detail.

Recall that one assumption for the proposed algorithm is that the $(2M+Q-1)\times Q(J-1)$ matrix $\mathbf{U}_Q^{(J)}$ must have full row rank. Inequality (3.31) is a necessary condition but is not sufficient since whether $\mathbf{U}_Q^{(J)}$ has full rank or not ultimately depends on the content of $\mathbf{U}_Q^{(J)}$. As long as the contents of $\mathbf{U}_Q^{(J)}$ are chosen from a finite constellation, then there is always a nonzero probability that $\mathbf{U}_Q^{(J)}$ is rank-deficient. To see this, simply consider the extreme case where the contents of $\mathbf{U}_Q^{(J)}$ are always chosen as identical symbols. All subspace-based blind methods suffer from the possibility of rank deficiency of the data matrix. In this section we will study how this probability of rank deficiency changes when J and Q change. To facilitate our discussion, we formally define the probability of $\mathbf{U}_Q^{(J)}$ having full rank as follows.

Definition 3.1: Consider a constellation $\mathcal{S}$ (which has at least two elements) and an $M\times M$ nonsingular precoder $\mathbf{R}$. Let each element of the $M\times J$ matrix $\mathbf{S}=\left[\begin{array}{cccc}\mathbf{s}(0) & \mathbf{s}(1) & \cdots & \mathbf{s}(J-1)\end{array}\right]$ be independently selected from the constellation $\mathcal{S}$ with equal probabilities. Let $\mathbf{u}_M(n)=\mathbf{R}\mathbf{s}(n)$, and let $\mathbf{U}_Q^{(J)}$ be defined as in Eq. (3.25). For $J\geq 2, Q\geq 1$, the probability that $\mathbf{U}_Q^{(J)}$ has full rank will be denoted as $P_{\mathcal{S},\mathbf{R}}(J,Q)$. □

□

Obviously, $P_{\mathcal{S},\mathbf{R}}(J,Q)=0$ whenever $(J-2)Q<2M-1$. Also, we have $P_{\mathcal{S},\mathbf{R}}(J+1,Q)\geq P_{\mathcal{S},\mathbf{R}}(J,Q)$ and $P_{\mathcal{S},\mathbf{R}}(J,Q+1)\geq P_{\mathcal{S},\mathbf{R}}(J,Q)$. The former inequality comes from the fact that the row rank of a matrix never decreases when additional columns are appended, and the latter can be verified by the following theorem. These inequalities show that both increasing J and increasing Q have the potential to increase the probability that $\mathbf{U}_Q^{(J)}$ has full rank.

Theorem 3.3: If $\mathbf{U}_Q^{(J)}$ has full row rank $(2M+Q-1)$, then $\mathbf{U}_{Q+1}^{(J)}$ also has full row rank $(2M+Q)$. □

Proof: See Appendix 3.8.1.

□

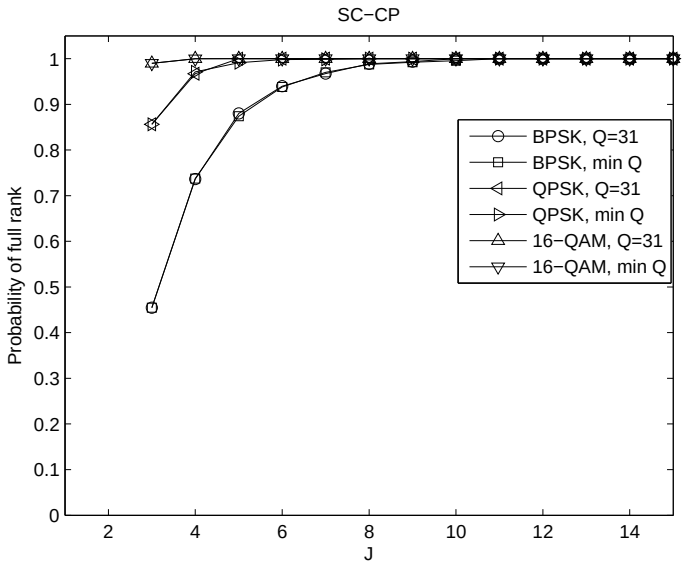

Figure 3.5: The probability of $\mathbf{U}_Q^{(J)}$ having full rank in SC-CP systems.

When J approaches infinity, it can be shown that $\lim_{J\to\infty} P_{\mathcal{S},\mathbf{R}}(J,Q) = 1$ for any constellation $\mathcal{S}$ and precoder $\mathbf{R}$ (and any $Q \geq 1$). However, this is not the case when we increase Q. The probability of full rank of $\mathbf{U}_Q^{(J)}$ always stops increasing when $Q \geq 2M-1$, which can be verified by the following theorem.

Theorem 3.4: If $\mathbf{U}_Q^{(J)}$ does not have full rank when $Q = 2M-1$, then $\mathbf{U}_Q^{(J)}$ does not have full rank for any Q. □

Proof: See Appendix 3.8.1.

□ Combining Theorems 3.3 and 3.4, we immediately have

$$P_{\mathcal{S},\mathbf{R}}(J,Q) = P_{\mathcal{S},\mathbf{R}}(J,2M-1)$$

for any $Q \geq 2M-1$.

We perform simulations with three commonly used constellations in communications: BPSK, QPSK, and 16-QAM. The $M \times M$ precoder $\mathbf{R}$ is chosen as $\mathbf{I}_M$ for SC-CP systems and $\mathbf{W}^\dagger$ for OFDM systems. Although the exact probability of $\mathbf{U}_Q^{(J)}$ having full rank can be actually obtained by testing all possible transmitted data, an exhaustive simulation is barely feasible. For each $J \geq 3$, the simulations are performed under two values of $Q = 2M-1$ and $Q = \lceil (2M-1)/(J-2) \rceil$. When

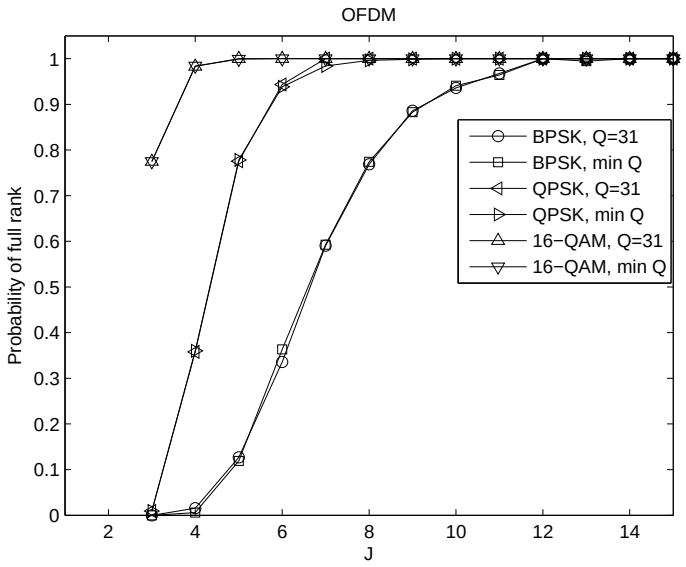

Figure 3.6: The probability of $\mathbf{U}_Q^{(J)}$ having full rank in OFDM systems.

$Q = 2M - 1$, the simulation gives an upper bound of $P_{\mathcal{S},\mathbf{R}}(J, Q)$ for a given J, and the simulation where $Q = \lceil (2M-1)/(J-2) \rceil$ gives a lower bound of nonzero $P_{\mathcal{S},\mathbf{R}}(J, Q)$. M is chosen as 16.

Figures 3.5 and 3.6 show the results when the precoder is chosen as an identity matrix and an IDFT matrix, respectively. Some comments on these results are made below.

1. As expected, the probability of $\mathbf{U}_Q^{(J)}$ having full rank is smaller when a smaller constellation is used or when J is smaller. When $J \geq 12$, the probability becomes very close to unity for all combinations of constellations and precoders. When a 16-QAM constellation is used, the probability is already very high when $J = 5$.

2. It should be especially noted that the probability of $\mathbf{U}_Q^{(J)}$ having full rank is significantly smaller when $\mathbf{R}$ is chosen as the IDFT matrix than when $\mathbf{R}$ is an identity matrix. An explanation of this phenomenon can be found in Appendix 3.8.2. This phenomenon suggests the proposed algorithm is more stable when operated in SC-CP systems than in OFDM systems when the constellation is small and/or when J is small.

3. Finally, although the theory suggests $P_{\mathcal{S},\mathbf{R}}(J, 2M-1) \geq P_{\mathcal{S},\mathbf{R}}(J, \lceil (2M-1)/(J-2) \rceil)$, in simulation the above two quantities look almost the same so that a conjecture may be made that $P_{\mathcal{S},\mathbf{R}}(J, Q) = P_{\mathcal{S},\mathbf{R}}(J, \lceil (2M-1)/(J-2) \rceil)$ for any $Q \geq \lceil (2M-1)/(J-2) \rceil$. This conjecture, however, has not yet been verified or disproved at the time of writing of this chapter.

3.6 Simulation Results and Discussions

In this section, we conduct several Monte Carlo simulations to demonstrate the performance of the proposed method under different system parameters: the number of collected blocks J, the repetition index Q, and the forgetting factor α. The block size M is chosen as 64, and the length of cyclic prefix is $L = 16$. The sample period is 1μs, and so the block length is 80 μs. We assume perfect block synchronization in all simulations. Note that in practice a blind block synchronization must be done before blind channel estimation can be performed. Recall that all previously reported algorithms in the literature use $Q = 1$.

3.6.1 Static Channels

We first test our methods in static channel environments. The channel is an FIR filter whose order is upper bounded by the CP length $L = 16$. The constellation of source symbols is QPSK, and the precoder $\mathbf{R}$ is chosen as the identity matrix (i.e., an SC-CP system). The simulation is performed over 500 different channels generated by Rayleigh fading statistics according to Table 3.1. The normalized least squared channel estimation error, denoted as E_{ch}, is used as the figure of merit for channel estimation and is defined as follows:

$$E_{ch} = \frac{1}{N_{ch}} \left[\sum_{k=1}^{N_{ch}} \min_{c \in \mathbb{C}} \frac{||c\hat{\mathbf{h}}_k - \mathbf{h}_k||^2}{||\mathbf{h}_k||^2} \right],$$

where N_{ch} is the number of channel estimates performed, $\mathbf{h}_k$ is the true channel vector, and $\hat{\mathbf{h}}_k$ is the channel estimate with a scalar ambiguity as defined in Eq. (3.29).

Tap	Delays (μs)	Avg. Power (dB)	Tap	Delays (μs)	Avg. Power (dB)
1	0	0.0	9	8	-6.9
2	1	-0.9	10	9	-7.8
3	2	-1.7	11	10	-4.7
4	3	-2.6	12	11	-7.3
5	4	-3.5	13	12	-9.9
6	5	-4.3	14	13	-12.5
7	6	-5.2	15	14	-13.7
8	7	-6.1	16	15	-18.0

Table 3.1: Power delay profile of the channel model used in Section 3.6

The simulation results for normalized channel estimation error E_{ch} is shown in Figure 3.7, and the corresponding bit-error-rate (BER) plot is presented in Figure 3.8. When $J = 86$ and $Q = 1$, the algorithm simply does not work since inequality (3.31) is not satisfied. This means the previously reported methods are unable to perform blind channel estimation using only 86 blocks. When we choose $Q = 2$, the algorithm works with a fairly satisfactory result. When $Q = 3$, the system performance further improves.

When the number of received blocks is $J = 129$, the algorithm works, but not very well, with $Q = 1$. In view of inequality (3.31), this is the minimum number of blocks J needed for any previously reported algorithm ($Q = 1$). If we use $Q = 2$, the performance has a significant boost. This suggests that choosing Q larger than necessary sometimes yields a better performance. When $J = 257$, the performance is even better since more data are available for blind estimation. Using $Q = 2$ stills slightly improves the system performance, but the improvement is not as large as in the previous cases. It is worthy to note that the performance curves of three cases where "$J = 86; Q = 3$," "$J = 129; Q = 2$," and "$J = 257; Q = 1$" are very close to each other. Recognizing that $(J-1)Q$ are very close to each other in these three cases, this phenomenon suggests that the system performance could be directly proportional to the number of column of $\mathbf{Y}_Q^{(J)}$ ($(J-1)Q$) as defined in Eq. (3.24) regardless of the actual number of accumulated received blocks (J).

We repeated the same simulation settings for other constellations and precoders $\mathbf{R}$. Figure 3.9 depicts the BER performance where a 16-QAM constellation and a precoder $\mathbf{R} = \mathbf{I}_M$ are used. The BER performance of the case where a QPSK constellation and a precoder $\mathbf{R} = \mathbf{W}^\dagger$ (i.e., an OFDM system) are used are shown in Figure 3.10. All these results exhibit similar characteristics to the case described in the previous paragraph.

3.6.2 Simulations with smaller J

We also test our algorithm when the number of available received blocks are smaller, with nine different values of J ranging from 3 to 64. Note that $J = 3$ is the smallest integer that satisfies inequality (3.30). The repetition index Q is chosen as

$$Q = \left\lceil \frac{2M-1}{J-2} \right\rceil + 3$$

for each J. Here we choose repetition indices larger by three than needed, in order to achieve a better system performance. Other system parameters are the same as in the first simulation in Section

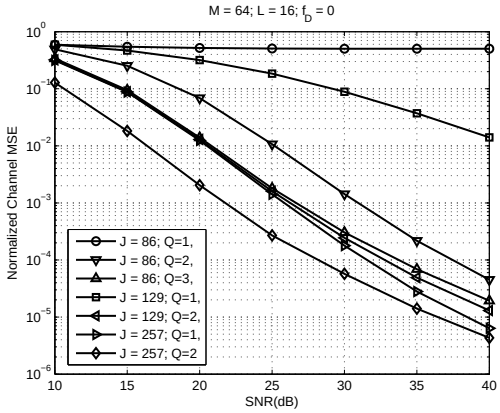

Figure 3.7: Normalized mean squared error of channel estimation for static channels with the QPSK constellation in SC-CP systems.

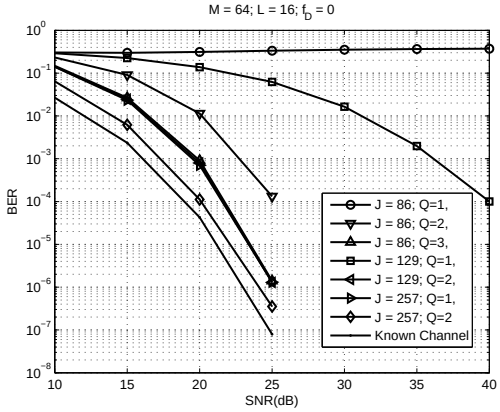

Figure 3.8: Bit error rate performance for static channels with the QPSK constellation in SC-CP systems.

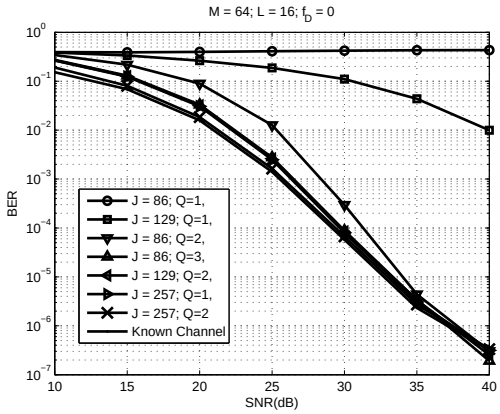

Figure 3.9: Bit error rate performance for static channels with the 16-QAM constellation in SC-CP systems.

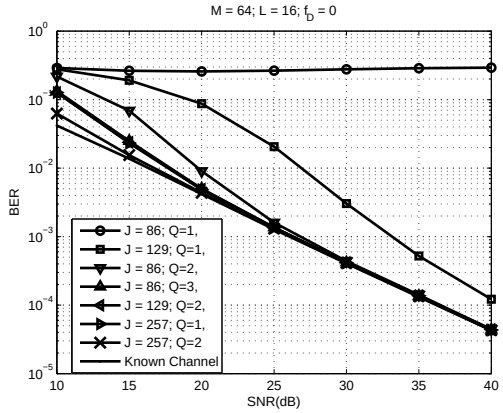

Figure 3.10: Bit error rate performance for static channels with the QPSK constellation in OFDM systems.

V-A. The BER performance is shown in Figure 3.11. When $J = 3$, the BER decreases slowly as SNR increases. This demonstrates the theoretical limit on the number of received blocks required for the proposed system, as argued in Sec. 3.3.2. However, when J is smaller than 10, the BER performances as shown in Figure 3.11 are usually unrealistic in practice. Also, a small J requires a large Q, which imposes a very demanding computational complexity. These observations largely limit the applicability of the proposed algorithm with these extremely small J in practical situations.

When the number of available received blocks is larger, the BER performance is much better. When $J = 10$ and $Q = 19$, a BER of around 10^{-5} is achieved when SNR is 30 dB. When $J = 20$ and $Q = 11$, the BER is on the order of 10^{-5} when SNR is 25 dB. The SNR margin between the BER curves of this case ($J = 20$) and of the case of known channel is around 5 dB at BER$= 10^{-4}$. When $J = 30$ and $J = 40$, this margin reduces to around 4 dB and 3dB, respectively. These results are considered acceptable BER in some practical applications (note that the presented results are all un-coded BER). Since $J = 30$ is slightly less than half the block size $M = 64$, we can argue that *the minimum number of received blocks required in a practical situation is on the order of half block size*. Three more similar simulations results with $M = 32$, $M = 128$, $M = 256$ strengthen this argument. Due to high similarity and space limit, they are not shown here. Compared to previously reported subspace-based blind algorithms [32, 5, 21], which always require a number of received blocks larger than *twice the block size*, the introduction of repetition index indeed largely reduces the required number of received blocks.

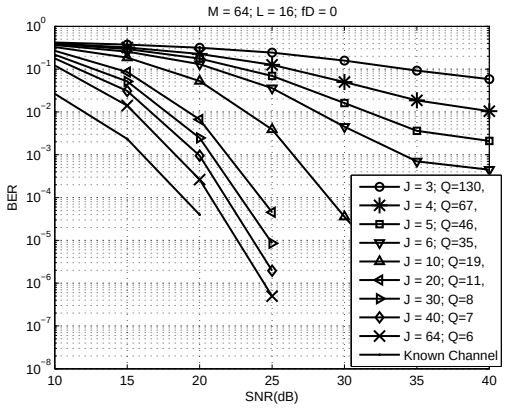

Figure 3.11: Bit error rate performance for static channels with the QPSK constellation in SC-CP systems when J is small.

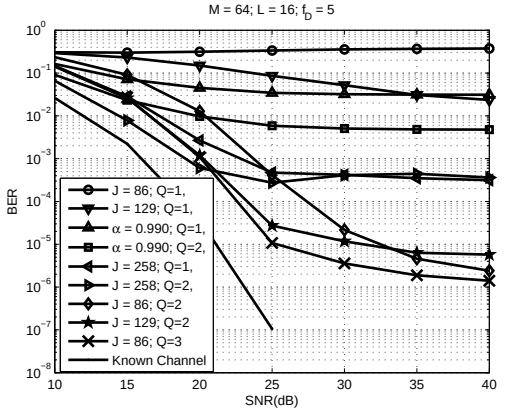

Figure 3.12: Bit error rate performance for blind estimation systems when the Doppler frequency is 5 Hz (5.4 km/hr).

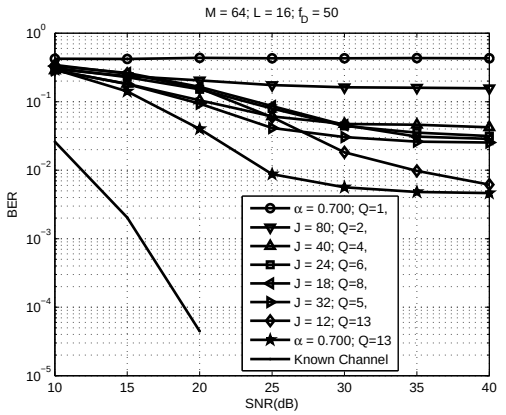

Figure 3.13: Bit error rate performance for blind estimation systems when the Doppler frequency is 50 Hz (54 km/hr).

3.6.3 Time-Varying Channels

We now test our algorithm in an environment of time-varying channels. For time-varying channels there is always a dilemma for subspace-based blind channel estimation algorithms in choosing the number of accumulated blocks (J). When J is large, the channel state may have changed significantly during data accumulation so that the estimation results could be meaningless. When J is small, the performance would be poor due to very limited amount of available data. With the introduction of repetition index Q, this problem can be solved to a certain extent.

In our simulation, the channel model considered is a random FIR channel with an order upper bounded by the CP length whose characteristics is shown in Table I. A standard Jakes' Doppler spectrum is used, and Rayleigh fading statistics are assumed for all taps[18]. A channel estimate is obtained using data of J consecutive blocks and then used to equalize the middle N_B blocks of the J blocks, where N_B is usually chosen as an integer small than or equal to J. One reason of doing this is, in the context of time-varying channels, the channel estimate obtained from J blocks may not be very accurate for the first few and the last few of the J blocks. In order to equalize each received block, a channel estimate is obtained every N_B blocks.

For the first simulation, the Doppler frequency is chosen as 5 Hz, which corresponds to an object speed 1.5 m/s (5.4 km/hr) if the carrier frequency is 1 GHz. The symbol duration is 10^{-6} seconds. This setting implies that the channel coefficients become totally uncorrelated in around 0.08 seconds (i.e., coherence interval), equal to 80,000 symbol durations, or 1,000 received blocks. A channel estimate is performed once for a time duration of 50 blocks (i.e., $N_B = 50$). The plot of BER performance is shown in Figure 3.12. In the low SNR region, the case where $J = 258$ and $Q = 2$ has the best performance. However, in the high SNR region, the case where $J = 86$ and $Q = 3$ becomes the best. Note that in the high SNR region, except for a few cases (where inequality (3.30) is not satisfied or is satisfied with a very small margin), the BER is greater when J is larger. This is because when channel noise is small, the channel estimation error comes solely from channel variation due to accumulation of a large number of blocks. In the low-SNR region, curves with similar values $(J-1)Q$ tend to have similar performances, just like what has been observed in static channel environments. We also compare an adaptive scheme where a forgetting factor $\lambda = 0.99$ is used. When $Q = 1$, the performance is not very good. Now if we choose $Q = 2$, a considerable improvement over $Q = 1$ is observed. Although the performance of forgetting factor schemes is not very good when SNR is high, they could be more promising than methods using a

fixed J in the low-SNR region.

Due to channel variation, the channel estimation error does not converge to zero even when the SNR is very high. As a consequence, the linear MMSE receiver defined in Eq. (3.34) becomes inaccurate when the SNR is large since the channel estimation error constitutes a larger variance than channel noise. In the simulation for the BER plot, we slightly adjust the linear MMSE equalizer defined in Eq. (3.34) as

$$\mathbf{\Lambda}_{k,k} = \begin{cases} \frac{E_s \hat{H}^*(W_M^k)}{E_s|\hat{H}(W_M^k)|^2+N_0} & \text{if } N_0 \geq N_t \\ \frac{E_s \hat{H}^*(W_M^k)}{E_s|\hat{H}(W_M^k)|^2+N_t} & \text{if } N_0 < N_t \end{cases}, \tag{3.44}$$

where N_t is the threshold noise level. In this case we choose $N_t = 10^{-3}$ since the channel mean square error approaches at a value greater than or equal to 10^{-3} in most settings (the plot for channel mean square error is not shown due to space limit).

For the second simulation, the Doppler frequency is chosen as 50 Hz, which corresponds to an object speed 15 m/s (54 km/hr) if the carrier frequency is 1 GHz. The symbol duration is 10^{-6} seconds. This setting implies that the coherence interval is around 8×10^{-3} seconds, equal to 8,000 symbol durations, or 100 received blocks. Since the channel is varying much faster than the previous case, we need to choose a much smaller J. The number of blocks J is ranging from 12 to 80, the parameter Q is chosen as the minimum value for each J, and N_B is chosen as $J/2$ for each J. The BER plot is shown in Figure 3.13. A modified linear MMSE receiver as defined in Eq. (3.44) with $N_t = 10^{-2}$ is used when producing the BER plot. When $J = 80$, the performance is fairly poor since the estimated channel coefficients are hardly accurate due to channel variation. When the number of received blocks J is reduced, the performance becomes better, and $J = 32$ yields the best performance in the low-SNR region among all values of J chosen in this simulation. When an even smaller J is chosen, performance in low-SNR region becomes worse again due to lack of data available for estimation. For high-SNR region, "$J = 12; Q = 13$" has the best performance. We also test the algorithm with a forgetting factor chosen as $\alpha = 0.7$ and repetition index as $Q = 13$. In this setting the data obtained 12 blocks earlier will be given a weighting of $\alpha^{12} \approx 0.0138$. If we use 1% as a threshold, we could say that the autocorrelation matrix (as defined in Eq. (3.33)) contains effective information from 12 composite blocks. This setting outperforms all other settings using a fixed J, which suggests the forgetting factor technique is more promising in a fast-varying channel environment. It should be especially noted that using a large repetition index $Q = 13$ makes it possible to choose a forgetting factor as small as 0.7. As shown in the plots, the same forgetting

factor does not work at all for $Q = 1$.

In all our simulations above, we used $M = 64$. However, in some applications, M can have a much larger value (e.g., $M = 1024$). In this case, the task of blind estimation is more sensitive to time-varying channels. The number of blocks J needs to be chosen even smaller to fit in a coherence interval. Note that J can be chosen as small as three. This implies the requirement of a larger repetition index Q. As we learned in Section 3.5, the problem of rank deficiency of $\mathbf{U}_Q^{(J)}$ may arise. However, since M is large, the probability of rank deficiency would be much smaller. So the proposed algorithm has the potential to work well in the case of time-varying channels and a large M. The only concern here may be a high complexity as can be seen in Section 3.3.5.

3.6.4 Simulation Results for Semi-Blind

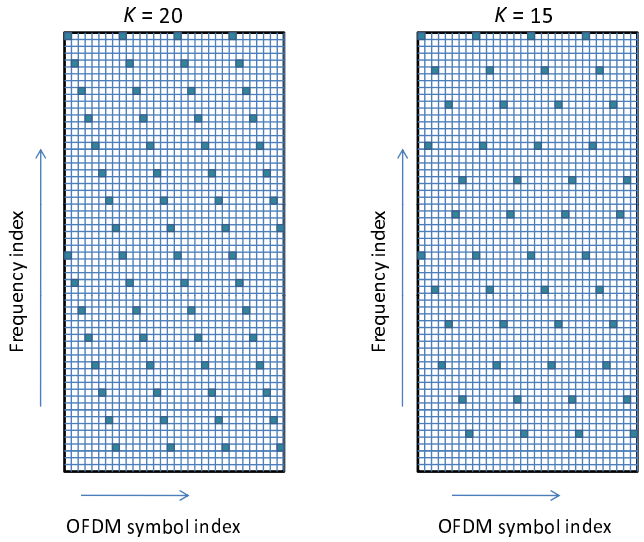

Figure 3.14: Pilot positions for $K = 20$ (left) and $K = 15$ (right).

In this subsection, we present the simulation results of the proposed semi-blind algorithm. We choose $M = 64$ and $L = 15$. The data symbols are chosen from a 64-QAM constellation to demonstrate the capability of the proposed algorithm with a large constellation. We use a 16-tap Rayleigh random channel whose power delay profile is defined as in Table 3.1. One thousand realizations of the channel are used in the simulation. We use two different pilot symbol configurations. In configuration 1, as shown in the left part of Figure 3.14, pilot samples are placed in 16 different frequency bins. In configuration 2, as depicted in the right part of Figure 3.14, only 12 different frequency bins

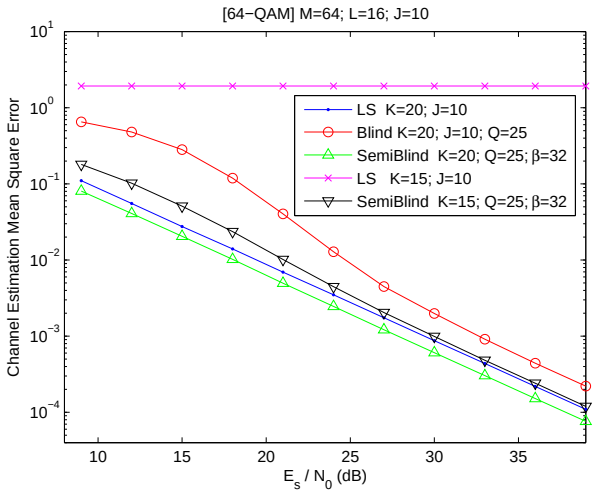

Figure 3.15: Comparison of pilot-based and semi-blind methods in channel estimation mean square error performance.

are used for pilot samples. The pilot samples are chosen so that they are uniformly distributed in an OFDM symbol to achieve the optimal positions [64]. In both configurations the pilot patterns repeat for every 8 OFDM symbols. Note that for a 16-tap channel, a pure pilot-assisted scheme requires pilot samples to be placed in at least 16 frequency bins. Each pilot sample has an absolute value $\sqrt{E_s}$, where $E_s = 42$ is the average sample energy for a 64-QAM constellation.

Ten blocks are used for each channel estimate ($J = 10$). Channel estimation is performed for every 5 OFDM symbols, i.e., for the kth channel estimate, t is chosen as $5k$. The repetition index is chosen as $Q = 25$ so that inequality (3.30) is satisfied. Notice that it is the idea of repetition index that makes it possible to choose the number of blocks as small as 10. It can be observed that for each channel estimation, $K = 20$ pilot samples are available for configuration 1, while $K = 15$ for configuration 2. The parameter β defined in (3.42) is 32. This value is chosen to give the best system performance based on empirical observations. The performance metric in channel estimation mean square error is defined as

$$E_{ch} = E\left[\frac{1}{N_{ch}}\sum_{k=0}^{N_{ch}}||\hat{\mathbf{h}}_k - \mathbf{h}||^2\right],$$

where the expectation is taken over 1,000 different channel realizations, N_{ch} is the number of total channel estimates for each channel realization, and $\hat{\mathbf{h}}_k$ is the kth channel estimate. Figure 3.15 shows the simulation results. For the least square pure pilot-assisted method, configuration 2 ($K = 15$) does not work, while configuration 1 ($K = 20$) has a satisfactory performance. The

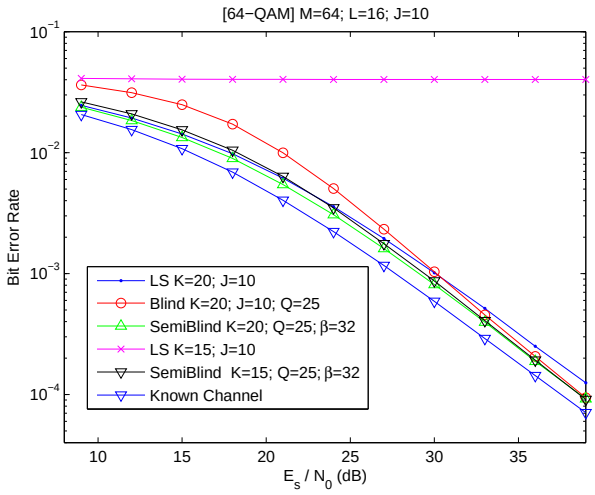

Figure 3.16: Comparison of pilot-based and semi-blind methods in bit error rate performance.

pure blind method works properly, but the performance is obviously worse than the pure pilot-assisted method with $K = 20$. When a semi-blind technique with $\beta = 32$ is used, the performances for both $K = 20$ and $K = 15$ are better than those of pure pilot-assisted method.

Based on the estimated channel coefficients, a linear minimum mean square error (L-MMSE) equalizer is used in OFDM symbol recovery [60]. The kth channel estimate $\hat{\mathbf{h}}_k$ is used for equalizing the OFDM symbol numbers $5k + 3$ to $5k + 7$. Equalized symbols then go through detection devices and bit error rate (BER) performance of the system is evaluated which is shown in Figure 3.16. We see that the semi-blind method with $K = 15$ has an even better performance than the pure pilot-assisted method with $K = 20$ when the E_s/N_0 ratio is greater than 23 dB. This suggests the proposed semi-blind algorithm does reduce the number of pilot samples for achieving the same BER performance.

3.7 Conclusions

In this chapter we proposed a generalized algorithm for subspace-based blind channel estimation in cyclic prefix systems. The repetition index (Q) was introduced as a new system parameter. By using a repetition index larger than unity, the number of received blocks (J) is significantly reduced compared to previously reported methods so that the proposed algorithm is more feasible in time-varying channel environments. A necessary condition on the system parameters J and Q for the

algorithm to work is derived. The number of received blocks $J \geq 3$ can be chosen depending on the speed of channel variation to yield the best performance. The generalization can also be applied to blind methods using a forgetting factor α.

Simulation shows that when the number of received blocks J and the repetition index Q are properly chosen, the generalized algorithm outperforms previously reported special cases, especially in a time-varying channel environment. The proposed method can be directly applied to existing systems such as OFDM, SC-CP, etc., without any modification of the transmitter structure.

We also proposed a semi-blind channel estimation algorithm in OFDM systems based on a combination of a pure pilot-assisted algorithm and the blind algorithm proposed in this chapter. The proposed semiblind algorithm is presumably the first one to be applicable with any type of communication constellations and a limited number of received blocks. Simulation results confirm the improvement in system performance of the semi-blind algorithm over the direct pilot-assisted algorithm. They also suggest that fewer pilot samples can be used to achieve the same BER performance when a semi-blind algorithm is employed.

In the future, many aspects are worthy of further investigation. For example, developing the strategy to find the optimal J and Q or the optimal α and Q given knowledge of channel variation can be a challenging yet important problem. Extending this scheme for multi-input-multi-output (MIMO) channels is also of great interest. As for the semiblind algorithm, it may be interesting to analytically derive the optimal parameter β. The optimal design of the pilot symbol configurations (i.e., pilot position, value, etc.) for the semi-blind algorithm is still an unknown but important issue.

3.8 Appendix

3.8.1 Proofs of Theorems

Proof of Theorem 3.3: Assume $\mathbf{U}_{Q+1}^{(J)}$ does not have full row rank. Then there exists a nonzero row vector $\mathbf{v}^T = \begin{bmatrix} v_1 & \cdots & v_{2M+Q} \end{bmatrix}$ such that $\mathbf{v}^T\mathbf{U}_{Q+1}^{(J)} = \mathbf{0}^T$. From the definition in Eq. (3.25), we obtain that $\mathbf{v}^T$ is a left annihilator of $\mathbf{U}_{Q+1}(n)$ for $1 \leq n \leq J-1$. The notation of $\mathbf{U}_Q(n)$ was defined in Eq. (3.22). Notice that $\mathbf{U}_Q(n)$ is a submatrix of $\mathbf{U}_{Q+1}(n)$ and can be obtained by removing the first row and the first column of $\mathbf{U}_{Q+1}(n)$, or by removing the last row and the last column of $\mathbf{U}_{Q+1}(n)$. This means that both $\mathbf{v}_1^T = \begin{bmatrix} v_1 & \cdots & v_{2M+Q-1} \end{bmatrix}$ and $\mathbf{v}_2^T = \begin{bmatrix} v_2 & \cdots & v_{2M+Q} \end{bmatrix}$ are

left annihilators of $\mathbf{U}_Q(n)$ for $1 \le n \le J$. So $\mathbf{v}_1^T \mathbf{U}_Q^{(J)} = \mathbf{v}_2^T \mathbf{U}_Q^{(J)} = \mathbf{0}^T$. Since $\mathbf{v}^T$ is nonzero, at least one of $\mathbf{v}_1^T$ and $\mathbf{v}_2^T$ must also be nonzero. This implies that $\mathbf{U}_Q^{(J)}$ does not have full rank and contradicts the assumption. □

Proof of Theorem 3.4: Let $\tilde{\mathbf{U}}_Q^{(J)} = \mathbf{K}\mathbf{U}_Q^{(J)}$ where

$$\mathbf{K} = \mathbf{I}_{2M+Q-1} - \begin{bmatrix} \mathbf{0}_{(M+Q-1)\times M} & \mathbf{I}_{M+Q-1} \\ \mathbf{0}_{M\times M} & \mathbf{0}_{(M+Q-1)\times M} \end{bmatrix}.$$

Then, we have rank($\tilde{\mathbf{U}}_Q^{(J)}$) = rank($\mathbf{U}_Q^{(J)}$) since $\mathbf{K}$ is nonsingular. Also define $\tilde{\mathbf{U}}_Q(n) = \mathbf{K}\mathbf{U}_Q(n)$ where $\mathbf{U}_Q(n)$ is defined as in Eq. (3.22). It can be shown that $\tilde{\mathbf{U}}_Q(n)$ can be written as

$$\tilde{\mathbf{U}}_Q(n) = \begin{bmatrix} [\mathbf{T}(n)]^T & [\mathbf{C}(n)]^T \end{bmatrix}^T,$$

where $\mathbf{T}(n) = \mathcal{T}_Q\left(\mathbf{u}_M(n-1) - \mathbf{u}'_M(n)\right)$ is an $(M+Q-1)\times Q$ Toeplitz matrix and the $M \times Q$ matrix

$$\mathbf{C}(n) = \begin{bmatrix} [\mathbf{u}'_M(n)]_M^1 & [\mathbf{u}'_M(n)]_{M+1}^2 & \cdots & [\mathbf{u}'_M(n)]_{2M+Q-2}^{M+Q-1} \end{bmatrix}$$

has a "circulant" structure. For simplicity, hereafter we denote $\mathbf{a}(n) = \mathbf{u}_M(n-1) - \mathbf{u}'_M(n)$ and $\mathbf{b}(n) = \mathbf{u}'_M(n)$. We also define polynomials in x as $A(x) = \begin{bmatrix} 1 & x & \cdots & x^{M-1} \end{bmatrix} \mathbf{a}(n)$ and $B(x) = \begin{bmatrix} 1 & x & \cdots & x^{M-1} \end{bmatrix} \mathbf{b}(n)$. $\tilde{\mathbf{U}}_Q(n)$ is a $(2M+Q-1)\times Q$ matrix and has at least $(2M-1)$ linearly independent left annihilators. These annihilators can always be written in the following forms, regardless of the value of Q:

$$\mathbf{v}_k^\dagger(n) = \left[\begin{array}{cccc|c} 1 & \alpha_k & \cdots & \alpha_k^{M+Q-2} & \mathbf{0}_{1\times M} \end{array}\right], 1 \le k \le M-1 \tag{3.45}$$

and

$$\mathbf{v}_{M-1+k}^\dagger(n) = \left[\begin{array}{c|c} B(W_M^{-k})\mathbf{w}_k^\dagger & -A(W_M^{-k})\mathbf{x}_k^\dagger \end{array}\right], 1 \le k \le M, \tag{3.46}$$

where $\{\alpha_1, \alpha_2, \cdots, \alpha_{M-1}\}$ are distinct roots of the polynomial $A(x)$, $\mathbf{w}_k^\dagger = \begin{bmatrix} 1 & W_M^{-k} & \cdots & W_M^{-k(M+Q-2)} \end{bmatrix}$, and $\mathbf{x}_k^\dagger = \begin{bmatrix} 1 & W_M^{-k} & \cdots & W_M^{-k(M-1)} \end{bmatrix}$. Please note that annihilators in the form of Eq. (3.45) come because of the Toeplitz structure of $\mathbf{T}(n)$ and annihilators in the form of Eq. (3.46) come because $A(W_M^{-k})$ and $B(W_M^{-k})$, the DFT coefficients of $\mathbf{a}(n)$ and $\mathbf{b}(n)$, respectively, cancel each other when $\tilde{\mathbf{U}}_Q(n)$ is multiplied by $\mathbf{v}_{M-1+k}^\dagger$ defined inEq. (3.46). Here we omit the index n in polynomials $A(x)$ and $B(x)$ for the sake of notational simplicity. Also note that vectors $\mathbf{v}_k, 1 \le k \le 2M-1$, are always linearly independent as long as 1) the polynomial $A(x)$ has degree $M-1$; 2) all roots of

$A(x)$ are distinct; and 3) none of roots of $A(x)$ is on the DFT grid. When any of these is not true, a slight modification of Eqs. (3.45) and (3.46) can be found so that they are still linearly independent.

If $\tilde{\mathbf{U}}_Q^{(J)}$ is rank-deficient and there exists any left annihilator of $\tilde{\mathbf{U}}_Q^{(J)}$, in the form of either Eq. (3.45) or Eq. (3.46), then $\tilde{\mathbf{U}}_Q^{(J)}$ is rank-deficient for all Q, since the same form of vectors will continue to be annihilators of $\tilde{\mathbf{U}}_Q^{(J)}$. Now, we will prove that if $\tilde{\mathbf{U}}_{2M-1}^{(J)}$ is rank-deficient (as assumed in the theorem statement), then at least an annihilator in the form of either Eq. (3.45) or Eq. (3.46) will be a common annihilator for all $\tilde{\mathbf{U}}_Q(n)$. Suppose this is not the case and there exist two nonzero $\tilde{\mathbf{U}}_Q(n)$, say, $\tilde{\mathbf{U}}_Q(1)$ and $\tilde{\mathbf{U}}_Q(2)$, without loss of generality, which do not have common annihilators. Since $\tilde{\mathbf{U}}_Q^{(J)}$ is rank-deficient when $Q = 2M-1$ (as assumed in the theorem statement), there exists a nonzero $(4M-2)$-row vector $\mathbf{v}^\dagger$ such that $\mathbf{v}^\dagger \tilde{\mathbf{U}}_{2M-1}^{(J)} = \mathbf{0}^T$. Clearly $\mathbf{v}^\dagger$ is also an annihilator of $\tilde{\mathbf{U}}_{2M-1}(1)$ and $\tilde{\mathbf{U}}_{2M-1}(2)$. Thus, $\mathbf{v}^\dagger$ can be decomposed into the following form:

$$\mathbf{v}^\dagger = \sum_{k=1}^{2M-1} c_k \mathbf{v}_k^\dagger(1) = \sum_{k=1}^{2M-1} d_k \mathbf{v}_k^\dagger(2),$$

where $\mathbf{v}_k^\dagger(n), 1 \le k \le 2M-1, n = 1, 2$ are as defined in Eqs. (3.45) and (3.46) with $Q = 2M-1$. So we have

$$\mathbf{V} \begin{bmatrix} \mathbf{c} \\ -\mathbf{d} \end{bmatrix} = \mathbf{0}, \tag{3.47}$$

where $\mathbf{c}$ and $\mathbf{d}$ are $(2M-1)$-column vectors containing coefficients c_k and d_k, respectively, and $\mathbf{V}$ is a $(4M-2) \times (4M-2)$ matrix whose columns are $\mathbf{v}_k(n)$, $1 \le k \le 2M-1, n = 1, 2$. Since the annihilators of $\tilde{\mathbf{U}}_Q(1)$ and $\tilde{\mathbf{U}}_Q(2)$ are linearly independent, $\mathbf{V}$ has full rank. Thus, Eq. (3.47) implies $\mathbf{c} = \mathbf{d} = \mathbf{0}$ and hence $\mathbf{v}^\dagger = \mathbf{0}^T$. This contradicts the assumption that $\tilde{\mathbf{U}}_{2M-1}^{(J)}$ is rank-deficient. This completes the proof. □

3.8.2 Probability of $\mathbf{U}_Q^{(J)}$ having full rank for different precoders

We now explain why the probability of $\mathbf{U}_Q^{(J)}$ having full rank is much smaller when $\mathbf{R} = \mathbf{W}$ than $\mathbf{R} = \mathbf{I}$. As explained in the proof of Theorem 3.4, if $\mathbf{U}_Q^{(J)}$ does not have full rank for $Q \ge 2M-1$, then a row vector $\mathbf{v}^\dagger$ in the form of either Eq. (3.45) or Eq. (3.46) will be a common annihilator of $\tilde{\mathbf{U}}_Q(n)$. The probability of this depends on how many possible values of these vectors there are. Focusing on Eq. (3.46), since $\mathbf{w}_k^\dagger$ and $\mathbf{x}_k^\dagger$ are fixed, the variety of this form of annihilators comes from the values of $A(W_M^{-k})$ and $B(W_M^{-k})$, which are Fourier transforms of $\mathbf{a}(n)$ and $\mathbf{b}(n)$. If there is no precoding (i.e., $\mathbf{R} = \mathbf{I}$), the number of possible values of $A(W_M^{-k})$ and $B(W_M^{-k})$ can be quite

large. On the contrary, when an IDFT precoder is used (i.e., $\mathbf{R} = \mathbf{W}^{\dagger}$), $A(W_M^{-k})$ and $B(W_M^{-k})$ can only be symbols in the constellation or the difference of two of them. Since the possible values of $A(W_M^{-k})$ and $B(W_M^{-k})$ are much fewer, it is more likely that a common annihilator of $\tilde{\mathbf{U}}_Q^{(J)}$ in this form exists, so the probability of $\mathbf{U}_Q^{(J)}$ having full rank is smaller in OFDM systems.

Chapter 4

Blind Block Synchronization for Transceivers Using Redundant Precoders

In Chapters 2 and 3, we studied blind channel estimation in block transmission systems using linear redundant precoding. These algorithms, as well as other blind algorithms studied in the literature [45, 36, 49, 76, 5, 32, 31, 24, 35], assume that block boundaries of the received streams are perfectly known to the receiver. In practical applications, however, this assumption is usually not true since no extra known samples are transmitted. The problem of blind recovery of block boundaries of the received signal is therefore important. However, up to date, the problem of blind block synchronization has not yet been given as much attention as the blind channel estimation problem has. In this chapter, we consider the blind block synchronization problem in ZP and CP systems. For ZP systems, the first blind block synchronization algorithm was proposed by Scaglione *et al.* [45]. The blind synchronization algorithm uses the rank deficiency property of a matrix composed of received samples, which was first used in a blind equalization algorithm also proposed in [45]. The rank deficiency property of the aforementioned matrix is valid at perfect block synchronization but is no longer valid when a nonzero timing mismatch is present. The algorithm proposed in [45] shows that block synchronization algorithms can be connected with existing blind channel estimation/equalization algorithms that exploit matrix null spaces. The blind block synchronization problem in CP systems may be of more importance since it is a broader version of the timing synchronization or the symbol synchronization problem in the popular orthogonal frequency division multiplexing (OFDM) systems. A number of blind block synchronization algorithms for OFDM systems have been developed [33, 20, 1, 72, 34]. In particular, in [33] Negi and Cioffi proposed the

first blind OFDM symbol synchronization for frequency selective channels.

These previously reported methods, however, require a large amount of received data to obtain accurate statistics for successful block synchronization. As we examine these previously reported blind block synchronization algorithms, we find that block synchronization algorithms can be connected with existing blind channel estimation/equalization algorithms that exploit matrix null spaces. In recent years, more advanced blind channel estimation algorithms, including those presented in Chapters 2 and 3, were developed. These suggest more opportunities to develop new blind channel synchronization algorithms that may possess new features. The feature of using much less received data in the blind channel estimation algorithms can also be properly transferred to blind synchronization algorithms if we adopt the concept of repetition index. The blind block synchronization algorithm for ZP systems proposed in this chapter will explore this idea. Another novelty is that the proposed method for ZP systems is based on a subspace of dimension L rather than one as in [45] (where L is the channel order). This idea, combined with the repetition index, is shown to significantly improve the performance with sufficient amount of received data. As for CP systems, our approach to reduce the required amount of received data resorts to employing the idea of repetition index. As the idea of repetition index was recently extended to blind channel estimation in CP systems [60], we propose a new blind block synchronization algorithm in CP systems based on the foundation of [60]. Our proposed algorithm possesses two advantages over the previously reported methods: 1) In absence of noise, the proposed algorithm provides correct recovery of block boundaries using only three received blocks, whereas all previously reported algorithms require the number of received blocks to be no less than the block size. 2) When noise is present, simulation results as reported in Section 4.5 show that given the same amount of received data, the proposed algorithm has an obvious improvement in blind block synchronization error rate performance over the previously reported algorithm in [33].

The content of this chapter is mainly drawn from [59], and portions of it have been presented in [61] and submitted to [62].

4.1 Outline

The chapter will be organized as follows. In Section 4.2, the problems of interest, namely the blind block synchronization problems in ZP and CP systems, respectively, will be formulated.

In Sections 4.3 and 4.4, the proposed blind block synchronization algorithms in ZP and CP

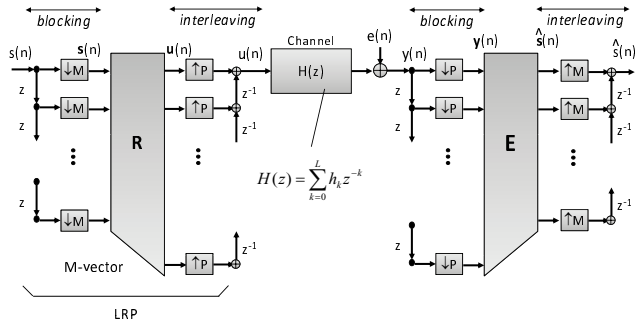

Figure 4.1: Block transmission systems using linear redundant precoders.

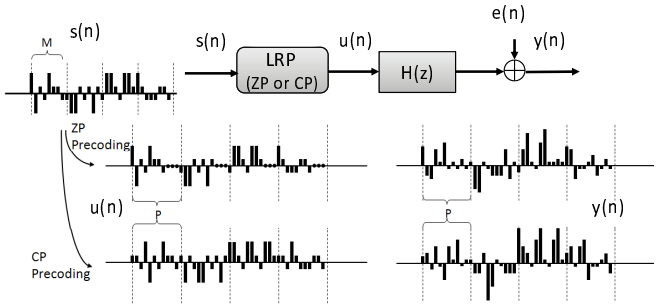

Figure 4.2: Illustration of blind block synchronization problem in ZP and CP systems.

systems, as well as their theoretical foundations, will be presented, respectively. In Section 4.5, simulation results are provided to evaluate the system performances of the proposed algorithms and to compare them with those of previously reported algorithms. Finally, the conclusions are made in Section 4.6.

4.2 Problem Formulation

4.2.1 Redundant Block Transmission Systems

Figure 4.1 shows the structure of a block transmission system. The data samples, $s(n)$, are blocked into vectors $\mathbf{s}(n)$ of size M. Let L be a positive integer indicating the redundancy inserted in each block, and assume $M > L$. The precoded vector, $\mathbf{u}(n)$, of size $P = M+L$ is obtained by multiplying a $P \times M$ matrix $\mathbf{R}$ with $\mathbf{s}(n)$. The vector sequence $\mathbf{u}(n)$ is then unblocked into a scalar sequence $u(n)$ before being sent over the channel. The channel is characterized as an FIR system with a

maximum order L, i.e.,

$$H(z) = \sum_{k=0}^{L_0} h_k z^{-k},$$

where $L_0 \leq L$. Assume h_0 and h_{L_0} are nonzero. Define $\mathbf{h}$ as the $(L+1)$-vector

$$\begin{bmatrix} h_0 & h_1 & \cdots & h_L \end{bmatrix}^T,$$

where the values of h_k are set to zeros for any k, $L_0 < k \leq L$. The integer L_0 is called the effective channel order. The signal at the channel output is corrupted by an additive white Gaussian noise $e(n)$. At the receiver side, the received sample stream $y(n)$ is blocked into vectors $\mathbf{y}(n)$ of size P. An equalizer, characterized by an $M \times P$ matrix $\mathbf{E}$, is used to recover the data blocks $\mathbf{s}(n)$.

While the redundant precoder can be designed as any rank-M matrix $\mathbf{R}$, we consider specifically two commonly used classes of LRPs in this paper: the zero-padding (ZP) precoders and the cyclic prefixing (CP) precoders. A block transmission system using a ZP or CP precoder is called a ZP system or an CP system, respectively.

In a ZP system, the matrix $\mathbf{R}$ has the form of

$$\mathbf{R} = \begin{bmatrix} \mathbf{R}_{zp} \\ \mathbf{0}_{L \times M} \end{bmatrix},$$

where $\mathbf{R}_{zp}$ is an $M \times M$ nonsingular matrix. Each precoded block $\mathbf{u}(n)$ is composed of a data part of length M followed by a zero block of length L. Due to trailing zero introduced in each block at the transmitter, each received block $\mathbf{y}(n)$ can be expressed as [45]

$$\mathbf{y}(n) = \mathcal{T}_M(\mathbf{h})\mathbf{R}_{zp}\mathbf{s}(n) + \mathbf{e}(n), \tag{4.1}$$

where $\mathbf{e}(n)$ is the blocked version of $e(n)$. Note that $\mathbf{y}(n)$ depends only on $\mathbf{s}(n)$ and not on $\mathbf{s}(k)$ where $k \neq n$, so the inter-block interference (IBI) is completely eliminated.

In a CP system, the precoder matrix $\mathbf{R}$ has the form of

$$\mathbf{R} = \left[\begin{array}{c|c} \mathbf{0}_{L \times (M-L)} & \mathbf{I}_L \\ \hline & \mathbf{I}_M \end{array}\right] \cdot \mathbf{R}_{cp},$$

where $\mathbf{R}_{cp}$ is an $M \times M$ nonsingular matrix. Each precoded block $\mathbf{u}(n)$ is composed of a cyclic prefix $\mathbf{u}_{cp}(n)$ of length L followed by the precoded data $\mathbf{u}_M(n) = \mathbf{R}_{cp}\mathbf{s}(n)$ of length M. The cyclic

prefix is a copy of the last L elements of the precoded data (i.e., $\mathbf{u}_{cp}(n) = [\mathbf{u}_M(n)]_{M-L+1:M}$). Each received block can be expressed as

$$\mathbf{y}(n) = \begin{bmatrix} \mathbf{y}_{cp}(n) \\ \mathbf{y}_M(n) \end{bmatrix} = \begin{bmatrix} \mathbf{H}_l \mathbf{u}_{cp}(n) + \mathbf{H}_u \mathbf{u}_{cp}(n-1) \\ \hline \mathbf{H}_{cir} \mathbf{u}_M(n) \end{bmatrix}, \tag{4.2}$$

where $\mathbf{H}_{cir}$ is an $M \times M$ circulant matrix [67] whose first column is $\begin{bmatrix} h_0 & \cdots & h_L & 0 & \cdots & 0 \end{bmatrix}^T$ and where

$$\mathbf{H}_l \triangleq \begin{bmatrix} h_0 & & \mathbf{0} \\ \vdots & \ddots & \\ h_{L-1} & \cdots & h_0 \end{bmatrix} \text{ and } \mathbf{H}_u \triangleq \begin{bmatrix} h_L & \cdots & h_1 \\ & \ddots & \vdots \\ \mathbf{0} & & h_L \end{bmatrix}$$

are $L \times L$ matrices. We can see that $\mathbf{y}_{cp}(n)$, the CP part of $\mathbf{y}(n)$, contains IBI, but $\mathbf{y}_M(n)$ is free from IBI. In particular, when $\mathbf{R}_{cp}$ is chosen as the normalized inverse DFT matrix, the CP system is equivalent to the popular OFDM system.

4.2.2 Blind Block Synchronization for LRP Systems

Figure 4.2 illustrates the precoded sample stream $u(n)$ and the received sample stream $y(n)$ of a ZP and a CP system, respectively. The dashed lines shown in the precoded sample streams and received sample streams depict the block boundaries. While the block boundaries are easy to trace in precoded sample streams $u(n)$ by recognizing the zero part or the cyclic prefix part, there does not seem to exist a clear rule of thumb to determine by inspection the block boundaries in the received sample streams $y(n)$ in either ZP or CP systems, as the signal has been convolved with the frequency selective channel $H(z)$. Furthermore, there is additive channel noise. A more sophisticated method must be employed to recover the block boundaries in received signals.

When the block synchronization is perfect between the transmitter and the receiver, the nth received block $\mathbf{y}(n)$ is

$$\mathbf{y}(n) = \begin{bmatrix} y(nP) & y(nP+1) & \cdots & y(nP+P-1) \end{bmatrix}^T.$$

Suppose the blocking was performed with an unknown timing mismatch $d \in [-P/2, P/2)$ between the transmitter and the receiver. Then the samples collected in the nth block will be

$$\mathbf{y}^{(d)}(n) = \begin{bmatrix} y(nP+d) & y(nP+d+1) & \cdots & y(nP+d+P-1) \end{bmatrix}^T.$$

The problem statement of this paper is explained as follows. In a ZP or CP system as described

in Section 4.2.1, given the received sample stream $y(n)$, with a possible unknown timing mismatch to the transmitter, how do we determine the optimal $d \in [-P/2, P/2)$ that represents the starting index of a received block without knowledge of $\mathbf{s}(n)$? Note that since the OFDM systems are a special case of CP systems, the block synchronization problem in CP systems is a broader version of the "timing synchronization" problem or the "symbol synchronization" problem in OFDM systems. Without loss of generality and for convenience of the presentation, we assume the "correct answer" is always $d = 0$. Furthermore, when the effective channel order L_0 is strictly smaller than the guard interval length L (i.e., trailing zeros or cyclic prefixes), we observe that

$$d = -L + L_0, -L + L_0 + 1, ..., 0$$

can all be considered "correct answers" since we can think of the equivalent channel vector as

$$\mathbf{h}^{(d)} = \left[\begin{array}{ccccc} \mathbf{0}_{1\times(-d)} & h_0 & \cdots & h_{L_0} & \mathbf{0}_{1\times(L-L_0+d)} \end{array} \right]^T$$

in this case. No interblock interference will occur due to a timing-mismatch d, $-L + L_0 \leq d \leq 0$. If the redundancy is minimal, i.e., $L = L_0$, then the only choice is $d = 0$.

4.3 Proposed Algorithm for ZP Systems

The basic idea of the proposed blind block synchronization algorithm for ZP systems stems from Eq. (4.1). Notice that $\mathcal{T}_M(\mathbf{h})\mathbf{R}_{zp}$ is a $P \times M$ matrix whose rank is M. In absence of noise, each received block, $\mathbf{y}(n)$, must be a linear combination of columns of $\mathcal{T}_M(\mathbf{h})\mathbf{R}_{zp}$ when the block synchronization is perfect. In other words, a $P \times J$ matrix $\mathbf{Y}_J$ composed of J received blocks,

$$\mathbf{Y}_J \triangleq \left[\begin{array}{cccc} \mathbf{y}(0) & \mathbf{y}(1) & \cdots & \mathbf{y}(J-1) \end{array} \right], \tag{4.3}$$

must have rank M for some sufficiently large $J \geq M$. This implies that $\mathbf{Y}_J$ has a L-dimensional null space if the block synchronization is perfect. This property has been exploited in the blind channel estimation algorithm reported first in [45]. On the other hand, the matrix

$$\mathbf{Y}_J^{(d)} \triangleq \left[\begin{array}{cccc} \mathbf{y}^{(d)}(0) & \mathbf{y}^{(d)}(1) & \cdots & \mathbf{y}^{(d)}(J-1) \end{array} \right]$$

usually has a larger rank when $d \neq 0$ than when $d = 0$ (this will be verified later). The task of blind block synchronization can thus be completed by finding an optimal $d \in [-P/2, P/2)$ such that the rank deficiency of $\mathbf{Y}_J^{(d)}$ is L. In presence of noise, the optimal d can be chosen such that the sum of the smallest L eigenvalues of $\mathbf{Y}_J^{(d)}\mathbf{Y}_J^{(d)\dagger}$ is minimized. It should be noted that this technique is different from the one reported in [45] and reviewed in Section 4.3.2.

However, the blind block synchronization technique requires the condition that $J \geq M$ as the blind channel estimation algorithm in [45] needs it to satisfy certain full rank condition. This means the receiver has to accumulate at least MP data samples in order to determine the block boundary correctly. In a fast-varying environment such as a wireless channel, we usually do not have the luxury to collect so many samples since the channel status may have changed significantly during the data accumulation.

In order to reduce the amount of required data, we will use the idea of "repetition index," which first arose in a blind channel estimation problem [49]. The idea of repetition index is to repeatedly use each received block and has successfully reduced the number of received blocks needed for blind channel estimation problem in ZP and CP systems, as reported in [36, 49, 60]. By properly applying this idea, we can develop blind block synchronization algorithms using less data. We shall present here the application of repetition index in blind block synchronization problems, and the readers interested in the blind channel estimation algorithms are referred to [36], [49], and [60].

4.3.1 Derivation of the Proposed Algorithm

Consider the noise-free case first. It can be verified [49] that Eq. (4.1) is equivalent to

$$\mathcal{T}_Q(\mathbf{y}(n)) = \mathcal{T}_{M+Q-1}(\mathbf{h})\mathcal{T}_Q(\mathbf{u}_M(n)), \tag{4.4}$$

where Q is any positive integer and $\mathbf{u}_M(n)$ denotes $\mathbf{R}_{zp}\mathbf{s}(n)$ in the context of ZP systems. The notation $\mathcal{T}_n(\cdot)$ was defined in Section II-A. Note that when $Q = 1$, Eq. (4.4) reduces to Eq. (4.1). When $Q > 1$, Eq. (4.4) is similar to Eq. (4.1) in the sense that $\mathcal{T}_{M+Q-1}(\mathbf{h})$ is also a full-banded Toeplitz matrix, except that the size of $\mathcal{T}_{M+Q-1}(\mathbf{h})$ is larger than that of $\mathcal{T}_M(\mathbf{h})$ by $Q - 1$. The parameter Q is called the repetition index since each received block is repeatedly used Q times. Note that $\mathcal{T}_Q(\mathbf{y}(n))$ is a $(P+Q-1)\times Q$ matrix, and each column of $\mathcal{T}_Q(\mathbf{y}(n))$ is a linear combination of columns of $\mathcal{T}_{M+Q-1}(\mathbf{h})$. This property leads us to develop a new blind block synchronization algorithm as follows.

Suppose J received blocks are available at the receiver. Consider the $(P+Q-1) \times JQ$ matrix

$$\mathbf{Y}_{J,Q} = \left[\begin{array}{cccc} \mathcal{T}_Q\left(\mathbf{y}(0)\right) & \mathcal{T}_Q\left(\mathbf{y}(1)\right) & \cdots & \mathcal{T}_Q\left(\mathbf{y}(J-1)\right) \end{array} \right]. \tag{4.5}$$

It is readily verified that

$$\mathbf{Y}_Q^{(J)} = \mathcal{T}_{M+Q-1}\left(\mathbf{h}\right) \mathbf{U}_Q^{(J)},$$

where

$$\mathbf{U}_Q^{(J)} = \left[\begin{array}{cccc} \mathcal{T}_Q(\mathbf{u}_M(0)) & \mathcal{T}_Q(\mathbf{u}_M(1)) & \cdots & \mathcal{T}_Q(\mathbf{u}_M(J-1)) \end{array} \right] \tag{4.6}$$

is a $(M+Q-1) \times JQ$ matrix. A necessary (but not sufficient) condition for $\mathbf{U}_Q^{(J)}$ to have full rank $M+Q-1$ is $JQ \geq M+Q-1$, or

$$J \geq 1 + \frac{M-1}{Q}. \tag{4.7}$$

Inequality (4.7) gives a lower bound on the required number of received blocks of the proposed blind synchronization algorithm with respect to the repetition index Q. When $\mathbf{U}_Q^{(J)}$ has full rank $M+Q-1$, the rank of $\mathbf{Y}_Q^{(J)}$ is also $M+Q-1$, and therefore the rank deficiency of $\mathbf{Y}_Q^{(J)}$ is exactly L. On the other hand, when a nonzero timing error $d \in [-P/2, P/2)$ is present, the matrix

$$\mathbf{Y}_{J,Q}^{(d)} = \left[\begin{array}{cccc} \mathcal{T}_Q\left(\mathbf{y}^{(d)}(0)\right) & \mathcal{T}_Q\left(\mathbf{y}^{(d)}(1)\right) & \cdots & \mathcal{T}_Q\left(\mathbf{y}^{(d)}(J-1)\right) \end{array} \right] \tag{4.8}$$

usually has strictly less than L zero eigenvalues, as verified in the following theorem.

Theorem 4.1: Consider the noise-free situation. Assume each channel coefficient $h_k, 0 \leq k \leq L$, is an independent complex Gaussian random variable, and each element of $\mathbf{s}(n)$ is i.i.d. and selected from a finite constellation. Then, with probability one there exists a sufficiently large J such that the following statement on the matrix $\mathbf{Y}_{J,Q}^{(d)}$ defined in (4.8) is true with probability one.

$$\begin{aligned} & \text{The number of zero eigenvalues of } \mathbf{Y}_{J,Q}^{(d)} \mathbf{Y}_{J,Q}^{(d)\,\dagger} \\ = \;& (P+Q-1) - \text{rank}(\mathbf{Y}_{J,Q}^{(d)} \mathbf{Y}_{J,Q}^{(d)\,\dagger}) \\ = \;& \begin{cases} L & \text{if } d = 0 \\ \max\{L - |d| - 2(Q-1), 0\} & \text{if } d \neq 0 \end{cases}. \end{aligned}$$

□

Proof: See Appendix. □

Theorem 4.1 gives the foundation of the proposed algorithm for ZP systems. We use the rank deficiency of the matrix $\mathbf{Y}_{J,Q}^{(d)}$ to determine the optimal block boundaries. When the block synchronization is perfect (i.e., $d = 0$), the rank deficiency of $\mathbf{Y}_{J,Q}^{(d)}$ is exactly L. When the amount of timing error $|d|$ increases, this value decreases gradually to zero. In particular, if $Q = 1$, the rank deficiency of $\mathbf{Y}_{J,Q}^{(d)}$ is $\max\{L-|d|, 0\}$. The decrease in the rank deficiency of $\mathbf{Y}_{J,Q}^{(d)}$ when $|d|$ increases is relatively smooth. When $Q \geq 2$, the rank deficiency of $\mathbf{Y}_{J,Q}^{(d)}$ has an abrupt decrease when $|d|$ increases from 0 to 1. Furthermore, if $Q \geq (L+1)/2$, the rank deficiency of $\mathbf{Y}_{J,Q}^{(d)}$ goes immediately to zero whenever a nonzero timing error is present. This sharper decrease in rank deficiency of $\mathbf{Y}_{J,Q}^{(d)}$ demonstrates the advantage of using a larger repetition index Q for blind block synchronization.

The use of a large repetition index Q has two major advantages. First of all, it requires less received data as suggested in inequality (4.7). If Q is selected sufficiently large (e.g., $Q = M-1$), J can be as small as 2. Secondly, the robustness of block boundary detection is potentially improved from the above discussions on Theorem 4.1. We now present the proposed blind block synchronization algorithm in ZP systems as follows.

Algorithm 1:

1. Choose the repetition index $Q \geq 1$ and the number of received blocks $J \geq 2$ so that inequality (4.7) is satisfied.

2. Collect $(J+1)P$ consecutive received samples, and form the matrix $\mathbf{Y}_{J,Q}^{(d)}$ as defined in Eq. (4.8) for each $d \in [-P/2, P/2)$.

3. Perform eigen-decomposition on the matrix $\mathbf{Y}_{J,Q}^{(d)}\mathbf{Y}_{J,Q}^{(d)\dagger}$ for each d, and take the L smallest eigenvalues $\sigma_{L,(d)}^2 \geq \sigma_{L-1,(d)}^2 \geq \cdots \geq \sigma_{2,(d)}^2 \geq \sigma_{1,(d)}^2 \geq 0$.

4. Calculate the cost function
$$\lambda_{zp,Q}(d) := \sum_{k=1}^{L} \sigma_{k,(d)}^2, \tag{4.9}$$
and decide the estimated timing mismatch
$$\hat{d} = \arg \min_{-\frac{P}{2} \leq d < \frac{P}{2}} \lambda_{zp,Q}(d).$$

□

4.3.2 Comparison with An Earlier Algorithm

We review here a blind block synchronization algorithm proposed earlier by Scaglione, Giannakis, and Barbarossa in [45] (which we call the SGB method from now on) and compare it with Algorithm 1. Suppose J consecutive blocks are collected at the receiver with a timing mismatch of d samples. Let $\mathbf{J}_n$ denote an $n \times n$ square shift matrix

$$\mathbf{J}_n = \begin{bmatrix} \mathbf{0}^T & 0 \\ \mathbf{I}_{n-1} & \mathbf{0} \end{bmatrix},$$

and consider the $P \times JL$ matrix

$$\mathcal{Y}_{SGB}^{(d)} \triangleq \begin{bmatrix} \mathbf{Y}_J^{(d)} & \mathbf{J}_P \mathbf{Y}_J^{(d)} & \cdots & \mathbf{J}_P^{L-1} \mathbf{Y}_J^{(d)} \end{bmatrix}. \tag{4.10}$$

The following claim has been proved (as Theorem 4 in [45]) regarding the rank of $\mathcal{Y}_{SGB}^{(d)} \mathcal{Y}_{SGB}^{(d)\dagger}$.

Claim: Consider the noise-free situation and assume $L_0 = L$. Then, $\mathcal{Y}_{SGB}^{(d)} \mathcal{Y}_{SGB}^{(d)\dagger}$ has full rank P when $d \neq 0$ and has rank $P-1$ when $d = 0$. □

The block synchronization problem can thus be solved by finding the only d which makes the matrix $\mathcal{Y}_{SGB}^{(d)} \mathcal{Y}_{SGB}^{(d)\dagger}$ rank deficient. In practice, when the noise is present, the cost function can be defined as

$$\lambda_{SGB}(d) \triangleq \min \left\{ \text{eigenvalues of } \mathcal{Y}_{SGB}^{(d)} \mathcal{Y}_{SGB}^{(d)\dagger} \right\}. \tag{4.11}$$

The optimal d can be chosen as

$$\hat{d} = \arg \min_{-\frac{P}{2} \leq d < \frac{P}{2}} \lambda_{SGB}(d).$$

The matrix $\mathcal{Y}_{SGB}^{(d)}$ defined in Eq. (4.10) was first proposed in [45] for blind direct channel equalization and was used in blind block synchronization. Note that when $d = 0$, the matrix $\mathcal{Y}_{SGB}^{(d)}$ happens to be a truncation of $\mathbf{Y}_{J,L}^{(d)}$ after a proper permutation of columns:

$$\mathcal{Y}_{SGB}^{(0)} \quad = \quad \begin{bmatrix} \mathbf{I}_P & \mathbf{0}_{P \times (L-1)} \end{bmatrix} \mathbf{Y}_{J,L}^{(0)} \mathcal{P} = \mathcal{H} \mathbf{U}_{J,L} \mathcal{P},$$

where $\mathcal{P}$ is a $JL \times JL$ permutation matrix, $\mathbf{U}_{J,L}$ is as defined in (4.6) with $Q = L$, and $\mathcal{H}$ is a $P \times (P-1)$ matrix defined as $\begin{bmatrix} \mathbf{I}_P & \mathbf{0}_{P \times (L-1)} \end{bmatrix} \mathcal{T}_{P-1}(\mathbf{h})$ (i.e., dropping the last $L-1$ rows of $\mathcal{T}_{P-1}(\mathbf{h})$).

The SGB method exploits the property that the rank deficiency of $\mathcal{Y}_{SGB}^{(0)}$ is unity when $d = 0$. In order to use this property properly, the matrix $\mathbf{U}_{J,L}$ must have full rank. This implies that $J \geq 1 + (M-1)/L$, which is equivalent to the requirement of Algorithm 1 with $Q = L$. Of course the SGB method was not developed from the point of view of a repetition index, but the fact that $\mathcal{Y}_{SGB}^{(d)}$ happens to be a truncation of $\mathbf{Y}_{J,L}^{(d)}$ suggests a potential performance degradation of the SGB algorithm from Algorithm 1 with $Q = L$. Indeed, this will be verified in the simulation results presented in Section 4.5.

4.4 Proposed Algorithm for CP Systems

In this section we consider the blind block synchronization problem in CP systems. The block synchronization problem in CP systems is a broader version of the so-called "timing-synchronization" or "OFDM symbol synchronization." Here we will tackle this problem without knowledge of the transmitted blocks and exploit a rank deficiency property that has been observed in an existing blind channel estimation algorithm for CP systems [60]. Unlike in ZP systems, where each received block is free from inter-block interference (IBI), a received block in CP systems, as indicated in Eq. (4.2), contains IBI in some part of it. This makes it difficult to express the received block as a linear combination of less than P linearly independent vectors, as we did in ZP systems. To overcome this problem, a concept of "composite block" composed of elements from two consecutive received blocks is employed, as described below.

4.4.1 Derivation of the Proposed Algorithm

The proposed approach to the blind block synchronization problem is derived from the blind channel estimation algorithm proposed in [60]. We first consider the situation where the noise is absent. Define a "composite block" whose elements are chosen from two consecutive received blocks:

$$\bar{\mathbf{y}}(n) = \begin{bmatrix} \mathbf{y}_M(n-1)^T & \mathbf{y}_{cp}(n)^T & \mathbf{y}_M(n)^T \end{bmatrix}^T.$$

It can be verified that [32]

$$\bar{\mathbf{y}}(n) = \tilde{\mathbf{H}}\tilde{\mathbf{u}}(n), \tag{4.12}$$

where

$$\tilde{\mathbf{H}} = \left[\begin{array}{c|c} \mathbf{H}_{cir} & \mathbf{0}_{M\times M} \\ \hline \left[\begin{array}{c|c} \mathbf{0}_{L\times(M-L)} & \mathbf{H}_u \end{array}\right] & \left[\begin{array}{c|c} \mathbf{0}_{L\times(M-L)} & \mathbf{H}_l \end{array}\right] \\ \hline \mathbf{0}_{M\times M} & \mathbf{H}_{cir} \end{array}\right],$$

$\tilde{\mathbf{u}}(n) = \left[\begin{array}{cc} \mathbf{u}_M(n-1)^T & \mathbf{u}_M(n)^T \end{array}\right]^T$, and $\mathbf{u}_M(n)$ denotes $\mathbf{R}_{cp}\mathbf{s}(n)$ in the context of CP systems. Note that here $\tilde{\mathbf{H}}$ has a size of $(2M+L)\times 2M$. This means each composite block, $\bar{\mathbf{y}}(n)$, of size $2M+L$, is a linear combination of $2M$ columns of $\tilde{\mathbf{H}}$, and is always limited to a $2M$-dimension subspace. This special property, however, is no longer true when the block synchronization is not correct (this will be verified later). This observation constitutes the basic idea of the proposed method for blind block synchronization.

Furthermore, employing the idea of repetition index, each received composite block $\bar{\mathbf{y}}(n)$ can be reformulated into a Q-column matrix $\bar{\mathbf{Y}}_Q(n)$ as defined below:

$$\bar{\mathbf{Y}}_Q(n) = \left[\begin{array}{cccc} \bar{\mathbf{y}}_{0,Q-1}(n) & \bar{\mathbf{y}}_{1,Q-2}(n) & \cdots & \bar{\mathbf{y}}_{Q-1,0}(n) \end{array}\right],$$

where each column is a $(2M+L+Q-1)$-vector defined as

$$\bar{\mathbf{y}}_{kl}(n) = \left[\begin{array}{c} [\mathbf{y}_M(n-1)]_{-k+1:M} \\ \mathbf{y}_{cp}(n) \\ [\mathbf{y}_M(n)]_{1:M+l} \end{array}\right]$$

for $k,l = 0,1,...,Q-1$. When block synchronization between the transmitter and the receiver is perfect, it can be shown that [60]

$$\bar{\mathbf{Y}}_Q(n) = \bar{\mathbf{H}}_Q\bar{\mathbf{U}}_Q(n), \tag{4.13}$$

where $\bar{\mathbf{H}}_Q$ and $\bar{\mathbf{U}}_Q(n)$ are defined as follows:

$$\bar{\mathbf{H}}_Q = \left[\begin{array}{ccc} \mathbf{H}_{cir} & & \mathbf{0}_{M\times(M+Q-1)} \\ \mathbf{0}_{(L+Q-1)\times(M-L)} & \mathcal{H}_{L+Q-1} & \mathbf{0}_{(L+Q-1)\times(M-L)} \\ \mathbf{0}_{M\times(M+Q-1)} & & \mathbf{H}_{cir2} \end{array}\right], \tag{4.14}$$

where $\mathbf{H}_{cir2}$ is obtained by moving the first L rows of $\mathbf{H}_{cir}$ to the bottom and $\mathcal{H}_{L+Q-1}$ is a $(L+Q-1)\times(2L+Q-1)$ Toeplitz matrix whose first row is $\left[\begin{array}{ccccccc} h_L & \cdots & h_0 & 0 & \cdots & 0 \end{array}\right]$ and whose first column is $\left[\begin{array}{ccccc} h_L & 0 & \cdots & 0 \end{array}\right]^T$. In (4.13),

$$\bar{\mathbf{U}}_Q(n) \triangleq \left[\begin{array}{cccc} \bar{\mathbf{u}}_{0,Q-1}(n) & \bar{\mathbf{u}}_{1,Q-2}(n) & \cdots & \bar{\mathbf{u}}_{Q-1,0}(n) \end{array}\right], \tag{4.15}$$

where

$$\bar{\mathbf{u}}_{kl}(n) \triangleq \left[\begin{array}{c} [\mathbf{u}_M(n-1)]_{-k+1:M} \\ [\mathbf{u}_M(n)]_{-L+1:M+l-L} \end{array}\right].$$

Note that $\bar{\mathbf{H}}_Q$ is a tall matrix with a size $(2M+Q+L-1)\times(2M+Q-1)$. So each column of $\bar{\mathbf{Y}}_Q(n)$ is limited to a $(2M+Q-1)$-dimension subspace. Also note that when $Q=1$, Eq. (4.13) reduces to (4.12). Now, consider J consecutive received blocks $\mathbf{y}(n)$, $n=0,1,...,J-1$ and the $(2M+L+Q-1)\times(J-1)Q$ matrix

$$\bar{\mathbf{Y}}_{J,Q} = \left[\begin{array}{cccc} \bar{\mathbf{Y}}_Q(1) & \bar{\mathbf{Y}}_Q(2) & \cdots & \bar{\mathbf{Y}}_Q(J-1) \end{array}\right]. \tag{4.16}$$

It is readily verified that

$$\bar{\mathbf{Y}}_{J,Q} = \bar{\mathbf{H}}_Q \bar{\mathbf{U}}_{J,Q},$$

where

$$\bar{\mathbf{U}}_{J,Q} = \left[\begin{array}{cccc} \bar{\mathbf{U}}_Q(1) & \bar{\mathbf{U}}_Q(2) & \cdots & \bar{\mathbf{U}}_Q(J-1) \end{array}\right] \tag{4.17}$$

is a $(2M+Q-1)\times Q(J-1)$ matrix. Suppose J is sufficiently large so that $\bar{\mathbf{U}}_{J,Q}$ has full rank $2M+Q-1$. Then the rank of $\mathbf{Y}_Q^{(J)}$ is exactly $2M+Q-1$, i.e., $\mathbf{Y}_Q^{(J)}\mathbf{Y}_Q^{(J)\dagger}$ has exactly L zero eigenvalues. This property, however, is no longer true when the block synchronization is not perfect. When a timing mismatch d is present, the matrix in (4.16) becomes

$$\bar{\mathbf{Y}}_{J,Q}^{(d)} = \left[\begin{array}{cccc} \bar{\mathbf{Y}}_Q^{(d)}(1) & \bar{\mathbf{Y}}_Q(2) & \cdots & \bar{\mathbf{Y}}_Q^{(d)}(J-1) \end{array}\right], \tag{4.18}$$

where

$$\bar{\mathbf{Y}}_Q^{(d)}(n) = \left[\begin{array}{cccc} \bar{\mathbf{y}}_{0,Q-1}^{(d)}(n) & \bar{\mathbf{y}}_{1,Q-2}^{(d)}(n) & \cdots & \bar{\mathbf{y}}_{Q-1,0}^{(d)}(n) \end{array}\right],$$

$$\bar{\mathbf{y}}_{kl}^{(d)}(n) = \left[\begin{array}{c} \left[\mathbf{y}_M^{(d)}(n-1)\right]_{-k+1:M} \\ \mathbf{y}_{cp}^{(d)}(n) \\ \left[\mathbf{y}_M^{(d)}(n)\right]_{1:M+l} \end{array}\right],$$

$$\mathbf{y}_{cp}^{(d)}(n) \triangleq \left[\mathbf{y}^{(d)}(n)\right]_{1:L},$$

and

$$\mathbf{y}_{M}^{(d)}(n) \triangleq \left[\mathbf{y}^{(d)}(n)\right]_{L+1:P}.$$

The rank deficiency of the matrix $\bar{\mathbf{Y}}_{J,Q}^{(d)}$ is the key to the proposed blind block synchronization algorithm. The following theorem presents the theoretical foundation of the proposed algorithm for CP systems.

Theorem 4.2: Assume each channel coefficient $h_k, 0 \leq k \leq L$, is an independent complex Gaussian random variable, and each element of $\mathbf{s}(n)$ is i.i.d. and selected from a finite constellation. Then, with probability one there exists a sufficiently large J such that the following statement on the matrix $\bar{\mathbf{Y}}_{J,Q}^{(d)}$ defined in (4.18) is true with probability one.

$$\begin{aligned} & \text{The number of zero eigenvalues of } \bar{\mathbf{Y}}_{J,Q}^{(d)} \bar{\mathbf{Y}}_{J,Q}^{(d)\dagger} \\ = \; & (2M+L+Q-1) - \text{rank}(\bar{\mathbf{Y}}_{J,Q}^{(d)} \bar{\mathbf{Y}}_{J,Q}^{(d)\dagger}) \\ = \; & \begin{cases} L & \text{if } d = 0 \\ \max\{L-|d|-2(Q-1), 0\} & \text{if } d \neq 0 \end{cases}. \end{aligned}$$

□

Proof: See Appendix. □

The behavior of the rank deficiency of $\bar{\mathbf{Y}}_{J,Q}^{(d)}$ is exactly equal to that of $\mathbf{Y}_{J,Q}^{(d)}$ in ZP systems as presented in Theorem 4.1, even though the sizes of $\bar{\mathbf{Y}}_{J,Q}^{(d)}$ and $\mathbf{Y}_{J,Q}^{(d)}$ are completely different. Similar comments can therefore be made as follows. When $Q = 1$, the rank deficiency of $\bar{\mathbf{Y}}_{J,Q}^{(d)}$ is $\max\{L-|d|, 0\}$, and when $Q \geq (L+1)/2$, the rank deficiency of $\bar{\mathbf{Y}}_{J,Q}^{(d)}$ is $L \cdot \delta[d]$, where $\delta[\cdot]$ denotes the discrete Delta function. An advantage is present for using a larger Q: the reduction in the rank deficiency of $\bar{\mathbf{Y}}_{J,Q}^{(d)}$ when $d \neq 0$ is more significant. This potentially improves the accuracy of blind block synchronization performance.

We should note that a necessary (but not sufficient) condition for $\bar{\mathbf{U}}_{J,Q}$ to have full rank is [60]:

$$J \geq 2 + \frac{2M-1}{Q}. \tag{4.19}$$

Although (4.19) is not sufficient, the probability that $\bar{\mathbf{U}}_{J,Q}$ has full rank is usually very high in the simulation shown in Section 4.5. Inequality (4.19) also shows that, when the repetition index Q is chosen sufficiently large (e.g., $Q = 2M - 1$), the proposed algorithm can work with only *three* received blocks in absence of noise!

In presence of noise, the optimal d can be chosen as the one which minimizes the sum of the smallest L eigenvalues of $\mathbf{Y}_{J,Q}^{(d)} \mathbf{Y}_{J,Q}^{(d)\,\dagger}$. The proposed algorithm can be summarized as follows.

Algorithm 2:

1. Choose the repetition index $Q \geq 1$ and the number of received blocks $J \geq 3$ so that (4.19) is satisfied.

2. Collect $(J+1)P$ consecutive received samples, and form the matrix $\bar{\mathbf{Y}}_{J,Q}^{(d)}$ as in Eq. (4.18) for each $d \in [-P/2, P/2)$.

3. Perform eigen-decomposition on the matrix $\bar{\mathbf{Y}}_{J,Q}^{(d)} \bar{\mathbf{Y}}_{J,Q}^{(d)\,\dagger}$, and take the L smallest eigenvalues $\sigma_{L,(d)}^2 \geq \sigma_{L-1,(d)}^2 \geq \cdots \geq \sigma_{2,(d)}^2 \geq \sigma_{1,(d)}^2 \geq 0$.

4. Calculate the cost function $\lambda_{cp,Q}(d) := \sum_{k=1}^{L} \sigma_{k,(d)}^2$, and decide the estimated timing mismatch $\hat{d} = \arg\min_{-\frac{P}{2} \leq d < \frac{P}{2}} \lambda_{cp,Q}(d)$. □

4.4.2 Comparisons with a Previously Reported Algorithm

In [33], a block synchronization algorithm was proposed by Negi and Cioffi based on the estimated rank of the autocorrelation matrix of received blocks. The basic idea of the Negi-Cioffi algorithm is to use the $(M + L - L_0) \times J$ matrix

$$\mathcal{Y}_{NC}^{(d)} = \left[\begin{array}{ccc} \left[\mathbf{y}_{cp}^{(d)}(0)\right]_{L_0+1:L} & \cdots & \left[\mathbf{y}_{cp}^{(d)}(J-1)\right]_{L_0+1:L} \\ \hline \mathbf{y}_{M}^{(d)}(0) & \cdots & \mathbf{y}_{M}^{(d)}(J-1) \end{array} \right].$$

Define

$$\mathbf{u}^{(d)}(n) = \left[\begin{array}{cccc} u(nP+d) & u(nP+d+1) & \cdots & u(nP+d+P-1) \end{array} \right]^T.$$

Then it can be verified that

$$\mathcal{Y}_{NC}^{(d)} = \mathcal{H}_{L_0} \mathbf{U}_{NC}^{(d)},$$

where $\mathcal{H}_{L_0}$ is a $(P - L_0) \times P$ Toeplitz matrix whose first row is $\left[\begin{array}{ccccccc} h_{L_0} & \cdots & h_0 & 0 & \cdots & 0 \end{array} \right]$ and

whose first column is $\left[\begin{array}{cccc} h_{L_0} & 0 & \cdots & 0 \end{array}\right]^T$, and

$$\mathbf{U}_{NC}^{(d)} = \left[\begin{array}{cccc} \mathbf{u}^{(d)}(0) & \mathbf{u}^{(d)}(1) & \cdots & \mathbf{u}^{(d)}(J-1) \end{array}\right]$$

is a $P \times J$ matrix. When $d = 0$, $\mathbf{U}_{NC}^{(d)}$ has rank M and the matrix $\mathcal{Y}_{NC}^{(d)}$ has a $L - L_0$ rank deficiency. When $d \neq 0$, the rank of $\mathbf{U}_{NC}^{(d)}$ is larger than M and the rank deficiency of $\mathcal{Y}_{NC}^{(d)}$ will not exceed $L - L_0$. This provides a way to determine the block boundaries by finding the d which gives $\mathcal{Y}_{NC}^{(d)}$ the smallest rank. In order to make the method work, $L - L_0$ must be a positive integer, which implies that the effective channel order L_0 must be strictly less than the cyclic prefix length L. In our proposed Algorithm 2, $L - L_0$ does not have to be positive. Another difference between the Negi-Cioffi algorithm and Algorithm 2 resides in the matrix $\mathbf{U}_{NC}^{(d)}$. In order to make $\mathbf{U}_{NC}^{(d)}$ rank M, a condition $J \geq M$ must be satisfied, which means the minimum number of received blocks is equal to the block size. As a comparison with (4.19), we find that the required number of received blocks for Algorithm 2 is always smaller than that of the Negi-Cioffi algorithm whenever the repetition index Q is chosen greater than 2.

In [33], the optimal d is chosen by estimating the rank of $\mathcal{Y}_{NC}^{(d)}$ using a minimum description length (MDL) criterion, assuming the channel noise variance is known. However, our proposed algorithm does not assume known channel noise variance. In order to make a fair comparison between Algorithm 2 and the Negi-Cioffi algorithm, in our simulations presented in Section 4.5, we will slightly modify the optimal d decision procedure in the Negi-Cioffi algorithm by using the following cost function:

$$\lambda_{NC}(d) \triangleq \sum_{k=1}^{L-L_0} \sigma_{k,(d)}^2, \tag{4.20}$$

where $\sigma_{k,(d)}^2$ is the kth smallest eigenvalue of $\mathcal{Y}_{NC}^{(d)} \mathcal{Y}_{NC}^{(d)\,\dagger}$. The optimal d is chosen as the one which minimizes the value of $\lambda_{NC}(d)$.

4.5 Simulation Results and Discussions

In this section, we conduct simulations to evaluate the performances of Algorithms 1 and 2 and compare each of them with well known algorithms. In all simulations, the number of data samples per block is chosen as $M = 16$, and the length of guard intervals per block is $L = 4$ (which implies

$P = 20$). The constellation of data samples is QPSK. In the plots, $E_s = E[|s_k(n)|^2]$ and $N_0 = E[|e(n)|^2]$.

4.5.1 Simulation Results for Zero Padding Systems

We first present simulation results for zero padding systems. The precoder is chosen as $\mathbf{R}_{zp} = \mathbf{I}_M$. We test Algorithm 1 with $Q = 1, 2, 3$ and compare the performances with that of the SGB algorithm proposed in [45]. Simulations are first conducted with two different fixed fourth order FIR channels. Channel 1 has zero locations at $(0.8, -0.8, 0.5j, -0.5j)$ and is a minimum-phase system. Channel 2 has zero locations at $(1.2, -0.9, 0.7j, -0.7)$. As suggested in (4.7), the number of received blocks must be at least $J \geq M = 16$. We choose $J = 20$, that is, $(J + 1)P = 420$ consecutive received samples $y(n)$ are available for blind block synchronization. For each blind synchronization attempt, 420 samples $y(n)$ are collected, and the cost functions $\lambda(d)$ as defined in (4.9) and (4.11) (i.e., $\lambda_{zp,Q}(d)$ and $\lambda_{SGB}(d)$ for Algorithm 1 and the SGB method, respectively) are evaluated for each $d \in [-P/2, P/2)$. A successful block synchronization is declared when $\lambda(d)$ gives the minimum value at $d = 0$. Over 20,000 block synchronization attempts are conducted in the simulations in different E_s/N_0 levels ranging from -20 dB to 50 dB, and the block synchronization error rates are calculated accordingly. We also calculated the average values of $\lambda(d)$ over all block synchronization attempts in a noise-free environment.

Figure 4.3 shows the average value of the cost functions $\lambda(d)$ versus the timing mismatch $d \in [-P/2, P/2)$ with Channel 1. For a clearer view of the values of $\lambda(d)$ in the neighborhood of $d = 0$, a close-up window is put at the top of each plot. As expected, $\lambda(d) = 0$ when $d = 0$ and is nonzero otherwise for all curves. The robustness of a particular algorithm against noise perturbation with respect to a specific Q may be roughly evaluated by looking at the values $\Delta^{k,Q}_{\text{left}}$ and $\Delta^{k,Q}_{\text{right}}$. When an additive noise is present, the values of $\lambda(d)$ will change, and an algorithm may mistakenly decide the optimal timing mismatch as $d = -1$ or $d = 1$. Therefore, larger values of $\Delta^{k,Q}_{\text{left}}$ and $\Delta^{k,Q}_{\text{right}}$, in Figure 4.3, represent a larger margin against noise perturbation and suggest a better performance for a particular algorithm.

As we can see in Figure 4.3, the SGB method has a good $\Delta^{k,Q}_{\text{left}}$ but a relatively small $\lambda(1)$. Algorithm 1 with $Q = 2$ or 3 has a much better $\Delta^{k,Q}_{\text{right}}$, but both $\Delta^{k,Q}_{\text{left}}$ and $\Delta^{k,Q}_{\text{right}}$ are poor with $Q = 1$. These observations can be explained from the point of view of Theorem 4.1. In Theorem 4.1, the number of zero eigenvalues of $\mathbf{Y}^{(d)}_{J,Q}\mathbf{Y}^{(d)\,\dagger}_{J,Q}$ is L when $d = 0$, and it decreases to $L - 2Q + 1$ when

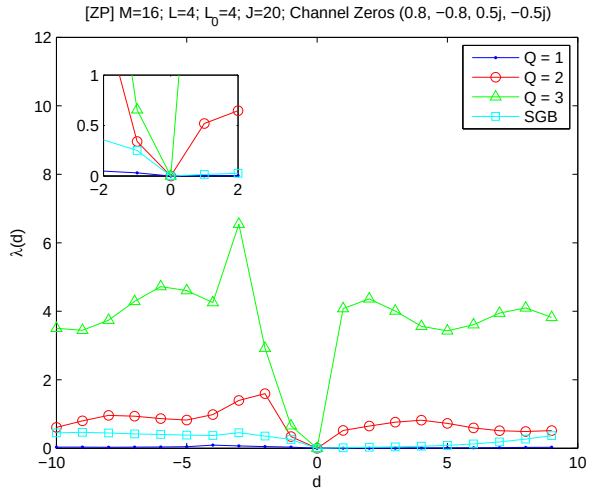

Figure 4.3: Function $\lambda(d)$ v.s. time mismatch d for a channel with zeros at $(0.8, -0.8, 0.5j, -0.5j)$ in absence of noise.

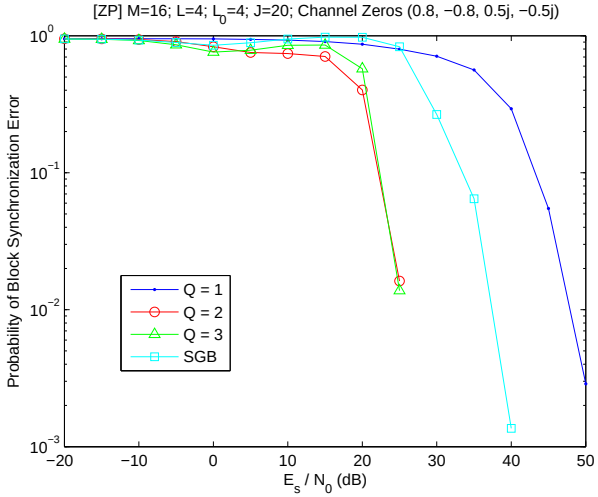

Figure 4.4: Blind block synchronization error rate performance for a channel with zeros at $(0.8, -0.8, 0.5j, -0.5j)$ when $J = 20$ in ZP systems.

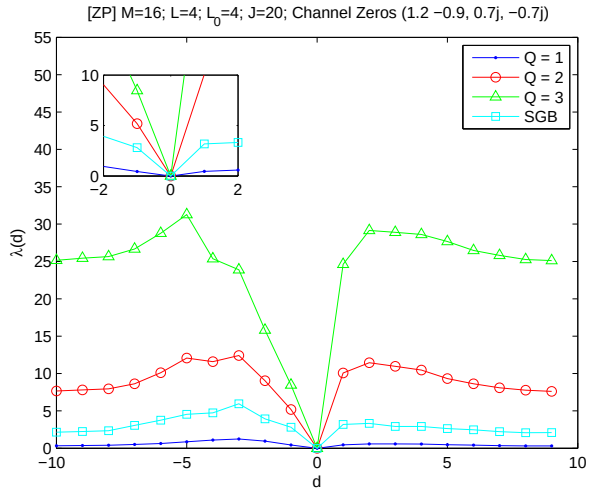

Figure 4.5: Function $\lambda(d)$ v.s. time mismatch d for a channel with zeros at $(1.2, -0.9, 0.7j, -0.7j)$ in absence of noise when $J = 20$.

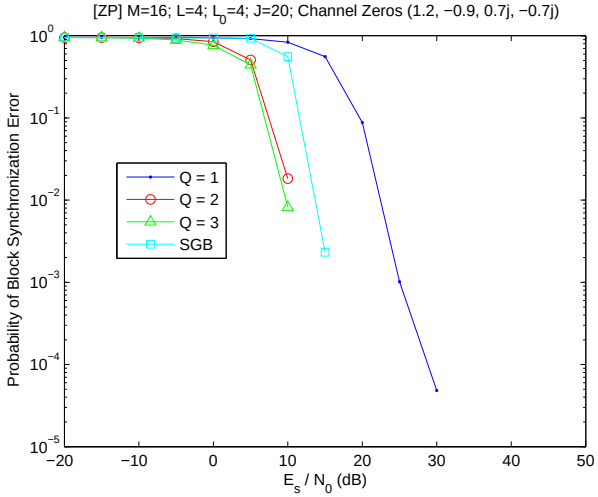

Figure 4.6: Blind block synchronization error rate performance for a channel with zeros at $(1.2, -0.9, 0.7j, -0.7j)$ when $J = 20$ in ZP systems.

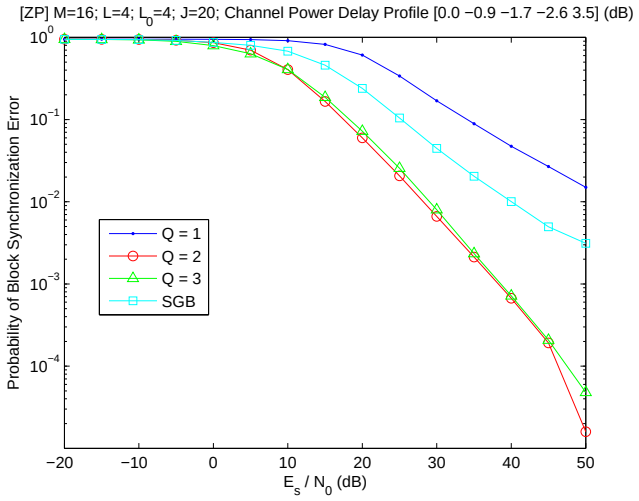

Figure 4.7: Blind block synchronization error rate performance for a Rayleigh random channel with $J = 20$ in ZP systems.

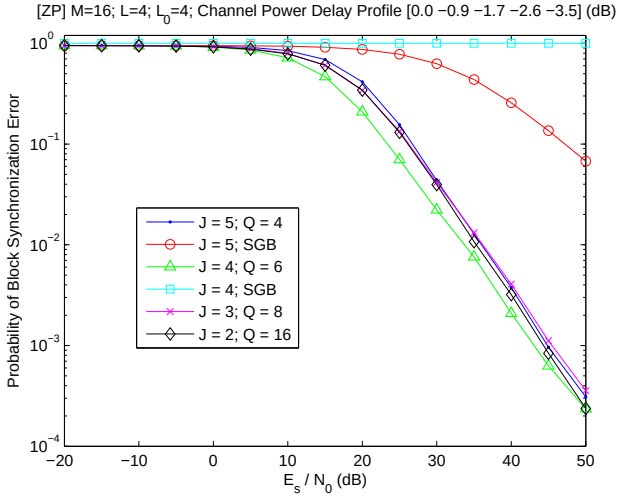

Figure 4.8: Blind block synchronization error rate performance for a Rayleigh random channel with small J in ZP systems.

$d = 1$ (if $L \geq 2Q - 1$), so $\lambda(1)$ is obtained by adding up $2Q - 1$ nonzero eigenvalues of $\mathbf{Y}_{J,Q}^{(d)} \mathbf{Y}_{J,Q}^{(d)\dagger}$. When $Q = 1$, $\lambda(1)$ is obtained by a single nonzero eigenvalue, which can be very close to zero with a certain probability. When $Q = 2$, $\lambda(1)$ is obtained by adding three nonzero eigenvalues, and the probability that all of them are very small will drop significantly. Simulations under a noisy environment, as shown in Figure 4.4, confirm the intuitive expectation that the algorithms (for various Q) perform better for larger values of $\Delta_{\text{left}}^{k,Q}$and $\Delta_{\text{right}}^{k,Q}$. Clearly, Algorithm 1 with $Q = 2$ has a significant gain (more than 10 dB!) over the SGB algorithm. Increasing Q from 2 to 3, however, does not further improve the performance. Algorithm 1 with $Q = 1$, however, requires a 50-dB E_s/N_0 ratio to achieve a satisfactory error rate, which is considered infeasible in practice.

We now show the simulation results for Channel 2, which contains channel zeros both inside and outside the unit circle and so is neither a minimum phase nor a maximum phase system. In the noiseless environment, the plot of $\lambda(d)$ versus timing mismatch d is shown in Figure 4.5. We observe that the SGB method has a much larger $\Delta_{\text{right}}^{k,Q}$than it does with Channel 1, a minimum phase system. Yet Algorithm 1 with $Q \geq 2$ possesses even larger $\Delta_{\text{left}}^{k,Q}$and $\Delta_{\text{right}}^{k,Q}$than the SGB algorithm. The block synchronization error rate performance is plotted in Figure 4.6. Algorithm 1 with $Q = 2$ still has a roughly 5-dB gain over the SGB method. Again, the performance of Algorithm 1 with $Q = 3$ is not significantly better than that with $Q = 2$. Algorithm 1 with $Q = 1$ still has the poorest performance in this plot. From Figures 4.4 and 4.6 for Channels 1 and 2, respectively, we find that the block synchronization error rate performance depends not only on the algorithms, but also on the channels. Minimum phase channels appear to be less favorable for blind block synchronization in general than other types of channels.

Simulation results presented so far are based on fixed channels. We now try the comparison in a fourth order Rayleigh random channel with a power delay profile $[0.0 - 0.9 - 1.7 - 2.6 - 3.5]$ (dB). Over 4,000 independent realizations of the channel are used in the simulation, and for each channel realization four block synchronization attempts are performed (i.e., four different sets of data samples $s(n)$ are used). Figure 4.7 shows the average block synchronization error rate performances for all cases. As we can see, Algorithm 1 with $Q = 2$ has a roughly 10 dB gain over the SGB algorithm. Increasing Q from 2 to 3 does not significantly improve the system performance.

Finally, in this subsection, we demonstrate the capability of Algorithm 1 to conduct blind block synchronization with extremely limited received data. We choose J ranging from 2 to 5, and the repetition index Q is properly chosen so that inequality (4.7) is satisfied. Figure 4.8 shows the

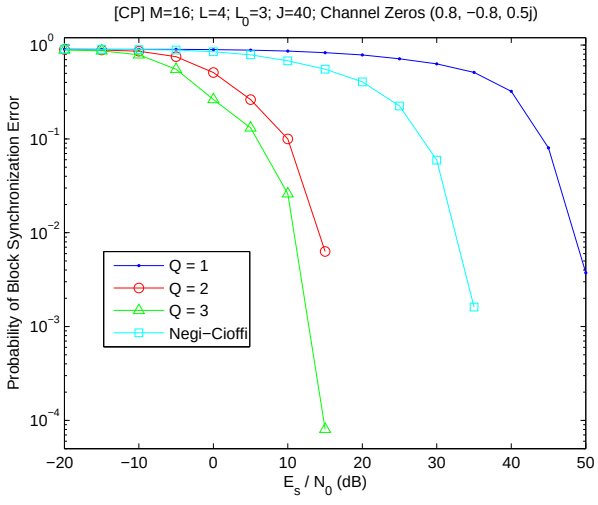

Figure 4.9: Blind block synchronization error rate performance for a channel with zeros at $(0.8, -0.8, 0.5j)$ when $J = 40$ in CP systems.

simulation plot. As discussed in Section 4.3.2, the SGB algorithm is similar to Algorithm 1 with $Q = L = 4$ except for some omissions of data. As shown in the plot, when $J = 5$, the SGB method indeed has a much worse performance than Algorithm 1 with $Q = 4$. Furthermore, when $J = 4$, the SGB algorithm fails, while Algorithm 1 continues to work even when J is as small as 2. Note that when $J = 2$, the number of available consecutive received samples is only $(J + 1)P = 60$. Even though the block synchronization error rate performance is satisfactory only when the E_s/N_0 value is very high, Algorithm 1 is presumably the first one to perform blind block synchronization properly with such limited received data.

4.5.2 Simulation Results for Cyclic Prefix Systems

We now present simulation results for cyclic prefix systems. The precoder is chosen as $\mathbf{R}_{cp} = \mathbf{I}_M$. We test Algorithm 2 with $Q = 1, 2, 3$ and compare the performances with that of the Negi-Cioffi algorithm [33]. As suggested in inequality (4.19), J must be chosen as at least $2M + 1 = 37$ for Algorithm 2 with $Q = 1$ to work. We choose $J = 40$, that is, $(J + 1)P = 820$ consecutive received samples $y(n)$ are available for blind block synchronization.

We first test the algorithm with third-order channels (i.e., $L_0 = 3$). Note that a cyclic prefix of length $L = 4$ allows a maximum channel order to be four to avoid interblock interference. The reason why we chose only third-order channels is for proper comparison with the Negi-Cioffi algo-

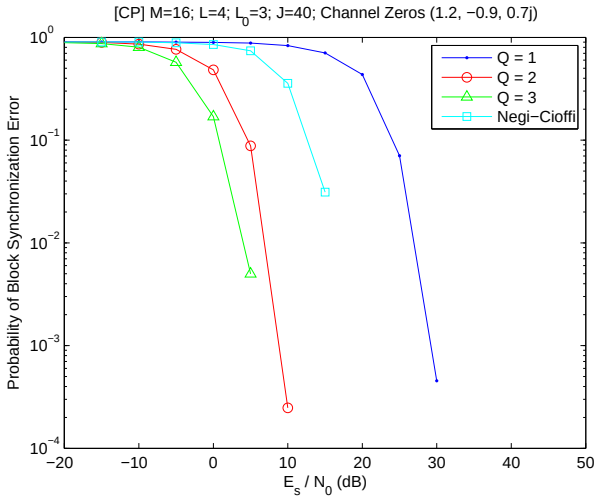

Figure 4.10: Blind block synchronization error rate performance for a channel with zeros at $(1.2, -0.9, 0.7j)$ when $J = 40$ in CP systems.

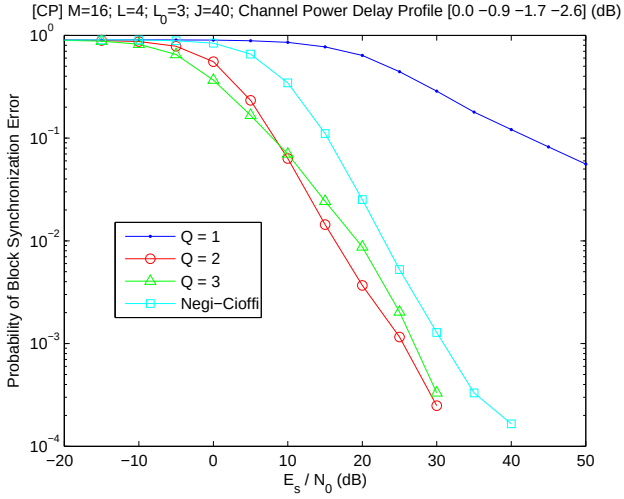

Figure 4.11: Blind block synchronization error rate performance for a third-order Rayleigh random channel with $J = 40$ in CP systems.

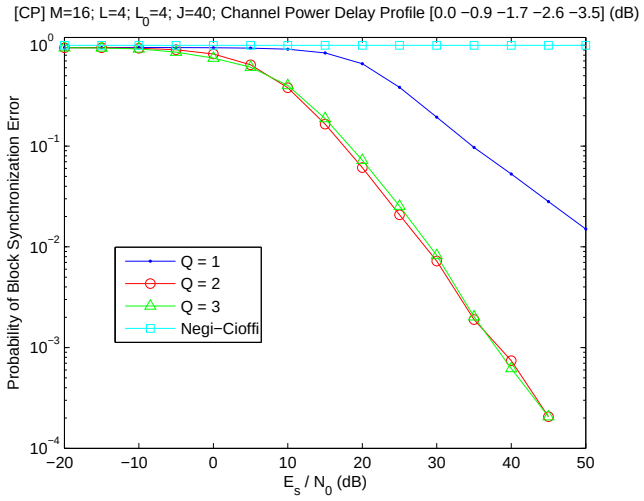

Figure 4.12: Blind block synchronization error rate performance for a fourth-order Rayleigh random channel with $J = 40$ in CP systems.

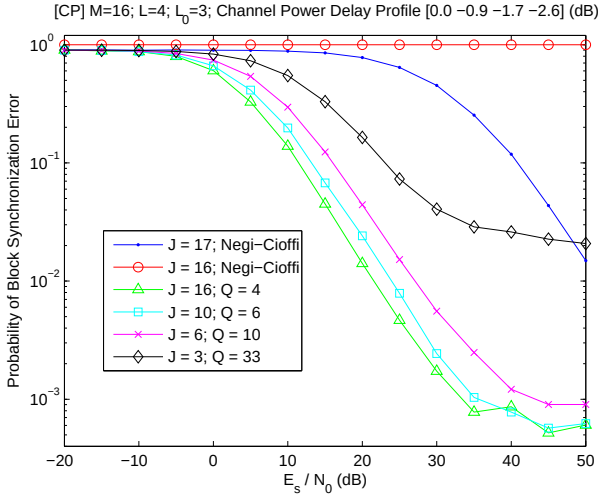

Figure 4.13: Blind block synchronization error rate performance for a third-order Rayleigh random channel in CP systems when J is small.

rithm due to its restriction (see Section 4.4.2). In the simulations, we use the cost function defined in (4.20) for the Negi-Cioffi algorithm.

Simulations are first conducted with two different fixed third order FIR channels. Channel 3 has zero locations at $(0.8, -0.8, 0.5j)$ and is a minimum-phase system. Channel 4 has zero locations at $(1.2, -0.9, 0.7j)$. Figure 4.9 shows the simulation results with Channel 3. We see that when $Q = 1$, Algorithm 2 works properly in the high-SNR region, but with a rather unsatisfactory performance. Algorithm 2 with $Q = 2$ has a much better performance and has a 20-dB gain over the Negi-Cioffi algorithm. Increasing Q from 2 to 3 further improves the performance. Figure 4.10 shows the simulation results with Channel 4. While the relative performances among all cases do not change, the performances are obviously better than those in Figure 4.9 in all cases. This suggests all blind block synchronization algorithms have poorer performance for minimum phase channels than for other types of channels.

We now perform the simulation in a third-order Rayleigh random channel with a power delay profile $[0.0 - 0.9 - 1.7 - 2.6]$ dB, and the results are shown in Figure 4.11. Algorithm 2 with $Q = 2$ has a 10-dB gain over the Negi-Cioffi algorithm. Increasing Q from 2 to 3 does not significantly improve the system performance.

Recall that we chose $L_0 = 3 < L$ in previous simulations due to a restriction of the Negi-Cioffi algorithm. Now we conduct simulations with a fourth order Rayleigh channel to verify that Algorithm 2 also works in the situation where $L = L_0$. As shown in Figure 4.12, Algorithm 2 works fine with all Q, while the Negi-Cioffi algorithm fails.

Finally, in this subsection, we demonstrate the capability of Algorithm 2 to conduct blind block synchronization with small amount of received data. We choose J ranging from 3 to 16, and the repetition index Q is properly chosen so that inequality (4.19) is satisfied. We also compare the performances with those of the Negi-Cioffi algorithm with $J = 16$ and 17. Figure 4.13 shows the simulation plot. As discussed in Section 4.4.2, the Negi-Cioffi algorithm requires at least $M = 16$ blocks to work properly. From the simulation plot, we see that it does not even work with $J = 16$. When $J = 17$, the Negi-Cioffi algorithm appears to work, but with a somewhat poor performance. On the other hand, Algorithm 2 with $Q = 4$ already works when $J = 16$ with a fairly satisfactory performance. As the parameter J decreases, the performance of Algorithm 2 (with a properly chosen Q) degrades slowly. Even when $J = 3$ (which implies the number of available consecutive received sample is only $(J+1)P = 80$), Algorithm 2 still possesses a much better performance than

the Negi-Cioffi algorithm with $J = 17$.

4.6 Conclusions

In this chapter we proposed two algorithms for blind block synchronization in zero-padding (ZP) systems and in cyclic prefix (CP) systems, respectively. Both algorithms use a parameter called repetition index (Q) which can be chosen as any positive integer. The CP algorithm can be directly applied to blind symbol synchronization problem in the popular orthogonal frequency division multiplexing (OFDM) systems. Theoretical results prove the validity of the proposed algorithms in the noiseless case and suggest that the algorithms would have a better performance when the repetition index is larger in the noisy case. The proposed algorithms are capable of blindly recovering the block boundaries using much less received data than previously reported algorithms. This feature makes the proposed algorithms more favorable in an environment of fast-varying channels. Simulation results of the proposed algorithm not only demonstrate the capability to work properly with a limited amount of received data but also reveal significant improvement in block synchronization error rate performance over previously reported algorithms.

In the future, performance evaluation of the proposed algorithms for time-varying channels will be important for a more realistic scenario. A theoretical analysis of the system performance is also of interest.

4.7 Appendix

Proof of Theorem 4.1: We first consider the case $d = 0$.

$$\mathbf{y}(n) = \mathcal{H} \left[\begin{array}{c} \mathbf{0}_{L\times 1} \\ \hline \mathbf{u}(n) \\ \hline \mathbf{0}_{L\times 1} \end{array} \right] = \mathcal{T}_M(\mathbf{h})\,\mathbf{u}(n),$$

where $\mathcal{H}$ is the $P \times (P + L)$ Toeplitz matrix Toeplitz matrix whose first column is $[h_L, 0, ..., 0]^T$ and whose first row is $[h_L, ..., h_0, 0, ..., 0]$.

When $d = 0$, it can be shown that

$$\mathcal{T}_Q\left(\mathbf{y}^{(0)}(n)\right) = \mathcal{T}_{M+Q-1}(\mathbf{h})\,\mathcal{T}_Q\left(\mathbf{u}^{(0)}(n)\right).$$

With probability one, for sufficiently large J, the matrix

$$\mathbf{Y}_{J,Q}^{(d)} = \mathcal{T}_{M+Q-1}\left(\mathbf{h}\right)\mathbf{U}_{Q}^{(J)}$$

has rank $M+Q-1$. This implies $\mathbf{Y}_{J,Q}^{(d)}\mathbf{Y}_{J,Q}^{(d)\ \dagger}$ has exactly L zero eigenvalues.

When $d \neq 0$,

$$\mathbf{y}^{(d)}(n) = \mathcal{H}\mathbf{u}^{(d)}(n),$$

where $\mathbf{u}^{(d)}(n) = \left[\begin{array}{c} \mathbf{0}_{(L-d)\times 1} \\ \hline \mathbf{u}(n) \\ \hline \mathbf{0}_{L\times 1} \\ \hline \left[\mathbf{u}(n+1)\right]_{1:d} \end{array}\right]$ when $0 < d \leq L$ and $\mathbf{u}^{(d)}(n) = \left[\begin{array}{c} \left[\mathbf{u}(n)\right]_{d-L+1:M} \\ \hline \mathbf{0}_{L\times 1} \\ \hline \left[\mathbf{u}(n+1)\right]_{1:d} \end{array}\right]$ when $L < d \leq P/2$.

The qth column of $\mathcal{T}_Q\left(\mathbf{y}^{(d)}(n)\right)$ can be written as

$$\left[\begin{array}{c} \mathbf{0}_{(q-1)\times 1} \\ \mathbf{y}^{(d)}(n) \\ \mathbf{0}_{(Q-q)\times 1} \end{array}\right] = \mathcal{H}_Q \left[\begin{array}{c} v_{q-1} \\ \vdots \\ v_1 \\ \mathbf{u}^{(d)}(n) \\ x_1 \\ \vdots \\ x_{Q-q} \end{array}\right],$$

where $\mathcal{H}_Q$ is a $(P+L+Q-1)\times(P+Q-1)$ Toeplitz matrix whose first column is $[h_L, 0, ..., 0]^T$ and whose first row is $[h_L, ..., h_0, 0, ..., 0]$ and sequences $\{x_k\}$ and $\{v_k\}$ are defined as follows.

$$\begin{aligned} [x_{-L+1}, x_{-L+2}, \cdots, x_0]^T &\triangleq \left[\mathbf{u}^{(d)}(n)\right]_{P:P+L} \\ [v_0, v_{-1}, \cdots, v_{-L+1}]^T &\triangleq \left[\mathbf{u}^{(d)}(n)\right]_{1:L} \end{aligned}$$

$$\begin{aligned} x_l &\triangleq -\frac{1}{h_0}\left[\sum_{k=1}^{L} h_k x_{l-k}\right], l = 1, ..., Q-1. \\ v_l &\triangleq -\frac{1}{h_L}\left[\sum_{k=0}^{L-1} h_k v_{l-L+k}\right], l = 1, ..., Q-1. \end{aligned}$$

So

$$\mathcal{T}_Q\left(\mathbf{y}^{(d)}(n)\right) = \mathcal{H}_Q \mathbf{U}_Q^{(d)}(n),$$

where

$$\mathbf{U}_Q^{(d)}(n) = \mathcal{T}_Q\left(\mathbf{u}^{(d)}(n)\right) + \mathbf{V}$$

and $\mathbf{V}$ is a $(P+L+Q-1)\times Q$ Toeplitz matrix whose first column is $\begin{bmatrix} \mathbf{0}_{1\times(P+L)} & x_1 & \cdots & x_{Q-1} \end{bmatrix}^T$ and whose first row is $\begin{bmatrix} 0 & v_1 & \cdots & v_{Q-1} \end{bmatrix}$.

Denote $n(L,Q,d)$ as the number of pairs of identical rows in $\mathbf{U}_Q^{(d)}(n)$. When $Q \leq L+1$, the zero block $\mathbf{0}_{L\times 1}$ in $\mathbf{u}^{(d)}(n)$ accounts for $(L-Q-1)$ zero rows in $\mathbf{U}_Q^{(d)}(n)$. Furthermore, if $0 < d \leq L-Q+1$, the zero block $\mathbf{0}_{(L-d)\times 1}$ in $\mathbf{u}^{(d)}(n)$ accounts for $(L-Q-1-d)$ zero rows in $\mathbf{U}_Q^{(d)}(n)$. If $L-Q-1 < d < P/2$, the zero block $\mathbf{0}_{(L-d)\times 1}$ does not account for any zero rows in $\mathbf{U}_Q^{(d)}(n)$ (when $d > L$, $\mathbf{0}_{(L-d)\times L}$ does not even exist). The above arguments can be extended to the case when $-P/2 \leq d < 0$ due to symmetry. So, when $Q \leq L+1$,

$$n(L,Q,d) = \underbrace{(L-Q+1)}_{\text{from } \mathbf{0}_{L\times 1}} + \underbrace{\max\{L-Q+1-|d|, 0\}}_{\text{from } \mathbf{0}_{(L-d)\times 1}}.$$

When $Q > L+1$, neither blocks $\mathbf{0}_{L\times 1}$ nor $\mathbf{0}_{(L-d)\times 1}$ in $\mathbf{u}^{(d)}(n)$ account for any zero rows. So

$$n(L,Q,d) = 0$$

when $Q > L+1$.

Now $\mathbf{Y}_{J,Q}^{(d)} = \mathcal{H}_Q \mathbf{U}_{J,Q}^{(d)} = \mathcal{H}'_Q \mathbf{U}'^{(d)}_{J,Q}$, where $\mathbf{U}'^{(d)}_{J,Q}$ is obtained by eliminating the $n(L,Q,d)$ zeros rows in $\mathbf{U}_{J,Q}^{(d)}$ and $\mathcal{H}'_Q$ is obtained by eliminating the corresponding columns in $\mathcal{H}_Q$. We are interested in the value of the number of rows of $\mathcal{H}'_Q$ minus the number of columns of $\mathcal{H}'_Q$. Denote this value as $n(\mathcal{H}'_Q)$. This value represents the column rank deficiency of $\mathcal{H}'_Q$ if $n(\mathcal{H}'_Q) \geq 0$. It is readily

verified that $n(\mathcal{H}'_Q) = n(L,Q,d) - L$, and so the column rank deficiency of $\mathcal{H}'_Q$ is $\max\{n(\mathcal{H}'_Q), 0\}$. Due to the random nature of $\mathbf{u}(n)$, $\{x_k\}$, and $\{v_k\}$, with probability one, there exists a sufficiently large J such that $\mathbf{U}'^{(d)}_{J,Q}$ has full rank $(P+L+Q-1-n(L,Q,d))$. The rank deficiency of $\mathbf{Y}^{(d)}_{J,Q}\mathbf{Y}^{(d)\ \dagger}_{J,Q}$ is $\max\{n(L,Q,d)-L, 0\}$. When $Q > L+1$, $n(L,Q,d) = 0$, so the rank deficiency of $\mathbf{Y}^{(d)}_{J,Q}\mathbf{Y}^{(d)\ \dagger}_{J,Q}$ is zero. When $Q \leq L+1$ and when $|d| \geq L-Q+1$, $n(L,Q,d) = L-Q+1$, so the rank deficiency of $\mathbf{Y}^{(d)}_{J,Q}\mathbf{Y}^{(d)\ \dagger}_{J,Q}$ is $\max\{-Q+1, 0\} = 0$. When $Q \leq L+1$ and when $|d| \leq L-Q+1$, $n(L,Q,d) = 2L-2Q+2-|d|$, so the rank deficiency of $\mathbf{Y}^{(d)}_{J,Q}\mathbf{Y}^{(d)\ \dagger}_{J,Q}$ is $\max\{2L-2Q+2-|d|-L, 0\} = L-|d|-2(Q-1)$.

In summary, with probability one, the number of zero eigenvalues of $\mathbf{Y}^{(d)}_{J,Q}\mathbf{Y}^{(d)\ \dagger}_{J,Q}$ is $\max\{L - |d| - 2(Q-1), 0\}$ when $d \neq 0$. This completes the proof. □

Proof of Theorem 4.2:

We first consider the case $d = 0$.

$$\bar{\mathbf{y}}(n) = \mathcal{H}\left[\begin{array}{c}\mathbf{u}_{cp}(n-1)\\ \hline \mathbf{u}_M(n-1)\\ \hline \mathbf{u}'_M(n)\\ \hline \mathbf{u}_{cp}(n)\end{array}\right] = \bar{\mathbf{H}}\bar{\mathbf{u}}(n),$$

where $\mathcal{H}$ is the $(2M+L) \times (2M+2L)$ Toeplitz matrix whose first column is $[h_L, 0, ..., 0]^T$ and whose first row is $[h_L, \cdots, h_0, 0, ..., 0]$, and $\mathbf{u}'_M(n)$ is a permutation of $\mathbf{u}_M(n)$ defined as $\mathbf{u}'_M(n) = [\mathbf{u}_M(n)]_{-L+1:M-L}$.

With probability one there exists a sufficiently large J such that

$$\mathbf{Y}^{(d)}_{J,Q} = \bar{\mathbf{H}}_Q \mathbf{U}^{(J)}_Q,$$

where $\bar{\mathbf{H}}_Q$ is a $(2M+L+Q-1)\times(2M+Q-1)$ matrix which has full column rank $(2M+Q-1)$ with probability one and $\mathbf{U}_{J,Q}$ has full row rank. The rank of $\mathbf{Y}^{(d)}_{J,Q}$ is thus exactly equal to $2M+Q-1$ since $\bar{\mathbf{H}}$ has full column rank $2M+Q-1$ and $\mathbf{U}^{(0)}_{J,Q}$ has full row rank $2M+Q-1$. This implies $\mathbf{Y}^{(d)}_{J,Q}\mathbf{Y}^{(d)\dagger}_{J,Q}$ has exactly $(2M+L+Q-1)-(2M+Q-1) = L$ zero eigenvalues.

When $d \neq 0$, we have

$$\bar{\mathbf{y}}^{(d)}(n) = \mathcal{H}\bar{\mathbf{u}}^{(d)}(n),$$

where $\bar{\mathbf{u}}^{(d)}(n) = \left[\begin{array}{c} [\mathbf{u}_{cp}(n-1)]_{d+1:L} \\ \hline \mathbf{u}_M(n-1) \\ \mathbf{u}'_M(n) \\ \mathbf{u}_{cp}(n) \\ \hline [\mathbf{u}_{cp}(n+1)]_{1:d} \end{array}\right]$ when $0 < d \leq L$ and $\bar{\mathbf{u}}^{(d)}(n) = \left[\begin{array}{c} [\mathbf{u}_M(n-1)]_{(d-L+1):M} \\ \hline \mathbf{u}'_M(n) \\ \mathbf{u}_{cp}(n) \\ \hline \mathbf{u}_{cp}(n+1) \\ [\mathbf{u}_M(n+1)]_{1:d-L} \end{array}\right]$ when $L < d \leq P/2$.

Now, from the definition of $\bar{\mathbf{Y}}_Q^{(d)}(n)$, the qth column of $\bar{\mathbf{Y}}_Q^{(d)}(n)$ can be expressed as

$$\left[\begin{array}{c} \left[\mathbf{y}_M^{(d)}(n-1)\right]_{M-q+1:M} \\ \hline \bar{\mathbf{y}}^{(d)}(n) \\ \hline \left[\mathbf{y}_M^{(d)}(n)\right]_{1:Q-q} \end{array}\right] = \mathcal{H}_{2Q} \left[\begin{array}{c} v_{q-1} \\ \vdots \\ v_1 \\ \hline \bar{\mathbf{u}}^{(d)}(n) \\ \hline x_1 \\ \vdots \\ x_{Q-q} \end{array}\right], q = 1, 2, ..., Q,$$

where $\mathcal{H}_{2Q}$ is a $(2M+L+Q-1)\times(2P+Q-1)$ Toeplitz matrix whose first column is $\left[\begin{array}{cccc} h_L & 0 & \cdots & 0 \end{array}\right]^T$ and whose first row is $\left[\begin{array}{ccccccc} h_L & \cdots & h_0 & 0 & \cdots & 0 \end{array}\right]$ and sequences $\{x_k\}$ and $\{v_k\}$ are defined as follows. The values of x_k and v_k when $k \leq 0$ are defined as

$$\begin{aligned} [x_{-L+1}, x_{-L+2}, \cdots, x_0]^T &\triangleq \left[\bar{\mathbf{u}}^{(d)}(n)\right]_{2P-L+1:2P} \\ [v_0, v_{-1}, \cdots, v_{-L+1}]^T &\triangleq \left[\bar{\mathbf{u}}^{(d)}(n)\right]_{1:L}. \end{aligned}$$

The values of x_k and v_k when $k > 0$ are defined recursively as

$$x_l \triangleq \frac{1}{h_0}\left[\left[\mathbf{y}_M^{(d)}(n)\right]_l - \sum_{k=1}^{L} h_k x_{l-k}\right]$$

and

$$v_l \triangleq \frac{1}{h_L}\left[\left[\mathbf{y}_M^{(d)}(n-1)\right]_{M+1-l} - \sum_{k=0}^{L-1} h_k v_{l-L+k}\right]$$

for $l = 1, ..., Q-1$. So

$$\bar{\mathbf{Y}}_Q^{(d)}(n) = \mathcal{H}_{2Q}\bar{\mathbf{U}}_Q^{(d)}(n),$$

where

$$\bar{\mathbf{U}}_Q^{(d)}(n) = \mathcal{T}_Q\left(\bar{\mathbf{u}}^{(d)}(n)\right) + \mathbf{V}$$

and $\mathbf{V}$ is a $(2P+Q-1)\times Q$ Toeplitz matrix whose first column is $\left[\begin{array}{ccccc} \mathbf{0}_{1\times 2P} & x_1 & \cdots & x_{Q-1} \end{array}\right]^T$ and whose first row is $\left[\begin{array}{ccccc} 0 & v_1 & \cdots & v_{Q-1} \end{array}\right]$.

Denote $n(L,Q,d)$ as the number of pairs of identical rows in $\bar{\mathbf{U}}_Q^{(d)}(n)$. When $Q \leq L+1$, the segment $\mathbf{u}_{cp}(n)$ in $\bar{\mathbf{u}}^{(d)}(n)$ accounts for $(L-Q-1)$ pairs of identical rows in $\bar{\mathbf{U}}_Q^{(d)}(n)$ (recall that $\mathbf{u}_{cp}(n) = [\mathbf{u}'_M(n)]_{1:L}$.) Furthermore, if $0 < d \leq L-Q+1$, the segment $[\mathbf{u}_{cp}(n-1)]_{d+1:L}$ accounts for $(L-Q-1-d)$ pairs of identical rows in $\bar{\mathbf{U}}_Q^{(d)}(n)$. If $L-Q-1 < d < P/2$, on the other hand, the segment $[\mathbf{u}_{cp}(n-1)]_{d+1:L}$ will not account for any pairs of identical rows (when $d > L$, this segment does not even exist). The above arguments can be extended to the case when $-P/2 \leq d < 0$ due to symmetry. So, when $Q \leq L+1$,

$$n(L,Q,d) \;=\; \underbrace{(L-Q+1)}_{\text{from } \mathbf{u}_{cp}(n)} + \underbrace{\max\{L-Q+1-|d|,0\}}_{\text{from } [\mathbf{u}_{cp}(n-1)]_{d+1:L}}.$$

When $Q > L+1$, neither segments $\mathbf{u}_{cp}(n)$ nor $[\mathbf{u}_{cp}(n-1)]_{d+1:L}$ in $\bar{\mathbf{u}}^{(d)}(n)$ account for any pairs of identical rows. So

$$n(L,Q,d) = 0$$

when $Q > L+1$.

Now $\bar{\mathbf{Y}}_{J,Q}^{(d)} = \mathcal{H}_{2Q}\bar{\mathbf{U}}_{J,Q}^{(d)} = \mathcal{H}'_{2Q}\bar{\mathbf{U}}'^{(d)}_{J,Q}$, where $\mathbf{U}'^{(d)}_{J,Q}$ is obtained by eliminating the $n(L,Q,d)$ duplicated rows in $\mathbf{U}_{J,Q}^{(d)}$ and $\mathcal{H}'_{2Q}$ is obtained by merging the corresponding column pairs of $\mathcal{H}_{2Q}$. We are interested in the value of the number of rows of $\mathcal{H}'_{2Q}$ minus the number of columns of $\mathcal{H}'_{2Q}$. Denote this value as $n(\mathcal{H}'_{2Q})$. This value represents the column rank deficiency of $\mathcal{H}'_{2Q}$ if $n(\mathcal{H}'_{2Q}) \geq 0$. It is readily verified that $n(\mathcal{H}'_{2Q}) = n(L,Q,d) - L$, and so the column rank deficiency of $\mathcal{H}'_{2Q}$ is $\max\{n(\mathcal{H}'_{2Q}),0\}$. Due to the random nature of $\mathbf{u}_M(n)$, $\{x_k\}$, and $\{v_k\}$, with probability one, there exists a sufficiently large J such that $\bar{\mathbf{U}}'^{(d)}_{J,Q}$ has full rank $(2P+Q-1-n(L,Q,d))$. The rank deficiency of $\bar{\mathbf{Y}}_{J,Q}^{(d)}\bar{\mathbf{Y}}_{J,Q}^{(d)\,\dagger}$ is $\max\{n(L,Q,d)-L,0\}$. When $Q > L+1$, $n(L,Q,d) = 0$, so the rank deficiency of $\bar{\mathbf{Y}}_{J,Q}^{(d)}\bar{\mathbf{Y}}_{J,Q}^{(d)\,\dagger}$ is zero. When $Q \leq L+1$ and when $|d| \geq L-Q+1$, $n(L,Q,d) = L-Q+1$, so the rank deficiency of $\bar{\mathbf{Y}}_{J,Q}^{(d)}\bar{\mathbf{Y}}_{J,Q}^{(d)\,\dagger}$ is $\max\{-Q+1,0\} = 0$. When $Q \leq L+1$ and when $|d| \leq L-Q+1$, $n(L,Q,d) = 2L-2Q+2-|d|$, so the rank deficiency of $\bar{\mathbf{Y}}_{J,Q}^{(d)}\bar{\mathbf{Y}}_{J,Q}^{(d)\,\dagger}$ is $\max\{2L-2Q+2-|d|-L,0\} = L-|d|-2(Q-1)$.

In summary, with probability one, the number of zero eigenvalues of $\bar{\mathbf{Y}}_{J,Q}^{(d)}\bar{\mathbf{Y}}_{J,Q}^{(d)\,\dagger}$ is $\max\{L-$

$|d| - 2(Q-1), 0\}$ when $d \neq 0$. This completes the proof. $\square$

Chapter 5

Performance Analysis of Blind Estimation Algorithms in ZP Systems

In this chapter, we analyze the performance of the generalized blind channel estimation algorithm for ZP systems proposed in Chapter 2. From Chapter 2, we know the generalized algorithm contains a parameter called the repetition index Q; when $Q = 1$, it reduces to the SGB algorithm proposed in [45]. When Q is equal to the size of a received block, the algorithm reduces to the MNP algorithm [36], which allows blind estimation with as few as two received blocks. Even though the performance with two blocks is usually not satisfactory, with repetition index Q and the number of received blocks adjusted appropriately, the performance of the generalized algorithm is superior to those of the SGB and MNP algorithms, as documented in detail Chapter 2.

The goal here is to quantify this performance improvement theoretically. We study the channel estimation error (MSE) in the algorithm of [49] and compare it with the corresponding Cramer-Rao bound. Performance analysis for subspace-based algorithms has been studied in the literature since the advent of directional-of-arrival (DOA) estimation algorithms such as the famous multiple signal classification (MUSIC) algorithm. Since the subspace algorithms involve nonlinear operations of singular value decomposition (SVD), many studies resort to first-order small perturbation analysis (see, e.g. [22]) which gives an accurate performance analysis when the noise level is low, i.e., in the high-SNR region. In [2], the performance of the SGB algorithm in [45] was analyzed based on small perturbation analysis. By generalizing the work in [2], we will derive in this chapter performance analysis of the generalized algorithm proposed in Chapter 2. Analysis in this chapter gives an explanation for the performance of different algorithms we have observed in simulation results presented in Chapter 2.

The Cramer-Rao lower bound (CRB) for an estimation problem is independent from algorithms

and is smaller than the MSE of any algorithm that solves the problem, so the CRB has long been a useful tool to evaluate the efficiency of a particular algorithm. In [2] fundamental work has been reported which derives the CRB of the blind channel estimation problem in ZP systems. By comparing the CRB with the analytical performance of the SGB method, it has been found that the SGB algorithm is efficient in high-SNR region when the number of received blocks goes to infinity. When the number of received blocks is small, however, we use the CRB expression given in [58] which is a correction of that in [2]. There is an obvious gap between the performance of the SGB algorithm, and the corrected CRB given in [58] when a small number of received blocks are available. Both theory and simulation results suggest that the performance of the generalized algorithm is usually closer to the CRB when the repetition index is larger but the performance does not achieve the CRB for any repetition index. The material in the chapter is mainly drawn from [57] and [58].

5.1 Outline

The rest of the chapter is organized as follows. Section 5.2 briefly gives the problem statement and reviews the generalized algorithm proposed in Chapter 2. In Section 5.3 we derive the theoretical performance of the generalized algorithm and compare it with the Cramer-Rao bound. In Section 5.4 simulation results are given to compare the theoretical performance, performance obtained by simulation, and the CRB. Finally, the conclusion is given in Section 5.5. An appendix is provided to elaborate the corrected version of the CRB reported in [58].

5.2 Review of the Generalized Algorithm

5.2.1 Problem Formulation

Consider a sequence of discrete-time information symbols $s(n)$, which is blocked into vectors of size M. Let $\mathbf{s}(n) = \begin{bmatrix} s_0(n) & s_1(n) & \cdots & s_{M-1}(n) \end{bmatrix}^T$, where $s_k(n) := s(Mn+k)$ for $k = 0, 1, ..., M-1$. Each block $\mathbf{s}(n)$ is precoded by a linear transformation characterized by an $M \times M$ nonsingular matrix $\mathbf{F}$ so that $\mathbf{u}(n) = \mathbf{F}\mathbf{s}(n)$. Each precoded block $\mathbf{u}(n)$ is appended at the end with a block of L zeros, forming a vector $\mathbf{u}_P(n) = \begin{bmatrix} \mathbf{u}(n)^T & \mathbf{0}_{1\times L}^T \end{bmatrix}^T$ of size $P = M + L$. The vector signal $\mathbf{u}_P(n)$ is unblocked into scalar form $u(n)$ before being sent over the channel. The channel is characterized as a linear time-invariant (LTI) finite impulse response (FIR) system whose order is upper-bounded

by L:

$$H(z) = \sum_{k=0}^{L} h(k) z^{-k}.$$

Also define $\mathbf{h} = \begin{bmatrix} h(0) & h(1) & \cdots & h(L) \end{bmatrix}^T$ as the $(L+1)$-vector containing the channel coefficients. The channel output is corrupted by an additive complex white Gaussian noise $e(n)$ with variance σ_v^2. At the receiver side, the symbol stream $y(n)$ is blocked into vectors of size P which can be written as $\mathbf{y}(n) = \begin{bmatrix} y_0(n) & y_1(n) & \cdots & y_{P-1}(n) \end{bmatrix}^T$, where $y_k(n) := y(Pn+k)$ for $k = 0, 1, ..., P-1$. Assuming the block synchronization between the transmitter and the receiver is perfect, it can be shown that [45]

$$\mathbf{y}(n) = \mathbf{HFs}(n) + \mathbf{e}(n),$$

where $\mathbf{H} := \mathcal{T}_M(\mathbf{h})$ is a *full-banded Toeplitz matrix* and $\mathbf{e}(n)$ is the blocked version of the additive noise $e(n)$. Suppose we collect J received blocks in a $P \times J$ matrix $\mathbf{Y}^{(J)} = \begin{bmatrix} \mathbf{y}(0) & \mathbf{y}(1) & \cdots & \mathbf{y}(J-1) \end{bmatrix}$. Then it is clear that

$$\mathbf{Y}^{(J)} = \mathbf{HU}^{(J)} + \text{noise}, \tag{5.1}$$

where $\mathbf{U}^{(J)} = \begin{bmatrix} \mathbf{u}(0) & \mathbf{u}(1) & \cdots & \mathbf{u}(J-1) \end{bmatrix}$ contains unknown transmitted blocks.

The problem of blind channel estimation can be stated as follows. Given $P \times J$ matrix $\mathbf{Y}^{(J)}$, how do we estimate the channel coefficients $\mathbf{h}$ blindly (i.e., when $\mathbf{s}(n)$ is unknown)? This problem was first formulated and solved by Scaglione et. al [45]. We will study here the performance of a generalization of the SGB algorithm proposed in [49].

5.2.2 Generalized Algorithm

In this subsection we review the generalized algorithm proposed in Chapter 2. We start with a subroutine that is used by both SGB algorithm and the generalized algorithm.

Subroutine 1: $(\hat{\mathbf{h}}, \tilde{\mathbf{R}}, \tilde{\mathcal{U}}) = ZPBLIND(\mathbf{Z})$

Input: Matrix $\mathbf{Z}$ of user-defined size $p \times k$.

Outputs: $(L+1)$-vector $\hat{\mathbf{h}}$, $p \times L$ matrix $\tilde{\mathbf{R}}$, and $(L+1) \times mL$ matrix $\tilde{\mathcal{U}}$, where $m := p - L$.

1. Take SVD on $\mathbf{Z}$ and denote this as

$$\mathbf{Z} = \begin{bmatrix} \overline{\mathbf{R}} & \tilde{\mathbf{R}} \end{bmatrix} \begin{bmatrix} \mathbf{\Sigma}_s & & \\ & \mathbf{\Sigma}_n & \mathbf{0} \end{bmatrix} \begin{bmatrix} \overline{\mathbf{V}}^\dagger \\ \tilde{\mathbf{V}}^\dagger \end{bmatrix}, \tag{5.2}$$

where $\mathbf{\Sigma}_n$ has size $L \times L$ and contains the L smallest singular values of $\mathbf{Z}$. Columns of $\tilde{\mathbf{R}}$, denoted as $\tilde{\mathbf{r}}_l$, $l = 1, 2, ..., L$ are the corresponding left singular vectors. (*Remark:* In particular, if $\mathbf{Z}$ can be written as $\mathbf{Z} = \mathcal{T}_m(\mathbf{h})\,\mathbf{U}$, where the $m \times k$ matrix $\mathbf{U}$ has rank m, then it can be shown that $\mathbf{\Sigma}_n = \mathbf{0}$, $\tilde{\mathbf{R}}\mathbf{Z} = \mathbf{0}$, and $\tilde{\mathbf{R}}\mathcal{T}_m(\mathbf{h}) = \mathbf{0}$, i.e., columns of $\tilde{\mathbf{R}}$, $\tilde{\mathbf{r}}_l$, $l = 1, 2, ..., L$, are annihilators of $\mathcal{T}_m(\mathbf{h})$.)

2. Construct the $(L+1) \times m$ Hankel matrix

$$\tilde{\mathcal{U}}_l := \begin{bmatrix} \tilde{r}_l(1) & \tilde{r}_l(2) & \cdots & \tilde{r}_l(m) \\ \tilde{r}_l(2) & \tilde{r}_l(3) & \cdots & \tilde{r}_l(m+1) \\ \vdots & \vdots & \vdots & \vdots \\ \tilde{r}_l(L+1) & \tilde{r}_l(L+2) & \cdots & \tilde{r}_l(p) \end{bmatrix} \tag{5.3}$$

for $l = 1, 2, ..., L$, where $\tilde{r}_l(i)$ represents the ith element of $\tilde{\mathbf{r}}_l$. Construct matrix $\tilde{\mathcal{U}} := \begin{bmatrix} \tilde{\mathcal{U}}_1 & \tilde{\mathcal{U}}_2 & \cdots & \tilde{\mathcal{U}}_L \end{bmatrix}$. (*Remark:* If $\tilde{\mathbf{R}}\mathcal{T}_m(\mathbf{h}) = \mathbf{0}$, it is readily verified that $\mathbf{h}^\dagger\tilde{\mathcal{U}} = \mathbf{0}^\dagger$.)

3. Let $\hat{\mathbf{h}} = \arg\min_{\bar{\mathbf{h}}} ||\bar{\mathbf{h}}^\dagger\tilde{\mathcal{U}}||^2$.

Subroutine 1 produces an output $\hat{\mathbf{h}}$ proportional to $\mathbf{h}$ (i.e., $\hat{\mathbf{h}} = \alpha\mathbf{h}$ for some $\alpha \in \mathbb{C}$) if the input $\mathbf{Z}$ can be written as $\mathbf{Z} = \mathcal{T}_m(\mathbf{h})\,\mathbf{U}$, where $\mathbf{U}$ has rank m. When $\mathbf{Z}$ is corrupted with small additive noise, then columns of $\tilde{\mathbf{R}}$ are approximately annihilators of $\mathcal{T}_m(\mathbf{h})$, and an estimate of $\mathbf{h}$ is outputted (with a scalar ambiguity). These properties were first used by Scaglione *et al.* in [45] when developing the SGB algorithm. In fact, the SGB algorithm simply runs $(\hat{\mathbf{h}}, \tilde{\mathbf{R}}, \tilde{\mathcal{U}}) = \mathit{ZPBLIND}(\mathbf{Y}^{(J)})$ (under the assumption that $\mathbf{U}^{(J)}$ has full rank M) and takes $\hat{\mathbf{h}}$ as the estimated channel coefficients.

Although the SGB algorithm uses Subroutine 1 as its kernel routine, it does not take advantage of the flexibility on input matrix size of Subroutine 1 (it always uses $p = P$). The generalized algorithm in [49], on the other hand, fully exploits this flexibility by using an extra parameter, namely the repetition index Q, as described below.

Algorithm 1: $\hat{\mathbf{h}} = \mathit{GENERAL}(\mathbf{Y}^{(J)}, Q)$

Inputs: $P \times J$ matrix $\mathbf{Y}^{(J)}$ and repetition index $Q \geq 1$.

Output: channel estimate as an $(L+1)$-vector $\hat{\mathbf{h}}$.

1. Construct the $(P+Q-1)\times JQ$ matrix

$$\mathbf{Y}_Q^{(J)} = \left[\begin{array}{cccc} \mathcal{T}_Q\left(\mathbf{y}(0)\right) & \mathcal{T}_Q\left(\mathbf{y}(1)\right) & \cdots & \mathcal{T}_Q\left(\mathbf{y}(J-1)\right) \end{array} \right].$$

2. Perform the subroutine $(\hat{\mathbf{h}}, \tilde{\mathbf{R}}, \tilde{\mathcal{U}}) = \mathit{ZPBLIND}(\mathbf{Y}_Q^{(J)})$ and output $\hat{\mathbf{h}}$. □

The generalized algorithm is based on the idea that Eq. (5.1) implies

$$\mathbf{Y}_Q^{(J)} = \mathcal{T}_{M+Q-1}\left(\mathbf{h}\right)\mathbf{U}_Q^{(J)} + \text{noise}, \tag{5.4}$$

where

$$\mathbf{U}_Q^{(J)} = \left[\begin{array}{cccc} \mathcal{T}_Q\left(\mathbf{u}(0)\right) & \mathcal{T}_Q\left(\mathbf{u}(1)\right) & \cdots & \mathcal{T}_Q\left(\mathbf{u}(J-1)\right) \end{array} \right]. \tag{5.5}$$

Note that the noise autocorrelation in (5.4) is different from that in (5.1). When $Q=1$, the generalized algorithm reduces to SGB algorithm. Also, when $Q=P$, the generalized algorithm is equivalent to the MNP algorithm [36]. The matrix $\mathbf{U}_Q^{(J)}$ must have full rank so that Algorithm 1 works, which implies $J \geq 1 + \lceil (M-1)/Q \rceil$.

5.3 Performance Analysis in Additive Noise

When evaluating the MSE performance of blind estimation algorithms, it is natural to compare the estimated channel $\hat{\mathbf{h}}$ and the true channel $\mathbf{h}$. However, due to an intrinsic scalar ambiguity presented in all blind channel estimation algorithms, the comparison should be done after normalizing this unknown scalar. There are many options for doing this. Here we adopted an option presented in [2], where the channel coefficient with the largest magnitude is assumed known. That is, $h(d)$, where $d \in [0, L]$ satisfies $|h(d)| \geq |h(l)|, \forall l \neq d$, is known. After normalizing the estimated channel vector by letting $\tilde{\mathbf{h}} = (h(d)/\hat{h}(d))\hat{\mathbf{h}}$, the channel estimation error can be defined as an L-vector

$$\Delta\mathbf{h} = \mathbf{I}_{L,d}(\tilde{\mathbf{h}} - \mathbf{h}), \tag{5.6}$$

where $\mathbf{I}_{L,d}$ is an $L \times (L+1)$ matrix obtained by removing the dth row of $\mathbf{I}_{L+1}$. We first review a result on estimating $\Delta\mathbf{h}$ presented in [2] using small perturbation analysis. In Lemma 5.1 presented below, we assume the perturbation $\Delta\mathbf{X}$ is small compared to $\mathbf{X}$. That is, assume the first-order

approximation

$$(\mathbf{X}+\Delta\mathbf{X})^{\dagger}(\mathbf{X}+\Delta\mathbf{X}) \approx \mathbf{X}^{\dagger}\mathbf{X}+\Delta\mathbf{X}^{\dagger}\mathbf{X}+\mathbf{X}^{\dagger}\Delta\mathbf{X}$$

is accurate. We also assume $h(d)$ is known to the receiver and the output of *ZPBLIND*, $\hat{\mathbf{h}}$, has applied the scalar ambiguity normalization based on the knowledge of $h(d)$.

Lemma 5.1: Let $\mathbf{X}=\mathcal{T}_m(\mathbf{h})\,\mathbf{U}$, where $m\times k$ matrix $\mathbf{U}$ has rank m. Let $\mathbf{Y}=\mathbf{X}+\Delta\mathbf{X}$, where $\Delta\mathbf{X}$ is a small perturbation to $\mathbf{X}$. Perform subroutine *ZPBLIND* on $\mathbf{X}$ and $\mathbf{Y}$, and denote them as $(\hat{\mathbf{h}},\mathbf{R}_1,\mathcal{U}_1)=$ *ZPBLIND*$(\mathbf{Y})$ and $(\mathbf{h}_1,\tilde{\mathbf{R}},\hat{\mathcal{U}})=$ *ZPBLIND*$(\mathbf{X})$, respectively. Consider error vector $\Delta\mathbf{h}$ as defined in (5.6). Then the first-order approximation of $\Delta\mathbf{h}$ can be expressed as

$$\Delta\mathbf{h}^{\dagger} \;\approx\; \mathrm{vec}^{T}(\Delta\mathbf{X}^{\dagger})\left(\tilde{\mathbf{R}}\otimes\mathbf{U}^{\#*}\right)\tilde{\mathcal{V}}^{\#},$$

where $\tilde{\mathcal{V}}:=\mathbf{I}_{L,d}\tilde{\mathcal{U}}$. □

Proof: See (28) in [2]. □

Notice that $\tilde{\mathbf{R}}$ and $\tilde{\mathcal{V}}$ depend only on $\mathbf{U}$ and $\mathbf{h}$ and not on the noise perturbation $\Delta\mathbf{X}$. Using Lemma 5.1, we can derive the MSE performance of the generalized algorithm in [49] by computing the autocorrelation matrix of $\Delta\mathbf{h}$, as described below.

Theorem 5.1: Consider $\mathbf{Y}^{(J)}$ as defined in Eq. (5.1) and Q as the repetition index. Perform Algorithm 1: $\hat{\mathbf{h}}=$ *GENERAL*$(\mathbf{Y}^{(J)},Q)$. Then the autocorrelation matrix of the channel estimation error vector $\Delta\mathbf{h}$ (defined in (5.6)) can be expressed as

$$\begin{aligned}&\mathbf{C}_{hh,Q}=E[\Delta\mathbf{h}\Delta\mathbf{h}^{\dagger}]\\ \approx\;&\sigma_v^2\tilde{\mathcal{V}}_Q^{\#\dagger}\left(\tilde{\mathbf{R}}_Q^{\dagger}\otimes\mathbf{U}_Q^{(J)\#T}\right)(\mathbf{I}_J\otimes\mathbf{B}_Q)\left(\tilde{\mathbf{R}}_Q\otimes\mathbf{U}_Q^{(J)\#*}\right)\tilde{\mathcal{V}}_Q^{\#}.\end{aligned} \tag{5.7}$$

Here, $\mathbf{U}_Q^{(J)}$ is defined as in (5.5), and $\mathbf{B}_Q$ is defined as

$$\mathbf{B}_Q=\begin{bmatrix}\mathbf{B}_{11}&\cdots&\mathbf{B}_{1Q}\\ \vdots&\vdots&\vdots\\ \mathbf{B}_{Q1}&\cdots&\mathbf{B}_{QQ}\end{bmatrix},\mathbf{B}_{kl}=\begin{bmatrix}\mathbf{0}_{(k-1)\times(P+Q-1)}\\ \mathbf{K}_l\\ \mathbf{0}_{(Q-k)\times(P+Q-1)}\end{bmatrix},$$

and $\mathbf{K}_l=\begin{bmatrix}\mathbf{0}_{(P+Q-1)\times(l-1)}&\mathbf{I}_P&\mathbf{0}_{(P+Q-1)\times(Q-l)}\end{bmatrix}$. In (5.7), $\tilde{\mathbf{R}}_Q$ and $\tilde{\mathcal{V}}_Q$ are obtained by

performing

$$(\hat{\mathbf{h}}', \tilde{\mathbf{R}}_Q, \tilde{\mathcal{U}}_Q) = \mathit{ZPBLIND}(\mathcal{T}_{M+Q-1}(\mathbf{h})\,\mathbf{U}_Q^{(J)})$$

and letting $\tilde{\mathcal{V}}_Q = \mathbf{I}_{L,d}\tilde{\mathcal{U}}_Q$.

□

Proof: Using Lemma 5.1, the autocorrelation matrix of $\Delta\mathbf{h}$ can be written as

$$E[\Delta\mathbf{h}\Delta\mathbf{h}^\dagger] = \tilde{\mathcal{V}}^{\#\dagger}\left(\tilde{\mathbf{R}}^\dagger \otimes \mathbf{U}^{\#T}\right)\mathbf{R}_{\Delta\mathbf{X}}\left(\tilde{\mathbf{R}} \otimes \mathbf{U}^{\#*}\right)\tilde{\mathcal{V}}^{\#}, \tag{5.8}$$

where $\mathbf{R}_{\Delta\mathbf{X}} := E[\mathrm{vec}(\Delta\mathbf{X}_Q^{(J)})\mathrm{vec}^\dagger(\Delta\mathbf{X}_Q^{(J)})]$. The perturbation matrix $\Delta\mathbf{X}_Q^{(J)}$ can be written as

$$\Delta\mathbf{X}_Q^{(J)} = \left[\begin{array}{cccc} \mathcal{T}_Q(\mathbf{e}(0)) & \mathcal{T}_Q(\mathbf{e}(1)) & \cdots & \mathcal{T}_Q(\mathbf{e}(J-1)) \end{array}\right].$$

One can verify that the $(P+Q-1)JQ \times (P+Q-1)JQ$ matrix $\mathbf{R}_{\Delta\mathbf{X}}$ can be written as $\mathbf{R}_{\Delta\mathbf{X}} = \sigma_v^2(\mathbf{I}_J \otimes \mathbf{B}_Q)$, and the proof of the theorem is complete. □

Corollary 5.1: When $Q = 1$, the channel estimation error autocorrelation matrix can be expressed as

$$\mathbf{C}_{hh,1} \;=\; \sigma_v^2\tilde{\mathcal{V}}^{\#\dagger}\left(\mathbf{I}_L \otimes \mathbf{U}^{(J)\#T}\mathbf{U}^{(J)\#*}\right)\tilde{\mathcal{V}}^{\#},$$

which agrees with the analytical performance of SGB algorithm derived in [2]. □

Proof: Immediate from Theorem 5.1 using $\mathbf{B}_Q = \mathbf{I}_P$ and the fact that columns of $\tilde{\mathbf{R}}_Q$ are orthogonal to each other. □

5.3.1 Cramer-Rao Bound

In [2], a Cramer-Rao lower bound (CRB) for the zero-padding blind channel estimation problem was derived. We use the corrected version CRB presented in [58] as follows:

$$\mathbf{C}_{CR} = \sigma_v^2\left[\tilde{\mathcal{V}}\left(\mathbf{I}_{L\times L} \otimes \mathbf{U}^{(J)*}\mathbf{U}^{(J)T}\right)\tilde{\mathcal{V}}^\dagger\right]^{-1}. \tag{5.9}$$

The Cramer-Rao bound presented in Eq. (5.11) is a lower bound for the performance of *all* algorithms which attempt to solve the blind estimation problem described in Section 5.2.1, including

the SGB algorithm [45], the MNP algorithm [36], and the generalized algorithm [49]. More details of the correction of the CRB are presented in the Appendix.

5.4 Simulations

In this section we perform Monte Carlo simulation for the generalized blind channel estimation algorithm [49] with different repetition indices and compare the performances obtained by simulations and theory, and the Cramer-Rao Bound at different SNR values.

In our simulations, the block size is chosen as $M = 12$, and the channel order is chosen as $L = 4$. The QPSK constellation is used to generate i.i.d. symbols $s(n)$, and the linear precoder $\mathbf{F}$ is chosen as $\mathbf{I}_M$. The channel coefficients (elements of $\mathbf{h}$) are chosen as i.i.d., zero-mean, unit variance complex Gaussian random variables. The simulation is performed using 100 independent realizations of channel coefficients and 10 independent realizations of symbol streams $s(n)$ (totally 1000 different pairs of $\mathbf{S}^{(J)}$ and $\mathbf{h}$). Theoretical preformances in Eq. (5.7) and the CRB in Eq. (5.11) are computed accordingly and averaged over these 1000 pairs of $\mathbf{S}^{(J)}$ and $\mathbf{h}$. Furthermore, to solve the scalar ambiguity problem, the channel coefficient with the largest magnitude, $h(d)$, is assumed known to the receiver. Two separate simulation settings are considered: the first one uses 16 received blocks ($J = 16$), and the second one uses $J = 5$.

Figure 5.1 depicts the result of the first simulation setting, where $J = 16$. We compare the MSE performances with $Q = 1$ and $Q = 2$. Both theoretical and simulation performances are plotted for each case. The Cramer-Rao bound is plotted as the benchmark. We have the following observations. First of all, in both cases of $Q = 1$ and $Q = 2$, the simulation results are very close to theory in the high SNR region. This validates the small perturbation assumption given in Lemma 5.1. Secondly, performance of $Q = 2$ is better than that of $Q = 1$ with a considerable margin. However, the system with $Q = 2$ does not achieve the CRB yet. Increasing Q might further improve the performance toward the CRB, but we omit these curves here due to space limit.

In Figure 5.2, simulation results are shown for the case when $J = 5$. We choose $Q = 3$ and $Q = P(= M + L = 16)$ in this simulation. Notice that $Q = P$ represents the MNP algorithm [36]. The simulation results approach the theoretical values when SNR goes to infinity. In high SNR region, the performance for $Q = P$ is obviously better than that for $Q = 3$. But it still does not achieve the CRB. Notice that in this case, we need $Q \geq 3$ in order to satisfy the full rank assumption as described in Section II-B.

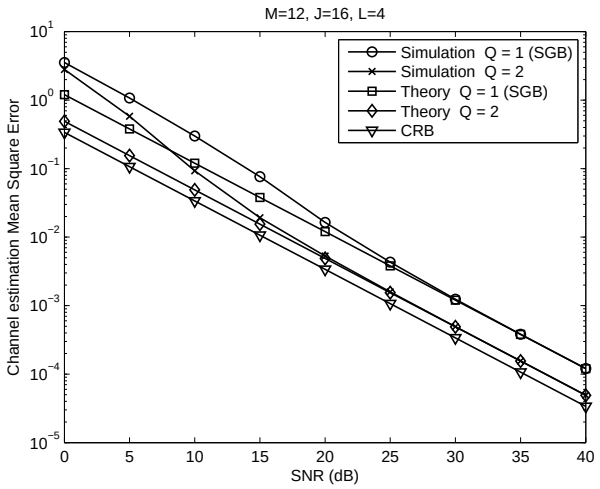

Figure 5.1: Channel estimation MSE versus SNR obtained by simulations, theoretical values in (5.7), and CRB in (5.11) with 16 blocks.

5.5 Conclusions

In this chapter we derived the theoretical performance of the generalized blind channel estimation algorithm proposed in Chapter 2 for ZP systems in the high-SNR range. Simulation results and theory both suggest that when the repetition index is larger, the performance is usually better when SNR is large. A Cramer-Rao bound (CRB) presented in [2] and corrected in [58] is used as a benchmark of the algorithm performance. When the repetition index Q is large, the performance curve tends to approach the CRB but does not appear to achieve it.

In the future, a formal proof that the generalized algorithm does not achieve the CRB for any Q is desirable. It also remains an open question whether there exists another blind channel estimation algorithm that has a performance achieving the CRB.

5.6 Appendix

In [2], important work has been done to analyze the SGB algorithm [45] which solves the blind channel estimation problem in ZP systems. The performance of the algorithm in [45] in high SNR region was shown to be as in (33) of [2]. The Cramer-Rao bound (CRB) of the above mentioned blind estimation problem was shown to be as in (49) of [2]. The coincidence of (33) and (49) led the authors of [2] to claim that the algorithm in [45] is statistically efficient (i.e., achieves the CRB) at

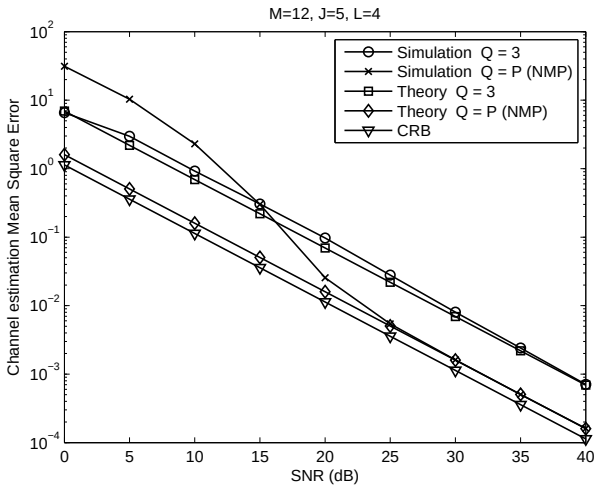

Figure 5.2: Channel estimation MSE versus SNR obtained by simulations, theoretical values in (5.7), and CRB in (5.11) with 5 blocks.

high SNR values. However, we have found an error in the derivation of (49), which invalidates this claim. Eq. (49) of [2] was derived from (80) in Appendix B of [2]. The second equality of (80) is not valid in general since it is conditioned on the validity of the matrix identity

$$(\mathbf{ABA}^H)^{-1} = \mathbf{A}^{H\dagger}\mathbf{B}^{-1}\mathbf{A}^{\dagger}, \tag{5.10}$$

where $\mathbf{A}$ is a full rank matrix with more columns than rows and $\mathbf{B}$ is a square positive definite matrix. But a simple example shows that this identity is not true in general: set

$$\mathbf{A} = \begin{bmatrix} 1 & 0 & 0 \\ 0 & 1 & 0 \end{bmatrix}, \text{ and } \mathbf{B} = \begin{bmatrix} 1 & 0 & 0 \\ 0 & 1 & 1 \\ 0 & 1 & 2 \end{bmatrix}.$$

Then, the left hand side of (5.10) is $\mathbf{I}_2$ whereas the right hand side is $\begin{bmatrix} 1 & 0 \\ 0 & 2 \end{bmatrix}$.

A correction to the CRB, however, is easy to make. The corrected CRB can be simply taken as the first equality of (80) of [2]:

$$\mathbf{C}_{CR} = \sigma_v^2 \left[\tilde{\mathcal{V}}\left[\mathbf{I}_{L\times L} \otimes (\mathbf{F}^*\mathbf{S}_N^*\mathbf{S}_N^T\mathbf{F}^T)\right]\tilde{\mathcal{V}}^H\right]^{-1} \tag{5.11}$$

(in the original text [2], σ_v^2 appeared in the denominator, which was presumably a typographical

error).

We conduct numerical simulations to compare

$$\mathbf{C}_{hh} \approx \sigma_v^2 \tilde{\mathcal{V}}^{\dagger H} \left[\mathbf{I}_{L\times L} \otimes \left(\mathbf{F}^{-T} (\mathbf{S}_N^* \mathbf{S}_N^T)^{-1} \mathbf{F}^{-*} \right) \right] \tilde{\mathcal{V}}^{\dagger}$$

from (33) of [2] and the corrected CRB in (5.11). The simulation setting basically follows that in [2]: the channel order is chosen as $L = 4$, and the channel coefficients are i.i.d., zero-mean, unit variance complex Gaussian random variables. The data length per block is $M = 12$, and the number of blocks N ranges from 8 to 1000. Elements of the data matrix $\mathbf{S}_N$ were generated using the QPSK constellation, and $\mathbf{F}$ is chosen as $\mathbf{I}_M$. One hundred independent realizations of channel coefficients and 10 independent realizations of data blocks $\mathbf{S}_N$ are used (totally 1000 different pairs of $\mathbf{S}_N$ and $\mathbf{h}$). Traces of $\mathbf{C}_{hh}$ and $\mathbf{C}_{CR}$ in (5.11) are computed for these 1000 realizations, and the averages are reported in Table I.

N	$\mathrm{tr}(\mathbf{C}_{hh})/\sigma_v^2$	$\mathrm{tr}(\mathbf{C}_{CR})/\sigma_v^2$	$\frac{\mathrm{tr}(\mathbf{C}_{hh})-\mathrm{tr}(\mathbf{C}_{CR})}{\mathrm{tr}(\mathbf{C}_{CR})}$
8	–	1.7752	–
12	184.01	1.3373	136.6002
14	6.8590	1.0981	5.2462
16	3.5362	0.9760	2.6233
20	1.7197	0.7414	1.3196
100	0.1614	0.1448	0.1147
1000	1.5149×10^{-2}	1.4986×10^{-2}	0.0109

Table 5.1: Comparison of Eq. (33) in [2] and Eq. (5.11); the data length per block is $M = 12$

We find from Table I that there is a significant discrepancy between the corrected CRB in (5.11) and the performance of the algorithm in [45] (Eq. (33) in [2]), especially when N is small. Furthermore, when $N < M$, the inverse of $\mathbf{S}_N^* \mathbf{S}_N^T$ in (33) of [2] does not exist, but $\mathbf{C}_{CR}$ in (5.11) still gives a finite value. This suggests there might exist algorithms (e.g., see [36, 49, 57]) other than [45] which solve the aforementioned blind estimation problem when $N < M$. On the other hand, when N is large, the difference between traces of $\mathbf{C}_{hh}$ and $\mathbf{C}_{CR}$ tends to shrink, but it never goes to zero. This observation is accounted for by the following lemma, where we use notations from the singular value decomposition of the $L \times LM$ full-rank matrix $\tilde{\mathcal{V}}$:

$$\tilde{\mathcal{V}} = \mathbf{U} \begin{bmatrix} \mathbf{D} & \mathbf{0} \end{bmatrix} \begin{bmatrix} \mathbf{V}_1 & \mathbf{V}_2 \end{bmatrix}^H, \tag{5.12}$$

where $\mathbf{U}$ is a unitary matrix, $\mathbf{D}$ is a diagonal matrix with positive diagonal entries, and $\mathbf{V} := \begin{bmatrix} \mathbf{V}_1 & \mathbf{V}_2 \end{bmatrix}$ is a unitary matrix. $\mathbf{V}_1$ and $\mathbf{V}_2$ are the first L and the last $(M-1)L$ columns of $\mathbf{V}$, respectively.

Lemma 5.2: If $N \geq M$, then $\text{tr}(\mathbf{C}_{hh}) \geq \text{tr}(\mathbf{C}_{CR})$, with equality if and only if

$$\mathbf{V}_1^H \mathbf{B} \mathbf{V}_2 = \mathbf{0}, \tag{5.13}$$

where $\mathbf{B} := \mathbf{I}_{L\times L} \otimes (\mathbf{F}^* \mathbf{S}_N^* \mathbf{S}_N^T \mathbf{F}^T)$ and $\mathbf{V}_1$ and $\mathbf{V}_2$ are defined as in (5.12).

□

Proof: Since both $\mathbf{C}_{hh}$ and $\mathbf{C}_{CR}$ are positive definite (p.d.), the statement $\text{tr}(\mathbf{C}_{hh}) \geq \text{tr}(\mathbf{C}_{CR})$ is equivalent to the statement that $\mathbf{C}_{hh} - \mathbf{C}_{CR}$ is a positive semi-definite matrix. We first observe that $\mathbf{B}$ is p.d. since $\mathbf{F}^* \mathbf{S}_N^* \mathbf{S}_N^T \mathbf{F}^T$ is p.d. Recall the SVD of $\tilde{\mathcal{V}}$ as in (5.12), where $\mathbf{U}$ and $\mathbf{V} := [\mathbf{V}_1, \mathbf{V}_2]$ are unitary matrices and $\mathbf{D}$ is a diagonal matrix with positive diagonal entries. Define $\mathbf{B}_2 := \mathbf{V}^H \mathbf{B} \mathbf{V}$, which is obviously also p.d. Partition $\mathbf{B}_2$ and $\mathbf{B}_2^{-1}$ into

$$\mathbf{B}_2 = \begin{bmatrix} \mathbf{B}_{11} & \mathbf{B}_{12} \\ \mathbf{B}_{12}^H & \mathbf{B}_{22} \end{bmatrix} \text{ and } \mathbf{B}_2^{-1} = \begin{bmatrix} \mathbf{B}'_{11} & \mathbf{B}'_{12} \\ \mathbf{B}'^H_{12} & \mathbf{B}'_{22} \end{bmatrix},$$

respectively, so that $\mathbf{B}_{11}$ and $\mathbf{B}'_{11}$ have the same size as $\mathbf{D}$ ($L \times L$). Then we have

$$\begin{aligned} \mathbf{C}_{CR} &= \sigma_v^2 (\tilde{\mathcal{V}} \mathbf{B} \tilde{\mathcal{V}}^H)^{-1} = \sigma_v^2 \mathbf{U} ([\mathbf{D} \;\; \mathbf{0}] \mathbf{B}_2 [\mathbf{D} \;\; \mathbf{0}]^T)^{-1} \mathbf{U}^H \\ &= \sigma_v^2 \mathbf{U} \mathbf{D}^{-1} \mathbf{B}_{11}^{-1} \mathbf{D}^{-1} \mathbf{U}^H \end{aligned}$$

and

$$\begin{aligned} \mathbf{C}_{hh} &= \sigma_v^2 \tilde{\mathcal{V}}^{\dagger H} \mathbf{B}^{-1} \tilde{\mathcal{V}}^{\dagger} = \sigma_v^2 \mathbf{U} [\mathbf{D}^{-1} \;\; \mathbf{0}] \mathbf{B}_2^{-1} [\mathbf{D}^{-1} \;\; \mathbf{0}]^T \mathbf{U}^H \\ &= \sigma_v^2 \mathbf{U} \mathbf{D}^{-1} \mathbf{B}'_{11} \mathbf{D}^{-1} \mathbf{U}^H. \end{aligned}$$

Therefore, $\mathbf{C}_{CR} \leq \mathbf{C}_{hh}$ if and only if

$$\mathbf{B}_{11}^{-1} \leq \mathbf{B}'_{11} = \mathbf{B}_{11}^{-1} + \mathbf{B}_{11}^{-1} \mathbf{B}_{12} \mathbf{\Delta}_{B11}^{-1} \mathbf{B}_{12}^H \mathbf{B}_{11}^{-1},$$

where $\mathbf{\Delta}_{B11} := \mathbf{B}_{22} - \mathbf{B}_{12}^H \mathbf{B}_{11}^{-1} \mathbf{B}_{12}$ is the Schur complement [17] of $\mathbf{B}_{11}$ in $\mathbf{B}_2$. Since $\mathbf{B}_2$ is p.d.,

both $\mathbf{B}_{11}$ and $\mathbf{\Delta}_{B11}$ are also p.d. (see theorem (7.7.6) of [17]), so $\mathbf{B}_{11}^{-1} \leq \mathbf{B}'_{11}$ is readily verified, with equality if and only if $\mathbf{B}_{12} = \mathbf{0}$, which is equivalent to (5.13). □

Using Lemma 5.1, we find that (33) in [2] achieves the CRB if and only if (5.13) is satisfied. Eq. (5.13) can be satisfied only in one of two possible ways described as follows.

1. If $\mathbf{B}$ is the identity matrix or a positive multiple thereof, i.e., $\mathbf{S}_N^* \mathbf{S}_N^T = c\mathbf{I}_M$ for some positive constant c, then Eq. (5.13) is satisfied. This is extremely unlikely to happen since elements of $\mathbf{S}_N$ are i.i.d. random symbols. However, we should note that $(1/N)\mathbf{S}_N^* \mathbf{S}_N^T$ tends to approach $c\mathbf{I}_M$ for some $c > 0$ as N goes to infinity. This explains to some extent why the discrepancy between tr$(\mathbf{C}_{hh})$ and tr$(\mathbf{C}_{CR})$ approaches zero as $N \to \infty$.

2. On the other hand, if $\mathbf{B} \neq c\mathbf{I}$, then columns of $\mathbf{V}_1$ and $\mathbf{V}_2$ must match the eigenvectors of $\mathbf{B}$ in order to make (5.13) true. But this is also extremely unlikely since $\tilde{\mathcal{V}}$ depends on, besides $\mathbf{S}_N$, the random channel coefficients which we have no control of.

So, the gap existing between (33) of [2] and the corrected CRB (5.11) suggests that there might exist algorithms other than [45] which yield a better performance than [45] in high-SNR region. Indeed there are such algorithms as reported in [36, 49, 57].

Chapter 6

Theoretical Issues on Linear Precoders that Preserve Signal Richness

In this chapter and the next, we will study a mathematical concept, namely *signal richness*, that is highly related to the blind algorithms we have studied in Chapter 2. Vectorized signals are often considered to be "rich" if they satisfy certain fullness properties appropriate for an application under discussion. The property is especially important for subspace-based blind channel estimation algorithms. In this chapter, we consider the following definition of signal richness. A sequence of $M \times 1$ vectors $\mathbf{x}(n), n \geq 0$, is said to be **rich** or **rank-rich** if the matrix

$$\left[\begin{array}{cccc} \mathbf{x}(0) & \mathbf{x}(1) & \cdots & \mathbf{x}(K_x) \end{array} \right]$$

has rank M for sufficiently large K_x [69]. The definition of signal richness given above first arose in the blind algorithm proposed in [45], referred to as the SGB algorithm. It serves as a *necessary and sufficient* condition on the channel input vectorized signal for channel identifiability in the SGB algorithm, a special case of the generalized blind algorithm proposed in Chapter 2. For different algorithms in various systems, the exact definition of signal richness may be different. For the generalized algorithm proposed in Chapter 2 with a repetition index Q, a generalized (and more relaxed) definition of signal richness can be established and will be studied in detail in the next chapter.

Now, the channel input signal is usually a precoded version of the source signal. We are therefore interested in the effect of the precoder on the signal richness property. Let the linear time

invariant system be characterized by the $M \times M$ polynomial matrix

$$\mathbf{H}(z) = \sum_{k=0}^{N} \mathbf{h}(k) z^{-k}$$

so that the output of the system is

$$\mathbf{y}(n) = \sum_{k=0}^{N} \mathbf{h}(k)\mathbf{x}(n-k).$$

We say the system $\mathbf{H}(z)$ is **richness preserving** (RP) if for any rank-rich input $\mathbf{x}(n)$, the output $\mathbf{y}(n)$ is also rank-rich. Obviously, if the precoder is characterized as a constant (i.e., memoryless; or $\mathbf{H}(z) = \mathbf{h}(0)$) nonsingular matrix, the signal richness property will not be altered due to the precoding. However, there are some other applications (e.g., [37]) which use a precoder as a polynomial matrix with memory. The conditions under which the linear precoders will preserve richness of the vectorized signals are much less obvious. In this chapter, we will explore this question and find the necessary and sufficient conditions on such linear precoders. This fundamental mathematical problem, rather than the applications, will be the focus of this chapter and will be explored in depth. Several examples will be presented to clarify the issues involved in the problem. Paraunitary and unimodular matrices can be shown not to preserve richness unless they are constant matrices (or a delayed version in the paraunitary case). Some richness preserving properties of cascaded systems are also investigated. A structured proof of the necessary and sufficient conditions is presented. The relationship between persistent excitation (PE) and our definitions of richness is also described.

The richness preserving problem can also be formulated for the generalized definition of signal richness which arises in the blind algorithm proposed in Chapter 2 with a repetition index greater than unity. We will delay our exploration of this more advanced problem until next chapter. The material in the chapter is mainly drawn from [48], and portions of it have been presented at [69], [50], and [68].

6.1 Outline

This chapter is organized as follows. In Section 6.2, the first definition of richness will be given and several examples will be presented to clarify the issue. A set of necessary and sufficient conditions

will be presented in Section 6.3. In Section 6.4 we will explore more properties of richness preserving systems, including cascaded systems, and enriching systems, and we will also show that paraunitary (PU) matrices and unimodular matrices cannot satisfy the necessary conditions unless they are constant matrices (with a possible delay in the PU case). In Section 6.5 a strict definition of richness and the necessary and sufficient conditions on LTI systems that preserve richness according to this definition will be given. The proof of the main theorems will be given in Section 6.6. In Section 6.7 we will connect the relationship between strict richness defined in Section 6.5 and persistent excitation (PE) in the literature on control theory [14, 41, 43, 4]. Conclusions and open issues are presented in Section 6.8.

6.2 Formulation and Examples

Definition 6.1: A sequence of $M \times 1$ vectors $\mathbf{x}(n), n \geq 0$ is said to be **rich** if there exists an integer K_x such that the matrix

$$\left[\begin{array}{cccc} \mathbf{x}(0) & \mathbf{x}(1) & \cdots & \mathbf{x}(K_x)) \end{array} \right]$$

has rank M. □

Consider an LTI FIR causal system $\mathbf{H}(z) = \sum_{k=0}^{N} \mathbf{h}(k) z^{-k}$. Then, the output of this system is rich if there exists an integer K_y such that

$$\mathcal{Y} = \left[\begin{array}{cccc} \mathbf{y}(0) & \mathbf{y}(1) & \cdots & \mathbf{y}(K_y) \end{array} \right]$$

has rank M. Note that $\mathcal{Y} = \mathcal{H}\mathcal{X}$, where

$$\mathcal{H} = [\mathbf{h}(0)\ \mathbf{h}(1)\ \cdots\ \mathbf{h}(N)]$$

and

$$\mathcal{X} = \left[\begin{array}{ccccc} \mathbf{x}(0) & \mathbf{x}(1) & \mathbf{x}(2) & \cdots & \mathbf{x}(K_y) \\ \mathbf{0} & \mathbf{x}(0) & \mathbf{x}(1) & \cdots & \mathbf{x}(K_y - 1) \\ \mathbf{0} & \mathbf{0} & \mathbf{x}(0) & \cdots & \mathbf{x}(K_y - 2) \\ \vdots & \vdots & & \ddots & \vdots \\ \mathbf{0} & \mathbf{0} & \mathbf{0} & \cdots & \mathbf{x}(K_y - N) \end{array} \right].$$

The matrix $\mathcal{H}$ has size $M \times M(N+1)$. With ρ_y, ρ_h, and ρ_x denoting the ranks of $\mathcal{Y}$, $\mathcal{H}$ and $\mathcal{X}$ respectively, we have from Sylvester's inequality [17]:

$$\rho_h + \rho_x - M(N+1) \leq \rho_y \leq \min(\rho_h, \rho_x).$$

Observe that if the output matrix $\mathcal{Y}$ has to have rank M, it is necessary that the filter matrix $\mathcal{H}$ have rank M. For example, if one of the $\mathbf{h}(n)$'s has rank M, this is satisfied. We will produce examples to demonstrate that this necessary condition is in fact not sufficient. In fact the examples also show that many standard systems such as unimodular and paraunitary matrices do not preserve richness!

6.2.1 Examples that Do not Preserve Richness

Example 6.1: To demonstrate that the rank-M property of the filter matrix $\mathcal{H}$ is not sufficient, consider the following example with $M = 2$:

$$\mathbf{H}(z) = \begin{bmatrix} 1 & 1 \\ 1 & 1 \end{bmatrix} + z^{-1} \begin{bmatrix} 1 & -1 \\ -1 & 1 \end{bmatrix}.$$

Then,

$$\mathcal{H} = \begin{bmatrix} 1 & 1 & 1 & -1 \\ 1 & 1 & -1 & 1 \end{bmatrix}$$

and has rank $M = 2$. Suppose the input signal is

$$\mathbf{x}(0) = \begin{bmatrix} 1 \\ -1 \end{bmatrix}, \mathbf{x}(1) = \begin{bmatrix} -1 \\ -1 \end{bmatrix},$$

with $\mathbf{x}(n) = \mathbf{0}$ otherwise. Clearly this input is rich because $\begin{bmatrix} \mathbf{x}(0) & \mathbf{x}(1) \end{bmatrix}$ has rank two. The output can have only three nonzero samples, so that the largest output matrix we need to look at is:

$$[\mathbf{y}(0)\ \mathbf{y}(1)\ \mathbf{y}(2)] = \begin{bmatrix} \mathbf{h}(0) & \mathbf{h}(1) \end{bmatrix} \begin{bmatrix} \mathbf{x}(0) & \mathbf{x}(1) & \mathbf{0} \\ \mathbf{0} & \mathbf{x}(0) & \mathbf{x}(1) \end{bmatrix}.$$

We have

$$[\mathbf{y}(0)\ \mathbf{y}(1)\ \mathbf{y}(2)] = \begin{bmatrix} 1 & 1 & 1 & -1 \\ 1 & 1 & -1 & 1 \end{bmatrix} \begin{bmatrix} 1 & -1 & 0 \\ -1 & -1 & 0 \\ 0 & 1 & -1 \\ 0 & -1 & -1 \end{bmatrix}$$
$$= \begin{bmatrix} 0 & 0 & 0 \\ 0 & -4 & 0 \end{bmatrix},$$

which shows that the output matrix has rank one. Thus, richness of the input is not preserved at the output even though the matrix $\mathcal{H}$ has full rank M. In this example, $\mathbf{H}(z)$ happens to be a **paraunitary** matrix [67], that is, it satisfies $\widetilde{\mathbf{H}}(z)\mathbf{H}(z) = d\mathbf{I}$ for some positive d. Thus, paraunitary matrices do not necessarily preserve richness. □

Example 6.2: Consider again $M = 2$ and let

$$\mathbf{H}(z) = \begin{bmatrix} 1+z^{-1} & -z^{-1} \\ z^{-1} & 1-z^{-1} \end{bmatrix} = \begin{bmatrix} 1 & 0 \\ 0 & 1 \end{bmatrix} + z^{-1} \begin{bmatrix} 1 & -1 \\ 1 & -1 \end{bmatrix}.$$

Then,

$$\mathcal{H} = \begin{bmatrix} 1 & 0 & 1 & -1 \\ 0 & 1 & 1 & -1 \end{bmatrix}$$

and has rank $M = 2$. Consider the input

$$\mathbf{x}(0) = \begin{bmatrix} 0 \\ 1 \end{bmatrix}, \mathbf{x}(1) = \begin{bmatrix} 1 \\ 1 \end{bmatrix},$$

with $\mathbf{x}(n) = \mathbf{0}$ otherwise. Then the output matrix is

$$[\mathbf{y}(0)\ \mathbf{y}(1)\ \mathbf{y}(2)] = \begin{bmatrix} 1 & 0 & 1 & -1 \\ 0 & 1 & 1 & -1 \end{bmatrix} \begin{bmatrix} 0 & 1 & 0 \\ 1 & 1 & 0 \\ 0 & 0 & 1 \\ 0 & 1 & 1 \end{bmatrix}$$
$$= \begin{bmatrix} 0 & 0 & 0 \\ 1 & 0 & 0 \end{bmatrix},$$

which has rank one. Again, richness of the input is not preserved at the output, though $\mathcal{H}$ has full

rank M. In this example $\mathbf{H}(z)$ happens to be a **unimodular** matrix[67], that is, $\det \mathbf{H}(z) = 1$ for all z so that its inverse is an FIR matrix as well. The example shows that unimodular matrices do not necessarily preserve richness. □

6.2.2 Examples that Preserve Richness

If $\mathbf{H}(z)$ is an invertible memoryless system (i.e., a constant nonsingular matrix), it obviously preserves richness since multiplication with a nonsingular matrix does not change the rank of a matrix. A generalization of this special case has been found in [69] to be sufficient to preserve richness.

Example 6.3: An Nth order FIR system of the form

$$\mathbf{H}(z) = \mathbf{A}\left(g_0 + g_1 z^{-1} + \cdots + g_N z^{-N}\right)$$

preserves richness if $\mathbf{A}$ is a nonsingular matrix and $g_0 \neq 0$. To see this, suppose there exists a rich input sequence $\mathbf{x}(n)$ such that the output $\mathbf{y}(n)$ is not rich. Then, there exists a vector $\mathbf{v} \neq \mathbf{0}$ such that

$$\mathbf{v}^\dagger \mathbf{y}(n) = \mathbf{0}, \forall n$$

For $n = 0$, we have $g_0 \mathbf{v}^\dagger \mathbf{A}\mathbf{x}(0) = \mathbf{0}$. Since $g_0 \neq 0$, we obtain $\mathbf{w}^\dagger \mathbf{x}(0) = \mathbf{0}$, where $\mathbf{w}$, defined as $\mathbf{A}^\dagger \mathbf{v}$, is also a nonzero vector. For $n = 1$, we have $g_0 \mathbf{v}^\dagger \mathbf{x}(1) + g_1 \mathbf{v}^\dagger \mathbf{A}\mathbf{x}(0) = \mathbf{0}$, which implies $\mathbf{w}^\dagger \mathbf{x}(1) = \mathbf{0}$ because the second term is zero. For $n = 2$ we have $g_0 \mathbf{v}^\dagger \mathbf{x}(2) + g_1 \mathbf{v}^\dagger \mathbf{A}\mathbf{x}(1) + g_2 \mathbf{v}^\dagger \mathbf{A}\mathbf{x}(0) = \mathbf{0}$, and this implies $\mathbf{w}^\dagger \mathbf{x}(2) = \mathbf{0}$ since the last two terms are zero. Proceeding like this, we see that $\mathbf{w}^\dagger \mathbf{x}(n) = \mathbf{0}$ for all n, contradicting the assumption that $\mathbf{x}(n)$ is rich. □

Example 6.4: An RP example that does not have the form of the previous example is [69]:

$$\mathbf{H}(z) = \begin{bmatrix} 1 & a \\ 0 & 0 \end{bmatrix} + z^{-1} \begin{bmatrix} 0 & 0 \\ 1 & a \end{bmatrix},$$

where a is an arbitrary number.

To see this, assume the input $\mathbf{x}(n)$ is rich. Denote $x_n = \begin{bmatrix} 1 & a \end{bmatrix} \mathbf{x}(n)$. Then, x_n cannot be zero for all n since $\mathbf{x}(n)$ is rich. Now we have

$$\mathbf{y}(0) = \begin{bmatrix} 1 & a \\ 0 & 0 \end{bmatrix} \mathbf{x}(0) = \begin{bmatrix} x_0 \\ 0 \end{bmatrix}$$

and

$$\mathbf{y}(n) = \begin{bmatrix} 1 & a \\ 0 & 0 \end{bmatrix} \mathbf{x}(n) + \begin{bmatrix} 0 & 0 \\ 1 & a \end{bmatrix} \mathbf{x}(n-1) = \begin{bmatrix} x_n \\ x_{n-1} \end{bmatrix}$$

for $n \geq 1$. Suppose x_k is the first nonzero number in the sequence $\{x_n\}$. Then,

$$\begin{bmatrix} \mathbf{y}(k) & \mathbf{y}(k+1) \end{bmatrix} = \begin{bmatrix} x_k & x_{k+1} \\ 0 & x_k \end{bmatrix}$$

is a full-rank matrix, so $\mathbf{y}(n)$ is rich for any rich input $\mathbf{x}(n)$. □

6.3 Main Theorem

In this section we will describe the necessary and sufficient conditions for an LTI system to preserve richness. The proof of the theorem will be given in Section 6.6.

Theorem 6.1: An Nth order, $M \times M$ polynomial matrix

$$\mathbf{H}(z) = \sum_{k=0}^{N} \mathbf{h}(k) z^{-k}$$

is a **richness preserving (RP)** LTI system **if and only if** either one of the following conditions is true:

(a) There exist a nonsingular $M \times M$ matrix $\mathbf{A}$ and constants $g_0, g_1, \cdots, g_N$ of which at least one is nonzero such that $\mathbf{h}(k) = g_k \mathbf{A}$.

(b) There exist a nonzero row vector $\mathbf{v}^\dagger$ and a set of column vectors $\mathbf{a}_0, \mathbf{a}_1, \cdots, \mathbf{a}_N$ such that $\mathbf{h}(k) = \mathbf{a}_k \mathbf{v}^\dagger$ for any k, and $\begin{bmatrix} \mathbf{a}_0 & \mathbf{a}_1 & \cdots & \mathbf{a}_N \end{bmatrix}$ has full rank M.

□

It is obvious that conditions (a) and (b) cannot be satisfied at the same time. We can hence say there are two types of RP matrices, namely Type A and Type B, according to the statement of Theorem 6.1. Examples 6.3 and 6.4 in the previous section serve as special cases for Type A and Type B RP matrices, respectively.

For a Type A matrix, each nonzero coefficient matrix is nonsingular. For Type B matrices, each nonzero coefficient matrix has unit rank. *There are no other types of examples!* Notice in particular

that the order N and the size M of a Type B matrix must satisfy $N \geq M-1$ to meet the full rank criterion of $\left[\begin{array}{cccc} \mathbf{a}_0 & \mathbf{a}_1, & \cdots & \mathbf{a}_N \end{array} \right]$.

The rank of each nonzero coefficient matrix of a RP matrix is always the same, and we call it the *coefficient rank*. In addition, the coefficient rank of a RP system can only be either unity or full. For a RP system where the first coefficient matrix is nonsingular, a useful corollary of Theorem 6.1 is as follows:

Corollary 6.1: Consider the Nth order, $M \times M$ FIR systems $\mathbf{H}(z) = \sum_{k=0}^{N} \mathbf{h}(k) z^{-k}$ and assume $\mathbf{h}(0)$ is nonsingular. Then $\mathbf{H}(z)$ is RP **if and only if** there exist a nonsingular $M \times M$ matrix $\mathbf{A}$ and constants $g_0, g_1, \cdots, g_N$ where $g_0 \neq 0$ such that $\mathbf{h}(k) = g_k \mathbf{A}$. □

When the first coefficient matrix $\mathbf{h}(0)$ of a RP system is singular but nonzero, it must be a Type B RP system, as stated in the following corollary:

Corollary 6.2: Consider the Nth order, $M \times M$ FIR system $\mathbf{H}(z) = \sum_{k=0}^{N} \mathbf{h}(k) z^{-k}$ with size $M \times M$, and assume $\mathbf{h}(0) \neq \mathbf{0}$ is singular. Then, $\mathbf{H}(z)$ is RP **if and only if** there exist a nonzero row vector $\mathbf{v}^\dagger$ and $N+1$ column vectors $\mathbf{a}_0, \mathbf{a}_1, \cdots \mathbf{a}_N$ such that $\mathbf{h}(n) = \mathbf{a}_n \mathbf{v}^\dagger$, $\left[\begin{array}{cccc} \mathbf{a}_0 & \mathbf{a}_1 & \cdots & \mathbf{a}_N \end{array} \right]$ has full rank, and $\mathbf{a}_0 \neq \mathbf{0}$. □

The proofs of the preceding two corollaries will be automatically covered when we prove Theorem 6.1 in Section 6.6. In these corollaries we have not considered the case where $\mathbf{h}(0) = \mathbf{0}$. If this is true, however, $\mathbf{H}(z)$ is simply a delayed version of another LTI system whose first coefficient is nonzero. Since $\mathbf{H}(z)$ is RP if and only if $z^{-m}\mathbf{H}(z)$ is RP for any m, the assumption $\mathbf{h}(0) \neq \mathbf{0}$ is not a loss of generality.

6.3.1 Proof of a Special Case

We will give the proof of a special case of Corollary 6.1 where we assume $\mathbf{h}(0)$ is nonsingular. Although the proof of this special case will be definitely covered when we prove Theorem 6.1 in Section 6.6, the reader might find this insightful.

Special Case of Corollary 6.1: Consider the first order, 2×2 FIR system

$$\mathbf{H}(z) = \mathbf{h}(0) + z^{-1}\mathbf{h}(1),$$

and assume $\mathbf{h}(0)$ is nonsingular. Then, $\mathbf{H}(z)$ is RP if and only if $\mathbf{h}(1) = \rho\mathbf{h}(0)$ for some scalar constant ρ.

Proof: The proof of sufficiency is self-evident in view of Example 6.3. As for necessity, since $\mathbf{h}(0)$ is nonsingular, we can write $\mathbf{H}(z) = \mathbf{h}(0)(\mathbf{I} + \mathbf{B}z^{-1})$. The nonsingular factor $\mathbf{h}(0)$ does not affect the rank of the output matrix, so $\mathbf{H}(z)$ is RP if and only if $(\mathbf{I} + \mathbf{B}z^{-1})$, which has the form

$$\mathbf{G}(z) = \mathbf{I} + z^{-1} \begin{bmatrix} a & b \\ c & d \end{bmatrix},$$

preserves richness. Consider the input

$$\mathbf{x}(0) = \begin{bmatrix} 0 \\ 1 \end{bmatrix}, \mathbf{x}(1) = \begin{bmatrix} -b \\ a \end{bmatrix},$$

with $\mathbf{x}(n) = \mathbf{0}$ otherwise. This produces the output

$$\mathbf{y}(0) = \begin{bmatrix} 0 \\ 1 \end{bmatrix}, \mathbf{y}(1) = \begin{bmatrix} 0 \\ a+d \end{bmatrix}, \mathbf{y}(2) = \begin{bmatrix} 0 \\ ad-bc \end{bmatrix},$$

and $\mathbf{y}(n) = \mathbf{0}$ otherwise. We see that if $b \neq 0$, then $\begin{bmatrix} \mathbf{x}(0) & \mathbf{x}(1) \end{bmatrix}$ has rank 2, and hence the input is rich while the output $\mathbf{y}(n)$ is not. Therefore, $b = 0$ is a necessary condition for richness preservation. A slight variation of this construction shows that $c = 0$ is necessary as well. Thus, in order to preserve richness $\mathbf{G}(z)$ has to be of the form

$$\mathbf{G}(z) = \mathbf{I} + z^{-1} \begin{bmatrix} a & 0 \\ 0 & d \end{bmatrix}.$$

If we now choose the input

$$\mathbf{x}(0) = \begin{bmatrix} 1 \\ 1 \end{bmatrix}, \mathbf{x}(1) = \begin{bmatrix} d \\ a \end{bmatrix},$$

with $\mathbf{x}(n) = \mathbf{0}$ otherwise, then

$$\mathbf{y}(0) = \begin{bmatrix} 1 \\ 1 \end{bmatrix}, \mathbf{y}(1) = \begin{bmatrix} a+d \\ a+d \end{bmatrix}, \mathbf{y}(2) = \begin{bmatrix} ad \\ ad \end{bmatrix},$$

with $\mathbf{y}(n) = \mathbf{0}$ otherwise. If $a \neq d$, then the input is rich whereas the output is not. This shows that $a = d$ is a necessary condition. Thus, $\mathbf{G}(z) = \mathbf{I} + \rho\mathbf{I}z^{-1}$, so $\mathbf{h}(1) = \rho\mathbf{h}(0)$ indeed.

□

6.4 Properties of Richness-Preserving Systems

6.4.1 Cascaded Systems

In this subsection we are interested in richness preserving properties of cascaded systems. It is obvious that the product of RP systems is also RP. We will show that the product is Type A RP if all the subsystems are Type A RP, and it would be Type B RP if *any of them* is Type B RP.

Theorem 6.2: If $\mathbf{A}_1(z), \mathbf{A}_2(z)$ are Type A RP matrices and $\mathbf{B}_1(z), \mathbf{B}_2(z)$ are Type B RP matrices, then

(1) $\mathbf{A}_1(z)\mathbf{A}_2(z)$ is a Type A RP matrix,

(2) $\mathbf{A}_1(z)\mathbf{B}_1(z)$ is a Type B RP matrix,

(3) $\mathbf{B}_1(z)\mathbf{A}_1(z)$ is a Type B RP matrix,

(4) $\mathbf{B}_1(z)\mathbf{B}_2(z)$ is a Type B RP matrix.

□

Proof: Let $\mathbf{A}_1(z) = g_1(z)\mathbf{A}_1, \mathbf{A}_2(z) = g_2(z)\mathbf{A}_2$, where $\mathbf{A}_1, \mathbf{A}_2$ are invertible constant $M \times M$ matrices and $g_1(z), g_2(z)$ are nonzero polynomials in z^{-1}. Then the product $\mathbf{A}_1\mathbf{A}_2 = g_1(z)g_2(z)\mathbf{A}_1\mathbf{A}_2$ is clearly a Type A RP matrix. Furthermore, let $\mathbf{B}_1(z) = \sum_{k=0}^{N_1} \mathbf{a}_k\mathbf{v}_1^\dagger z^{-k}$ and $\mathbf{B}_2(z) = \sum_{k=0}^{N_2} \mathbf{b}_k\mathbf{v}_2^\dagger z^{-k}$, then $\mathbf{A}_1(z)\mathbf{B}_1(z) = g_1(z)\mathbf{A}_1 \sum_{k=0}^{N_1} \mathbf{a}_k\mathbf{v}_1^\dagger z^{-k} = \sum_{l=0}^{N} g_l z^{-l} \sum_{k=0}^{N_1} \mathbf{a}'_k z^{-k}\mathbf{v}_1^\dagger = \sum_{k=0}^{N_1+N} \mathbf{a}''_k z^{-k}\mathbf{v}_1^\dagger$ is Type B RP since both $\mathbf{a}'_k$'s and $\mathbf{a}''_k$'s still span a full dimensional space. And $\mathbf{B}_1(z)\mathbf{A}_1(z) = (\sum_{k=0}^{N_1} \mathbf{a}_k z^{-k})g_1(z)$ $\mathbf{v}_1^\dagger\mathbf{A}_1 = (\sum_{k=0}^{N_1+N} \mathbf{a}'_k z^{-k})\mathbf{v}'^\dagger$ is also Type B RP. Finally $\mathbf{B}_1(z)\mathbf{B}_2(z) = (\sum_{k=0}^{N_1} \mathbf{a}_k\mathbf{v}_1^\dagger z^{-k})(\sum_{l=0}^{N_2} \mathbf{b}_l\mathbf{v}_2^\dagger z^{-l}) =$ $\sum_{k=0}^{N_1+N_2} \mathbf{a}'_k\mathbf{v}_2^\dagger z^{-k}$ is also a Type B RP matrix. □

If some of the subsystems are non-RP, however, it does not imply the whole system is non-RP. A trivial example is a cascade of the unimodular matrix in Example 2 with its inverse, which is also causal and unimodular. Since the product is identity it preserves richness. But both of the factors in the product are non-RP systems. In fact, for a cascaded system to be RP, although it is sufficient that all the subsystems are RP, this is not necessary. An interesting question that comes up here is this: if $\mathbf{F}(z)\mathbf{H}(z)\mathbf{G}(z)$ is a richness preserving system and both $\mathbf{F}(z)$ and $\mathbf{G}(z)$ are RP, is $\mathbf{H}(z)$ also RP? The answer depends on the types of $\mathbf{F}(z)$ and $\mathbf{G}(z)$, and is given in the following two theorems.

Theorem 6.3: Suppose $\mathbf{A}(z)$ is a Type A RP matrix. Then, the statement "$\mathbf{A}(z)\mathbf{H}(z)$ is RP" implies that $\mathbf{H}(z)$ is RP. Similarly, the statement "$\mathbf{H}(z)\mathbf{A}(z)$ is RP" also implies that $\mathbf{H}(z)$ is RP. □

This theorem states that if a Type A RP system is going to connect with another system, the resulting cascaded system is RP only when the new system is also RP. On the contrary, Type B RP systems do not have this property. We can see this in the following examples.

Example 6.5: Let $\mathbf{B}(z) = \begin{bmatrix} 1 & 0 \\ z^{-1} & 0 \end{bmatrix}$, which is a Type B RP system, and

$$\mathbf{H}_1(z) = \begin{bmatrix} 1 & 1 \\ 0 & 0 \end{bmatrix}.$$

Then,

$$\mathbf{B}(z)\mathbf{H}_1(z) = \begin{bmatrix} 1 & 0 \\ z^{-1} & 0 \end{bmatrix} \begin{bmatrix} 1 & 1 \\ 0 & 0 \end{bmatrix} = \begin{bmatrix} 1 & 1 \\ z^{-1} & z^{-1} \end{bmatrix}$$

is RP, although $\mathbf{H}_1(z)$ is not RP. On the other hand, let

$$\mathbf{H}_2(z) = \begin{bmatrix} 1+z^{-1} & -1 \\ z^{-1} & 0 \end{bmatrix}.$$

We have

$$\mathbf{H}_2(z)\mathbf{B}(z) = \begin{bmatrix} 1+z^{-1} & -1 \\ z^{-1} & 0 \end{bmatrix} \begin{bmatrix} 1 & 0 \\ z^{-1} & 0 \end{bmatrix} = \begin{bmatrix} 1 & 0 \\ z^{-1} & 0 \end{bmatrix}$$

is also RP, while $\mathbf{H}_2(z)$ is not. □

Actually, for any given Type B RP system, we can always find a non-rich system such that the product of the two systems is RP, as stated in the following theorem.

Theorem 6.4: If $\mathbf{B}(z)$ is a Type B RP matrix, then there exist non-RP systems $\mathbf{H}_1(z)$ and $\mathbf{H}_2(z)$ such that $\mathbf{B}(z)\mathbf{H}_1(z)$ and $\mathbf{H}_2(z)\mathbf{B}(z)$ are both RP. □

The proofs of these two theorems require some lemmas which will be introduced in the following two subsections. The proofs will be given in Section 6.4.4.

6.4.2 Enriching Systems

We can define a system to be *enriching* if there exists a non-rich input such that the output of the system is rich. An enriching system, when following a non-RP system, could possibly make the overall system become RP again. We will show that Type A RP matrices are *not* enriching, while all Type B RP matrices are enriching.

Lemma 6.1: If $\mathbf{A}(z)$ is a Type A RP system, then the input $\mathbf{x}(n)$ is rich if and only if the output $\mathbf{y}(n)$ is rich. □

Proof: Obviously, if $\mathbf{x}(n)$ is rich, then so is $\mathbf{y}(n)$. Now suppose $\mathbf{x}(n)$ is non-rich. We need to show that $\mathbf{y}(n)$ is also non-rich. Let

$$\mathbf{A}(z) = \sum_{k=0}^{N} g_k \mathbf{A} z^{-k},$$

where $\mathbf{A}$ is an invertible constant matrix. We have

$$\mathbf{y}(n) = \sum_{k=0}^{N} g_k \mathbf{A}\mathbf{x}(n-k) = \sum_{k=0}^{N} g_k \mathbf{x}'(n-k),$$

where $\mathbf{x}'(n) = \mathbf{A}\mathbf{x}(n)$ is also non-rich since $\mathbf{A}$ does not change the rank of a signal. This implies $\mathbf{y}(n)$, a linear combination of $\mathbf{x}'(k)$, is also non-rich. □

This lemma states that Type A RP systems are never enriching. Type-B RP systems, on the contrary, can be shown to be enriching. An example of this is when

$$\mathbf{H}(z) = \begin{bmatrix} 1 & a \\ 0 & 0 \end{bmatrix} + z^{-1} \begin{bmatrix} 0 & 0 \\ 1 & a \end{bmatrix},$$

and we let the input $\mathbf{x}(n) = [1 \quad 0]^T$ for all n, which is obviously non-rich. Then, we obtain $\mathbf{y}(0) = [1 \quad 0]^T$ and $\mathbf{y}(1) = [1 \quad 1]^T$, implying the output $\mathbf{y}(n)$ is rich, and hence $\mathbf{H}(z)$ is enriching. More generally we have:

Lemma 6.2: If $\mathbf{B}(z)$ is a Type B RP system, then there exists a non-rich input $\mathbf{x}(n)$ such that the output is rich. □

Proof: For $\mathbf{B}(z) = \sum_{k=0}^{N} \mathbf{a}_k \mathbf{v}^\dagger z^{-k}$, let $\mathbf{x}(n) = \mathbf{v}/||\mathbf{v}||^2$ for all n, which is obviously non-rich. Then it can be shown that $\mathbf{y}(n) = \sum_{k=0}^{n} \mathbf{a}_k$ for $0 \leq n \leq N$, so we have

$$[\mathbf{y}(0)\ \mathbf{y}(1) \cdots \mathbf{y}(N)] = [\mathbf{a}_0\ \mathbf{a}_1 \cdots \mathbf{a}_N] \begin{bmatrix} 1 & 1 & \cdots & 1 \\ 0 & 1 & \cdots & 1 \\ \vdots & \ddots & \ddots & \vdots \\ 0 & \cdots & 0 & 1 \end{bmatrix},$$

which implies the matrix $[\mathbf{y}(0)\ \mathbf{y}(1) \cdots \mathbf{y}(N)]$ has full rank since it is the product of two full-rank matrices, so $\mathbf{y}(n)$ is rich, and hence any Type B RP system is enriching. □

6.4.3 Restriction on Output Range

Consider the cascaded system $\mathbf{F}(z)\mathbf{G}(z)$. If rich signals which are rendered non-rich by $\mathbf{F}(z)$ can never be produced as outputs of $\mathbf{G}(z)$, then the product $\mathbf{F}(z)\mathbf{G}(z)$ can be RP. We will show that a Type A RP system $\mathbf{G}(z)$ can produce any output if the first coefficient matrix $\mathbf{g}(0)$ is nonzero. For any Type B RP system, on the contrary, we can always find an output that it cannot generate.

Lemma 6.3: If $\mathbf{A}(z)$ is a Type A RP matrix, and the first coefficient matrix $\mathbf{h}(0)$ is nonzero, then for any output sequence $\mathbf{y}(n)$, there exists unique $\mathbf{x}(n)$ such that the output of $\mathbf{A}(z)$ is $\mathbf{y}(n)$. □

Proof: For any $n \geq 0$ we have

$$\mathbf{y}(n) = \sum_{k=0}^{N} g_k \mathbf{A}\mathbf{x}(n-k),$$

where we assume $\mathbf{x}(n) = \mathbf{0}$ for all $n < 0$. This implies

$$\mathbf{A}^{-1}\mathbf{y}(n) = g_0\mathbf{x}(n) + \sum_{k=1}^{N} g_1\mathbf{x}(n-k),$$

and hence

$$\mathbf{x}(n) = \frac{1}{g_0}\left[\mathbf{A}^{-1}\mathbf{y}(n) - \sum_{k=1}^{N} g_1\mathbf{x}(n-k)\right]$$

can be uniquely decided for any $n \geq 0$, given any output signal $\mathbf{y}(n)$. □

Lemma 6.4: If $\mathbf{B}(z)$ is a Type B RP matrix, then there exists $\mathbf{y}(n)$ that cannot be output of $\mathbf{B}(z)$. □

Proof: Suppose

$$\mathbf{B}(z) = \sum_{k=0}^{N} \mathbf{a}_k \mathbf{v}^\dagger z^{-k}.$$

Then for any input $\mathbf{x}(n)$, we have $\mathbf{y}(0) = \mathbf{a}_0\mathbf{v}^\dagger\mathbf{x}(0)$, which is confined to be a scalar multiple of $\mathbf{a}_0$, so $\mathbf{B}(z)$ cannot produce output $\mathbf{y}(n)$ where $\mathbf{y}(0)$ is not proportional to $\mathbf{a}_0$. □

6.4.4 Proof of Theorems 3 and 4

Proof of Theorem 6.3: First let $\mathbf{x}(n)$ be the input to $\mathbf{H}(z)$, $\mathbf{x}_1(n)$ be the output of $\mathbf{H}(z)$ and the input of $\mathbf{A}(z)$, and $\mathbf{y}(n)$ be the output $\mathbf{A}(z)$. Suppose $\mathbf{H}(z)$ is not RP but $\mathbf{A}(z)\mathbf{H}(z)$ is RP. Then there exists $\mathbf{x}(n)$ such that $\mathbf{x}_1(n)$ is non-rich. From Lemma 1 we know $\mathbf{y}(n)$ is also non-rich. Hence the system $\mathbf{A}(z)\mathbf{H}(z)$ is not RP, contradicting the assumption, so $\mathbf{H}(z)$ has to be RP if $\mathbf{A}(z)\mathbf{H}(z)$ is RP.

Conversely, let $\mathbf{x}(n)$ be the input of the cascaded system $\mathbf{H}(z)\mathbf{A}(z)$ and $\mathbf{y}(n)$ be the output of $\mathbf{H}(z)\mathbf{A}(z)$. In addition, we assume $\mathbf{A}(z) = z^{-m}\mathbf{A}'(z)$, where m is a nonnegative integer and $\mathbf{A}'(z)$ is a causal Type A RP system with first coefficient matrix nonzero. Then, the cascaded system can be viewed as a cascade of $\mathbf{A}'(z)$ followed by $\mathbf{H}(z)z^{-m}$. Let $\mathbf{x}_1(n)$ be the output of the subsystem $\mathbf{A}'(z)$ and the input of the subsystem $\mathbf{H}(z)z^{-m}$. Suppose $\mathbf{H}(z)$ is not RP. Then, $\mathbf{H}(z)z^{-m}$ is also not RP, so there exists input sequence $\mathbf{x}_1(n)$ such that the output $\mathbf{y}(n)$ of $\mathbf{H}(z)z^{-m}$ is not rich. By Lemma 3 we can find an input $\mathbf{x}(n)$ for $\mathbf{A}'(z)$ such that the output is $\mathbf{x}_1(n)$. Also, by Lemma 1 this $\mathbf{x}(n)$ must be rich, so we can use this $\mathbf{x}(n)$ to be the input of the whole system $\mathbf{H}(z)\mathbf{A}(z)$ and generate the non-rich output $\mathbf{y}(n)$, so $\mathbf{H}(z)$ must be RP if $\mathbf{H}(z)\mathbf{A}(z)$ is RP. □

Proof of Theorem 6.4: Let $\mathbf{B}(z) = \sum_{k=0}^{N}\mathbf{a}_k\mathbf{v}^\dagger z^{-k}$. Assume $||\mathbf{v}|| = 1$. Take an arbitrary nonzero row vector $\mathbf{w}^\dagger$ and let $\mathbf{H}_1(z) = \mathbf{v}\mathbf{w}^\dagger$, which is a singular constant matrix and is obviously non-RP. Then, it can be shown that $\mathbf{B}(z)\mathbf{H}_1(z) = \sum_{k=0}^{N}\mathbf{a}_k\mathbf{w}^\dagger z^{-k}$ is also RP!

Suppose $\mathbf{a}_0$ and $\mathbf{a}_N$ are nonzero. Let $\mathbf{H}_2(z) = \mathbf{I}_M + \mathbf{a}_0\mathbf{a}_N^\dagger z^{-1}$. Since the coefficient matrices have different ranks, $\mathbf{H}_2(z)$ is not RP. But the product $\mathbf{H}_2(z)\mathbf{B}(z)$ can be shown to have the form $\sum_{k=0}^{N+1}\mathbf{b}_k\mathbf{v}^\dagger z^{-k}$, where $\mathbf{b}_0 = \mathbf{a}_0, \mathbf{b}_k = \mathbf{a}_k + c_{k-1}\mathbf{a}_0$ for $1 \le k \le N$, and $\mathbf{b}_{N+1} = \mathbf{a}_0 c_N$, where $c_k = \mathbf{a}_k^\dagger\mathbf{a}_N$ are constants. One can verify that the matrix $[\mathbf{b}_0\mathbf{b}_1\cdots\mathbf{b}_N]$ is a full rank matrix and hence $\mathbf{H}_2(z)\mathbf{B}(z)$ is Type B RP. □

6.4.5 Paraunitary and Unimodular matrices

In Examples 6.1 and 6.2 we have seen that paraunitary matrices and unimodular matrices are not necessarily RP. Using Theorem 6.1, we can actually show that FIR paraunitary and unimodular matrices cannot preserve richness unless they are constant matrices (with a possible delay in the PU case):

Corollary 6.3: If a paraunitary matrix $\mathbf{H}(z)$ is RP, then $\mathbf{H}(z)$ is a constant unitary matrix or a delayed version of it. □

Proof: Without loss of generality, assume $\mathbf{h}(0) \neq \mathbf{0}$. Suppose $\mathbf{H}(z) = \sum_{k=0}^{N} \mathbf{h}(k) z^{-k}$ is paraunitary and richness preserving but not a constant matrix (i.e., $N > 0$ and $\mathbf{h}(N)$ is nonzero). From properties of paraunitary matrices we know both $\mathbf{h}(0)$ and $\mathbf{h}(N)$ are singular [67]. Using Corollary 6.2 of Theorem 6.1, there exist row vector $\mathbf{v}^\dagger$ and $N+1$ column vectors $\mathbf{a}_0, \mathbf{a}_1, \cdots, \mathbf{a}_N$ such that $\mathbf{H}(z) = \sum_{k=0}^{N} \mathbf{a}_k \mathbf{v}^\dagger z^{-k}$, so $\widetilde{\mathbf{H}}(z) = \sum_{l=0}^{N} \mathbf{v}\mathbf{a}_l^\dagger z^{l}$ and

$$\widetilde{\mathbf{H}}(z)\mathbf{H}(z) = \sum_{k=0}^{N} \sum_{l=0}^{N} \mathbf{v}\mathbf{a}_l^\dagger \mathbf{a}_k \mathbf{v}^\dagger z^{-(k-l)}.$$

The constant term (z^0) of $\widetilde{\mathbf{H}}(z)\mathbf{H}(z)$ would be

$$\sum_{k=0}^{N} \mathbf{v}\mathbf{a}_k^H \mathbf{a}_k \mathbf{v}^\dagger = \left[\sum_{k=0}^{N} \mathbf{a}_k^\dagger \mathbf{a}_k \right] \mathbf{v}\mathbf{v}^\dagger$$

since $\mathbf{a}_k^\dagger \mathbf{a}_k$ are all constants. The matrix $\mathbf{v}\mathbf{v}^\dagger$ obviously has rank one. This contradicts $\widetilde{\mathbf{H}}(z)\mathbf{H}(z) = \mathbf{I}_M$, completing the proof. □

Corollary 6.4: If a unimodular matrix $\mathbf{H}(z)$ is richness preserving, then $\mathbf{H}(z)$ is a constant matrix.□

Proof: If $\mathbf{H}(z) = \sum_{k=0}^{N} \mathbf{h}(k) z^{-k}$ is unimodular, $\det(\mathbf{h}(0)) = \det(\mathbf{H}(\infty)) = 1$, so $\mathbf{h}(0)$ must be nonsingular. If $\mathbf{H}(z)$ is also RP, it must satisfy condition (a) in Theorem 1. Then, $\mathbf{H}(z) = \left(\sum_{k=0}^{N} g_k z^{-k} \right) \mathbf{A}$ and $\det(\mathbf{H}(z)) = \left(\sum_{k=0}^{N} g_k z^{-k} \right)^M \det(\mathbf{A}) = 1$, where $\mathbf{A}$ is nonsingular, so we have $g_k = 0$ for $k > 0$, and hence $\mathbf{H}(z)$ must be a constant matrix. □

6.5 Strict Definition of Richness

In practical applications, the new definition of richness given below might be more useful:

Definition 6.2: A sequence of $M \times 1$ vectors $\mathbf{x}(n), n \geq 0$ is said to be **strictly rich** (SR) if for any positive integer n_0, there exists an integer K_{n_0} such that the matrix

$$\left[\begin{array}{cccc} \mathbf{x}(n_0) & \mathbf{x}(n_0+1) & \cdots & \mathbf{x}(n_0+K_{n_0}) \end{array} \right]$$

has rank M. □

Observe that a strictly rich signal is also rich according to the old definition. Conversely, a rich signal is not necessarily strictly rich. Furthermore, we will find that some systems that preserve richness according to the old definition no longer preserve strict richness. For example, we showed that Type A RP system $\mathbf{H}(z) = \begin{bmatrix} 1 & 0 \\ 0 & 1 \end{bmatrix} + z^{-1} \begin{bmatrix} 1 & 0 \\ 0 & 1 \end{bmatrix}$ preserves richness. However, if we let $\mathbf{x}(2n) = \begin{bmatrix} 1 & 0 \end{bmatrix}^T$ and $\mathbf{x}(2n+1) = \begin{bmatrix} 0 & 1 \end{bmatrix}^T$ for all nonnegative n, then the output would be $\mathbf{y}(0) = \begin{bmatrix} 1 & 0 \end{bmatrix}^T$ and $\mathbf{y}(n) = \begin{bmatrix} 1 & 1 \end{bmatrix}^T$ for any positive n. Here, the input $\mathbf{x}(n)$ is both rich and strictly rich, but the output $\mathbf{y}(n)$ is not strictly rich. The necessary and sufficient condition for LTI systems to preserve strict richness is summarized in the following theorem.

Theorem 6.5: An Nth order, $M \times M$ polynomial matrix

$$\mathbf{H}(z) = \sum_{k=0}^{N} \mathbf{h}(k) z^{-k}$$

is a **strict-richness preserving** (SRP) LTI system **if and only if** there exists nonnegative integer n and an invertible $M \times M$ matrix $\mathbf{A}$ such that
$\mathbf{H}(z) = z^{-n}\mathbf{A}$. □

In view of this theorem, we find if a system is SRP then it is also RP. We will prove Theorems 6.1 and 6.5 together in Section 6.6.

6.6 Proof of the Main Theorems

6.6.1 Sketch of the Proof

In this section, we will prove Theorems 6.1 and 6.5 step by step. We will first show that conditions described in Theorems 6.1 and 6.5 are sufficient (Section 6.6.2). Then we will present Lemma 5, which shows that necessary conditions for Theorem 1 are also necessary for Theorem 5 (Section 6.6.3). From Section 6.6.7 to Section 6.6.6, necessary conditions of Theorem 6.1 will be developed. In particular, a term *coefficient rank* will be defined for all RP systems to denote the ranks of all nonzero coefficient matrices since they will prove to be the same (Section 6.6.5). The coefficient rank will later on prove to be either unity or M. Finally, for the case of unity coefficient rank,

we will show condition (b) is necessary, and for the case of full coefficient rank, condition (a) is necessary (Section 6.6.6).

In Section 6.6.7, we will show that Type A and Type B RP systems cannot preserve strict richness unless they are a constant invertible matrix with a possible delay.

6.6.2 Proof of Sufficiency

We first prove conditions (a) and (b) in Theorem 6.1 are sufficient for preserving richness.

Proof: If $\mathbf{H}(z)$ satisfies condition (a), by Theorem 6.1 in [69], it is RP. Suppose $\mathbf{H}(z)$ satisfies condition (b) but is not RP. Then there exists a rich input $\mathbf{x}(n)$ such that the output $\mathbf{y}(n)$ is not rich, i.e., there exists a row vector $\mathbf{w}^\dagger$ such that $\mathbf{w}^\dagger \mathbf{y}(n) = 0, \forall n$. Using $\mathbf{y}(n) = \sum_{k=0}^{N} \mathbf{h}(k)\mathbf{x}(n-k)$, we have the following equations:

$$\begin{aligned} (\mathbf{w}^\dagger \mathbf{a}_0)(\mathbf{v}^\dagger \mathbf{x}(0)) &= 0 \\ (\mathbf{w}^\dagger \mathbf{a}_0)(\mathbf{v}^\dagger \mathbf{x}(1)) + (\mathbf{w}^\dagger \mathbf{a}_1)(\mathbf{v}^\dagger \mathbf{x}(0)) &= 0 \\ &\vdots \\ \textstyle\sum_{k=0}^{N} (\mathbf{w}^\dagger \mathbf{a}_k)(\mathbf{v}^\dagger \mathbf{x}(N-k)) &= 0. \end{aligned} \tag{6.1}$$

If $\mathbf{v}^\dagger \mathbf{x}(0)$ is not zero, then from the first equation we have $\mathbf{w}^\dagger \mathbf{a}_0 = 0$. Substituting this into the second equation, we get

$$(\mathbf{w}^\dagger \mathbf{a}_1)(\mathbf{v}^\dagger \mathbf{x}(0)) = 0,$$

so $\mathbf{w}^\dagger \mathbf{a}_1$ has to be zero. Repeating these substitutions we will have $\mathbf{w}^\dagger \mathbf{a}_k = 0, \forall k, 0 \le k \le N$. This contradicts the statement that $[\mathbf{a}_0, \mathbf{a}_1, ..., \mathbf{a}_N]$ has rank M, so $\mathbf{v}^\dagger \mathbf{x}(0)$ has to be zero. Substituting this into (6.1) and repeating the same derivations, we will have $\mathbf{v}^\dagger \mathbf{x}(1) = \mathbf{0}$ as well. Repeating this we get $\mathbf{v}^\dagger \mathbf{x}(n) = 0$ for all n. This violates richness of the input $\mathbf{x}(n)$, so condition (b) is also sufficient. □

The sufficiency for Theorem 6.5 is self-evident.

6.6.3 Relationship between RP and SRP Systems

We know that strict richness implies richness, but not vice versa. Therefore, it is not obvious that an SRP system is also RP. We will show, however, that this is the case.

Lemma 6.5: Given $M \times M$ polynomial matrix $\mathbf{H}(z) = \sum_{k=0}^{N} \mathbf{h}(k) z^{-k}$, if there exists a rich causal

signal $\mathbf{x}(n)$ which has a finite support such that $\mathbf{y}(n) = \sum_{k=0}^{N} \mathbf{h}(k)\mathbf{x}(n-k)$ is non-rich, then $\mathbf{H}(z)$ is neither RP nor SRP. □

Proof: By definition, $\mathbf{H}(z)$ is not RP. Suppose $\mathbf{x}(n)$ has length L, that is, $\mathbf{x}(n) = \mathbf{0}$ for all $n \geq L$. Then it is clear that $\mathbf{y}(n) = \sum_{k=0}^{N} \mathbf{h}(k)\mathbf{x}(n-k) = \mathbf{0}$ for all $n \geq L+N$. Now consider a new signal $\mathbf{x}'(n) = \mathbf{x}(n \bmod (N+L))$. Since $\mathbf{x}(n)$ is rich, we have $\mathbf{x}'(n)$ is strictly rich. Then, using the facts that $\mathbf{x}(n) = \mathbf{0}$ for all $n \geq L$ and that $\mathbf{y}(n)$ is not rich, we find $\mathbf{y}'(n) = \sum_{k=0}^{N} \mathbf{h}(k)\mathbf{x}'(n-k) = \sum_{k=0}^{N} \mathbf{h}(k)\mathbf{x}((n-k) \bmod (N+L)) = \sum_{k=0}^{N} \mathbf{h}(k)\mathbf{x}([n \bmod (N+L)]-k) = \mathbf{y}(n \bmod (N+L))$ is also not strictly rich. Therefore, $\mathbf{H}(z)$ is not SRP. □

We will use this lemma to show that SRP is stronger than RP. In the following lemmas, we will derive necessary conditions for Theorem 1 by constructing rich input signals that have non-rich output for a system that does not satisfy these conditions. All of the input signals we construct will have finite support, and hence the necessary conditions for Theorem 1 are also those for Theorem 5.

6.6.4 Lemmas for Proof of Necessity

Lemma 6.6: If an $M \times M$ polynomial matrix $\mathbf{H}(z) = \sum_{k=0}^{N} \mathbf{h}(k)z^{-k}$ is RP, then there exist $M \times M$ diagonal matrices $\mathbf{D}_k$ and an $M \times M$ constant matrix $\mathbf{A}$, each row of which is nonzero, such that $\mathbf{h}(k) = \mathbf{D}_k\mathbf{A}$. □

Proof: For $0 \leq k \leq N$, we assume

$$\mathbf{h}(k) = \begin{bmatrix} \mathbf{a}_{1k} & \mathbf{a}_{2k} & \cdots & \mathbf{a}_{Mk} \end{bmatrix}^T,$$

where

$$\mathbf{a}_{ik}^T = \begin{bmatrix} a_{i1k} & a_{i2k} & \cdots & a_{iMk} \end{bmatrix}$$

is the ith row of $\mathbf{h}(k)$. Focusing on the ith row of $\mathbf{H}(z)$, we use

$$\mathbf{b}_k^T = \begin{bmatrix} b_{1k} & b_{2k} & \cdots & b_{Mk} \end{bmatrix}$$

to denote $\mathbf{a}_{ik}^T$ for simplicity. Since $\mathbf{H}(z)$ is richness preserving, any row of $\mathbf{H}(z)$ cannot be all zeros. So there exists b_{jk} that is nonzero. Without loss of generality, assume $b_{10} \neq 0$. Construct the input as:

$$\begin{aligned}
\mathbf{x}(0) &= b_{20}\mathbf{e}_1 - b_{10}\mathbf{e}_2 \\
\mathbf{x}(1) &= b_{21}\mathbf{e}_1 - b_{11}\mathbf{e}_2 \\
&\vdots \\
\mathbf{x}(N) &= b_{2N}\mathbf{e}_1 - b_{1N}\mathbf{e}_2 \\
\mathbf{x}(m(N+1)+k) &= b_{(m+2),k}\mathbf{e}_1 - b_{1k}\mathbf{e}_{m+2}, \\
&\quad 0 \le m \le M-2, 0 \le k \le N.
\end{aligned}$$

For simplicity, we will use $\mathbf{x}_m(k)$ to denote $\mathbf{x}(m(N+1)+k)$

By the definitions above, one can verify the following things for $0 \le m \le M-2,\ 0 \le k, l \le N$.

(1) $\mathbf{b}_k^T \mathbf{x}_m(k) = 0$.

(2) $\mathbf{b}_k^T \mathbf{x}_m(l) + \mathbf{b}_l^T \mathbf{x}_m(k) = 0$.

Using these results, it can be shown that

$$\begin{aligned}
[\mathbf{y}(n)]_i &= \left[\sum_{k=0}^{N} \mathbf{h}(k)\mathbf{x}(n-k)\right]_i \\
&= \sum_{k=0}^{N} \mathbf{b}_k^T \mathbf{x}(n-k) = 0.
\end{aligned}$$

Hence, the output $\mathbf{y}(n)$ is not rich. Since $\mathbf{H}(z)$ is richness preserving, $\mathbf{x}(n)$ must also be not rich. Define the $M \times M$ matrix

$$\mathbf{X}_1 = \left[\begin{array}{ccccccc} \mathbf{x}(0) & \mathbf{x}(1) & \mathbf{x}_1(0) & \mathbf{x}_2(0) & \cdots & \mathbf{x}_{M-2}(0) \end{array}\right].$$

One can verify the absolute value of the determinant of $\mathbf{X}_1$ is $|\det(\mathbf{X}_1)| = |b_{10}|^{M-2}|b_{10}b_{21} - b_{11}b_{20}|$. Since $\mathbf{x}(n)$ is not rich, $\det(\mathbf{X}_1) = 0$. Since b_{10} is nonzero, we get $b_{10}b_{21} = b_{11}b_{20}$, or $b_{21} = d_{i1}b_{20}$, where d_{i1} is chosen as b_{11}/b_{10}. Now we define another $M \times M$ matrix by replacing $\mathbf{x}(1)$ in the definition of $\mathbf{X}_1$ with another $\mathbf{x}_m(1)$, and we obtain $b_{(m+2),1} = d_{i1}b_{(m+2),0}$. These results for all m imply that $\mathbf{b}_1 = d_{i1}\mathbf{b}_0$, or $\mathbf{a}_{i1} = d_{i1}\mathbf{a}_{i0}$.

If we replace $\mathbf{x}(1)$ in the definition of $\mathbf{X}_1$ with $\mathbf{x}_m(k)$, we can show that $\exists d_{ik}$ such that $\mathbf{b}_k = d_{ik}\mathbf{b}_0$, or $\mathbf{a}_{ik} = d_{ik}\mathbf{a}_{i0}$. Finally, define $\mathbf{v}_i = \mathbf{a}_{i0}$ and $d_{i0} = 1$. Then, we have $\mathbf{a}_{ik} = d_{ik}\mathbf{v}_i$ for all i and k. The reader has to note that here we assign $\mathbf{v}_i$ as $\mathbf{a}_{i0}$ just because of the assumption that b_{10} is nonzero without loss of generality. If $b_{10} = 0$, we can find another b_{jk} that is nonzero and do similar derivation, and $\mathbf{v}_i$ here will be assigned as another $\mathbf{a}_{ik}$ rather than $\mathbf{a}_{i0}$. After all, $\exists d_{ik}, \mathbf{v}_i \neq \mathbf{0}$ such

that $\mathbf{a}_{ik} = d_{ik}\mathbf{v}_i$ is still true for all i and k. Now we simply assign

$$\mathbf{A} = \begin{bmatrix} \mathbf{v}_1 & \mathbf{v}_2 & \cdots & \mathbf{v}_M \end{bmatrix}^T$$

and

$$\mathbf{D}_k = \text{diag}\begin{bmatrix} d_{1k} & d_{2k} & \cdots & d_{Mk} \end{bmatrix}.$$

Then, the proof is complete. □

Lemma 6.6 will play an important role in the proof of necessity for both conditions (a) and (b) of Theorem 6.1. Some other useful lemmas will be presented here.

Lemma 6.7: $\mathbf{H}(z)$ is RP if and only if $\mathbf{AH}(z)$ is RP, where $\mathbf{A}$ is any nonsingular $M \times M$ matrix. □

Proof: This lemma becomes obvious when we recognize that $\mathbf{x}(n)$ is rich if and only if $\mathbf{Ax}(n)$ is rich for any nonsingular matrix $\mathbf{A}$. □

Lemma 6.8: $\mathbf{H}(z)$ is RP if and only if $z^{-k}\mathbf{H}(z)$ is RP, where k is any nonnegative integer. □

Proof: This is self-evident. □

Lemma 6.7 allows us to do invertible row operations on $\mathbf{H}(z)$ since each invertible row operation corresponds to a nonsingular matrix. Lemma 6.8 allows us to assume $\mathbf{h}(0) \neq \mathbf{0}$ for an RP matrix $\mathbf{H}(z)$.

6.6.5 Coefficient Rank of an RP System

Lemma 6.9: For an FIR system $\mathbf{H}(z) = \sum_{k=0}^{N} \mathbf{h}(k)z^{-k}$ which preserves richness, the ranks of all nonzero coefficient matrices must be the same. We call this value the *coefficient rank* of an RP system. □

Proof: Suppose $\mathbf{h}(j)$ has the smallest rank ρ among all nonzero $\mathbf{h}(k)$ ($\rho > 0$). By Lemma 7, we can do invertible row operations on $\mathbf{H}(z)$ such that $\mathbf{h}(j)$ can be expressed as

$$\mathbf{h}(j) = \begin{bmatrix} \mathbf{v}_1 & \mathbf{v}_2 & \cdots \mathbf{v}_\rho & \mathbf{v}_\rho & \cdots & \mathbf{v}_\rho \end{bmatrix}^T,$$

where $\mathbf{v}_1, ..., \mathbf{v}_\rho$ are linearly independent nonzero column vectors. By Lemma 6, there exists a constant matrix $\mathbf{A}$ and a diagonal matrix $\mathbf{D}_j$ such that $\mathbf{h}(j) = \mathbf{D}_j\mathbf{A}$. Since each row of $\mathbf{h}(j)$ is nonzero, all diagonal entries of $\mathbf{D}_j$ must be nonzero and $\mathbf{A}$ also has rank ρ.

Now for any other nonzero coefficient matrix $\mathbf{h}(k)$, there exists a diagonal matrix $\mathbf{D}_k$ such that $\mathbf{h}(k) = \mathbf{D}_k\mathbf{A}$, so rank($\mathbf{h}(k)$)$\leq$ rank($\mathbf{A}$) $= \rho$. Since $\mathbf{h}(j)$ has the smallest nonzero rank ρ, we have rank($\mathbf{h}(k)$) $= \rho$. □ In the following two lemmas, we will prove the coefficient rank of an RP system can only be unity or M.

Lemma 6.10: If an RP system with the form $\mathbf{H}(z) = \sum_{k=0}^{N} \mathbf{D}_k\mathbf{A}z^{-k}$ has coefficient rank ρ, where $\mathbf{D}_k$'s are diagonal matrices and $\mathbf{A}$ is a constant matrix, then rank($\mathbf{A}$) $= \rho$. □

Proof: If $\mathbf{H}(z)$ has only one nonzero coefficient matrix, then the statement is self-evident. Now we assume $\mathbf{H}(z)$ has at least two nonzero coefficient matrices and, without loss of generality, assume $\mathbf{h}(0)$ and $\mathbf{h}(l)$ are nonzero. Since $\mathbf{h}(0) = \mathbf{D}_0\mathbf{A}$, we have rank($\mathbf{A}$) $\geq$ rank($\mathbf{h}(0)$) $= \rho$. Suppose rank($\mathbf{A}$) $> \rho$. Then, without loss of generality we can assume the first $\rho + 1$ rows of $\mathbf{A}$, namely $\mathbf{a}_1^T, \cdots, \mathbf{a}_\rho^T, \mathbf{a}_{\rho+1}^T$, are linearly independent. Since rank($\mathbf{h}(0)$) $= \rho$, we can further assume the first row of $\mathbf{h}(0)$ is zero, while rows 2, 3, ..., $(\rho + 1)$ are nonzero. Let d_{ik} denote the ith diagonal entry of $\mathbf{D}_k$. Now we have $d_{10} = 0$ and $d_{i0} \neq 0$ for $2 \leq i \leq \rho + 1$. Since $\mathbf{H}(z)$ is RP, there exists a coefficient matrix whose first row is nonzero. Assume $\mathbf{h}(l)$ satisfies this and, thus, $d_{1l} \neq 0$. Since rank($\mathbf{h}(l)$) $= \rho$, at least one of the first $\rho + 1$ rows of $\mathbf{h}(l)$ must be zero. Assume the second row is zero, which means $d_{2l} = 0$. By Lemma 7 we can do an invertible row operation on $\mathbf{H}(z)$ by adding the second row into the first row and produce another RP system $\mathbf{H}'(z) = \sum_{k=0}^{N} \mathbf{h}'(k)z^{-k}$. Now the first rows of $\mathbf{h}'(0)$ and $\mathbf{h}'(l)$ are $d_{20}\mathbf{a}_2^T$ and $d_{1l}\mathbf{a}_1^T$, respectively. They are both nonzero and are linearly independent. This makes it impossible for $\mathbf{H}'(z)$ to be written as the form in Lemma 6 and causes a contradiction. Therefore, rank($\mathbf{A}$) $= \rho$ must be true. □

Lemma 6.11: The coefficient rank of an RP system can only be unity or M. □

Proof: Suppose there exists an RP matrix $\mathbf{H}(z)$ that has a coefficient rank ρ where $2 \leq \rho \leq M - 1$. By Lemmas 6.2 and 6.3, we can assume $\mathbf{h}(0) \neq \mathbf{0}$ and do invertible row operations on $\mathbf{H}(z)$ such that

$$\mathbf{h}(0) = \begin{bmatrix} \mathbf{a}_1 & \mathbf{a}_2 & \cdots & \mathbf{a}_\rho & \mathbf{0} & \cdots & \mathbf{0} \end{bmatrix}^T.$$

Since $\rho < M$, the last row of $\mathbf{h}(0)$ must be a zero vector. The last rows of other $\mathbf{h}(k)$, however, cannot be all zeros. By Lemma 6.6, there exist a constant matrix $\mathbf{A}$ and a diagonal matrix $\mathbf{D}_0$ such

that $\mathbf{h}(0) = \mathbf{D}_0\mathbf{A}$. By Lemma 6.10 we know rank$(\mathbf{A}) = \rho$, so the last row of $\mathbf{A}$, namely $\mathbf{v}_2^T$, must be a linear combination of $\mathbf{a}_1^T, \mathbf{a}_2^T, \cdots, \mathbf{a}_\rho^T$.

Since $\rho \geq 2$, we can find an i, $1 \leq i \leq \rho$ such that $\mathbf{a}_i$ and $\mathbf{v}_2$ are linearly independent. For convenience we define $\mathbf{v}_1 = \mathbf{a}_i$. Now we can find a set of linearly independent vectors $\mathbf{w}_1, \mathbf{w}_2, \cdots, \mathbf{w}_M$ such that $\mathbf{w}_1$ is orthogonal to $\mathbf{v}_2$, $\mathbf{w}_2$ is orthogonal to $\mathbf{v}_1$, and $\mathbf{w}_3$, $\mathbf{w}_4$, ..., $\mathbf{w}_M$ are orthogonal to both $\mathbf{v}_1$ and $\mathbf{v}_2$. (For example, we can let $\mathbf{w}_1 = \mathbf{v}_1 - \frac{\mathbf{v}_1^T\mathbf{v}_2}{||\mathbf{v}_2||^2}\mathbf{v}_2$). Furthermore, we can assume $\mathbf{v}_1^T\mathbf{w}_1 = \mathbf{v}_2^T\mathbf{w}_2 = 1$.

Now we focus on the ith and the Mth rows of $\mathbf{H}(z)$. They are $\mathbf{v}_1^T + \sum_{n=1}^N p_n\mathbf{v}_1^T z^{-n}$ and $\sum_{n=1}^N q_n\mathbf{v}_2^T z^{-n}$, respectively, where $\{q_n\}_{n=1}^N$ are not all zeros. Construct the input sequence as:

$$\begin{aligned}
\mathbf{x}(n) &= \mathbf{w}_{n+3}, 0 \leq n \leq M-3 \\
\mathbf{x}(M-2) &= \mathbf{w}_2 \\
\mathbf{x}(M-2+k) &= q_k\mathbf{w}_1 + p_k\mathbf{w}_2, 1 \leq k \leq N \\
\mathbf{x}(n) &= \mathbf{0}, \forall n \geq M+N-1.
\end{aligned}$$

Then, one can verify that $[\mathbf{y}(n)]_i = [\mathbf{y}(n)]_M$ for all n, and hence $\mathbf{y}(n)$ is not rich. But the input $\mathbf{x}(n)$ is rich. This contradicts the assumption that $\mathbf{H}(z)$ is RP, so the coefficient rank of $\mathbf{H}(z)$ can only be unity or M. □

6.6.6 Completion of Proof of Necessity for RP Systems

Now we are ready to prove conditions (a) and (b) are necessary for richness preserving property.

Proof: Let $\mathbf{H}(z)$ be RP. By Lemma 6.8 we assume $\mathbf{h}(0) \neq \mathbf{0}$. If $\mathbf{h}(0)$ is singular, the coefficient rank of $\mathbf{H}(z)$ must be unity by Lemma 6.11, so there exist a nonzero row vector $\mathbf{v}^T$ and column vectors $\mathbf{a}_0, \mathbf{a}_1, \cdots, \mathbf{a}_N$ such that $\mathbf{h}(k) = \mathbf{a}_k\mathbf{v}^T$. Now we only need to prove $[\mathbf{a}_0, \mathbf{a}_1, ..., \mathbf{a}_N]$ has full rank. If this is not true, we can find an annihilator $\mathbf{w}^T$ for all $\mathbf{a}_k$. Then, no matter what the input is, the output $\mathbf{y}(n)$ will have an annihilator $\mathbf{w}^T$, and thus $\mathbf{H}(z)$ becomes richness-destroying. So $[\mathbf{a}_0, \mathbf{a}_1, ..., \mathbf{a}_N]$ must have rank M, and thus condition (b) must be true.

If $\mathbf{h}(0)$ is nonsingular, the coefficient rank of $\mathbf{H}(z)$ must be M. By Lemma 6.7 we assume $\mathbf{h}(0) = \mathbf{I}$ without loss of generality. Using Lemma 6.6, $\mathbf{H}(z)$ must have the form

$$\mathbf{H}(z) = \mathbf{I} + \sum_{k=1}^{N} z^{-k}\text{diag}\left(\begin{bmatrix} a_{k1} & a_{k2} & \cdots & a_{kM} \end{bmatrix}\right).$$

Suppose there exist i, j, k such that $a_{ki} \neq a_{kj}$ and $i \neq j$. Let

$$\begin{aligned} \mathbf{x}(0) &= \mathbf{e}_i + \mathbf{e}_j \\ \mathbf{x}(n) &= a_{nj}\mathbf{e}_i + a_{ni}\mathbf{e}_j, 1 \leq n \leq N \\ \{\mathbf{x}(n)\}_{n=N+1}^{M+N-2} &= \{\mathbf{e}_l | 1 \leq l \leq M, l \neq i, l \neq j\} \\ \mathbf{x}(n) &= \mathbf{0}, \forall n \geq M+N-1. \end{aligned}$$

Since $a_{ki} \neq a_{kj}$, one can verify that $\mathbf{x}(n)$ is rich. It is also easy to verify the following things for $1 \leq k \leq N$:

(1) $[\mathbf{x}(0)]_i = [\mathbf{x}(0)]_j$.

(2) $a_{ki}[\mathbf{x}_k]_i = a_{kj}[\mathbf{x}(k)]_j$.

(3) $[\mathbf{x}(k)]_i + a_{ki}[\mathbf{x}(0)]_i = [\mathbf{x}(k)]_j + a_{kj}[\mathbf{x}(0)]_j$.

(4) $a_{li}[\mathbf{x}(k)]_i + a_{ki}[\mathbf{x}(l)]_i = a_{lj}[\mathbf{x}(k)]_j + a_{kj}[\mathbf{x}(l)]_j$,
$1 \leq l \leq N$.

(5) $a_{ki}[\mathbf{x}(l)]_i = a_{kj}[\mathbf{x}(l)]_j, N+1 \leq l \leq M+N-2$.

Using these facts, we can show $[\mathbf{y}(n)]_i = [\mathbf{y}(n)]_j, n \geq 0$, and hence $\mathbf{y}(n)$ is not rich. Therefore, in order to let $\mathbf{H}(z)$ preserve richness, $a_{ki} = a_{kj}$ must be true for any $i \neq j$ and any k. This means each coefficient matrix of $\mathbf{H}(z)$ is proportional to identity matrix and hence condition (a) must be true. □

The proof of Theorem 6.1 is now complete. In addition, by Lemma 6.5, we know the necessary conditions in Theorem 6.1 are also necessary for SRP systems. In the next subsection, we will show that SRP systems require even stronger necessary conditions and complete the proof of Theorem 6.5.

6.6.7 Necessary Conditions for Preserving Strict Richness

Lemma 6.12: If a Type A RP matrix $\mathbf{A}(z)$ preserves strict richness, then it must be a constant invertible matrix with a possible delay. □

Proof: Assume $\mathbf{A}(z) = g(z)\mathbf{A}$, where $\mathbf{A}$ is an invertible constant matrix and $g(z)$ is a nonzero polynomial of z^{-1}. Suppose the contrary, then the polynomial $g(z)$ must have at least two terms

and hence have at least one zero other than infinity. Suppose $g(\alpha) = 0$. Let the input $\mathbf{x}(n) = \alpha^n \mathbf{A}^{-1}\mathbf{e}_{(n \bmod M)+1}$. Then, for all $n \geq N$, we have

$$\begin{aligned}\sum_{i=1}^{M} [\mathbf{y}(n)]_i &= \sum_{i=1}^{M} \mathbf{e}_i^T \left[\sum_{k=0}^{N} g_k \mathbf{A}\mathbf{x}(n-k)\right] \\ &= \sum_{k=0}^{N} g_k \alpha^{n-k} \left[\sum_{i=1}^{M} \mathbf{e}_i^T \mathbf{e}_{((n-k) \bmod M)+1}\right] \\ &= \alpha^n g(\alpha) = 0.\end{aligned}$$

This means row vector $\begin{bmatrix} 1 & 1 & \cdots & 1 \end{bmatrix}$ is an annihilator of $\mathbf{y}(n)$ for all $n \geq N$. Therefore, $\mathbf{y}(n)$ is not strictly rich, and the proof is complete. □

Lemma 6.13: Type-B RP matrices $\mathbf{B}(z)$ do not preserve strict richness. □

Proof: Suppose $\mathbf{B}(z) = \left(\sum_{k=0}^{N} \mathbf{a}_k z^{-k}\right) \mathbf{v}_1^T$ and assume $||\mathbf{v}_1|| = 1$. We can find $\mathbf{v}_2, \mathbf{v}_3, \cdots \mathbf{v}_M$ such that $||\mathbf{v}_k|| = 1$ and $\mathbf{v}_i^T \mathbf{v}_j = 0, \forall i \neq j$. Let $\mathbf{w}_1 = \mathbf{v}_1$ and $\mathbf{w}_k = \mathbf{v}_1 + \mathbf{v}_k$ for $k \geq 2$. Then, we have $\mathbf{v}_1^T \mathbf{w}_k = 1, \forall k$. Let the input $\mathbf{x}(n) = \mathbf{w}_{(n \bmod M)+1}$, and clearly it is strictly rich. However, for all $n \geq N$, we have $\mathbf{y}(n) = \sum_{k=0}^{N} \mathbf{a}_k \mathbf{v}_1^T \mathbf{x}(n-k) = \sum_{k=0}^{N} \mathbf{a}_k$, independent from n. This implies $\mathbf{y}(n)$ is not strictly rich, so Type B RP matrices cannot preserve strict richness. □

Using Lemmas 6.5, 6.12, and 6.13, the proof of Theorem 6.5 is now complete.

6.7 Relationship with Persistent Excitation

The definition of strict richness given in Section 6.5 happens to be related to the concept of "persistent excitation" in the literature on control theory. The property of persistent excitation is relevant to the stability and convergence of adaptive systems [43],[4]. The exact definition of persistent excitation can vary with respect to different applications. In [41] (page 1060), a sequence of $M \times 1$ vectors $\mathbf{x}(n)$ is called *persistently exciting* (PE) if there exists a finite integer K such that the matrix

$$\begin{bmatrix} \mathbf{x}(n) & \mathbf{x}(n+1) & \cdots & \mathbf{x}(n+K) \end{bmatrix}$$

has rank M for sufficiently large n. It is clear from the definition that PE implies SR, but the converse is not true. This can be seen by constructing a sequence of 2×1 vectors $\mathbf{x}(n)$ as:

$$\mathbf{x}(n) = \begin{cases} \begin{bmatrix} 1 \\ 0 \end{bmatrix}, & \text{if } n = 2^{2k} \quad \forall k \in \mathbb{N} \\ \begin{bmatrix} 0 \\ 1 \end{bmatrix}, & \text{if } n = 2^{2k+1} \quad \forall k \in \mathbb{N} \\ \begin{bmatrix} 0 \\ 0 \end{bmatrix}, & \text{otherwise.} \end{cases}$$

It is readily verified that $\mathbf{x}(n)$ is SR but not PE. Although the definitions of SR and PE are not exactly equivalent, it can still be shown that for an LTI $M \times M$ system to preserve the property of PE is the same as to preserve SR, as stated in Theorem 6.5. The proof of this is rather involved and will be presented elsewhere.

An even stronger definition of PE can be found in [14] and [43]. Therein, the sequence $\mathbf{x}(n)$ is called persistently exciting if there exist positive integers L, n_0, and $\alpha > 0$ such that for any vector $\mathbf{v} \in \mathbb{C}^M$ and any integer $n \geq n_0$, $|\mathbf{v}^\dagger \mathbf{x}(k)| > \alpha$ for some k satisfying $n \leq k \leq n + L$.

However, in many applications of control theory, the property of PE is applied to signals which are often called "regressors," [14] that is, the sequence of $M \times 1$ vectors $\mathbf{x}(n)$ comes from a sequence of scalars $x_n, n \geq 0$ and can be written as

$$\mathbf{x}(n) = \begin{bmatrix} x_n & x_{n-1} & \cdots & x_{n-M+1} \end{bmatrix}^T.$$

This constraint limits the degrees of freedom of choices of sequence $\mathbf{x}(n)$. If we take into account this constraint when studying PE signals, the problem of preserving PE becomes a totally different problem. The similarity between the definitions of SR and PE, nevertheless, suggests that there might exist some application in control or adaptive filtering to which the theory of richness preservation can be applied.

6.8 Concluding Remarks and Open Issues

Necessary and sufficient conditions have been found for multiple-input-multiple-output (MIMO) LTI FIR systems that are richness preserving (RP) and strict-richness preserving (SRP). The results

show that most standard systems with memory do not generally preserve richness, including paraunitary and unimodular matrices. The similarity of, and relationship between, signal richness and persistent excitation have also been described and discussed. This relation suggests that there might be some applications of the results of this chapter in the control theory literature.

Under the definitions of richness considered in this chapter, it remains to investigate conditions on infinite impulse response (IIR) systems that preserve richness. It is also interesting to consider the case where the input and the output of the LTI system have different sizes.

Another issue of interest is the evaluation of the probability for an LTI system to preserve richness. For an LTI system that does not satisfy necessary conditions in Theorem 6.1, we can manage to find a rich input sequence such that the output of the system is not rich. In practical applications, however, the probability of appearance of such input could almost be zero! This suggests there may exist some LTI systems that, although not satisfying necessary conditions of Theorems 6.1 and 6.5, still preserve richness with probability one. These systems would still be very useful in practical applications. The RP conditions for such systems are characterized probabilistically and furthermore depend on the statistics of the class of allowed inputs. A study of such systems could be challenging and important.

It would also be of interest to study the case of wide sense stationary (WSS) signals. In this case, richness can be defined with respect to the autocorrelation matrices (e.g. nonsingularity) of the signal. Development of RP conditions is equivalent to finding the conditions under which an LTI system preserves such nonsingular property.

Chapter 7

Generalized Signal Richness Preservation Problem and Vandermonde-Form Preserving Matrices

In the previous chapter, we studied the signal richness preservation problem. In this chapter, we will extend the study for a more generalized definition of signal richness. As we have seen in Chapter 2, using a generalized blind channel estimation algorithm in zero-padding (ZP) systems with a repetition index larger than unity, the signal richness property required for the input sequence is relaxed. The generalized signal richness has been defined in Section 2.5, with the repetition index Q as its parameter. An $M \times 1$ sequence $\mathbf{x}(n), n \geq 0$ is said to be $(1/Q)$-rich if there exists a finite integer J such that the $(M+Q-1) \times JQ$ matrix

$$\mathbf{U}_Q^{(J)} = \left[\begin{array}{cccc} \mathcal{T}_Q\left(\mathbf{s}(0)\right) & \mathcal{T}_Q\left(\mathbf{s}(1)\right) & \cdots & \mathcal{T}_Q\left(\mathbf{s}(J-1)\right) \end{array} \right]$$

has full row rank $M+Q-1$. Notice that when $Q=1$, the generalized definition of signal richness reduces to traditional signal richness, as discussed in the previous chapter. When $Q = M-1$, it becomes equivalent to the coprimality property stated in [36]. We will elaborate the generalized definition and study many properties thereof. Under this new definition of signal richness, the richness-preserving conditions on the linear precoders become a different problem. Finding out these conditions will be helpful as a guideline to choose the ZP precoders when a generalized blind algorithm proposed in Chapter 2 is used.

In this chapter, we will focus on the theoretical issues of the generalized signal richness preser-

vation problem and find out the necessary and sufficient conditions for linear precoders to preserve generalized signal richness. In order to solve the problem, a special class of square matrices, namely the "Vandermonde-form preserving" (VFP) matrices, is introduced and found to be highly relevant to the problem. Several properties of VFP matrices are studied in detail. The necessary and sufficient conditions of the problem have been found, and a systematic proof is also presented. The material of this chapter is mainly drawn from [56], and portions of it have been presented in [54].

7.1 Outline

The rest of the chapter is organized as follows. In Section 7.2, we give a definition of generalized signal richness and briefly describe several important properties thereof. Some examples will be given to clarify these properties. In Section 7.3, we will address the problem of preserving generalized signal richness. In Section 7.4, the class of Vandermonde-form preserving (VFP) matrices will be introduced and several properties of VFP matrices will be studied in detail. In Section 7.5, the necessary and sufficient conditions for linear precoders to preserve generalized richness will be presented. In Section 7.6, some deeper issues on $(1/Q)$-richness will be studied. For example, the relation between such richness and the "rank" of a signal is studied. Finally, Section 7.7 gives the conclusion and possible future directions.

7.1.1 Notations

Besides notations defined in Section 1.4, some more notations specifically used in this chapter is defined as follows. If $\mathcal{A}$ and $\mathcal{B}$ are multisets (a multiset is like a set, but it may contain identical elements repeated a finite number of times[19]), $\mathcal{A} \biguplus \mathcal{B}$, $\mathcal{A} \bigcap \mathcal{B}$, and $\mathcal{A} \bigcup \mathcal{B}$ denote the multisets defined as follows: if an element occurring exactly a times in $\mathcal{A}$ and b times in $\mathcal{B}$, it occurs exactly $a + b$ times in $\mathcal{A} \biguplus \mathcal{B}$, exactly $\min(a, b)$ times in $\mathcal{A} \bigcap \mathcal{B}$, and exactly $\max(a, b)$ times in $\mathcal{A} \bigcup \mathcal{B}$.

7.2 Generalized Signal Richness

7.2.1 Definition of Generalized Signal Richness

Definition 7.1: A sequence of $M \times 1$ vectors $\mathbf{s}(n), n \geq 0$, over the field $\mathbb{C}$ is said to be *rich* if there exists a finite integer J such that the $M \times J$ matrix

$$\left[\begin{array}{cccc} \mathbf{s}(0) & \mathbf{s}(1) & \cdots & \mathbf{s}(J-1) \end{array} \right]$$

has full row rank M. □

□

The definition of the *generalized signal richness* for an $M \times 1$ signal will be given in Definitions 2 and 3 as follows. We first build up the definition of a notation $\mathbf{s}_Q(n)$, representing a *shifted and repeated* version of $\mathbf{s}(n)$, using the following examples.

Example 7.1: $\mathbf{s}_1(n)$ is $\mathbf{s}(n)$ itself. □ □

Example 7.2: Consider a sequence of 3×1 vectors $\mathbf{s}(n)$ defined as

$$\left[\begin{array}{ccc} \mathbf{s}(0) & \mathbf{s}(1) & \mathbf{s}(2) \end{array} \right] = \left[\begin{array}{ccc} 1 & 4 & 7 \\ 2 & 5 & 8 \\ 3 & 6 & 9 \end{array} \right],$$

and $\mathbf{s}(n) = 0$ for $n \geq 3$. Then, $\mathbf{s}_2(n)$ can be expressed as

$$\left[\begin{array}{cccccc} \mathbf{s}_2(0) & \mathbf{s}_2(1) & \mathbf{s}_2(2) & \mathbf{s}_2(3) & \mathbf{s}_2(4) & \mathbf{s}_2(5) \end{array} \right] \tag{7.1}$$

$$= \left[\begin{array}{cccccc} 1 & 0 & 4 & 0 & 7 & 0 \\ 2 & 1 & 5 & 4 & 8 & 7 \\ 3 & 2 & 6 & 5 & 9 & 8 \\ 0 & 3 & 0 & 6 & 0 & 9 \end{array} \right], \tag{7.2}$$

and $\mathbf{s}_2(n) = 0$ for $n \geq 6$. And $\mathbf{s}_3(n)$ can be expressed as

$$[\mathbf{s}_3(0), \mathbf{s}_3(1), \mathbf{s}_3(2), \mathbf{s}_3(3), \mathbf{s}_3(4), \mathbf{s}_3(5), \mathbf{s}_3(6), \mathbf{s}_3(7), \mathbf{s}_3(8)] \tag{7.3}$$

$$= \begin{bmatrix} 1 & 0 & 0 & 4 & 0 & 0 & 7 & 0 & 0 \\ 2 & 1 & 0 & 5 & 4 & 0 & 8 & 7 & 0 \\ 3 & 2 & 1 & 6 & 5 & 4 & 9 & 8 & 7 \\ 0 & 3 & 2 & 0 & 6 & 5 & 0 & 9 & 8 \\ 0 & 0 & 3 & 0 & 0 & 6 & 0 & 0 & 9 \end{bmatrix}, \tag{7.4}$$

and $\mathbf{s}_3(n) = 0$ for $n \geq 9$. □ □

The formal definition of $\mathbf{s}_Q(n)$ is given as follows.

Definition 7.2: Given a positive integer Q and a sequence of $M \times 1$ vectors $\mathbf{s}(n)$ over the field $\mathbb{C}$, $\mathbf{s}_Q(n)$ is a sequence of $(M + Q - 1) \times 1$ vectors defined as

$$\mathbf{s}_Q(nQ + k) = \begin{bmatrix} \mathbf{0}_{k \times 1} \\ \mathbf{s}(n) \\ \mathbf{0}_{(Q-k-1) \times 1} \end{bmatrix}$$

for $n \geq 0, k = 0, 1, ..., Q - 1$. □ □

Note that the matrices shown in Eqs. (7.2) and (7.4) are similar to Sylvester's resultant matrices [19] in the manner of Toeplitz-like structures. The definition of generalized signal richness is given as follows.

Definition 7.3: An $M \times 1$ sequence $\mathbf{s}(n), n \geq 0$ is said to be $(1/Q)$-*rich* if $\mathbf{s}_Q(n)$ is rich. □

□

Note that when $Q = 1$, Definition 3 reduces to the conventional signal richness given in Definition 1. For the example given in Example 2, we can verify that $\mathbf{s}(n)$ is $(1/2)$-rich and $(1/3)$-rich, but not 1-rich.

An alternative definition of $(1/Q)$-richness can be given immediately by using the following theorem.

Theorem 7.1 ($(1/Q)$-richness): Given an $M \times 1$ vector sequence $\mathbf{s}(n), n \geq 0$, $\mathbf{s}(n)$ is $(1/Q)$-rich if and only if there does not exist a nonzero $Q \times M$ Hankel matrix $\mathbf{H}$ such that $\mathbf{H}\mathbf{s}(n) = \mathbf{0}, \forall n \geq 0$. □

Proof: See Appendix. □

7.2.2 Properties of $(1/Q)$-richness

It can be shown that the condition of $(1/Q)$-richness is stronger when the integer Q is smaller, as shown in the following lemma.

Lemma 7.1: If a sequence of $M \times 1$ vectors $\mathbf{s}(n), n \geq 0$ is $(1/Q)$-rich, then $\mathbf{s}(n)$ is $(1/(Q+1))$-rich. □

Proof: The proof of this lemma becomes straightforward when we use the result of Theorem 1. Suppose $\mathbf{s}(n)$ is $(1/Q)$-rich, but not $(1/(Q+1))$-rich. Then there exists a nonzero $(Q+1) \times M$ Hankel matrix $\mathbf{V}$ such that $\mathbf{V}\mathbf{s}(n) = \mathbf{0}$ for all n. Let $\mathbf{V}_1$ and $\mathbf{V}_2$ be $Q \times M$ Hankel matrices whose rows are composed of the first Q rows of $\mathbf{V}$ and the last Q rows of $\mathbf{V}$, respectively. Note that at least one of $\mathbf{V}_1$ and $\mathbf{V}_2$ is nonzero, and $\mathbf{V}\mathbf{s}(n) = \mathbf{0}$ implies $\mathbf{V}_k\mathbf{s}(n) = \mathbf{0}$ for $k = 1, 2$. This violates the assumption that $\mathbf{s}(n)$ is $(1/Q)$-rich. □

Lemma 7.1 states a basic property of generalized signal richness: the smaller the value of Q is, the "stronger" the condition of $(1/Q)$-richness is. For example, if an $M \times 1$ sequence $\mathbf{s}(n)$ is 1-rich, or simply *rich*, then it is $(1/2)$-rich, $(1/3)$-rich, and $(1/Q)$-rich for any positive integer Q. This is why we use the notation of $(1/Q)$-richness. On the contrary, a $(1/2)$-rich signal $\mathbf{s}(n)$ is not necessarily 1-rich. We can thus define a *measure* of generalized signal richness, namely the *degree of non-richness* for a given $M \times 1$ sequence $\mathbf{s}(n)$, as follows.

Definition 7.4: Given an $M \times 1$ sequence $\mathbf{s}(n), n \geq 0$, the *degree of non-richness* of $\mathbf{s}(n)$ is defined as:

$$Q_{min} \triangleq \min_{Q} \left(\mathbf{s}(n) \text{ is } \frac{1}{Q}\text{-rich} \right). \tag{7.5}$$

□

If $\mathbf{s}(n)$ is not $(1/Q)$-rich for any Q, then $Q_{min} = \infty$. The property of an infinite degree of non-richness can be described in the following lemma, in which we use the notation of $\mathbf{p}_M(x)$ to denote

the column vector:

$$\mathbf{p}_M(x) = \begin{bmatrix} 1 & x & x^2 & \cdots & x^{M-1} \end{bmatrix}^T.$$

Lemma 7.2: Consider a sequence of $M \times 1$ vectors $\mathbf{s}(n), n \geq 0$. The following statements are equivalent.

1. $\mathbf{s}(n)$ is not $(1/Q)$-rich for any Q.
2. The degree of non-richness of $\mathbf{s}(n)$ is infinity.
3. Either $\mathbf{p}_M^T(\alpha)\mathbf{s}(n) = 0, \forall n$ for some $\alpha \in \mathbb{C}$ or $\begin{bmatrix} 0 & 0 & \cdots & 1 \end{bmatrix} \mathbf{s}(n) = 0, \forall n$.
4. Polynomials $p_n(x) = \mathbf{p}_M^T(x)\mathbf{s}(n), n \geq 0$ either share a common zero $\alpha \in \mathbb{C}$ or all have orders less than $M - 1$.

□

Proof: See Chapter 2.

□

Lemma 7.1 suggests that if the value of Q is larger, the less "rich" is the signal $\mathbf{s}(n)$. By definition, a 1-rich signal has "full rank". If $\mathbf{s}(n)$ is not 1-rich but has only one annihilator $\mathbf{v}^T$ (i.e., $\mathbf{v}^T\mathbf{s}(n) = 0$), intuitively it is still likely to be $(1/2)$-rich, or $(1/Q)$-rich for other larger Q. Lemma 7.2 suggests, however, this is not the case if the annihilator happens to be in the form defined in condition 3) of Lemma 7.2. If an $M \times 1$ sequence $\mathbf{s}(n)$ has a finite degree of non-richness, or $\mathbf{s}(n)$ is $(1/Q)$-rich for some integer Q, then it can be shown that the maximum possible value of Q_{min} is $M - 1$, as described in the following lemma.

Lemma 7.3: If $M > 1$ and an $M \times 1$ sequence $\mathbf{s}(n)$ is not $(1/(M-1))$-rich, then it is not $(1/Q)$-rich for any Q. □

Proof: See Chapter 2. □

With Lemma 7.3, we can see that for an $M \times 1$ sequence $\mathbf{s}(n)$, $(1/(M-1))$-richness is the weakest form of generalized richness. Given a $M \times 1$ vector sequence $\mathbf{s}(n)$, the degree of non-richness can only be one of values $1, 2, ..., M - 1$, or ∞.

7.2.3 Vandermonde Form Vectors and Generalized Zero Location

Consider a $1 \times M$ complex-valued row vector $\mathbf{v}^T = \begin{bmatrix} v_1 & v_2 & \cdots & v_M \end{bmatrix}$ which has the form

$$\mathbf{v}^T = c \begin{bmatrix} 1 & \alpha & \alpha^2 & \cdots & \alpha^{M-1} \end{bmatrix} \tag{7.6}$$

for some $c, \alpha \in \mathbb{C}, c \neq 0$. We call a vector in the form of Eq. (7.6) a *Vandermonde form vector* since it can be a row of a Vandermonde matrix. Now, consider the vector

$$\mathbf{v}^T = \begin{bmatrix} 0 & 0 & \cdots & 0 & c \end{bmatrix} \tag{7.7}$$

for some $c \in \mathbb{C}, c \neq 0$. In view of condition 3) of Lemma 7.2, for generality we want to include vectors as in Eq.(7.7) into the definition of Vandermonde form vectors. A formal definition of Vandermonde form vectors is given as follows.

Definition 7.5: [Vandermonde Form Vectors] A row vector $\mathbf{v}^T = \begin{bmatrix} v_1 & v_2 & \cdots & v_M \end{bmatrix}$ is said to be in the "*Vandermonde form*" if there exist $\alpha, \beta \in \mathbb{C}$, $|\alpha|^2 + |\beta|^2 > 0$, such that

$$\mathbf{v}^T = \begin{bmatrix} \beta^{M-1} & \alpha\beta^{M-2} & \cdots & \alpha^{M-2}\beta & \alpha^{M-1} \end{bmatrix}.$$

The set of M-vectors in Vandermonde form, denoted as $\mathcal{V}_M$, is defined as

$$\mathcal{V}_M^T = \left\{ \mathbf{v}^T | \mathbf{v} \in \mathbb{C}^M \text{ and } \mathbf{v}^T \text{ is in the Vandermonde form} \right\}. \square$$

$\square$

By the definition above, we have

$$\begin{aligned} \mathbf{v}^T &= \begin{bmatrix} \beta^{M-1} & \alpha\beta^{M-2} & \cdots & \alpha^{M-2}\beta & \alpha^{M-1} \end{bmatrix} \\ &= \begin{cases} \beta^{M-1} \cdot \mathbf{p}_M^T\left(\frac{\alpha}{\beta}\right) & \text{if } \beta \neq 0 \\ \begin{bmatrix} 0 & 0 & \cdots & \alpha^{M-1} \end{bmatrix} & \text{if } \beta = 0 \end{cases}. \end{aligned}$$

An straightforward observation on Definition 7.5 is described below.

Property 7.1: If $M \leq 2$, a nonzero $M \times 1$ row vector $\mathbf{v}^T$ is always a Vandermonde form vector. $\square$

Proof: Self-evident. □

In view of Definition 7.5, it would be useful if we define a *Vandermonde ratio* for each M-row vector in Vandermonde form.

Definition 7.6 (Vandermonde ratio): For a row vector $\mathbf{v}^T \in \mathcal{V}_M$,

$$\mathbf{v}^T = \left[\begin{array}{ccccc} \beta^{M-1} & \alpha\beta^{M-2} & \cdots & \alpha^{M-2}\beta & \alpha^{M-1} \end{array} \right],$$

where $\alpha, \beta \in \mathbb{C}$, the "*Vandermonde ratio*" $\gamma \in \mathbb{C} \bigcup \{\infty\}$ is defined as

$$\gamma = \left\{ \begin{array}{ll} \frac{\alpha}{\beta} & \text{if } \beta \neq 0 \\ \infty & \text{if } \beta = 0 \end{array} \right. .$$

□ □

Lemma 7.4: Let $\mathbf{v}^T$ be a $1 \times M$ Vandermonde vector with Vandermonde ratio $\gamma \in \mathbb{C} \bigcup \{\infty\}$. Let $\mathbf{y}$ be an $M \times 1$ nonzero vector. Then, $\mathbf{v}^T\mathbf{y} = 0$ if and only if

1. Polynomial $\mathbf{p}_M^T(x)\mathbf{y}$ has a zero at γ if $\gamma \in \mathbb{C}$.
2. Polynomial $\mathbf{p}_M^T(x)\mathbf{y}$ has a degree less than $M-1$ if $\gamma = \infty$.

□

Proof: See Appendix. □

Now, let us turn our attention to the sequence of polynomials $p_n(x) = \mathbf{p}_M^T(x)\mathbf{s}(n), n = 0, 1, 2, \cdots$. Lemma 7.2 states that $\mathbf{s}(n)$ has an infinite degree of non-richness if and only if the polynomials $p_n(x)$ either a) have a common factor or b) all have an order less than $M-1$. Conditions a) and b), although seemingly unrelated to each other, can be unified in one statement using the following definition.

Definition 7.7: Given an $M \times 1$ nonzero column vector $\mathbf{u}$, suppose $u(x) = \mathbf{p}_M^T(x)\mathbf{u}$ is an mth order polynomial, where $m+1 \leq M$, (i.e., $[\mathbf{u}]_l = 0, \forall l \in \{m+2, m+3, ..., M\}$). The "*zero locations*" of $\mathbf{u}$ are defined as a multiset $\mathcal{Z}_\mathbf{u}$ of $M-1$ elements from $\mathbb{C} \bigcup \{\infty\}$ (possibly with multiplicity), as follows:

$$\mathcal{Z}_\mathbf{u} = \{\alpha_1, \alpha_2, ..., \alpha_m, \infty, \cdots, \infty\},$$

where $\alpha_1, ..., \alpha_m$ are the zeros of the polynomial $\mathbf{p}_M^T(x)\mathbf{u}$ whose degree is m. The number of occurrences of ∞ is $M - m - 1$. □ □

Example 7.3: For examples, if $\mathbf{y} = \begin{bmatrix} 1 & -2 & 1 \end{bmatrix}^T$, then $\mathcal{Z}_{\mathbf{y}} = \{1, 1\}$.
If $\mathbf{y} = \begin{bmatrix} 1 & -2 & 1 & 0 \end{bmatrix}^T$, then $\mathcal{Z}_{\mathbf{y}} = \{1, 1, \infty\}$.
If $\mathbf{y} = \begin{bmatrix} 1 & -3 & 2 \end{bmatrix}^T$, then $\mathcal{Z}_{\mathbf{y}} = \{1, 1/2\}$.
If $\mathbf{y} = \begin{bmatrix} 1 & -3 & 2 & 0 & 0 \end{bmatrix}^T$, then $\mathcal{Z}_{\mathbf{y}} = \{1, 1/2, \infty, \infty\}$.
As an extreme case, if $\mathbf{y} = \begin{bmatrix} 1 & 0 & 0 & 0 \end{bmatrix}$, then $\mathcal{Z}_{\mathbf{y}} = \{\infty, \infty, \infty\}$. □ □

This definition may seem unusual at the first sight since infinity can never be a zero of a polynomial. Nevertheless, we gave this definition *on a vector* for convenience in our context and will find it useful in later discussions. So far, we have not given a formal definition of set of zero locations on a zero vector $\mathbf{0}$. However, there is no loss of generality in the following discussions to assume that

$$\mathcal{Z}_{\mathbf{0}} = \biguplus_{m=1}^{M-1} \left(\mathbb{C} \bigcup \{\infty\} \right),$$

which means any number in the complex plane is a zero location of the vector $\mathbf{0}$ with a multiplicity $M - 1$.

With the new definitions addressed above, we can rewrite Lemma 7.2 in a clearer manner.

Lemma 7.5 (Lemma 2 rewritten): Consider a sequence of $M \times 1$ vector $\mathbf{s}(n), n \geq 0$. The following statements are equivalent:

1. $\mathbf{s}(n)$ is not $(1/Q)$-rich for any Q.
2. The degree of non-richness of $\mathbf{s}(n)$ is infinity.
3. There exists a Vandermonde form vector $\mathbf{v}^T \in \mathcal{V}_M$ (with a Vandermonde ratio $\gamma \in \mathbb{C} \bigcup \{\infty\}$) such that $\mathbf{v}^T \mathbf{s}(n) = 0, \forall n \geq 0$.
4. $\exists \gamma \in \mathbb{C} \bigcup \{\infty\}$ such that $\gamma \in \bigcap_{n=0}^{\infty} \mathcal{Z}_{\mathbf{s}(n)}$ (i.e., vectors $\mathbf{s}(n), n \geq 0$ share a common zero $\gamma \in \mathbb{C} \bigcup \{\infty\}$.)

□ □

Using Lemmas 7.2 and 7.3, we readily obtain the following useful lemma.

Lemma 7.6: Column vectors $\mathbf{s}(n), n \geq 0$ have no common zeros if and only if $\mathbf{s}(n)$ is $(1/(M-1))$-rich. □

7.3 Preserving Generalized Signal Richness

7.3.1 Problem Statement

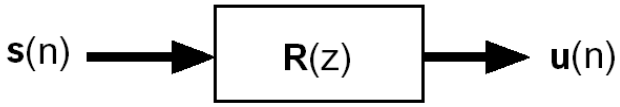

Figure 7.1: A multi-input multi-output LTI system.

In this section, we will describe the main problem addressed in this chapter. Consider an Nth order, M-input-M-output LTI causal system, depicted in Figure 7.1, with a transfer function $\mathbf{R}(z) = \sum_{k=0}^{N} \mathbf{R}_k z^{-k}$.

Definition 7.8: An $M \times M$ system $\mathbf{R}(z) = \sum_{k=0}^{N} \mathbf{R}_k z^{-k}$ is said to be $(1/Q)$-*richness preserving* if and only if for any $(1/Q)$-rich signal $\mathbf{s}(n)$, the output $\mathbf{u}(n) = \sum_{k=0}^{N} \mathbf{R}_k \mathbf{s}(n-k)$ is also a $(1/Q)$-rich signal. □ □

We want to find out the necessary and sufficient conditions for the LTI systems $\mathbf{R}(z)$ to be $(1/Q)$-richness preserving. The special case of this problem when $Q = 1$ was solved in Chapter 6 (also in [48]). In particular, for memoryless systems, an $M \times M$ constant matrix $\mathbf{R}$ preserves 1-richness if and only if $\mathbf{R}$ is nonsingular. However, in the case when $Q > 1$, a nonsingular memoryless system $\mathbf{R}$ does not necessarily preserve $(1/Q)$-richness. This can be seen in the following simple example.

Example 7.4: Let $\mathbf{s}(0) = \begin{bmatrix} 1 & -1 & 0 \end{bmatrix}^T$, $\mathbf{s}(1) = \begin{bmatrix} 1 & 1 & 2 \end{bmatrix}^T$, and $\mathbf{s}(n) = \mathbf{0}$ for $n > 1$. By

observing that

$$\mathbf{A} = \begin{bmatrix} 1 & 0 & 1 & 0 \\ -1 & 1 & 1 & 1 \\ 0 & -1 & 2 & 1 \\ 0 & 0 & 0 & 2 \end{bmatrix}$$

has full rank 4, we know that $\mathbf{s}(n)$ is (1/2)-rich. Now let

$$\mathbf{R} = \begin{bmatrix} 1 & 0 & 0 \\ 0 & 0 & 1 \\ 0 & 1 & 0 \end{bmatrix},$$

which is an invertible permutation matrix. Then we can obtain the output $\mathbf{u}(n) = \mathbf{R}\mathbf{s}(n)$ as $\mathbf{u}(0) = \begin{bmatrix} 1 & 0 & -1 \end{bmatrix}^T$ and $\mathbf{u}(1) = \begin{bmatrix} 1 & 2 & 1 \end{bmatrix}^T$. Note that if $\mathbf{v}^T = \mathbf{p}_3^T(-1) = \begin{bmatrix} 1 & -1 & 1 \end{bmatrix}$, then $\mathbf{v}^T\mathbf{u}(n) = 0$ for all n, so $\mathbf{u}(n)$ is not $(1/Q)$-rich for any Q. This suggests that an invertible constant precoder, although preserving the "rank" of a signal does not preserve $(1/Q)$-richness in general! □ □

In this chapter we will limit our focus of the problem on memoryless systems, as described below.

Main Problem: Given integers M, Q, where $M > 1$ and $1 \leq Q \leq M-1$, what are the necessary and sufficient conditions for an $M \times M$ matrix $\mathbf{R}$ to be $(1/Q)$-richness preserving?

7.3.2 The Special Case When $Q = M - 1$

From Lemmas 7.2, 7.3, and 7.6, we know that $\mathbf{s}(n)$ is $(1/(M-1))$-rich if and only if there is no row vector $\mathbf{v}^T \in \mathcal{V}_M$ such that $\mathbf{v}^T\mathbf{s}(n) = 0, \forall n \geq 0$. This suggests that a $(1/(M-1))$-richness preserving matrix $\mathbf{R}$ may have something to do with Vandermonde form vectors.

Theorem 7.2: An $M \times M$ matrix $\mathbf{R}$ preserves $1/(M-1)$-richness if and only if $\mathbf{v}^T\mathbf{R} \in \mathcal{V}_M$ for all $\mathbf{v}^T \in \mathcal{V}_M$. An $M \times M$ constant matrix $\mathbf{R}$ satisfying this condition is said to be a "*Vandermonde-form preserving*" (VFP) matrix. □

Proof: See Appendix. □

While a rigorous proof of Theorem 7.2 can be found in the Appendix, here we seek to present an intuitive understanding of it. Recall that signal $\mathbf{s}(n)$ being $1/(M-1)$-rich means that vectors

$\mathbf{s}(n), n \geq 0$ do not share a common zero $\gamma \in \mathbb{C} \bigcup \{\infty\}$ (see Definition 7.7). Denote the set of zeros of the vector $\mathbf{s}(n)$ as $\mathcal{Z}_{\mathbf{s}(n)}$. Then we have

$$\bigcap_{n=0}^{+\infty} \mathcal{Z}_{\mathbf{s}(n)} = \phi.$$

If the matrix $\mathbf{R}$ is chosen arbitrarily, the zeros of the vector $\mathbf{R}\mathbf{s}(n)$ for a given n, $\mathcal{Z}_{\mathbf{R}\mathbf{s}(n)}$, compared to $\mathcal{Z}_{\mathbf{s}(n)}$, are likely to "reshuffle randomly." This is mainly because the zero locations of a vector are a nonlinear function of the vector contents, so it is usually hard to decide $\mathcal{Z}_{\mathbf{R}\mathbf{s}(n)}$ simply by inspecting $\mathcal{Z}_{\mathbf{s}(n)}$. Hence, one usually can manage to find a sequence of vectors $\mathbf{s}(n)$ which do not share common zeros but vectors $\mathbf{R}\mathbf{s}(n)$ do share a common zero. On the other hand, if we choose $\mathbf{R}$ as a VFP matrix defined above, each zero of $\mathbf{R}\mathbf{s}(n)$ can be uniquely "predicted," given the zeros of $\mathbf{s}(n)$: suppose $\alpha \in \mathbb{C} \bigcup \{\infty\}$ is a zero of $\mathbf{s}(n)$, that is, there exists $\mathbf{v}^T \in \mathcal{V}_M$ with Vandermonde ratio α such that $\mathbf{v}^T\mathbf{s}(n) = 0$. Then, the Vandermonde ratio of $\mathbf{w}^T = \mathbf{v}^T\mathbf{R}$, say γ, must be a zero location of the vector $\mathbf{R}\mathbf{s}(n)$. As we will show in the Section 7.4.2, the transformation of zero locations, due to the VFP matrix, is a one-to-one mapping. Thus, if the vectors $\mathbf{s}(n)$ do not share a common zero, then vectors $\mathbf{R}\mathbf{s}(n)$ also will not have a common zero.

7.4 Vandermonde-form preserving Matrices

Given the knowledge that Vandermonde-form preserving (VFP) matrices preserves $(1/(M-1))$-richness, we will consider in this section the representation of general $M \times M$ Vandermonde-form preserving (VFP) matrices. We will also present several properties of VFP matrices which help to answer the problem addressed in the previous section.

7.4.1 Representation of Vandermonde-form preserving Matrices

We start from focusing on what VFP matrices look like. Obviously, the identity matrix $\mathbf{I}_M$ and any nonzero multiple of it are VFP matrices. A permutation matrix, however, is in general not a VFP matrix, such as the one given in Section 7.3.1. So, is there any VFP matrix other than a multiple of an identity matrix? First we recognize that a VFP matrix has the following property.

Lemma 7.7: If an $M \times M$ matrix $\mathbf{R}$ is a Vandermonde-form preserving matrix, then both the first row of $\mathbf{R}$ and the last row of $\mathbf{R}$, $[\mathbf{R}]_1$ and $[\mathbf{R}]_M$, are in $\mathcal{V}_M$. □

Proof: See Appendix. □

An identity matrix $\mathbf{I}_M$ certainly satisfies this condition since the first row and the last row, $\mathbf{e}_1^T$ and $\mathbf{e}_M^T$, respectively, are in Vandermonde form. Now if we choose the first row and the last row of an $M \times M$ matrix $\mathbf{R}$ as vectors in $\mathcal{V}_M$ other than $\mathbf{e}_1^T$ and $\mathbf{e}_M^T$, will we be able to construct a VFP matrix $\mathbf{R}$? The answer turns out to be yes if we choose the first row and the last row of $\mathbf{R}$ as two Vandermonde form vectors with different Vandermonde ratios. The following theorem gives the most general characterization of VFP matrices.

Theorem 7.3: An $M \times M$ matrix $\mathbf{R} = \begin{bmatrix} \mathbf{r}_1 & \mathbf{r}_2 & \cdots & \mathbf{r}_M \end{bmatrix}$ is Vandermonde-form preserving if and only if there exists a 2×2 invertible matrix

$$\mathbf{R}_2 = \begin{bmatrix} a & b \\ c & d \end{bmatrix}$$

such that

$$r_k(x) = (a + cx)^{M-k}(b + dx)^{k-1}, k = 1, 2, ..., M,$$

where $r_k(x)$ is the polynomial representation of the column vector $\mathbf{r}_k$, i.e., $r_k(x) = \mathbf{p}_M^T(x)\mathbf{r}_k$ (see definition of $\mathbf{p}_M(x)$ in Section 7.2.2). The 2×2 matrix $\mathbf{R}_2$ is called the *characteristic matrix* of the $M \times M$ VFP matrix $\mathbf{R}$. □

Proof: See Appendix. □

Theorem 7.3 essentially provides us a construction method of an $M \times M$ VFP matrix using a "seed" 2×2 nonsingular matrix

$$\mathbf{R}_2 = \begin{bmatrix} a & b \\ c & d \end{bmatrix}.$$

Note that $\mathbf{R}_2$ is always a VFP matrix as long as it is nonsingular (i.e., $ad - bc \neq 0$) since a 1×2 nonzero vector is always in the Vandermonde form. Besides, we can see that any $M \times M$ VFP matrix $\mathbf{R}_M$ can be parameterized by a 2×2 Vandermonde-form preserving matrix. Thus, the number of freedoms of $M \times M$ Vandermonde-form preserving matrices is always a constant for any $M > 1$. For convenience, we denote

$$\mathcal{R}_M\left(\begin{bmatrix} a & b \\ c & d \end{bmatrix}\right),$$

where $ad-bc \neq 0$, as the $M \times M$ Vandermonde-form preserving matrix generated with polynomials $a + cx$ and $b + dx$. For example,

$$\mathcal{R}_3\left(\begin{bmatrix} a & b \\ c & d \end{bmatrix}\right) = \begin{bmatrix} a^2 & ab & b^2 \\ 2ac & ad+bc & 2bd \\ c^2 & cd & d^2 \end{bmatrix}. \tag{7.8}$$

Some more numerical examples are presented below for a better "visual" understanding of VFP matrices.

Example 7.5: If we choose $\mathbf{R}_2 = \begin{bmatrix} 1 & 1 \\ 0 & 1 \end{bmatrix}$, then

$$\mathbf{R}_3 = \begin{bmatrix} 1 & 1 & 1 \\ 0 & 1 & 2 \\ 0 & 0 & 1 \end{bmatrix} \text{ and } \mathbf{R}_4 = \begin{bmatrix} 1 & 1 & 1 & 1 \\ 0 & 1 & 2 & 3 \\ 0 & 0 & 1 & 3 \\ 0 & 0 & 0 & 1 \end{bmatrix}.$$

If we choose $\mathbf{R}_2 = \begin{bmatrix} 2 & 1 \\ 1 & 0 \end{bmatrix}$, then

$$\mathbf{R}_3 = \begin{bmatrix} 4 & 2 & 1 \\ 4 & 1 & 0 \\ 1 & 0 & 0 \end{bmatrix} \text{ and } \mathbf{R}_4 = \begin{bmatrix} 8 & 4 & 2 & 1 \\ 12 & 4 & 1 & 0 \\ 6 & 1 & 0 & 0 \\ 1 & 0 & 0 & 0 \end{bmatrix}.$$

□ □

Example 7.6: A VFP matrix can also be a full matrix. If we choose $\mathbf{R}_2 = \begin{bmatrix} 1 & 2 \\ 1 & 1 \end{bmatrix}$, then

$$\mathbf{R}_3 = \begin{bmatrix} 1 & 2 & 4 \\ 2 & 3 & 4 \\ 1 & 1 & 1 \end{bmatrix} \text{ and } \mathbf{R}_4 = \begin{bmatrix} 1 & 2 & 4 & 8 \\ 3 & 5 & 8 & 12 \\ 3 & 4 & 5 & 6 \\ 1 & 1 & 1 & 1 \end{bmatrix}.$$

If we choose $\mathbf{R}_2 = \begin{bmatrix} 1 & 2 \\ 2 & 1 \end{bmatrix}$, then

$$\mathbf{R}_3 = \begin{bmatrix} 1 & 2 & 4 \\ 4 & 5 & 4 \\ 4 & 2 & 1 \end{bmatrix} \text{ and } \mathbf{R}_4 = \begin{bmatrix} 1 & 2 & 4 & 8 \\ 6 & 9 & 12 & 12 \\ 12 & 12 & 9 & 6 \\ 8 & 4 & 2 & 1 \end{bmatrix}.$$

If we choose $\mathbf{R}_2 = \begin{bmatrix} 1 & j \\ j & 1 \end{bmatrix}$, then

$$\mathbf{R}_3 = \begin{bmatrix} 1 & j & -1 \\ 2j & 0 & 2j \\ -1 & j & 1 \end{bmatrix} \text{ and } \mathbf{R}_4 = \begin{bmatrix} 1 & j & -1 & -j \\ 3j & -1 & j & -3 \\ -3 & j & -1 & 3j \\ -j & -1 & j & 1 \end{bmatrix}.$$

□ □

7.4.2 Zero-Location Transformation

The key reason that a VFP matrix preserves $1/(M-1)$-richness is that it transforms each zero location of a column vector (see Definition 7.7) with a transformation function. This function depends only on its characteristic matrix and is independent from any other zeros of the column vector. In this subsection we will explore how VFP matrices transform zero locations of a column vector.

Consider an $M \times 1$ vector $\mathbf{u}$ and the set of zero location

$$\mathcal{Z}_{\mathbf{u}} = \{\alpha_1, \alpha_2, ..., \alpha_{M-1}\},$$

where $\alpha_k \in \mathbb{C} \bigcup \{\infty\}$ for all $k = 1, 2, ..., M-1$, as defined in Definition 7.7. Now, consider an $M \times M$ VFP matrix $\mathbf{R}$ whose characteristic matrix is $\mathbf{R}_2 = \begin{bmatrix} a & b \\ c & d \end{bmatrix}$. Suppose the set of zero locations of $\mathbf{y} = \mathbf{R}\mathbf{u}$ is

$$\mathcal{Z}_{\mathbf{y}} = \{\beta_1, \beta_2, ..., \beta_{M-1}\}.$$

How can we find each element of $\mathcal{Z}_{\mathbf{y}}$ given its corresponding zero in $\mathcal{Z}_{\mathbf{u}}$ and the values of $\mathbf{R}_2$? This question is directly related to how the Vandermonde ratio of $\mathbf{w}^T$ is related to that of $\mathbf{v}^T$ when $\mathbf{w}^T = \mathbf{v}^T\mathbf{R}$, as presented in the following theorem.

Theorem 7.4: Suppose $\mathbf{v}^T \in \mathcal{V}_M$ has a Vandermonde ratio $\alpha \in \mathbb{C} \bigcup \{\infty\}$ and $\mathbf{R}_M$ is a VFP matrix

with a nonsingular characteristic matrix

$$\mathbf{R}_2 = \begin{bmatrix} a & b \\ c & d \end{bmatrix}.$$

Then, $\mathbf{w}^T = \mathbf{v}^T\mathbf{R}_M$ is also a Vandermonde form vector with Vandermonde ratio $\beta = f(\alpha)$, where $f : \mathbb{C}\bigcup\{\infty\} \rightarrow \mathbb{C}\bigcup\{\infty\}$ is called the *characteristic function* of $\mathbf{R}_M$, defined as

$$f(\alpha) = \lim_{x\rightarrow\alpha} \frac{b+dx}{a+cx}. \tag{7.9}$$

□

Proof: See Appendix. □

In view of Theorem 7.4, when $a + c\alpha = 0$, the function f gives the value of infinity. On the other hand, if α is infinity, the function gives the value d/c when $c \neq 0$ or gives the value ∞ when $c = 0$ and $d \neq 0$. Notice that c and d can not both be zero due to the nonsingularity of $\mathbf{R}_2$ matrix. Also note that the characteristic function of a VFP matrix depends only on the 2×2 characteristic matrix and not on the size of the VFP matrix. Some numerical examples are presented below to demonstrate Theorem 7.4 and clarify the concept.

Example 7.7: We take $\mathbf{R}_2 = \begin{bmatrix} 1 & 2 \\ 1 & 1 \end{bmatrix}$ as in Example 7.6. Then, the 4×4 VFP matrix characterized by $\mathbf{R}_2$ is

$$\mathbf{R}_4 = \begin{bmatrix} 1 & 2 & 4 & 8 \\ 3 & 5 & 8 & 12 \\ 3 & 4 & 5 & 6 \\ 1 & 1 & 1 & 1 \end{bmatrix}.$$

The characteristic function of $\mathbf{R}_4$ is

$$f(\alpha) = \lim_{x\rightarrow\alpha} \frac{2+x}{1+x}.$$

Let $\mathbf{v}^T = \begin{bmatrix} 1 & -3 & 9 & -27 \end{bmatrix}$, which has a Vandermonde ratio $\alpha = -3$. Then

$$\mathbf{w}^T = \mathbf{v}^T\mathbf{R}_4 = \begin{bmatrix} -8 & -4 & -2 & -1 \end{bmatrix}$$

has a Vandermonde ratio $\beta = (2-3)/(1-3) = 1/2$.

If $\mathbf{v}^T = \begin{bmatrix} 1 & -1 & 1 & -1 \end{bmatrix}$, which has a Vandermonde ratio $\alpha = -1$, then

$$\mathbf{w}^T = \mathbf{v}^T\mathbf{R}_4 = \begin{bmatrix} 0 & 0 & 0 & 1 \end{bmatrix}$$

has a Vandermonde ratio $\beta = \infty$.
If $\mathbf{v}^T = \begin{bmatrix} 0 & 0 & 0 & 1 \end{bmatrix}$, which has a Vandermonde ratio $\alpha = \infty$, then

$$\mathbf{w}^T = \mathbf{v}^T\mathbf{R}_4 = \begin{bmatrix} 1 & 1 & 1 & 1 \end{bmatrix}$$

has a Vandermonde ratio $\beta = 1/1 = 1$. □

□

From the discussions above, we find that a VFP matrix "bi-linearly" transforms the Vandermonde ratio of a Vandermonde form vector with the characteristic function f defined in Theorem 7.4. Note that the function f is a one-to-one and onto function. The inverse function of f can be expressed as

$$g(\beta) = \lim_{y \to \beta} \left(-\frac{ay - b}{cy - d} \right). \tag{7.10}$$

A direct corollary of Theorem 7.4 is presented below.

Corollary 7.1: If β is a zero with multiplicity m of an $M \times 1$ vector $\mathbf{u}$, then

$$\alpha = g(\beta) = \lim_{y \to \beta} \left(-\frac{ay - b}{cy - d} \right)$$

is a zero with multiplicity m of the vector $\mathbf{y} = \mathbf{R}_M\mathbf{u}$. □

Proof: Since $\beta \in \mathcal{Z}_{\mathbf{u}}$, we have $\mathbf{v}_\beta^T\mathbf{u} = \mathbf{0}$, where $\mathbf{v}_\beta^T \in \mathcal{V}_M$ whose Vandermonde ratio is β. From Theorem 7.4 there exists $\mathbf{v}_\alpha^T \in \mathcal{V}_M$ whose Vandermonde ratio is $\alpha = f^{-1}(\beta) = g(\beta)$ such that $\mathbf{v}_\beta^T = \mathbf{v}_\alpha^T\mathbf{R}_M$. Then, $\mathbf{v}_\alpha^T\mathbf{y} = \mathbf{v}_\alpha^T\mathbf{R}_M\mathbf{u} = \mathbf{v}_\beta^T\mathbf{u} = \mathbf{0}$. So $\alpha = g(\beta) \in \mathcal{Z}_{\mathbf{y}}$. □

Example 7.8: We choose the same $\mathbf{R}_4$ as in Example 7.7. Let $\mathbf{u} = \begin{bmatrix} 1 & -3 & 2 & 0 \end{bmatrix}^T$, which has

zeros at $\beta_1 = 1/2$, $\beta_2 = \infty$, and $\beta_3 = 1$, respectively. Then we have

$$\begin{aligned}\mathbf{y} &= \mathbf{R}_4\mathbf{u} \\ &= \begin{bmatrix} 1 & 2 & 4 & 8 \\ 3 & 5 & 8 & 12 \\ 3 & 4 & 5 & 6 \\ 1 & 1 & 1 & 1 \end{bmatrix} \begin{bmatrix} 1 \\ -3 \\ 2 \\ 0 \end{bmatrix} = \begin{bmatrix} 3 \\ 4 \\ 1 \\ 0 \end{bmatrix}.\end{aligned}$$

The zero locations of $\mathbf{y}$ are at $\alpha_1 = -3$, $\alpha_2 = -1$, and $\alpha_3 = \infty$. Note that α_k and β_k have the relationship as predicted in Corollary 7.1. The function g defined in Eq. (7.10) is thus called the *zero-location transformation* (ZLT) function of the VFP matrix $\mathbf{R}_M$. □ □

7.4.3 Other Properties of VFP matrices

Some other noteworthy properties of VFP matrices, although not directly related to solving the main problem, are briefly presented here. The reader can verify these with some effort.

1. First of all, VFP matrices are in general not Hermitian nor symmetric, even if the 2×2 characteristic matrix is. In fact, one can prove that for $M > 2$, if the $M \times M$ matrix $\mathbf{R}$ is both VFP and Hermitian, then $\mathbf{R}$ must be a diagonal matrix or an anti-diagonal matrix (i.e., $[\mathbf{R}]_{ij}$ could be nonzero only when $i + j = M + 1$).

2. VFP matrices are invertible. The inverse of a VFP matrix is also a VFP matrix. In addition, the characteristic function of the inverse of a VFP matrix (as defined in Eq. (7.9)) is the inverse function (as defined in Eq. (7.10)) of the characteristic function of the original VFP matrix.

3. The product of two VFP matrices is a VFP matrix. The characteristic function of the product is the composition of two characteristic functions of the original two VFP matrices.

4. DFT and IDFT matrices are in general not VFP unless $M = 2$. It can also be shown that Hadamard matrices are not VFP in general. This means some most commonly used precoders do not preserve $1/(M-1)$-richness. It can also be shown that a unitary matrix is not VFP unless it is the identity matrix (or a nonzero scaled version of it) or an anti-diagonal matrix with identical anti-diagonal entries.

5. Define the set of all characteristic functions

$$\begin{aligned}\mathcal{T}_{\mathbb{C}} &= \Big\{ f : \mathbb{C}\bigcup\{\infty\} \to \mathbb{C}\bigcup\{\infty\} \Big| \\ &\qquad f(\alpha) = \lim_{x\to\alpha} \frac{b+dx}{a+cx}, a, b, c, d \in \mathbb{C}, ad \neq bc \Big\}\end{aligned}$$

Then, $(\mathcal{T}_{\mathbb{C}}, \circ)$, where "$\circ$" denotes the function composition operation, is a group which is algebraically isomorphic to the group $(\mathcal{R}_M, \cdot)$, where $\mathcal{R}_M$ is the set of all $M \times M$ VFP matrices and "$\cdot$" is the matrix multiplication operation.

6. Eigenvalues and eigenvectors of a VFP matrix can be easily found given its size M and its 2×2 characteristic matrix. Suppose $\mathbf{R}_M$ is a VFP matrix with a characteristic matrix $\mathbf{R}_2 = \begin{bmatrix} a & b \\ c & d \end{bmatrix}$ whose eigenvalues are λ_1 and λ_2. Then, the M eigenvalues of $\mathbf{R}_M$ are

$$\left\{\lambda_1^{M-1}, \lambda_1^{M-2}\lambda_2, \cdots, \lambda_2^{M-1}\right\}.$$

So, the determinant of $\mathbf{R}_M$ is

$$\det(\mathbf{R}_M) = (\lambda_1\lambda_2)^{M(M-1)/2} = \det(\mathbf{R}_2)^{M(M-1)/2}.$$

Now suppose $\mathbf{u}_i$ is an eigenvector of $\mathbf{R}_2$ associated with the eigenvalue λ_i for $i = 1, 2$. That is, $\mathbf{R}_2 = \mathbf{U}_2\mathbf{\Lambda}_2\mathbf{U}_2^{-1}$, where $\mathbf{U}_2 = \begin{bmatrix} \mathbf{u}_1 & \mathbf{u}_2 \end{bmatrix}$ and $\mathbf{\Lambda}_2 = \text{diag}(\lambda_1, \lambda_2)$. Then it can be shown that $\mathbf{R}_M = \mathbf{U}_M\mathbf{\Lambda}_M\mathbf{U}_M^{-1}$, where $\mathbf{U}_M = \mathcal{R}_M(\mathbf{U}_2)$ (see definition in Eq. (7.8)) and $\mathbf{\Lambda}_M = \text{diag}(\lambda_1^{M-1}, \lambda_1^{M-2}\lambda_2, \cdots, \lambda_2^{M-1})$.

7. Using the property mentioned above, a VFP matrix with unit-norm eigenvalues can be easily constructed by simply choosing a characteristic matrix $\mathbf{R}_2$ whose eigenvalues λ_1 and λ_2 satisfy $|\lambda_1| = |\lambda_2| = 1$, but it should be noticed that matrices created in this way are usually still not unitary. In fact, one can show that for $M > 2$, an $M \times M$ VFP matrix $\mathbf{R}$ is in general not a normal matrix (i.e., $\mathbf{R}^\dagger\mathbf{R} = \mathbf{R}\mathbf{R}^\dagger$) [17] unless $\mathbf{R}$ is diagonal or anti-diagonal. This more general fact also explains properties 1) and 4) mentioned above.

7.4.4 VFP matrices as a Linear Precoder

In real applications when a VFP matrix is used as the precoder, we multiply the input vectors by the VFP matrix at the transmitter and multiply the inverse of the VFP matrix (which is also a VFP matrix) at the receiver after equalization. In many applications, we may want to choose an optimal VFP matrix that satisfies certain constraints (e.g., power constraint, noise reduction, etc.). Since all VFP matrices can be characterized using four parameters (see Theorem 7.3), an optimization problem can be formulated with respect to only four parameters according to the specific application. In addition, since a VFP matrix is in general not unitary as discussed above, at the receiver it can amplify the signal subspace and noise subspace with different values. Hence, if the channel state information is known to both the transmitter and the receiver, we can accordingly choose the optimal values of $\mathbf{R}_2$ such that the signal-to-noise-ratio (SNR) is maximized.

7.5 Main Theorem

Now let us return to the problem stated in Section III: what is the necessary and sufficient condition for an $M \times M$ matrix $\mathbf{R}$ to be $(1/Q)$-richness preserving for any Q, $1 \leq Q \leq M-1$? In Section III we have already shown that when $Q = 1$, $\mathbf{R}$ needs to be nonsingular, and when $Q = M-1$, $\mathbf{R}$ needs to be Vandermonde-form preserving (VFP). With properties of VFP matrices presented in the previous section, we are now ready to solve the general case of problem for any Q, $1 \leq Q \leq M-1$.

7.5.1 Necessary Conditions

We first show that the VFP condition is necessary for $M \times M$ matrix $\mathbf{R}$ to preserve $(1/Q)$-richness for any $Q \geq 2$. From Lemma 7.2, we learn that if some $\mathbf{v}^T \in \mathcal{V}_M$ is an annihilator of $\mathbf{s}(n)$, then $\mathbf{s}(n)$ cannot be $(1/Q)$-rich for any Q. On the other hand, if some $\mathbf{v}^T$ not in $\mathcal{V}_M$ is the only annihilator of $\mathbf{s}(n)$ (i.e., the signal space has rank deficiency equal to one), we can show that the degree of non-richness of $\mathbf{s}(n)$ is 2. Following this argument, we can easily obtain the following lemma.

Lemma 7.8: For $M > 1$, consider an $M \times M$ matrix $\mathbf{R}$. If $2 \leq Q \leq M-1$ and $\mathbf{R}$ is $(1/Q)$-richness preserving, then $\mathbf{R}$ must be VFP. □

Proof: See Appendix. □

Notice that when $Q = 1$, $\mathbf{R}$ is not necessarily VPF to be $(1/Q)$-richness preserving (nonsingularity is sufficient). Lemma 7.8 is true only when $Q \geq 2$.

7.5.2 Hankel-form Preservation

As for sufficient conditions of the main problem (for the case $Q \geq 2$), we explore in this subsection another property of VFP matrices.

Theorem 7.5 (Hankel-form Preservation): Given an $m \times n$ nonzero Hankel matrix $\mathbf{H} = [h_{ij}]$, let $\mathbf{R}_2$ be a 2×2 invertible matrix. Let $\mathbf{R}_m = \mathcal{R}_m(\mathbf{R}_2)$ and $\mathbf{R}_n = \mathcal{R}_n(\mathbf{R}_2)$ be $m \times m$ and $n \times n$ VFP matrices, respectively (the notation $\mathcal{R}_M(\cdot)$ was defined in Section 7.4.1). Then, $\mathbf{H}' = \mathbf{R}_m^T \mathbf{H} \mathbf{R}_n$ is also a nonzero Hankel matrix. □

Proof: See Appendix. □

Theorem 7.5 shows another capability of VFP matrices: besides preserving Vandermonde form vectors, they also preserve the property of Hankel matrices if we use two VFP matrices with the same characteristic matrix. An example is shown below.

Example 7.9: Let $\mathbf{R}_2 = \begin{bmatrix} 1 & 1 \\ 2 & 0 \end{bmatrix}$, $\mathbf{R}_3 = \mathcal{R}_3(\mathbf{R}_2)$, and

$$\mathbf{H} = \begin{bmatrix} h_1 & h_2 & h_3 \\ h_2 & h_3 & h_4 \end{bmatrix}$$

is a nonzero Hankel matrix. Then we have

$$\begin{aligned} & \mathbf{H}' = \mathbf{R}_2^T \mathbf{H} \mathbf{R}_3 \\ = & \begin{bmatrix} 1 & 2 \\ 1 & 0 \end{bmatrix} \begin{bmatrix} h_1 & h_2 & h_3 \\ h_2 & h_3 & h_4 \end{bmatrix} \begin{bmatrix} 1 & 1 & 1 \\ 4 & 2 & 0 \\ 4 & 0 & 0 \end{bmatrix} \\ = & \begin{bmatrix} h_1 + 6h_2 + 12h_3 + 8h_4 & h_1 + 4h_2 + 4h_3 & h_1 + 2h_2 \\ h_1 + 4h_2 + 4h_3 & h_1 + 2h_2 & h_1 \end{bmatrix} \end{aligned}$$

is also a nonzero Hankel matrix. □ □

7.5.3 Main Theorem

Using Theorem 7.5 and Lemma 7.8, the main problem described in Section III can now be completely answered by the following theorem.

Theorem 7.6 ($1/Q$-richness Preservation): For $M > 1$, $2 \leq Q \leq M-1$, an $M \times M$ matrix $\mathbf{R}_M$ is $(1/Q)$-richness preserving if and only if $\mathbf{R}_M$ is Vandermonde-form preserving. □

Proof: The necessity comes directly from Lemma 7.8. As for sufficiency, suppose a Vandermonde-form preserving matrix

$$\mathbf{R}_M = \mathcal{R}_M(\mathbf{R}_2)$$

is not $(1/Q)$-richness preserving for some $Q \geq 2$, where $\mathbf{R}_2$ is a 2×2 invertible matrix. Then there exists a $(1/Q)$-rich signal $\mathbf{s}(n)$ such that the output $\mathbf{y}(n) = \mathbf{R}_M\mathbf{s}(n)$ is not $(1/Q)$-rich. Using Theorem 7.1, there exists a $Q \times M$ nonzero Hankel matrix

$$\mathbf{V} = \begin{bmatrix} v_1 & v_2 & \cdots & v_M \\ v_2 & v_3 & \cdots & v_{M+1} \\ \vdots & \vdots & \ddots & \vdots \\ v_Q & v_{Q+1} & \cdots & v_{Q+M-1} \end{bmatrix}$$

such that $\mathbf{V}\mathbf{y}(n) = \mathbf{0}$ for all $n \geq 0$. This implies $\mathbf{V}\mathbf{R}_M\mathbf{s}(n) = \mathbf{0}$ for all $n \geq 0$. Let

$$\mathbf{R}_Q = \mathcal{R}_Q(\mathbf{R}_2).$$

We have $\mathbf{R}_Q^T\mathbf{V}\mathbf{R}_M\mathbf{s}(n) = \mathbf{0}$ for all $n \geq 0$. Using Theorem 7.5, we know that $\mathbf{R}_Q^T\mathbf{V}\mathbf{R}_M$ is also a Hankel matrix. Now, using Theorem 7.1 again, we conclude that $\mathbf{s}(n)$ is also not $(1/Q)$-rich, contradicting the assumption that it is $(1/Q)$-rich. So a Vandermonde-form preserving matrix must be $(1/Q)$-richness preserving for $Q \geq 2$. □

A summary of the answer of the main problem is given as follows. Given an $M \times M$ matrix $\mathbf{R}$, then

1. when $Q = 1$, $\mathbf{R}$ preserves $(1/Q)$-richness if and only if $\mathbf{R}$ is nonsingular;
2. when $2 \leq Q \leq M-1$, $\mathbf{R}$ preserves $(1/Q)$-richness if and only if $\mathbf{R}$ is a VFP matrix.

7.6 Other Relevant Issues on $(1/Q)$-richness

In this section we will discuss some deeper issues on $(1/Q)$-richness.

7.6.1 Relationship between degree of richness and rank of a signal

As we already know, given an M-vector signal, the degree of non-richness Q_{min} of the signal can only be one of the values $1, 2, ...M-1$, and ∞. The larger Q_{min} is, the "less rich" the signal is. By definition, a signal is 1-rich if and only if a matrix composed of finite sample vectors of $\mathbf{s}(n)$ has full rank M. This gives us an intuition that as the degree of non-richness of $\mathbf{s}(n)$ increases, the "rank" of $\mathbf{s}(n)$ should decrease. Before further discussion, we shall give a formal definition to the *rank* of a signal $\mathbf{s}(n)$ as follows.

Definition 7.9: The *rank* of an $M \times 1$ sequence $\mathbf{s}(n)$ is defined as

$$\text{rank}(\mathbf{s}(n)) \triangleq \max_{0 \le n_1 \le n_2 \le \cdots \le n_M} \text{rank}\left([\mathbf{s}(n_1), \mathbf{s}(n_2), \cdots, \mathbf{s}(n_M)]\right).$$

□ □

In other words, the rank of $\mathbf{s}(n)$ is the maximum number of linearly independent column vectors among $\mathbf{s}(n), n \ge 0$. The rank of an $M \times 1$ signal $\mathbf{s}(n)$ is an integer between zero and M. In particular, if $\text{rank}(\mathbf{s}(n)) = M$, then $Q_{min} = 1$. If $\text{rank}(\mathbf{s}(n)) \le 1$, then $Q_{min} = \infty$. If $\text{rank}(\mathbf{s}(n)) = M - 1$, then the degree of non-richness can be found in the following lemma, which we have already known when exploring necessary conditions of the main problem (See Section 7.5.1).

Lemma 7.9: If a sequence of $M \times 1$ vectors $\mathbf{s}(n)$ is not 1-rich but $\text{rank}(\mathbf{s}(n)) = M - 1$, then the degree of non-richness of $\mathbf{s}(n)$ is either 2 or ∞. □

Proof: See Appendix. □

While a high rank signal (as high as $M-1$) can have a "bad" degree of non-richness as depicted in Lemma 7.9, a signal with a low degree of non-richness always implies it has a sufficiently high rank, as explained in the following lemma.

Lemma 7.10: If an $M \times 1$ sequence $\mathbf{s}(n)$ has a finite degree of non-richness Q_{min}, then

$$\text{rank}(\mathbf{s}(n)) \geq \frac{M + Q_{min} - 1}{Q_{min}}.$$

In particular, if $\text{rank}(\mathbf{s}(n)) = 2$, then $Q_{min} = M - 1$. □

Proof: See Appendix. □

If $\mathbf{s}(n)$ has a degree of non-richness $Q_{min} = 1$, Lemma 7.10 says the obvious fact that $\text{rank}(\mathbf{s}(n)) = M$. If $Q_{min} = 2$, then the minimum rank $\mathbf{s}(n)$ must have is $(M + 1)/2$. As Q_{min} increases, the minimum rank required by $\mathbf{s}(n)$ is approximately inverse proportional to Q_{min}, around $1/Q_{min}$ of full rank. This is also a reason why we call $\mathbf{s}(n)$ $(1/Q)$-rich.

Now let us look at Lemma 7.10 from the view point of the rank of $\mathbf{s}(n)$. If we consider a signal $\mathbf{s}(n)$ with $\text{rank}(\mathbf{s}(n)) = 2$, then Lemma 7.10 says $Q_{min} \geq M - 1$. In other words, the degree of non-richness of $\mathbf{s}(n)$ is either $M - 1$ or infinity. More generally, consider an FIR signal with $\mathbf{s}(n) = \mathbf{0}, \forall n \geq J$, i.e., considering an $M \times J$ matrix

$$\mathbf{S} = \begin{bmatrix} \mathbf{s}(0) & \mathbf{s}(1) & \cdots & \mathbf{s}(J-1) \end{bmatrix}.$$

Then, the condition in Lemma 7.10 can be rewritten as

$$J \geq \text{rank}(\mathbf{S}) = \text{rank}(\mathbf{s}(n)) \geq \frac{M + Q_{min} - 1}{Q_{min}}. \tag{7.11}$$

This implies

$$Q_{min} \geq \left\lceil \frac{M-1}{\text{rank}(\mathbf{S}) - 1} \right\rceil \geq \left\lceil \frac{M-1}{J-1} \right\rceil. \tag{7.12}$$

The equality in the left part of inequality (7.12) always holds true when $M \leq 4$, as long as $\mathbf{s}(n)$ has no annihilator in the Vandermonde form (i.e., $Q_{min} = \infty$). This can be readily verified using Lemmas 7.9 and 7.10. When $M \geq 5$, there are, however, situations when this is not true, as can be seen in the following example.

Example 7.10: Let $M = 5$ and $\mathbf{s}(n)$ be chosen as

$$\begin{bmatrix} \mathbf{s}(0) & \mathbf{s}(1) & \mathbf{s}(2) \end{bmatrix} = \begin{bmatrix} 1 & 1 & 0 \\ -1 & 0 & 0 \\ -1 & -2 & 1 \\ -1 & -1 & -1 \\ 1 & 1 & 0 \end{bmatrix},$$

and $\mathbf{s}(n) = \mathbf{0}$ when $n \geq 3$.

Then, rank$(\mathbf{s}(n)) = 3$, so $Q_{min} \geq \lceil (5-1)/(3-1) \rceil = 2$ as indicated in (7.12), and vectors $\mathbf{s}(n), n \geq 0$ do not share a common zero ($\mathcal{Z}_{\mathbf{s}(0)} = \{1.7221, -0.6514 \pm 0.7587j, 0.5807\}$, $\mathcal{Z}_{\mathbf{s}(1)} = \{1.9052, -0.7881 \pm 0.4014j, 0.6710\}$, and $\mathcal{Z}_{\mathbf{s}(2)} = \{0, 0, 1, \infty\}$), so Q_{min} is finite. However, it can be verified that $\mathbf{s}(n)$ has two annihilators $\begin{bmatrix} 2 & 1 & 1 & 1 & 1 \end{bmatrix}$ and $\begin{bmatrix} 1 & 1 & 1 & 1 & 2 \end{bmatrix}$, and so the 2×5 Hankel matrix

$$\mathbf{H} = \begin{bmatrix} 2 & 1 & 1 & 1 & 1 \\ 1 & 1 & 1 & 1 & 2 \end{bmatrix}$$

satisfies $\mathbf{H}\mathbf{s}(n) = \mathbf{0}$. So $\mathbf{s}(n)$ is not $(1/2)$-rich and $Q_{min} > 2$ (actually $Q_{min} = 3$ since the Hankel matrix $\mathbf{H}$ cannot be extended into three rows in this case). □ □

We summarize the relationship between degree of non-richness and rank of an $M \times 1$ sequence $\mathbf{s}(n)$ in Table I.

	Q_{min}				
rank(s(n))	M=2	M=3	M=4	M=5	M=6
1	∞	∞	∞	∞	∞
2	1	2 or ∞	3 or ∞	4 or ∞	5 or ∞
3	-	1	2 or ∞	2, 3, 4, or ∞	3, 4, 5, or ∞
4	-	-	1	2 or ∞	2, 3, 4, 5, or ∞
5	-	-	-	1	2 or ∞
6	-	-	-	-	1

Table 7.1: Relationship between degree of non-richness and rank of $\mathbf{s}(n)$. Notice ambiguity of finite values for $M \geq 5$. See text.

7.6.2 Distribution of Degree of Non-richness

In this subsection we want to discuss the distribution of degree of non-richness for a sequence of $M \times 1$ vectors $\mathbf{s}(n)$ when all entries of $\mathbf{s}(n)$ come from a finite constellation. We perform a Monte Carlo experiment with 2,500,000 samples of $8 \times J$ matrices for each $J, 2 \leq J \leq 9$, whose entries are randomly chosen from commonly used communication constellations: BPSK, QPSK, and 16-QAM. BPSK constellation has an alphabet size of two (1 and -1). QPSK constellation has a size of four, and 16-QAM has a size of sixteen. Each $8 \times J$ matrix can represent a causal FIR 8-vector signal whose first J samples are nonzero. In Figures 7.2, 7.3, and 7.4, the length of each bar segment with specific color represents the proportion of samples which have the corresponding degree of non-richness Q_{min}. For example, in Figure 7.2, around 77% of samples of 8×9 matrices have a degree of non-richness $Q_{min} = 1$, while most of the rest have around 23%. In view of these figures, we find that the degree of non-richness tends to achieve the lower bound predicted in (7.12) when entries of the signal come from a larger constellation. This indicates that in real applications (see Chapter 2 for more detailed reference) where Q is given, it is usually sufficient to collect

$$J = \frac{M + Q - 1}{Q}$$

samples of vectors when a large constellation is used. On the contrary, when using a small constellation like BPSK, it is quite probable that the signal has a degree of non-richness larger than the lower bound described in (7.12).

As a final comment, in real applications when these signals are precoded by a VFP matrix, the degree of non-richness of the input signal is guaranteed not to decrease. However, since a VFP matrix would not turn a non-$(1/Q)$-rich signal into $(1/Q)$-rich, the degree of non-richness would not increase and thus would be always unchanged. On the contrary, for an arbitrary non-VFP matrix, although the property of $(1/Q)$-richness could sometimes be destroyed, it is sometimes possible that a non-VFP matrix turns a non-$(1/Q)$-rich signal into a $(1/Q)$-rich signal. Whether an arbitrary matrix increases or decreases the probability of $(1/Q)$-richness is not clear at the time of writing this chapter.

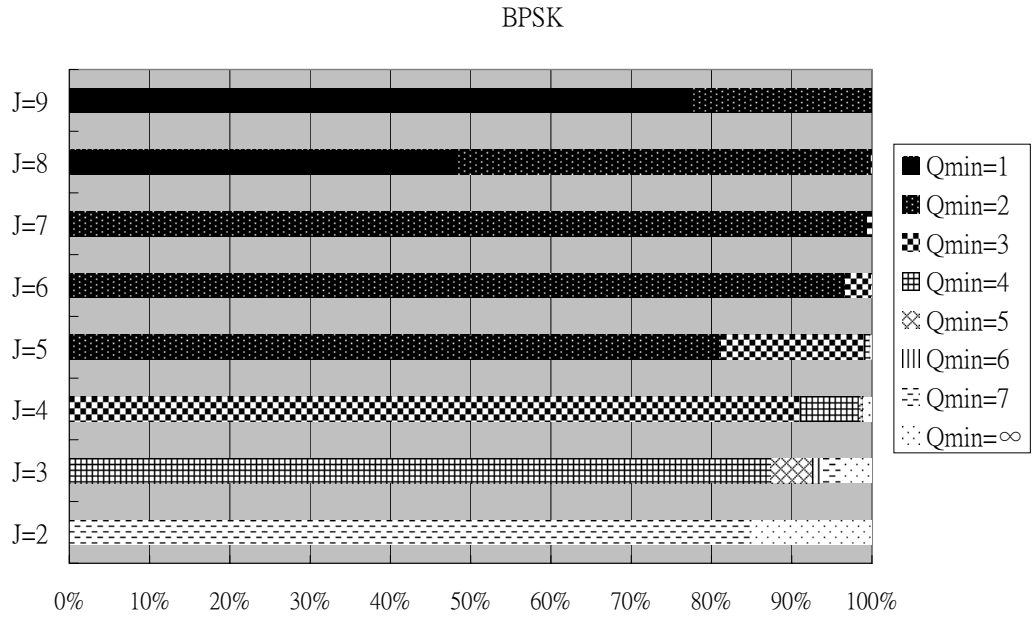

Figure 7.2: Distribution of degree of non-richness of signals whose entries are from BPSK constellation.

7.7 Concluding Remarks

In this chapter, we described a mathematical problem that arises in the blind channel estimation algorithm proposed in Chapter 2. We introduced Vandermonde-form preserving (VFP) matrices as a new subclass of invertible matrices which are highly relevant to the problem. Several properties of VFP matrices have been presented clearly, and the proof of the answer to the problem has been presented systematically.

In the future, it may be useful to consider the problem in general for a system with memory. That is, the transfer function of the precoder is an $M \times M$ polynomial matrix $\mathbf{R}(z) = \sum_{k=0}^{N} \mathbf{r}(k) z^{-k}$. It is also of interest to deal with a rectangular $P \times M$ system $\mathbf{R}(z)$. Finding other engineering applications of VFP matrices will also be interesting.

7.8 Appendix: Proof of Theorems

Proof of Theorem 7.1: If $\mathbf{s}(n)$ is not $(1/Q)$-rich, there exists a nonzero row vector

$$\mathbf{v}^T = \begin{bmatrix} v_1 & v_2 & \cdots & v_{Q+M-1} \end{bmatrix}$$

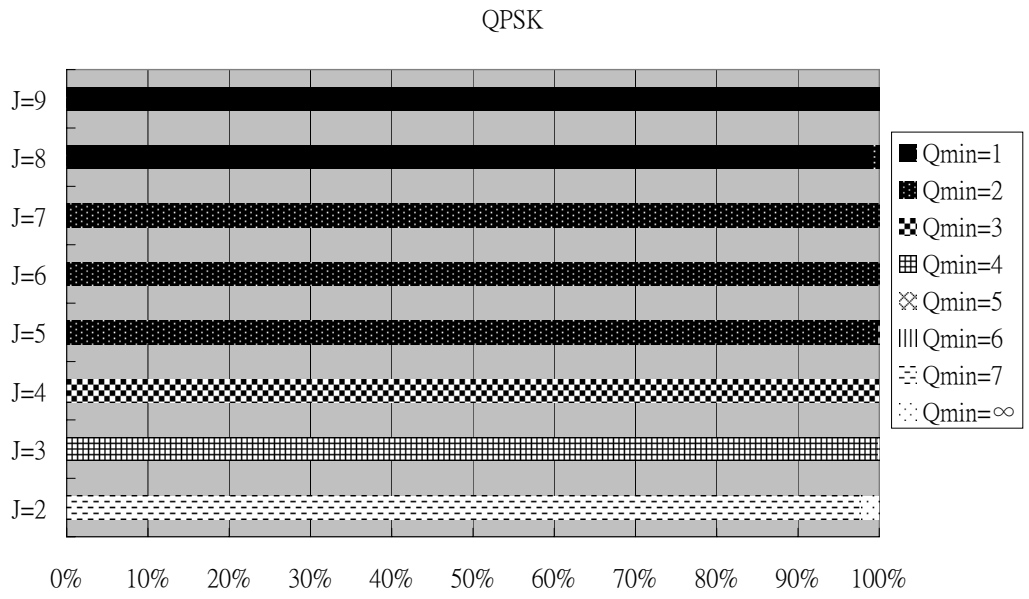

Figure 7.3: Distribution of degree of non-richness of signals whose entries are from QPSK constellation.

such that $\mathbf{v}^T\mathbf{s}_Q(n) = 0, \forall n \geq 0$. Then we have

$$\begin{bmatrix} v_k & v_{k+1} & \cdots & v_{k+M-1} \end{bmatrix} \mathbf{s}(n) = 0$$

for all k, $1 \leq k \leq Q$. This leads to

$$\underbrace{\begin{bmatrix} v_1 & v_2 & \cdots & v_M \\ v_2 & v_3 & \cdots & v_{M+1} \\ \vdots & \vdots & \ddots & \vdots \\ v_Q & v_{Q+1} & \cdots & v_{Q+M-1} \end{bmatrix}}_{\mathbf{V}} \mathbf{s}(n) \quad = \quad \mathbf{0}$$

for all $n \geq 0$ where $\mathbf{V}$ is a nonzero Hankel matrix.

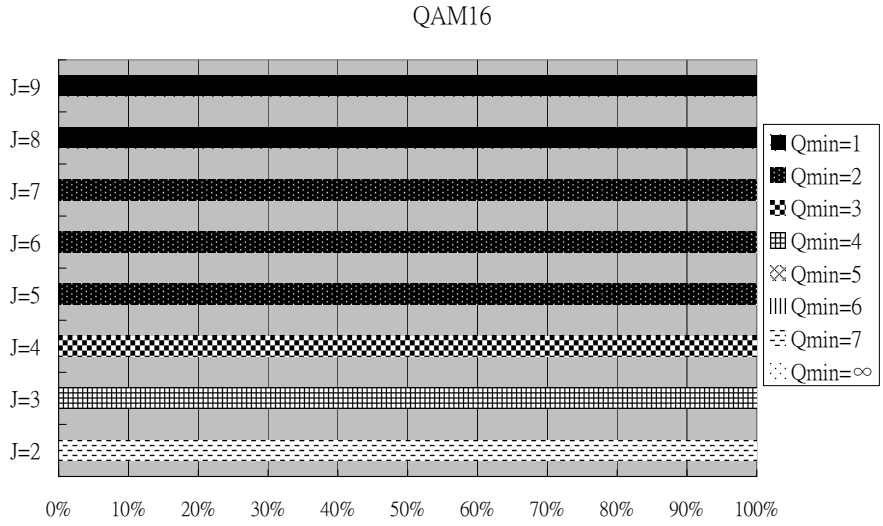

Figure 7.4: Distribution of degree of non-richness of signals whose entries are from 16-QAM constellation.

On the other hand, suppose there exists a nonzero $Q \times M$ Hankel matrix

$$\mathbf{V} = \begin{bmatrix} v_1 & v_2 & \cdots & v_M \\ v_2 & v_3 & \cdots & v_{M+1} \\ \vdots & \vdots & \ddots & \vdots \\ v_Q & v_{Q+1} & \cdots & v_{Q+M-1} \end{bmatrix}$$

such that $\mathbf{V}\mathbf{s}(n) = \mathbf{0}$ for all $n \geq 0$. It can be readily verified that the nonzero row vector

$$\mathbf{v}^T = \begin{bmatrix} v_1 & v_2 & \cdots & v_{Q+M-1} \end{bmatrix}$$

satisfies $\mathbf{v}^T \mathbf{s}_Q(n) = 0$, so $\mathbf{s}(n)$ is not $(1/Q)$-rich. □

Proof of Lemma 7.4: If $\gamma \in \mathbb{C}$, the statement is self-evident. If $\gamma = \infty$, then $\mathbf{v}^T = c\mathbf{e}_M^T$ for some $c \neq 0$, so $\mathbf{v}^T\mathbf{y} = 0 \Leftrightarrow \mathbf{e}_M^T\mathbf{y} = 0 \Leftrightarrow [\mathbf{y}]_M = 0 \Leftrightarrow$ polynomial $\mathbf{p}_M^T(x)\mathbf{y}$ does not have the term of x^{M-1} and, hence, has a degree less than $M-1$. □

Proof of Theorem 7.2: Suppose $\mathbf{R}$ is Vandermonde-form preserving (VFP) but does not preserve

$(1/(M-1))$-richness (i.e., there exists $\mathbf{s}(n)$ such that $\mathbf{s}(n)$ is $(1/(M-1))$-rich but $\mathbf{R}\mathbf{s}(n)$ is not). Then there exists $\mathbf{w}^T \in \mathcal{V}_M$ such that $\mathbf{w}^T\mathbf{R}\mathbf{s}(n) = 0$. This leads to $\mathbf{v}^T\mathbf{s}(n) = 0$, where $\mathbf{v}^T = \mathbf{w}^T\mathbf{R}$ is also in $\mathcal{V}_M$. This contradicts the fact that $\mathbf{s}(n)$ is $(1/(M-1))$-rich, so $\mathbf{R}$ being VFP implies it preserves $(1/(M-1))$-richness.

On the other hand, if $\mathbf{R}$ is not VFP, then there exists $\mathbf{w}^T \in \mathcal{V}_M$ such that $\mathbf{v}^T = \mathbf{w}^T\mathbf{R}$ is not in $\mathcal{V}_M$. We can thus create a $(1/(M-1))$-rich signal $\mathbf{s}(n)$ such that $\mathbf{v}^T\mathbf{s}(n) = 0, \forall n \geq 0$. (In fact, we can even create a $(1/2)$-rich signal $\mathbf{s}(n)$, which is stronger than a $(1/(M-1))$-rich signal. See also the proof of Lemma 7.8.) This implies $\mathbf{w}^T\mathbf{R}\mathbf{s}(n) = 0, \forall n \geq 0$, which means $\mathbf{R}\mathbf{s}(n)$ is not $(1/(M-1))$-rich. So $\mathbf{R}$ does not preserve $(1/(M-1))$-richness. □

Proof of Lemma 7.7: We first learn that both $\mathbf{e}_1^T$ and $\mathbf{e}_M^T$ are in $\mathcal{V}_M$ (with Vandermonde ratios 0 and ∞, respectively). Since $[\mathbf{R}]_1 = \mathbf{e}_1^T\mathbf{R}$, $[\mathbf{R}]_M = \mathbf{e}_M^T\mathbf{R}$, and $\mathbf{R}$ is Vandermonde-form preserving, the lemma is proved immediately. □

Proof of Theorem 7.3: Let $r_k(x)$ be the polynomial representation of the kth column of $\mathbf{R}$, i.e.,

$$\mathbf{p}_M^T(x)\mathbf{R} = \begin{bmatrix} r_1(x) & r_2(x) & \cdots & r_M(x) \end{bmatrix}.$$

Then we have

$$r_k(x)r_{k+2}(x) = r_{k+1}(x)^2 \tag{7.13}$$

for $k = 1, 2, ..., M-2$. (Otherwise we can find $\gamma \in \mathbb{C}$ such that $r_k(\gamma)r_{k+2}(\gamma) \neq r_{k+1}(\gamma)^2$ and, hence, $\mathbf{p}_M^T(\gamma)\mathbf{R} \notin \mathcal{V}_M$, while $\mathbf{p}_M^T(\gamma) \in \mathcal{V}_M$.)

We first argue that all columns of $\mathbf{R}$ must be nonzero. If $\mathbf{r}_k = \mathbf{0}$ for some k, then Eq. (7.13) implies that only $\mathbf{r}_1$ and $\mathbf{r}_M$ can be nonzero among $\mathbf{r}_k$'s. If only one of them is nonzero, say $\mathbf{r}_1 \neq \mathbf{0}$ and $\mathbf{r}_M = \mathbf{0}$, then there exists $\mathbf{v}^T \in \mathcal{V}_M$ such that $\mathbf{v}^T\mathbf{r}_1 = 0$ and hence $\mathbf{v}^T\mathbf{R} = \mathbf{0}^T \notin \mathcal{V}_M$. If both $\mathbf{r}_1$ and $\mathbf{r}_M$ are nonzero (which implies $M \geq 3$), then there exists $\gamma \in \mathbb{C}$ such that $r_1(\gamma)$ and $r_M(\gamma)$ are both nonzero. Choose $\mathbf{v}^T = \mathbf{p}_M^T(\gamma) \in \mathcal{V}_M$. Then, $p_M^T(\gamma)\mathbf{R} = \begin{bmatrix} r_1(\gamma) & 0 & \cdots & 0 & r_M(\gamma) \end{bmatrix} \notin \mathcal{V}_M$.

Since all columns of $\mathbf{R}$ are nonzero, Eq. (7.13) implies that there exist nonzero polynomials $p(x)$ and $q(x)$, which are co-prime to each other, such that

$$\frac{r_{k+2}(x)}{r_{k+1}(x)} = \frac{r_{k+1}(x)}{r_k(x)} = \frac{q(x)}{p(x)}$$

for $k = 1, 2, ..., M-2$. This leads to

$$r_M(x) = \frac{r_1(x)}{(p(x))^{M-1}} \cdot (q(x))^{M-1}.$$

Since $p(x)$ and $q(x)$ are co-prime to each other, we obtain that $(p(x))^{M-1}$ is a factor of $r_1(x)$. So

$$r_1(x) = c(x)(p(x))^{M-1}$$

for some nonzero polynomial $c(x)$. We now have

$$r_k(x) = c(x)(p(x))^{M-k}(q(x))^{k-1}, k = 1, 2, ..., M.$$

Note that $\deg(p(x)) \leq 1$ since otherwise $\deg(r_1(x)) \geq 2(M-1) > M-1$. Similarly we have $\deg(q(x)) \leq 1$. $p(x)$ and $q(x)$ cannot both be constants since otherwise there exists $\mathbf{v}^T \in \mathcal{V}_M$ such that $\mathbf{v}^T\mathbf{R} = \mathbf{0}^T \notin \mathcal{V}_M$. (This $\mathbf{v}^T$ can be chosen as $\mathbf{p}_M^T(\gamma)$ if γ is a zero of $c(x)$. If $c(x)$ is a constant, we can choose $\mathbf{v}^T$ as $\begin{bmatrix} 0 & \cdots & 0 & 1 \end{bmatrix}$.)

Now that at least one of $p(x)$ and $q(x)$ must be a first-order polynomial, $c(x)$ must be a constant, for otherwise either $\deg(r_1(x))$ or $\deg(r_M(x))$ would be greater than $M-1$. Without loss of generality, we can assume $c(x) = 1$. Now let $p(x) = a + cx$ and $q(x) = b + dx$. Since $p(x)$ and $q(x)$ are co-prime to each other and they cannot be constants simultaneously, this implies $ad - bc = 0$ and the proof of necessity is done.

The sufficiency is easily verified.

□

Proof of Theorem 7.4: From the proof of Theorem 7.3 we learn that

$$\mathbf{p}_M^T(x)\mathbf{R} = \begin{bmatrix} r_1(x) & r_2(x) & \cdots & r_M(x) \end{bmatrix},$$

where $r_k(x) = (a + cx)^{M-k}(b + dx)^{k-1}, k = 1, 2, ..., M$. Suppose $\mathbf{v}^T$ has a Vandermonde ratio α. When $\alpha \in \mathbb{C}$, $\mathbf{v}^T$ can be expressed as

$$\mathbf{v}^T = g \begin{bmatrix} 1 & \alpha & \alpha^2 & \cdots & \alpha^{M-1} \end{bmatrix}$$

for some $g \in \mathbb{C}$. The output $\mathbf{w}^T = \mathbf{v}^T\mathbf{R}$ is thus

$$\mathbf{w}^T = g \begin{bmatrix} r_1(\alpha) & r_2(\alpha) & \cdots & r_M(\alpha) \end{bmatrix}.$$

When $a + c\alpha \neq 0$, it is readily verified that the Vandermonde ratio of $\mathbf{w}^T$ is $\beta = r_{k+1}(\alpha)/r_k(\alpha)$ for all k, $1 \leq k \leq M$. This is

$$\beta = \frac{r_{k+1}(\alpha)}{r_k(\alpha)} = \frac{b + d\alpha}{a + c\alpha}.$$

If $a+c\alpha = 0$, then $\mathbf{w}^T = g \begin{bmatrix} 0 & \cdots & 0 & 1 \end{bmatrix}$, so $\beta = \infty$. Finally, when $\alpha = \infty$, $\mathbf{v}^T = g \begin{bmatrix} 0 & \cdots & 0 & 1 \end{bmatrix}$ for some g, so

$$\mathbf{w}^T = g \begin{bmatrix} c^{M-1} & c^{M-2}d & \cdots & d^{M-1} \end{bmatrix},$$

and $\beta = d/c$ when $c \neq 0$ and $\beta = \infty$ when $c = 0$. In summary,

$$\begin{aligned} \beta &= \begin{cases} \frac{b+d\alpha}{a+c\alpha} & \text{if } a + c\alpha \neq 0 \\ \infty & \text{if } a + c\alpha = 0 \text{ and } b + d\alpha \neq 0 \\ \frac{d}{c} & \text{if } a + c\alpha = 0 \text{ and } b + d\alpha = 0 \end{cases} \\ &= \lim_{x \to \alpha} \frac{b + dx}{a + cx}. \end{aligned}$$

□

Proof of Lemma 7.8: Assume $\mathbf{R}$ is not VFP. Then there exists $\mathbf{v}^T \in \mathcal{V}_M$ such that $\mathbf{w}^T = \mathbf{v}^T\mathbf{R} \notin \mathcal{V}_M$. Construct a vector sequence $\mathbf{s}(n), n \geq 0$ as follows. Let $\mathbf{s}(0), \mathbf{s}(1), \cdots, \mathbf{s}(M-2)$ be selected as $(M-1)$ linearly independent column vectors that are orthogonal to $\mathbf{w}^T \notin \mathcal{V}_M$. Let $\mathbf{s}(n) = \mathbf{0}$ for all $n \geq M-1$. Since $\mathbf{w}^T \notin \mathcal{V}_M$ is the only annihilator of $\mathbf{s}(n)$, there does not exist a $2 \times M$ nonzero Hankel matrix $\mathbf{H}$ such that $\mathbf{H}\mathbf{s}(n) = \mathbf{0}$, so $\mathbf{s}(n)$ is $(1/2)$-rich, and hence is $(1/Q)$-rich for any $Q \geq 2$. Now consider $\mathbf{u}(n) = \mathbf{R}\mathbf{s}(n)$. We have $\mathbf{v}^T\mathbf{u}(n) = \mathbf{v}^T\mathbf{R}\mathbf{s}(n) = \mathbf{w}^T\mathbf{s}(n) = \mathbf{0}$. By Lemma 7.2, $\mathbf{u}(n)$ is not $1/Q$-rich for any Q, so $\mathbf{R}$ is not $(1/Q)$-richness preserving for any $Q \geq 2$. □

The proof of Theorem 7.5 requires the following lemma.

Lemma 7.11: Let $\mathbf{H}$ be an $m \times n$ Hankel matrix whose entry values come from an $(m+n-1) \times 1$ vector $\mathbf{h}$. That is, $[\mathbf{H}]_{ij} = [\mathbf{h}]_{i+j-1} = h_{i+j-1}$. Let $\mathbf{u}$ and $\mathbf{v}$ be $m \times 1$ and $n \times 1$ column vectors, respectively, and $u(x) = \mathbf{p}_m^T(x)$ and $v(x) = \mathbf{p}_n^T(x)$ are the polynomials representing two vectors. Let $w(x) = u(x)v(x)$ and $\mathbf{w}$ be an $(m+n-1) \times 1$ vector whose polynomial representation is $w(x)$

(i.e., $w(x) = \mathbf{p}_{m+n-1}^T(x)\mathbf{w}$). Then

$$\mathbf{u}^T\mathbf{H}\mathbf{v} = \mathbf{w}^T\mathbf{h}.$$

□

Proof: The Lemma is immediately verified by observing that the coefficient associated with h_k in the sum $\mathbf{u}^T\mathbf{H}\mathbf{v}$ is $\sum_{l=1}^{m} u_l v_{k-l+1}$. (Assuming $v_l = 0$ when $l \leq 0$ or $l > n$.) □

Proof of Theorem 7.5: Denote the kth column of $\mathbf{R}_m$ as $\mathbf{r}_{m,k}$ and the lth column of $\mathbf{R}_n$ as $\mathbf{r}_{n,l}$. Let $r_{mk}(x) = \mathbf{p}_m^T(x)\mathbf{r}_{m,k}$ and $r_{nl}(x) = \mathbf{p}_n^T(x)\mathbf{r}_{n,l}$. From construction of VFP matrices we know $r_{mk}(x) = (a+cx)^{m-k}(b+dx)^{k-1}$ and $r_{nl}(x) = (a+cx)^{n-l}(b+dx)^{l-1}$. The kl-th entry of $\mathbf{H}'$, $[\mathbf{H}']_{kl}$, can be expressed as $\mathbf{r}_{m,k}^T\mathbf{H}\mathbf{r}_{n,l}$. Using Lemma 7.11, we have

$$[\mathbf{H}']_{kl} = \mathbf{w}_{k,l}^T\mathbf{h}, \tag{7.14}$$

where the polynomial representation of the $(m+n-1)\times 1$ vector $\mathbf{w}_{k,l}$ is $w_{kl}(x) = r_{mk}(x)r_{nl}(x) = (a+cx)^{m+n-k-l}(b+dx)^{k+l-2}$. The polynomial $w_{kl}(x)$ stays unchanged when $k+l$ is fixed, so from Eq. (7.14), the value of $[\mathbf{H}']_{kl}$ is a function of $(k+l)$, and hence $\mathbf{H}'$ is also a Hankel matrix. $\mathbf{H}'$ being nonzero is readily verified by observing that both $\mathbf{R}_n$ and $\mathbf{R}_m$ are invertible. □

Proof of Lemma 7.9: In view of proof of Lemma 7.8, this lemma is self-evident. □

Proof of Lemma 7.10: If $\mathbf{s}(n)$ has rank r, then rank$(\mathbf{s}_Q(n)) \leq rQ$. Since $\mathbf{s}(n)$ is Q-rich, then $\mathbf{s}_Q(n)$ is rich and hence rank$(\mathbf{s}_Q(n)) = M+Q-1 \leq rQ$. So $r \geq \frac{M+Q-1}{Q}$, and hence the proof is complete. □

Chapter 8

Conclusions

In this thesis, we have studied various important topics on blind channel estimation using linear redundant precoding. New algorithms were proposed which feature fast convergence speed and are much more applicable in fast-varying channel environments. Performance analysis is derived to confirm the improvements, and relevant theoretical issues are studied.

Two major types of linear redundant precoding, zero-padding (ZP) and cyclic prefixing (CP), are considered in this thesis. In Chapter 2, we proposed a generalized algorithm for blind channel estimation in ZP systems of which two previously reported subspace-based algorithms are special cases. The generalization uses an integer parameter called *repetition index* which represents the number of repeated uses of each received block. The minimum value of repetition index Q is found to be roughly inversely proportional to the number of available received blocks. Simulation shows that when the system parameter Q is properly chosen, the generalized algorithm outperforms previously reported special cases, especially in a time-varying channel environments. A frequency domain version of the generalized algorithm is also presented and is shown to outperform time domain approach at low SNR region for certain types of channels. The concept of *generalized signal richness* for a vector signal is introduced for the conditions of input signals on which the proposed algorithm works properly.

In Chapter 3, we extended the idea of repetition index to a more widely used class of redundant precoding systems: CP systems. A subspace-based generalized blind algorithm is proposed for CP systems. By using a repetition index larger than unity, the number of received blocks (J) is for the first time significantly reduced compared to previously reported methods so that the proposed algorithm is more feasible in time-varying channel environments. Theoretical limit allows the blind estimation to be performed using only three received blocks. Simulation shows that when the num-

ber of received blocks J and the repetition index Q are properly chosen, the generalized algorithm outperforms previously reported special cases. The proposed method can be directly applied to existing systems such as OFDM, SC-CP, etc., without any modification of the transmitter structure.

We also proposed a semi-blind channel estimation algorithm in OFDM systems based on a combination of the blind estimation algorithm in cyclic prefix systems and a pure pilot-assisted algorithm. The proposed algorithm is presumably the first one to be applicable with any types of communication constellations and a limited number of received blocks. Simulation results confirm the improvement in system performance of the semi-blind algorithm over the direct pilot-assisted algorithm. They also suggest that fewer pilot samples can be used to achieve the same BER performance when a semi-blind algorithm is employed.

In Chapter 4, the blind block synchronization problem in LRP systems is studied. Two algorithms which use the parameter repetition index were proposed for ZP and CP systems, respectively. The algorithm for CP systems can be directly applied to blind OFDM symbol synchronization problem. Theoretical results prove the validity of the proposed algorithms in the noiseless case. The proposed algorithms are capable of blindly recovering the block boundaries using much less received data than previously reported algorithms. This feature makes the proposed algorithms more favorable in an environment of fast-varying channels. Simulation results of the proposed algorithm not only demonstrate the capability to work properly with limited amount of received data but also reveal significant improvement in block synchronization error rate performance over previously reported algorithms.

Chapter 5 is a performance analysis of the generalized algorithm proposed in Chapter 2 in the high-SNR range. Theoretical analysis confirms the simulation results in Chapter 2 that when the repetition index is larger, the performance is usually better when SNR is large. A Cramer-Rao bound (CRB) is presented and used as a benchmark of the algorithm performance. When the repetition index Q is large, the performance curve tends to approach the CRB but does not appear to achieve it. However, the analysis, as well as simulation results, suggests that the generalized algorithm has a performance very close to the CRB even when the number of received blocks is very small.

In Chapters 6 and 7, the signal richness preservation problem has been studied. Chapter 6 considers the problem with respect to conventional definition of signal richness while Chapter 7 deals with the problem using the definition of generalized signal richness which first arises in Chap-

ter 2. In Chapter 6, necessary and sufficient conditions on linear FIR precoders which preserve conventional signal richness are found and proved. The results show that most standard systems with memory do not generally preserve signal richness, including paraunitary and unimodular matrices. In Chapter 7, necessary and sufficient conditions on linear memoryless precoders which preserve generalized signal richness with any repetition index Q are found. In order to solve the problem, a special class of nonsingular matrices called Vandermonde-form preserving (VFP) matrices are introduced. Several properties of VFP matrices have been presented, and the proof of the answer to the problem has been presented systematically.

There are various topics worthy of future research. First of all, the idea of repetition index can be applied to blind and semiblind channel estimation in MIMO systems. Also, the optimal number of pilot samples for semiblind systems which achieve capacity limit can be explored. A similar analysis can be conducted to evaluate the performance of blind channel estimation algorithm in CP systems proposed in Chapter 3 or in MIMO systems.

Bibliography

[1] A. Armada and M. Ramon, "Rapid prototyping of a test modem for terrestrial broadcasting of digital television, " *IEEE Trans. Consumer Electron.,* vol. 43, pp. 1100-1109, Nov. 1997.

[2] S. Barbarossa, A. Scaglione, and G. B. Giannakis, "Performance analysis of a deterministic channel estimator for block transmission systems with null guard intervals, " *IEEE Trans. SP*, vol. 50, pp. 684-695, Mar. 2002.

[3] A. Benveniste, M. Goursat, and G. Ruget, "Robust identification of a nonminimu phase system: blind adjustment of a linear equalizer in data communications," *IEEE Trans. on Automatic Control,* pp. 385-399, Jun. 1980.

[4] R. R. Bitmead, "Persistence of excitation conditions and the convergence of adaptive schemes," IEEE Trans. Inform. Theory, vol. IT-30, pp. 183-191, March 1986.

[5] X. Cai and A. Akansu, "A subspace method for blind channel identification in OFDM systems," in Proc. Int. Conf. Commun., vol 2, New Orleans, LA, pp. 929-933, Jun. 2000.

[6] N. Chotikakamthorn and H. B. Suzuki, "On identifiablity of OFDM blind channel estimation," in *Proc. ICC,* New Orleans, LA, Jul. 2000, pp. 929-933.

[7] T. Cui and C. Tellambura, "Semi-blind channel estimation and data detection for OFDM systems," in *Proc. ICASSP 2005*, Philadelphia, PA.

[8] Z. Ding and Y. Li, *Blind Equalization and Identification*, Marcel Dekker, Inc., 2001.

[9] Z. Ding and Y. Li, "On channel identification based on second order cyclic spectra," *IEEE Trans. SP,* vol. 42, pp. 1260 - 1264, May 1994.

[10] G. B. Giannakis, " Filterbanks for blind channel identification and equalization," *IEEE Signal Processing Letter,* vol. 4, no. 6, Jun. 1997.

[11] G. B. Giannakis, Y. Hua, P. Stoica, and L. Tong, *Signal Processing Advances in Wireless and Mobile Communications volume 1 – Trends in Channel Estimation and Equalization*, Prentice Hall, 2001.

[12] D. N. Godard, "Self-recovering equalization and carrier tracking in two-dimensional data communication systems," *IEEE Trans. on Communications,* COM-28:1867-1875, Nov. 1980.

[13] G. H. Golub and C. F. Van Loan, *Matrix Computations, 3rd Edition*, Johns Hopkins University Press, 1996.

[14] S. Haykin, *Adaptive Filter Theory*, 4th ed., Prentice-Hall, Upper Saddle River, NJ, 2002.

[15] R. W. Heath Jr. and G. B. Giannakis, "Exploting input cyclostationarity for blind channel identification in OFDM systems," *IEEE Trans. Signal Process.*, vol. 47, no. 3, pp. 848-856, Mar. 1999.

[16] K. Y. Ho and S. H. Leung, "A generalized semi-blind channel estimation for pilot-aided OFDM systems," in *Proc. ISCAS 2005*, Kobe, Japan, May 2005.

[17] R. A. Horn and C. R. Johnson, *Matrix Analysis*, Cambridge University Press, 1996.

[18] M. C. Jeruchim, P. Balaban, and K. S. Shanmugan, *Simulation of Communication Systems, Second Edition*, Kluwer Academic/Plenum, New York, 2000.

[19] D. E. Knuth, *The Art of Computer Programming Vol. 2, 3rd Edition*, Addison Wesley, 1997.

[20] D. Lee and K. Cheun, "A new symbol timing recovery algorithm for OFDM systems," *IEEE Trans. Consumer Elecron.,* vol 43, pp. 767-775, Aug. 1997.

[21] C. Li and S. Roy, "Subspace-based blind channel estimation for OFDM by exploiting virtual carriers," *IEEE Trans. Wireless Commun.*, vol. 2, no. 1, pp. 141-150, Jan. 2003.

[22] F. Li, H. Liu, and R. J. Vaccaro, "Performance analysis for DOA estimation algorithms: Further unification, simplification, and ovservations," IEEE Trans. Aerosp., Electron. Syste., vol. 29, pp. 1170-1184, Oct. 1993.

[23] Y. Li and Z. Ding, "Blind channel identification based on second order cyclostationary statistics," Proc. of ICASSP 1993, pp. 81-84, Minneapolis, MN.

[24] R. Lin and A. P. Petropulu, "Linear precoding assisted blind channel estimation for OFDM systems," *IEEE Trans. on Vehicular Technology*, vol. 54, no. 3, pp. 983-995, May 2005.

[25] Y. P. Lin and S. M. Phoong, "Perfect discrete multitone modulation with optimal transceivers," IEEE Trans. SP, vol. 48, pp. 1702-1711, Jun. 2000.

[26] H. Liu, and G. Xu, "A deterministic approach to blind symbol estimation," IEEE SP Letters, pp. 205-207, Dec. 1994.

[27] H. Liu, G. Xu, and L. Tong, "A deterministic approach to blind identification of multi-channel FIR systems," *Proc. 1994 IEEE ICASSP,* pp. 581-584, Adelaide, May 1994.

[28] J. H. Manton and W. D. Neumann, "Totally Blind Channel Identification by Exploiting Guard Intervals", *Systems and Control Letters,* vol. 48, no. 2, pp. 113-119, 2003.

[29] J. H. Manton, W. D. Neumann, and P. T. Norbury, "On the algebraic identifiability of finite impulse response channels driven by linearly precoded signals," *Systems and Control Letters,* vol. 54, pp. 125-134, Sep. 2004.

[30] E. Moulines, P. Duhamel, J. F. Cardoso, S. Mayrargue, "Subspace Methods for the Blind Identification of Multichannel FIR Filters," IEEE Trans. on SP, pp. 516-525, Feb. 1995.

[31] B. Muquet, M. de Courville, P. Duhamel, and V. Buzenac, "A subspace based blind and semi-blind channel identification method for OFDM systems," IEEE Workshop on Signal Processing Advances in Wireless Communications, pp. 170-173, May 1999.

[32] B. Muquet, M. de Courville, and P. Duhamel, "Subspace-based blind and semi-blind channel estimation for OFDM systems," *IEEE Trans. Signal Process.*, vol. 50, no. 7, pp. 1699-1712, Jul. 2002.

[33] R. Negi and J. M. Cioffi, "Blind OFDM symbol synchronization in ISI channels," *IEEE Trans. Commun.,* vol. 50, no. 9, pp. 1525-1534, Sept. 2002.

[34] A. Palin and J. Rinne, "Enhanced symbol synchronization method for OFDM system in SFM channel," in *Proc. IEEE Globecom,* Sydney, Australia, Nov. 1998, pp. 2788-2793.

[35] A. P. Petropulu, R. Zhang, and R. Lin, "Blind OFDM channel estimation through simple linear precoding," *IEEE Trans. on Wireless Communications*, vol. 3, no. 2, pp. 647-655, Mar. 2004.

[36] D. H. Pham and J. H. Manton, "A subspace algorithm for guard interval based channel identification and source recovery requiring just two received blocks", Proc. of ICASSP, pp. 317 - 320, Hong Kong, China, 2003.

[37] S.-M. Phoong and K.-Y. Chang, "Antipodal paraunitary matrices and their application to OFDM systems," IEEE Trans. Signal Process., vol. 53, no. 4, pp. 1374V1386, Apr. 2005.

[38] B. Porat and B. Friedlander, "Blind equalization of digital communication channels using high-order moments," IEEE Trans. SP, vol. 39, no. 2, pp. 522-526, Feb. 1991.

[39] W. Qiu, Y. Hua, and K. Abed-Meraim, "A subspace method for the computation of the GCD of polynomails," Automatica, vol. 33, no. 4, pp. 741-743, Apr. 1997.

[40] Y. Sato, "A method of self-recovering equalization for multi=level amplitude modulation," *IEEE Trans. on Communications,* COM-23:679-682, June 1975.

[41] A. H. Sayed, *Fundamentals of Adaptive Filtering*, John Wiley & Sons, Inc., Hoboken, NJ, 2003.

[42] R. O. Schmidt, *A signal subspace approach to multiple emitter location and spectral estimation*, Ph. D. dissertation, Stanford University, Stanford, CA.

[43] W. A. Sethares, *et al.*, "Parameter drift in LMS adaptive filters," IEEE Trans. Acoustic., Speech, Signal Processing, vol. ASSP-34, pp. 868-879, August 1986.

[44] A. Scaglione, G. B. Giannakis, and S. Barbarossa, "Redundant filter bank precoders and equalizers Part I: Unification and Optimal Designs," IEEE Trans. SP, vol. 47, pp. 2007-2022, Jul. 1999.

[45] A. Scaglione, G. B. Giannakis, and S. Barbarossa, "Redundant filter bank precoders and equalizers Part II: Blind Channel Estimation, Synchronization, and direct equalization", IEEE Trans. SP, vol. 47, pp. 1988-2006, Jul. 1999.

[46] S. V. Schell and D. L. Smith, "Improved performance of blind equalization using prior knowledge of transmitter filter," *Proc. 1994 IEEE MILCOM,* pp. 858-862, Fort Monmouth, NJ, Oct. 1994.

[47] O. Shalvi and E. Weinstein, "New criteria for blind deconvolution of non-minimum phase systems (channels)," IEEE Trans. Inform. Theory, vol. 36, pp. 312-321, Mar. 1990.

[48] B. Su, and P. P. Vaidyanathan, "Theoretical issues on LTI systems which preserve signal richness," IEEE Trans. Signal Processing, *IEEE Trans. on Signal Processing*, vol. 54, no. 3, pp. 1104-1113, Mar. 2006.

[49] B. Su and P. P. Vaidyanathan, "A generalized algorithm for blind channel identification with linear redundant precoders," *EURASIP Journal on Advances in Signal Processing*, vol. 2007, Article ID 25672, 13 pages, 2007.

[50] B. Su and P. P. Vaidyanathan, "Necessary and sufficient conditions for LTI systems to preserve signal richness" Proc. IEEE International Symposium on Circuits and Systems, Kobe, Japan, May 2005.

[51] B. Su and P. P. Vaidyanathan, "A generalization of deterministic algorithm for blind channel identification with filter bank precoders", Proc. of International Symposium on Circuits and Systems, Kos Island, Greece, May 2006.

[52] B. Su and P. P. Vaidyanathan, "On the persistency of excitation for blind channel estimation in cyclic prefix systems", Proc. of ISCAS, New Orleans, LA, May 2007.

[53] B. Su and P. P. Vaidyanathan, "Generalized subspace-based algorithms for blind channel estimation in cyclic prefix systems", *Proc. 40th Asilomar Conference on Signals, Systems, and Computers, Pacific Grove, CA, Nov. 2006*.

[54] B. Su and P. P. Vaidyanathan, "Vandermonde-form preserving matrices and the generalized signal richness preservation problem", *Proc. 40th Asilomar Conference on Signals, Systems, and Computers, Pacific Grove, CA, Nov. 2006*.

[55] B. Su and P. P. Vaidyanathan, "A semi-blind pilot-assisted channel estimation algorithm in OFDM systems", *Proc. 41th Asilomar Conference on Signals, Systems, and Computers,* Pacific Grove, CA, Nov. 2007.

[56] B. Su and P. P. Vaidyanathan, "Generalized signal richness preservation problem and Vandermonde-form preserving matrices," *IEEE Trans. on Signal Processing,* vol. 55, no. 5, part 2, pp. 2239-2250, May 2007.

[57] B. Su and P. P. Vaidyanathan, "Performance analysis of generalized zero-padded blind channel estimation algorithms," *IEEE Signal Processing Letter*, vol. 14, no. 11, pp. 789-792, Nov. 2007.

[58] B. Su and P. P. Vaidyanathan, "Comments on 'Performance analysis of a deterministic channel estimator for block transmission systems with null guard intervals', " *IEEE Trans. on Signal Processing,* vol. 56, no. 3, pp. 1308-1309.

[59] B. Su and P. P. Vaidyanathan, "New algorithms for blind block synchronization using redundant filterbank precoders," *Submitted to IEEE Trans. on Signal Processing*.

[60] B. Su and P. P. Vaidyanathan, "Subspace-based blind channel identification for cyclic prefix systems using few received blocks," *IEEE Trans. on Signal Processing*, vol. 55, no. 10, pp. 4979-4993, Oct. 2007.

[61] B. Su and P. P. Vaidyanathan, "New algorithms for blind block synchronization in zero-padding systems," Proc. of ICASSP 2007, Honolulu, Hawaii, Apr. 2007.

[62] B. Su and P. P. Vaidyanathan, "Blind block synchronization algorithms in cyclic prefix systems," Accepted by ISCAS 2008, Seattle, Washington, May 2008.

[63] L. Tong, B. M. Sadler, and M. Dong, "Pilot-assisted wireless transmissions: general model, design criteria, and signal processing," *IEEE Signal Processing Magazine,* vol. 21, no. 6, pp. 12-15, Nov. 2004.

[64] L. Tong, G. Xu, and T. Kailath, "A new approach to blind identification and equalization of multipath channels," in *Proc. 25th Asilomar Conf.*, pp. 856-860, 1991.

[65] L. Tong, G. Xu and T. Kailath, "A new approach to blind identification and equalization of multipath channels," Proc. 25th Asilomar Conf. on Signals, Systems, and Computers, Nov. 1991.

[66] L. Tong, G. Xu, and T. Kailath, "Blind identification and equalization based on second-order statistics: A time domain approach," IEEE Trans. Information Theory, vol. 40, no. 2, pp. 340-349, Mar. 1994.

[67] P. P. Vaidyanathan, *Multirate systems and filter banks,* Prentice-Hall, 1993.

[68] P. P. Vaidyanathan and B. Su, "Remarks on certain new methods for blind identification of FIR channels," Proc. IEEE Asil. Conf. Signals, Systems, and Computers, Nov. 2004.

[69] P. P. Vaidyanathan and B. Su, "Staying rich: LTI systems which preserve signal richness" Proc. IEEE International Conference on Acoustics, Speech, and Signal Processing, Philadelphia, PA, March 2005.

[70] P. P. Vaidyanathan and B. Vrcelj, "A frequency domain approach for blind identification with filter bank precoders," Proc. of ISCAS 2004, pp. 349-352, Vancouver, Canada.

[71] P. P. Vaidyanathan and B. Vrcelj, "Transmultiplexers as precoders in modern digital communication: a tutorial review," Proc. IEEE International Symposium on Circuits And Systems, Vancouver, Canada, May 2004.

[72] J. van de Beek, M. Sandell, and P. O. Borjesson, "ML estimation of time and frequency offset in OFDM systems," *IEEE Trans. Signal Processing*, vol. 45, pp. 1800-1805, July 1997.

[73] Z. Wang and G. B. Giannakis, "Wireless multicarrier communications: where Fourier meets Shannon, " *IEEE Signal Processing Mag.*, pp. 29-48, May 2000.

[74] G. Xu, H. Liu, L. Tong, T. Kailath, "A Least-Squares Approach to Blind Channel Identification," IEEE Trans. on SP, pp. 2982-2993, Dec. 1995.

[75] W. Yang, Y. Cai, and Y. Xun, "Semi-blind channel estimation for OFDM systems," in Proc. IEEE Vehicular Technology Conference, 2006. VTC 2006-Spring.

[76] S. Zhou and G. B. Giannakis, "Finite-alphabet based channel estimation for OFDM and related multicarrier systems," *IEEE Trans. Commun.*, vol. 49, pp. 1402-1414, Aug. 2001.

[77] X. Zhuang, Z. Ding, and A. L. Swindlehurst, "A statistical subspace method for blind channel identification in OFDM communications," in *Proc. ICASSP*, vol. 5, Istanbul, Turkey, pp. 2493-2496, June 2000.